



Universidade do Minho
Escola de Engenharia

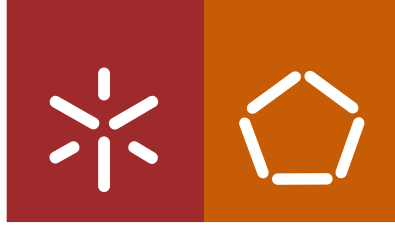
Jennifer Martins Noro

**Esterification of drugs: a tool to improve
hydrophobicity and encapsulation efficiency**

Jennifer Martins Noro Esterification of drugs: a tool to improve hydrophobicity and encapsulation efficiency

UMinho | 2021

janeiro de 2021



Universidade do Minho
Escola de Engenharia

Jennifer Martins Noro

**Esterification of drugs: a tool to improve
hydrophobicity and encapsulation efficiency**

Tese de Doutoramento
Doutoramento em Engenharia Química e Biológica

Trabalho efetuado sob a orientação do
Professor Doutor Artur Manuel Cavaco Paulo
e da
Doutora Carla Manuela Pereira Marinho da Silva

janeiro de 2021

DIREITOS DE AUTOR E CONDIÇÕES DE UTILIZAÇÃO DO TRABALHO POR TERCEIROS

Este é um trabalho académico que pode ser utilizado por terceiros desde que respeitadas as regras e boas práticas internacionalmente aceites, no que concerne aos direitos de autor e direitos conexos.

Assim, o presente trabalho pode ser utilizado nos termos previstos na licença abaixo indicada. Caso o utilizador necessite de permissão para poder fazer um uso do trabalho em condições não previstas no licenciamento indicado, deverá contactar o autor, através do RepositóriUM da Universidade do Minho.

Licença concedida aos utilizadores deste trabalho



Atribuição-NãoComercial-SemDerivações
CC BY-NC-ND

<https://creativecommons.org/licenses/by-nc-nd/4.0/>

Agradecimentos

A finalização desta tese representa a concretização de uma importante etapa do meu percurso académico, estando profundamente marcada por várias pessoas que direta ou indiretamente contribuíram para o seu sucesso. Assim, deixo-lhes aqui o meu maior e mais profundo agradecimento.

Em primeiro lugar, agradeço aos meus orientadores, ao Professor Artur Cavaco Paulo e à Doutora Carla Silva. Ao Professor Artur, pela oportunidade garantida e pela orientação e ajuda em todas as fases do projeto. À Carla, que para além de ser uma mentora de excelência, nunca me deixou fraquejar, impulsionando-me sempre a ser melhor e a atingir todos os meus objetivos. Agradeço-te não só pelas oportunidades, conversas e carinho, mas também pela tua profunda e sincera amizade.

Agradeço à Fundação para a Ciência e Tecnologia, pelo financiamento da minha bolsa de doutoramento (SFRH/BD/121673/2016) e à Universidade do Minho e Centro de Engenharia Biológica por garantirem todas as condições para a sua execução.

A todos os elementos do grupo de investigação de Bioprocessos e Bionanotecnologia, não só pela constante companhia, mas também pelo excelente espírito de cooperação e solidariedade assente durante todo o percurso. Especial gratidão à Diana, Filipa, Catarina, David e Artur, pela amizade e pelos momentos de alegria que nunca esquecerei. À Tarsila Castro, pela simpatia e dedicação na realização de todo o trabalho de modelação molecular, fundamentais nesta tese.

Um especial agradecimento ao Alfredo, que com toda a sua paciência, carinho e amor, contribuiu para que qualquer adversidade fosse superada. Foste um pilar capital desde o primeiro instante. Por fim, à minha família, sem os quais não seria possível concluir esta etapa. Agradeço aos meus pais, pela sua máxima dedicação, sacrifícios infindáveis e apoio incondicional incontestável. Pelos inúmeros ensinamentos e lições. Pelo amor que sempre senti e por tanto prezarem a minha educação. Agradeço-lhes especialmente por me ensinarem a apreciar as pequenas coisas, mas não me permitirem conformar, incentivando-me à superação e a lutar pelo meu futuro. À minha irmã Windy, que mesmo distante, sempre esteve (e sempre estará) presente. Vocês sempre foram o meu principal alicerce e sempre serão a estrela Polar que me guiará.

A todos o meu mais profundo e sincero agradecimento.

STATEMENT OF INTEGRITY

I hereby declare having conducted this academic work with integrity. I confirm that I have not used plagiarism or any form of undue use of information or falsification of results along the process leading to its elaboration.

I further declare that I have fully acknowledged the Code of Ethical Conduct of the University of Minho.

Esterificação de drogas: uma ferramenta para aumentar a hidrofobicidade e eficiência de encapsulação

Resumo

A necessidade de implementação de processos mais verdes e amigos do ambiente, continua a ser uma temática de grande importância para a comunidade científica. Das diferentes estratégias disponíveis para modificar e estabilizar compostos hidrofóbicos, o uso de enzimas para sua síntese e de nanoemulsões para o seu encapsulamento, são as abordagens mais comuns. Nesta tese, foram desenvolvidas nanoemulsões compostas por oligossacarídeos lipofílicos para a encapsulação de um composto hidrofóbico, o metotrexato (MTX). Enzimas, nomeadamente lipases ou proteases, foram aplicadas como catalisadores para a biossíntese de compostos hidrofóbicos com o objetivo de desenvolver alternativas ecológicas para futuras aplicações industriais. Primeiramente, a síntese de ciclo-oligossacarídeos lipofílicos (β -ciclodextrina, γ -ciclodextrina e ciclosforaose) foi realizada através da ligação de cadeias de palmitoilo aos grupos hidroxilo. As estruturas hidrofóbicas desenvolvidas revelaram propriedades emulsificantes quando submetidas a ultrassons. A sua estabilidade, baixo tamanho e baixa polidispersividade demonstraram o alto potencial destas emulsões como novos dispositivos para o encapsulamento e libertação do MTX.

Posteriormente, foram usadas duas abordagens enzimáticas para produzir pró-drogas de MTX. Inicialmente, lipases da *Thermomyces lanuginosus* (TL) e da *Cândida antarctica B* (CALB) foram utilizadas como catalisadores para a reação do MTX com triacilgliceróis e ciclodextrinas. Um meio aquoso, sob a ação de ultrassons, revelou ser uma estratégia eficaz para a síntese de pró-drogas de MTX, com o acoplamento de compostos não tóxicos. Na segunda abordagem, foi utilizada a α -quimiotripsina do *pâncreas de bovino* para a auto-polimerização do MTX. A protease revelou capacidade de produzir oligómeros de MTX até um máximo de 6 unidades. Foi assim estabelecida uma nova via para a produção de uma pró-droga de MTX polimérico, salientando o potencial desta protease para a catálise de substratos não naturais. Ao longo desta tese, foi também avaliado o efeito da modificação química de enzimas nas suas propriedades catalíticas. Numa primeira abordagem, as modificações foram realizadas através da PEGilação das lipases TL, CALB e de uma cutinase da *fusarium solani pisi*. Verificou-se que enquanto a PEGilação melhorou a atividade hidrolítica da CALB e da cutinase, a atividade da lipase TL permaneceu inalterada. O efeito dessa modificação foi também avaliado na atividade de polimerase das enzimas, na síntese de um poliéster, o poli(etileno glutarato). Das três enzimas estudadas, a lipase TL PEGuilada foi responsável pela maior produção de polímero, juntamente com um maior grau de polimerização (DP), em comparação com a forma nativa da enzima. Ambas as formas da CALB exibiram atividade de polimerase semelhante. O efeito da PEGuilação na cutinase não foi significativo, sendo detetado um pequeno aumento na conversão do polímero, em comparação com a enzima nativa, porém com menor DP. A segunda abordagem, implementada para a melhoria das propriedades catalíticas das lipases, baseou-se na ligação de pequenos ligandos hidrofóbicos, aldeídos e isotiocianatos, à lipase TL. O efeito dos ligandos na atividade hidrolítica e na estabilidade da enzima foi extensivamente estudado, tendo os dados revelado maior estabilidade a diferentes temperaturas e pHs, após a sua modificação. Além disso, a lipase modificada com 4 cadeias de dodecil (a partir do dodecil aldeído) apresentou excelente atividade catalítica, avaliada por reação com substratos de diferentes tamanhos de cadeia alifática (*p*-nitrofenil acetato a *p*-nitrofenil palmitato). Posteriormente, foi avaliada a atividade das enzimas na transesterificação do *p*-nitrofenil palmitato e na esterificação do ácido oleico, usando como substratos álcoois com diferentes tamanhos de cadeia (de metanol a eicosanol). A lipase modificada com 4 cadeias de dodecil, apresentou uma atividade superior, para ambas as reações, em comparação com a lipase nativa. Este incremento foi diretamente proporcional ao tamanho do álcool utilizado como substrato. Estas estratégias demonstraram a grande potencialidade das enzimas modificadas na biossíntese de produtos industriais de alto valor acrescentado.

Palavras-chave: enzimas, esterificação, metotrexato, modificação química, nanoemulsões.

Esterification of drugs: a tool to improve hydrophobicity and encapsulation efficiency

Abstract

The pursuit for green and environmentally friendly processes is still a great challenge among the scientific community. From the different strategies available to modify and stabilize hydrophobic compounds, the use of enzymes for their synthesis and of nanoemulsions for their encapsulation, are the most common approaches. In this thesis, nanoemulsions composed by lipophilic oligosaccharides were developed for the encapsulation of an hydrophobic compound, methotrexate (MTX). Enzymes, namely lipases or proteases, were applied as catalysts for the biosynthesis of hydrophobic compounds aiming to develop new eco-friendly routes for future industrial applications. Firstly, the synthesis of lipophilic cyclo-oligosaccharides (β -cyclodextrin, γ -cyclodextrin and cyclosophoraose) was carried out through the chemical coupling of palmitoyl chains to the hydroxylic groups. The hydrophobic structures showed emulsifying properties under ultrasonic energy. Their stability, narrow size, and low polydispersity demonstrated the high potential as new nanodevices for encapsulation and delivery of MTX.

Afterward, two different enzymatic approaches were used to produce MTX-prodrugs. In a first approach, lipases from *Thermomyces lanuginosus* (TL) and from *Candida antarctica B* (CALB) were applied as catalysts for the reaction of MTX with triacylglycerols and cyclodextrins. Aqueous medium, together with ultrasounds showed to be a successful route for the synthesis of MTX ester prodrugs, with the coupling of non-toxic compounds. The second approach included the use α -chymotrypsin from *bovine pancreas* for the self-polymerization of MTX. The protease revealed the ability to produce oligomers up to 6 MTX units. A novel pathway to produce a polymeric MTX prodrug was established, unravelling the potential of this protease for the catalysis of non-natural substrates. Along this thesis, the effect of the chemical modification of enzymes on their catalytic properties was also assessed. In a first approach, the chemical modifications were performed throughout PEGylation of lipase TL, CALB and cutinase from *fusarium solani pisi*. The data revealed that whereas PEGylation improved the hydrolytic activity of CALB and cutinase, it did not alter the activity of lipase TL. The effect of this modification was also evaluated throughout their polymerase activity in the synthesis of a polyester, poly(ethylene glutarate). From the three enzymes, PEGylated lipase TL was responsible for the highest polymer production with the highest degree of polymerization (DP), in comparison to the native form. Both CALB forms displayed similar polymerase activity. The effect of PEGylation on cutinase was not significant being detected a small increase of polymer conversion, however with lower DP, comparing with the native enzyme. The second approach for the improvement of lipases' catalytic properties covered the grafting of small hydrophobic aldehydes and isothiocyanates to the lipase TL. The effect of the linkers was extensively studied in terms of hydrolytic activity and stability, and the data obtained revealed higher temperature and pH stability after modification. Moreover, the lipase grafted with 4 dodecyl chains (from dodecyl aldehyde) showed outstanding catalytic activity, evaluated against a panoply of substrates differing in the aliphatic chain size (*p*-nitrophenyl acetate to *p*-nitrophenyl palmitate). Afterward, the enzymes' activity in the transesterification of *p*-nitrophenyl palmitate, and in the esterification of oleic acid was evaluated. Chain-size differentiated alcohols (methanol to eicosanol) were tested as substrates of the reactions. The modified lipase (with 4 dodecyl chains) showed superior activity for both reactions comparing to the native lipase. This increment was more directly proportional to the size of the alcohol used for the reaction. These strategies revealed high potentiality for the use of modified enzymes on the biosynthesis of industrial added-value products.

Keywords: chemical modification, enzymes, esterification, methotrexate, nanoemulsions.

Table of contents

Agradecimientos.....	iii
Resumo	v
Abstract	vi
List of Symbols and Abbreviations	xiii
List of Figures.....	xvii
List of Tables.....	xxiv
List of Schemes.....	xxvi
Chapter I.....	1
Thesis motivation and outline.....	1
1.1. Motivation and objectives.....	2
1.2. Thesis outline.....	4
Chapter II.....	7
Oil-based cyclo-oligosaccharide nanodevices for drug encapsulation.....	7
Abstract.....	8
2.1. Introduction.....	9
2.2. Materials and methods.....	10
2.2.1. Materials	10
2.2.2. Isolation of Cyclophoraose.....	11
2.2.3. Synthesis of modified cyclo-oligosaccharides	11
2.2.4. Nuclear Magnetic Resonance spectroscopy (NMR)	12
2.2.5. Matrix-Assisted Laser Desorption/Ionization Time-of-Flight (MALDI-TOF).....	12
2.2.6. Cyclo-oligosaccharide-palmitoyl conjugate nanoemulsions	12
2.2.7. Dynamic Light Scattering (DLS).....	12
2.2.8. Nanoparticle Tracking Analysis (NTA)	13
2.2.9. Differential Scanning Calorimetry (DSC)	13
2.2.10. Scanning Transmission Electron Microscopy (STEM)	13
2.2.11. Molecular Dynamics Simulations.....	13
2.2.12. Cellular viability assay.....	14
2.2.12.1. Cells and culture conditions	14
2.2.12.2. Cell viability assay.....	14
2.2.13. Stability of nanoemulsions in the presence of lipase	14

2.2.14.	Encapsulation and release of methotrexate	15
2.3.	Results and discussion	15
2.3.1.	Synthesis of hydrophobic cyclo-oligosaccharides by conjugation with palmitoyl chloride.....	15
2.3.2.	Cyclo-oligosaccharides-palmitoyl emulsification ability.....	18
2.3.3.	Microscopic observation	20
2.3.4.	Nanoemulsions stability over time	21
2.3.5.	Cytotoxicity of nanoemulsions	23
2.3.6.	Stability of nanoemulsions in the presence of lipase	24
2.3.7.	Encapsulation and release of methotrexate	25
2.4.	Conclusions	28
Chapter III	29
Ultrasound-assisted biosynthesis of novel methotrexate-conjugates	29
Abstract.....		30
3.1.	Introduction.....	31
3.2.	Materials and methods.....	32
3.2.1.	Materials	32
3.2.2.	General procedure	33
3.2.2.1.	MTX-acylglycerol (small carbon chain) conjugates.....	33
3.2.2.2.	MTX-acylglycerol (long carbon chain) conjugates	34
3.2.2.3.	MTX-cyclodextrin conjugates	34
3.2.3.	Nuclear Magnetic Resonance spectroscopy (NMR)	35
3.2.4.	Matrix-Assisted Laser Desorption/Ionization Time-of-Flight (MALDI-TOF).....	35
3.2.5.	Electrospray Ionization (ESI).....	36
3.3.	Results and discussion	36
3.3.1.	Methotrexate-acylglycerol conjugates.....	36
3.3.2.	Methotrexate-cyclodextrin conjugates	41
3.4.	Conclusions	44
Chapter IV	45
α-Chymotrypsin catalyses the synthesis of methotrexate oligomers	45
Abstract.....		46
4.1.	Introduction.....	47
4.2.	Materials and methods.....	48
4.2.1.	Materials	48

4.2.2.	General procedure for the synthesis of oligomeric methotrexate.....	48
4.2.3.	Activity of α -chymotrypsin	49
4.2.4.	Nuclear Magnetic Resonance spectroscopy (NMR)	49
4.2.5.	Matrix-Assisted Laser Desorption/Ionization Time-of-Flight (MALDI-TOF).....	49
4.2.6.	Electrospray Ionization (ESI).....	50
4.2.7.	Differential Scanning Calorimetry (DSC)	50
4.2.8.	Molecular Dynamics Simulations and docking.....	50
4.3.	Results and discussion	52
4.3.1.	α -Chymotrypsin-catalysed synthesis of oligomeric MTX	52
4.3.2.	Synthesis of dimeric MTX – proposed mechanism.....	54
4.3.3.	Molecular Dynamics Simulations.....	56
4.3.3.1.	NMR Spectroscopy	61
4.3.3.3.	DSC	63
4.4.	Conclusions	64
Chapter V.....	65	
Catalytic activation of esterases by PEGylation for polyester synthesis	65	
Abstract.....	66	
5.1. Introduction.....	67	
5.2. Materials and methods.....	68	
5.2.1. Materials	68	
5.2.2. Synthesis.....	68	
5.2.2.1. General procedure for the PEGylation of esterases.....	68	
5.2.2.2. General procedure for synthesis of poly(ethylene glutarate).....	69	
5.2.3. Enzyme characterization	69	
5.2.3.1. SDS-PAGE	69	
5.2.3.2. Esterase activity.....	69	
5.2.3.3. Protein quantification	70	
5.2.3.4. Degree of PEGylation	70	
5.2.3.5. Molecular Dynamics Simulations.....	70	
5.2.4. Polymer characterization	71	
5.2.4.1. Nuclear Magnetic Resonance spectroscopy (NMR)	71	
5.2.4.2. Matrix-Assisted Laser Desorption/Ionization Time-of-Flight (MALDI-TOF).....	72	
5.2.4.3. Fourier-transform infrared spectroscopy (FTIR)	72	
5.2.4.4. Differential Scanning Calorimetry (DSC)	72	

5.2.4.5.	Thermogravimetric Analysis (TGA)	73
5.3.	Results and discussion	73
5.3.1.	PEGylation and catalytic properties of PEGylated esterases.....	73
5.3.2.	Effect of PEGylation on the polymerase activity of esterases.....	77
5.3.3.	Molecular Dynamics Simulations.....	80
5.3.4.	Poly(ethylene glutarate) characterization	85
5.3.4.1.	NMR.....	86
5.3.4.2.	MALDI-TOF	87
5.3.4.3.	FTIR, DSC and TGA.....	88
5.4.	Conclusions	89
Chapter VI	91
Substrate's hydrophobicity and enzyme's modifiers play a major role on the activity of lipase from <i>Thermomyces lanuginosus</i>	91
Abstract.....		92
6.1.	Introduction.....	93
6.2.	Materials and methods.....	94
6.2.1.	Materials	94
6.2.2.	Synthesis.....	95
6.2.2.1.	Chemical modification of lipase from <i>Thermomyces lanuginosus</i>	95
6.2.2.2.	Synthesis of <i>p</i> -nitrophenyl benzoate.....	95
6.2.3.	Enzyme characterization	96
6.2.3.1.	Modification efficiency.....	96
6.2.3.2.	Matrix-Assisted Laser Desorption/Ionization Time-of-Flight (MALDI-TOF)	96
6.2.3.3.	Protein modification and SDS-PAGE	96
6.2.3.4.	Enzyme activity	96
6.2.3.5.	Kinetic parameters	97
6.2.3.6.	Molecular Dynamics Simulations.....	97
6.2.3.7.	Molecular docking and complexes simulations.....	97
6.2.3.8.	Linkers simulations.....	98
6.2.3.9.	Half-life time ($T_{1/2}$)	98
6.2.3.10.	Effect of the pH on the activity.....	99
6.2.3.11.	Effect of the temperature on the activity	99
6.2.3.12.	Circular Dichroism (CD)	99
6.2.3.13.	Fluorescence measurements	99

6.3.	Results and discussion	99
6.3.1.	Chemical modification of lipase from <i>Thermomyces lanuginosus</i>	99
6.3.2.	Hydrolytic activity.....	102
6.3.2.1.	Absolute activity.....	102
6.3.2.2.	Kinetic parameters	106
6.3.3.	Molecular Dynamics Simulations.....	108
6.3.4.	Stability of TL and modified lipases	112
6.3.5.	Circular dichroism	116
6.3.6.	Fluorescence analysis.....	116
6.4.	Conclusions	118
Chapter VII	119
Chemical modification of lipase from <i>Thermomyces lanuginosus</i> enhances transesterification and esterification activity	119
Abstract.....		120
7.1.	Introduction.....	121
7.2.	Materials and methods.....	122
7.2.1.	Materials	122
7.2.2.	Chemical modification of lipase TL.....	123
7.2.3.	Half-life time of the enzymes ($T_{1/2}$)	123
7.2.4.	Transesterification activity.....	123
7.2.5.	Esterification activity	124
7.2.6.	Products characterization	124
7.2.6.1.	Nuclear Magnetic Resonance spectroscopy (NMR)	124
7.2.6.2.	Gas Chromatography – Mass Spectrometry (GC-MS)	124
7.2.6.3.	Fourier-transform infrared spectroscopy (FTIR)	125
7.3.	Results and discussion	125
7.3.1.	Chemical modification of lipase TL.....	125
7.3.2.	Transesterification activity.....	126
7.3.3.	Esterification activity	129
7.3.3.1.	Effect of alcohol's chain-size	129
7.3.3.2.	Enzyme dosage vs temperature of reaction	130
7.3.4.	Products characterization	132
7.4.	Conclusions	134
Chapter VIII	135

Biotechnological approaches for the synthesis, modification and stabilization of hydrophobic compounds	135
Abstract.....	136
8.1. Introduction.....	137
8.2. Enzymes for the synthesis or modification of hydrophobic compounds	137
8.2.1. Synthesis and/or modification of hydrophobic drugs: practical applications	138
8.2.2. Polyester synthesis by enzymes	141
8.2.3. Other synthesis applications: cosmetic, food, biofuels, etc.	143
8.3. Improvement of enzymes' properties	144
8.3.1. Chemical modification of lipases	146
8.3.1.1. Catalytic properties of lipases.....	146
8.3.1.2. Modification of lipases with small molecules.....	148
8.3.1.3. Modification of lipases with macromolecules	149
8.4. Immobilization of lipases onto solid supports	156
8.4.1. Immobilization <i>vs</i> chemical modification: advantages and disadvantages	156
8.5. Nanoemulsions for the encapsulation of hydrophobic compounds	158
8.5.1. General description.....	158
8.5.2. Applications.....	158
8.6. Major remarks and future perspectives	160
References.....	163

List of Symbols and Abbreviations

^1H NMR: Proton Nuclear Magnetic Resonance

^{13}C NMR: Carbon Nuclear Magnetic Resonance

α : Alpha

α -CD: Alpha-cyclodextrin

Ala: Alanine

Asn: Asparagine

Asp: Aspartic acid

ATB: Automated Topology Builder

β : Beta

β -CD: Beta-cyclodextrin

BSA: Bovine Serum Albumin

C: Carbon

CALB: Lipase from *Candida antarctica* B

CBMA: Carboxyl betaine methacrylate

CD: Cyclodextrins

CHCA: α -Cyano-4-hydroxycinnamic acid

CNDE: *rac*-2-carboxyethyl-3-cyano-5-methylhexanoic acid ethyl ester

CTA: 2-(((ethylthio)-carbonothioyl)thio)propanoic acid

ρ : Conversion rate (Carothers equation)

Cys: Cyclosophoraose

Cys-PAL: Cyclosophoraose-palmitoyl conjugate

DEPT: Distortionless Enhancement by Polarization Transfer

DHB: 2,5-Dihydroxybenzoic acid

DLS: Dynamic Light Scattering

DFT: Density Functional Theory (quantum mechanical calculation method)

DMAPA: *N*[3-(dimethylamino)propyl]acrylamide

DMF: Dimethylformamide

DMSO: Dimethyl sulfoxide

DMSO- d_6 : Deuterated dimethyl sulfoxide

DP_{avg} : Average degree of polymerization

DP_{max}: Maximum degree of polymerization
DSC: Differential Scanning Calorimetry
ee: enantiomeric excess
ESI: Electrospray Ionization
FDA: Food and Drug Administration
FF: Force field
FTIR: Fourier-transform infrared spectroscopy
 γ : Gamma
 γ -CD: Gamma-cyclodextrin
GC-MS: Gas Chromatography – Mass Spectrometry
Gly: Glycine
Glu: Glutamic acid
HA: Heavy-atom
His: Histidine
HMBC: ¹H-¹³C Heteronuclear Multiple Bond Correlation
HPLC: High-Performance Liquid Chromatography
HSQC: ¹H-¹³C Heteronuclear Single Quantum Coherence
*k*_{cat}: turnover number
*K*_M: Michaelis-Menten constant
LCR: Lipases from *Candida rugosa*
LE: Ligand Efficiency
Leu: Leucine
LGA: Lamarckian Genetic Algorithm
LYP: Lysine residue with a poly(ethylene glycol) unit
Lys: Lysine
[M]: Monomeric repeating unit
MALDI-TOF: Matrix-Assisted Laser Desorption/Ionization Time-of-Flight
MD: Molecular Dynamics
Mn: Number average molecular weight
M.p.: Melting point
MTX: Methotrexate
MTX-CD: Methotrexate-cyclodextrin conjugate

MW: Molecular weight
 M_w : Weight average molecular weight
NHS: *N*-Hydroxysuccinimide
NIBMA: *N*-(iso-butoxymethyl) acrylamide
NMR: Nuclear Magnetic Resonance
NPT: Isothermal-isobaric ensemble, constant number of particles (N), pressure (P) and temperature (T)
NTA: Nanoparticle Tracking Analysis
NVT: Canonical ensemble, constant number of particles (N), volume (V) and temperature (T)
p: *para* (substituted)
P-Cys: Pentacosadiynoyl cyclophosphoramide
PAL: Palmitoyl
PAL-Cl: Palmitoyl chloride
PBS: Phosphate Buffer Saline
PDB: Protein Data Bank
PDI: Polydispersity Index
PEG: Poly(ethylene glycol)
PLA: Poly(lactic acid)
PLGA: Poly(lactide-co-glycolide)
PME: Particle-mesh Ewald
p-NP: *p*-Nitrophenol
p-NPAc: *p*-Nitrophenyl Acetate
p-NPB: *p*-Nitrophenyl Butyrate
p-NPH: *p*-Nitrophenyl Hexanoate
p-NPL: *p*-Nitrophenyl Laurate
p-NPO: *p*-Nitrophenyl Octanoate
p-NPP: *p*-Nitrophenyl Palmitate
p-NPPh: *p*-Nitrophenyl Benzoate
RMSD: Root Mean Square Deviation
RMSF: Root Mean Square Fluctuation
rt: room temperature
SASA: Solvent Accessible Surface Area

SD: Standard Deviation

SDS-PAGE: Sodium Dodecyl Sulfate Polyacrylamide Gel Electrophoresis

Ser: Serine

STEM: Scanning Transmission Electron Microscopy

$T_{1/2}$: Half-life time

T_g : Glass transition temperature (DSC)

T_m : Melting point temperature (DSC)

TBMA: *tert*-butyl methacrylate

TEMED: Tetramethylethylenediamine

TGA: Thermogravimetric Analysis

Thr: Threonine

TL: *Thermomyces lanuginosus*

TL1: lipase from *Thermomyces lanuginosus* modified with 1 unit of naphthyl isothiocyanate

TL2: lipase from *Thermomyces lanuginosus* modified with 1 unit of naphthyl aldehyde

TL3: lipase from *Thermomyces lanuginosus* modified with 7 units of butyraldehyde

TL4: lipase from *Thermomyces lanuginosus* modified with 7 units of hexyl aldehyde

TL5: lipase from *Thermomyces lanuginosus* modified with 4 units of dodecyl aldehyde

TLC: Thin Layer Chromatography

TNBSA: 2,4,6-Trinitrobenzene sulfonic acid

Tyr: Tyrosine

US: ultrasound

V_{max} : maximum rate

WB: water bath

η : Yield or catalytic efficiency

List of Figures

Figure 2.1. Synthesis of modified cyclo-oligosaccharides: A) reactional scheme of the conjugation of PAL-Cl with Cys; B) reactional scheme of the conjugation of PAL-Cl with β -CD (n=7) and γ -CD (n=8).....	16
Figure 2.2. Positive ion MALDI-TOF spectrum of: A) β -CD-PAL, B) γ -CD-PAL and C) Cys-PAL on DHB.....	17
Figure 2.3. ^1H NMR spectra of: A) Cys and Cys-PAL; B) β -CD and β -CD-PAL and C) γ -CD and γ -CD-PAL.....	18
Figure 2.4. Formulations photographs after emulsification with US: I) Cys (5 mg/mL); II) Cys-PAL (5 mg/mL); III) BSA (10 mg/mL) + Cys-PAL (5 mg/mL); IV) γ -CD (5 mg/mL); V) γ -CD-PAL (5 mg/mL); VI) BSA (10 mg/mL) + γ -CD-PAL (5 mg/mL); VII) β -CD (5 mg/mL); VIII) β -CD-PAL (5 mg/mL); IX) BSA (10 mg/mL) + β -CD-PAL (5 mg/mL) and X) BSA (10 mg/mL).....	19
Figure 2.5. Molecular dynamic simulations of Cys-PAL auto aggregation: I) cyclodextrin (red) surrounded by covalently bonded palmitic chains (green), before aggregation, II) 15 units of Cys-PAL self-aggregated; and BSA-Cys-PAL aggregation: III) BSA-Cys-PAL before nanoemulsion simulation, showing 6 units of BSA (in red) and 12 units of Cys-PAL (in cyan), IV) BSA-Cys-PAL after nanoemulsion simulation (one unit of Cys-PAL surrounded by several units of BSA).....	20
Figure 2.6. STEM images of nanoemulsions: A) Cys-PAL (5 mg/mL) (stained with uranyl acetate); B) γ -CD-PAL (5mg/mL); C) β -CD-PAL (5 mg/mL); D) BSA (10 mg/mL) + Cys-PAL (5 mg/mL) (stained with uranyl acetate); E) BSA (10 mg/mL) + γ -CD-PAL (5 mg/mL) (stained with uranyl acetate).....	21
Figure 2.7. Stability (size and PDI) of nanoemulsions during storage at 4 °C for 60 days (values are the mean \pm SD of 3 independent experiments).....	22
Figure 2.8. BJ5ta cell line viability after 72 h of contact with different concentrations (from 0.0625 mg/mL up to 1 mg/mL) of the four different nanoemulsion formulations, compared with cells (negative control) and cells incubated with 30 % (v/v) of DMSO (death control), determined by MTS assay. Values are the mean \pm SD of 2 independent experiments.....	24
Figure 2.9. ^1H NMR (in D_2O) of MTX free (in blue) and encapsulated in γ -CD-PAL nanoemulsions (in red).....	26

Figure 2.10. Release of MTX from the nanoemulsions over time (values are the mean \pm SD of 3 independent experiments).....	27
Figure 2.11. STEM microphotographs of nanoemulsions with MTX encapsulated: A) Cys-PAL-MTX before MTX release; B) Cys-PAL-MTX after MTX release; C) γ -CD-MTX before MTX release; D) γ -CD-MTX after MTX release.....	28
Figure 3.1. ^1H NMR spectra of A) free MTX and B) methotrexate-hexanoate conjugate (DMSO- d_6).....	40
Figure 3.2. ^1H NMR of MTX-CD (α , β and γ)-conjugates in DMSO- d_6 using lipase from <i>Thermomyces lanuginosus</i> in the US.....	43
Figure 3.3. MALDI-TOF of MTX-CD conjugates: A) α -CD conjugated with 1 MTX unit, B) β -CD conjugated with 2 MTX units, C) γ -CD conjugated with 3 MTX units; the upper image shows the proposed MTX-CD conjugates; all conjugates were obtained after reaction using lipase from <i>Thermomyces lanuginosus</i> in ultrasound.....	44
Figure 4.1. Proposed mechanism for the synthesis of a dimeric unit of methotrexate catalysed by α -chymotrypsin.....	55
Figure 4.2. A) Backbone RMSD of α -chymotrypsin, simulated at 310 K and physiological pH (black trace), and at 323 K and pH 9.5 (red trace), from the initial 3D structure (10XG); B) 3-D structure of bovine α -chymotrypsin (PDB ID: 10XG), from X-ray diffraction (I), highlighting in stick representation the catalytic triad: His57, Asp102 and Ser195. Green for cartoon/carbon, blue for nitrogen, red for oxygen and with for hydrogens; (II) shows the electrostatic distribution, where blue corresponds to positive areas and red to negative ones.....	57
Figure 4.3. A) Skeletal and 3-D methotrexate (MTX) structures at pH 7.0 and B) the deprotonated forms at pH 9.5. C) skeletal and 3-D structures of MTX dimer, at pH 9.5 and D) shows the trimer 3-D representation. The colour scheme use green for carbon, blue for nitrogen, red for oxygen and white for hydrogen.....	58
Figure 4.4. Docking poses showing the interaction of α -chymotrypsin with the different methotrexate species, and the respective binding energies obtained using AutoDock 4.0: A) α -chymotrypsin with methotrexate; B) α -chymotrypsin with dimeric methotrexate and C) α -chymotrypsin with trimeric methotrexate. Surface/cavities representation are in the right panel. Enzyme is represented in light grey, hydrogen bonds in yellow dashes and methotrexates following the scheme previous described in Figure 4.3	60

Figure 4.5. ^1H NMR (DMSO-d_6) spectra of A) methotrexate and B) oligomeric methotrexate synthesized by α -chymotrypsin.....	61
Figure 4.6. MALDI-TOF spectra of: A) control reaction carried without enzyme, and B) oligomeric methotrexate synthesized by α -chymotrypsin, and ESI spectra of: C) monomeric methotrexate and D) oligomeric methotrexate where the most abundant specie (100 %) is observed at m/z 975.36 corresponding to the dimeric MTX.....	62
Figure 4.7. Differential scanning calorimetry (DSC) curves of methotrexate (MTX) and oligomeric methotrexate; the black line corresponds to the monomer; the grey line corresponds to oligomeric MTX synthesized by α -chymotrypsin.....	63
Figure 5.1. SDS-PAGE gel of native and PEGylated esterases stained with Coomassie brilliant blue; A) GRS Protein Marker Blue (from Grisp, Portugal), B) Lipase from <i>Thermomyces lanuginosus</i> ; C) PEGylated lipase from <i>Thermomyces lanuginosus</i> ; D) Cutinase from <i>Fusarium solani pisi</i> ; E) PEGylated cutinase from <i>Fusarium solani pisi</i>	75
Figure 5.2. Absolute activity of esterases (native and PEGylated forms), at time zero, after 8 h, and after 50 days of incubation at 40 °C in phosphate buffer (pH 7.8). The activity was measured against <i>p</i> -NPB over 1 min and considering the same initial amount of protein; 1 U of enzyme activity was defined as the amount of enzyme required to convert the substrate (<i>p</i> -nitrophenyl butyrate) into <i>p</i> -nitrophenol in 1 min.....	76
Figure 5.3. Conversion (%) <i>vs</i> enzyme loading (U/mg) after synthesis of poly(ethylene glutarate).....	78
Figure 5.4. Conversion (%) and degree of polymerization (DP) for all the tested esterases under the optimized conditions: 2 h under US followed by 5 h under vacuum, at 40 °C; 65 U/mg. The graph bar corresponds to the conversion (%) and the graph line to the average DP.....	79
Figure 5.5. Lipase TL in water medium (A) and in substrates mixture medium (B) . Optimized structures of diethyl glutarate and ethylene glycol in united-atom GROMOS 54a7 FF representation (C) . Initial structures of lipase TL (green, 1TIB) and CALB (grey, 1TCA) (D) . PEGylated structures based on lipase TL and CALB: LP1 (LYP98), LP2 (LYP98, LYP74, LYP223 and LYP237), LP3 (LYP98, LYP24, LYP46, LYP127), LP4 (LYP98, LYP24, LYP46, LYP223, LYP237), LP5 (LYP46, LYP74, LYP127, LYP223, LYP237) and PEG-CALB (all Lys replaced by LYP). Lipases are represented in cartoon, with the lid region highlighted in cyan, the catalytic triad in yellow, and LYP residues in magenta.....	82

Figure 5.6. Backbone RMSD of lipase TL, CALB and PEGylated analogues in solvent (A-B) and in water (C-D).....	83
Figure 5.7. Middle conformations of lipase TL and PEGylated analogue LP1, in reactant mixture (A) and in water (B), highlighting the interior cavities and pockets surrounding the catalytic triad and lid regions.....	84
Figure 5.8. Middle conformations of CALB and PEGylated CALB, in reactant mixture (A) and in water (B), highlighting the cavities and pockets surrounding the catalytic triad and lid regions. Cartoon in grey, catalytic triad in yellow, lid-like region in cyan, LYP residues in magenta and the orange spheres represent the empty space (cavity or pocket) on each structure.....	85
Figure 5.9. ¹ H (A) and ¹³ C (B) NMR spectra of poly(ethylene glutarate) recorded in CDCl ₃	87
Figure 5.10. Positive ion MALDI-TOF spectra of poly(ethylene glycol) (DP _{max} = 16 and DP _{avg} = 5).....	88
Figure 5.11. FTIR spectra of A) diethyl glutarate; B) ethylene glycol; C) poly(ethylene glutarate) with a DP _{avg} = 3; D) poly(ethylene glutarate) with a DP _{avg} = 5.....	88
Figure 5.12. Graphics of A) DSC curve of poly(ethylene glutarate) with T _g = 77.29 ± 1.21 °C and T _m = 195.7 °C, and the respective monomers and B) TGA curves of the starting materials (diethyl glutarate and ethylene glycol) and the formed poly(ethylene glutarate).....	89
Figure 6.1. Proposed reactional scheme for the enzyme modification: A) native enzyme with an exposed lysine residue represented; B) enzyme modified with an aldehyde in the lysine residue, leading to a secondary amine; C) enzyme modified with an isothiocyanate in the lysine residue, leading to a thiourea; linkers used for lipase modification: i) naphthaldehyde; ii) butyraldehyde; iii) hexyl aldehyde; iv) dodecyl aldehyde; v) naphthyl isothiocyanate; vi) phenethyl isothiocyanate; vii) octyl isothiocyanate.....	100
Figure 6.2. SDS-PAGE of native lipase from <i>Thermomyces lanuginosus</i> and modified lipases (TL1-TL5).....	102
Figure 6.3. A) Proposed reactional scheme representing the hydrolysis of the ester substrates and the designation of each substrate according to the number of carbons in the aliphatic chain; B) Absolute hydrolytic activity of native lipase (TL) and of modified lipases with aromatic linkers (TL1 and TL2), and C) with aliphatic linkers (TL3-TL5), measured against different substrates: <i>p</i> -nitrophenyl benzoate (<i>p</i> -NPPH, 0C), <i>p</i> -nitrophenyl acetate (<i>p</i> -NPAC, 2C), <i>p</i> -nitrophenyl butyrate (<i>p</i> -NPB, 4C), <i>p</i> -nitrophenyl hexanoate (<i>p</i> -NPH, 6C), <i>p</i> -nitrophenyl	

octanoate (<i>p</i> -NPO, 8C), <i>p</i> -nitrophenyl laurate (<i>p</i> -NPL, 12C) and <i>p</i> -nitrophenyl palmitate (<i>p</i> -NPP, 16C).....	104
Figure 6.4. Activity of the modified lipases versus hydrophobic area of the linkers; activity measured against <i>p</i> -nitrophenyl acetate (<i>p</i> -NPAc, ●), <i>p</i> -nitrophenyl hexanoate (<i>p</i> -NPH, ▲) and <i>p</i> -nitrophenyl laurate (<i>p</i> -NPL, ■). The colour of the symbols in the graphs corresponds to the colour of each modified enzyme represented bellow the graph.....	105
Figure 6.5. Catalytic turnover ($\eta = k_{cat}/K_M$) of the native and modified enzymes calculated for the hydrolysis of <i>p</i> -nitrophenyl acetate (<i>p</i> -NPAc, 2C), <i>p</i> -nitrophenyl butyrate (<i>p</i> -NPB, 4C) and <i>p</i> -nitrophenyl octanoate (<i>p</i> -NPO, 8C).....	108
Figure 6.6. Middle structures characterized for lipase TL (A) and TL5 (C); Lid is highlighted in cyan, catalytic triad with the residues in green sticks and TL5 in blue sticks (C); (B) and (D) zoom in the active site, showing the pockets/cavities in yellow surface.....	109
Figure 6.7. A) Backbone RMSD of lipase TL and TL5 in water; B) amino acids RMSF.....	110
Figure 6.8. Representation of the best docking poses, interactions and $\Delta G_{binding}$ between <i>p</i> -nitrophenyl butyrate with native TL (A) and with TL5 (C); <i>p</i> -nitrophenyl octanoate with native TL (B) and with TL5 (D). Enzymes are represented in grey cartoon, sticks to highlight the amino acids residues participating in the binding, substrate in cyan ball and sticks, and hydrogen bonds in green dashed.....	111
Figure 6.9. Distance (nm) along simulation time from <i>p</i> -nitrophenyl butyrate or <i>p</i> -nitrophenyl octanoate to the Ser146 in catalytic triad.....	112
Figure 6.10. Stability of native and modified enzymes: A) Relative activity (%) at time zero, and after 4 months in solution at 4 °C and 37 °C; B) Half-life time (in hours) of the enzymes at 60 °C; C) Effect of temperature in the enzymes' activity after 10 min incubated at the respective temperatures (37 °C, 45 °C, 60 °C and 70 °C); D) Effect of pH in the enzymes' activity after 10 min incubated at the respective pH (1.81, 4.46, 6.41, 7.80, 9.40 and 10.5). The results presented were obtained using <i>p</i> -nitrophenyl butyrate as substrate. E) and G) same as C) but using <i>p</i> -nitrophenyl octanoate or <i>p</i> -nitrophenyl palmitate as substrate, respectively; F) and H) same as D) but using <i>p</i> -nitrophenyl octanoate or <i>p</i> -nitrophenyl palmitate as substrate, respectively.....	113
Figure 6.11. Electrostatic potential surface ($k_b T e_c^{-1}$) generated with PDB2PQR server and APBS plugin in PyMOL, at pH 10.5, for: A) TL with all Lys side chain protonated, and B) TL3 with	

all Lys converted to TL3 linker. On the left exterior surface and on the right the cavities/pocket representation.....	115
Figure 6.12. Circular dichroism of native lipase (TL) and modified lipases (TL1 to TL5).....	116
Figure 6.13. A) Fluorescence spectra of native (TL) and modified lipases (TL1-TL5) after excitation at 280 nm. B) Table of the maximum wavelength with the respective intensity value.....	117
Figure 7.1. A) Representative scheme for the modification of (I) native lipase from <i>Thermomyces lanuginosus</i> with dodecyl aldehyde to produce (II) modified lipase TL with 4 dodecyl chains; B) MALDI-TOF of the modified lipase, confirming the grafting of 4 dodecyl chains (MW of native= 29620.3) [326]; C) Half-life time of both enzymes at different temperatures.....	126
Figure 7.2. A) Reactional scheme for the transesterification reaction of <i>p</i> -nitrophenyl palmitate (<i>p</i> -NPP) with differentiated size-alcohols (methanol, pentanol and decanol), to produce <i>p</i> -nitrophenol and an aliphatic ester; B) Transesterification activity of native (full lines) and modified lipase (dash lines), using methanol (green), pentanol (red) and decanol (blue) as alcohol substrates. <i>K</i> values calculated after 7 h of reaction; C) GC-MS chromatograms of the products of the transesterification of <i>p</i> -NPP with methanol, catalysed by native and modified lipase (after 7 h of reaction).....	128
Figure 7.3. A) Reactional scheme for the esterification of oleic acid with differentiated chain-size alcohols; B) Reactional yield (%) of the esterification reaction of oleic acid with different alcohols catalysed by native and modified lipase TL (0.08 % w/v). Results obtained after 24 h of reaction, with the reactions performed at 37 °C; C) <i>K</i> values ($K = \frac{[\text{ester product}]}{[\text{oleic acid}]}$) regarding the effect of temperature (25, 37 and 50 °C), in the esterification of oleic acid with alcohols (methanol, decanol and eicosanol), using native <i>vs</i> modified lipase (0.08 % w/v) after 30 h of reaction.....	132
Figure 7.4. A) ¹ H NMR spectrum of propyl oleate, synthesized by reaction between oleic acid and propanol catalysed by the modified lipase; B) Retention time, <i>m/z</i> obtained after GC-MS analysis and theoretical molecular weight of all biosynthesised esters; C) FTIR spectra of oleic acid (black) and of propyl oleate (grey) synthesized by the modified lipase.....	134
Figure 8.1. Different fields of application where enzymes can be incorporated for the synthesis or modification of hydrophobic compounds (enzymes represented: A) lipase from <i>Candida antarctica</i> B PDB ID: 4K6G; B) cutinase from <i>Fusarium solani</i> PDB ID: 1CUS; C) α -chymotrypsin from <i>bovine pancreas</i> PDB ID: 1YPH; D) lipase from <i>Thermomyces lanuginosus</i> PDB ID: 5AP9).....	138

Figure 8.2. Some of the enzyme properties improved by chemical modification (enzyme represented: lipase from <i>Thermomyces lanuginosus</i> , PDB ID: 1TIB, modified aleatorily with four dodecyl chains through lysine residues using PyMOL).....	145
Figure 8.3. Examples of reactions performed by lipase-catalysis.....	147
Figure 8.4. Structure of lipase from <i>Thermomyces lanuginosus</i> (PDB ID: 1TIB) elucidating the lid in cyan and the catalytic triad Ser-His-Asp in magenta.....	148
Figure 8.5. Examples of enzyme immobilization strategies.....	156
Figure 8.6. Major advantages of both strategies: immobilization <i>vs</i> chemical modification of enzymes.....	157

List of Tables

Table 2.1. Mean size diameter (nm) and size distribution measured by DLS and NTA (values are the mean \pm SD of 3 independent experiments).....	23
Table 2.2. Particle size after assay (t= 0 h) and after 48 h in the presence of lipase (values are the mean \pm SD of 3 independent experiments).....	25
Table 2.3. Size, PDI and surface charge of nanoemulsions, before and after MTX release.....	27
Table 3.1. Experimental conditions and conversion yields for methotrexate-acylglycerol conjugates using immobilized CALB and free lipase from <i>Thermomyces lanuginosus</i> (TL) (results with standard deviation from at least 2 independent experiments).....	39
Table 3.2. Values of theoretical and experimental mass obtained by ESI and MALDI-TOF.....	40
Table 3.3. Reaction conditions and conversion yields obtained after conjugation of methotrexate with cyclodextrins using liquid lipase from <i>Thermomyces lanuginosus</i> (TL) (results with standard deviation from at least 2 independent experiments).....	42
Table 4.1. Reactional conditions tested for the α -chymotrypsin-assisted synthesis of methotrexate oligomers.....	53
Table 4.2. Conversion rate (%), average and maximum degree of polymerization (DP_{avg} and DP_{max}) analysed by MALDI-TOF and electrospray ionization (ESI), for the oligomerization of methotrexate, with and without α -chymotrypsin.....	54
Table 4.3. Number average molecular weight (Mn), weight average molecular weight (Mw), polydispersity (PDI), average and maximum degree of polymerization (DP_{avg} and DP_{max}) of the obtained oligomeric methotrexate catalysed by α -chymotrypsin at 50 °C after 1 week.....	63
Table 5.1. Percentage of amine residues modified by PEGylation and activity of esterases, before and after PEGylation.....	74
Table 5.2. Number average molecular weight (Mn), weight average molecular weight (Mw), polydispersity (PDI), average degree of polymerization (DP_{avg}), maximum degree of polymerization (DP_{max}) (calculated by MALDI-TOF) and conversion rate, after poly(ethylene glutarate) biosynthesis (2 h under US followed by 5 h under vacuum at 40 °C with the 65 U/mg of enzyme).....	86
Table 6.1. Modification degree and number of modified residues evaluated by MALDI-TOF and TNBSA assay, being TL the native enzyme, and the modified enzymes: TL1 modified with	

naphthyl isothiocyanate, TL2 modified with naphthyl aldehyde, TL3 modified with butyraldehyde, TL4 modified with hexyl aldehyde and TL5 modified with dodecyl aldehyde.....101

Table 6.2. Kinetic parameters of native and modified lipases (V_{\max} ($\mu\text{mol}/\text{mg}/\text{min}$), K_M (mM) and $\eta = k_{\text{cat}}/K_M$ ($\text{M}^{-1} \text{s}^{-1}$)) calculated for the hydrolysis of <i>p</i> -nitrophenyl acetate (<i>p</i> -NPAC), <i>p</i> -nitrophenyl butyrate (<i>p</i> -NPB) and <i>p</i> -nitrophenyl octanoate (<i>p</i> -NPO) under the conditions: substrate concentration varied between 1 and 350 mM, enzyme content (1 mg), performed at 37 °C for 1 min.....	107
Table 8.1. Examples of enzymes applied for the synthesis or modification of drugs.....	139
Table 8.2. Synthetic approaches for the biosynthesis of polyesters/polyamides.....	142
Table 8.3. Chemical modification of lipases: molecules grafted, experimental conditions and practical applications (2013-2020).....	151
Table 8.4. Recent examples of novel types of nanoemulsions encapsulating hydrophobic compounds, and their fields of applications.....	159

List of Schemes

- Scheme 3.1.** Reactional scheme of methotrexate-acylglycerols conjugates synthesis. Compound **1**, methotrexate; Compounds **2a-2c** were produced using US in the presence of immobilized CALB. Compounds **2d** and **2e** were produced using US and lipase from *Thermomyces lanuginosus*. **2a** was produced using glycerol tributyrates, **2b** using glycerol trivalerate, **2c** using glycerol trihexanoate, **2d** using glycerol tristearate and **2e** using triolein.....37
- Scheme 4.1.** Reactional scheme for the oligomerization of methotrexate.....52
- Scheme 5.1.** Proposed mechanism for the PEGylation of esterases; **A)** Lysine residue of an esterase; **B)** PEG-Aldehyde; **C)** Esterase-lysine-PEG as imine intermediate; **D)** Esterase-lysine-PEG.....73
- Scheme 5.2.** Reactional scheme for the synthesis of poly(ethylene glutarate) catalysed by esterase; **A)** diethyl glutarate; **B)** ethylene glycol; **C)** poly(ethylene glutarate); **D)** ethanol.....77

Chapter I

Thesis motivation and outline

1.1. Motivation and objectives

The main goal of this thesis was to study different approaches for the encapsulation and modification/synthesis of compounds with industrial applications.

Methotrexate (MTX) is a commercial drug, currently used for the treatment of numerous illnesses, such as cancer, rheumatoid arthritis, psoriasis, multiple sclerosis, among others [1, 2]. Similarly to many other drugs, several side-effects are associated to its usage [3]. Nevertheless, given its high efficacy, the pursuit in finding alternative routes for its administration, its continuously arising among the scientific community. Given the several drawbacks associated with its usage, in this thesis, MTX was chosen as the model drug, and different approaches were undertaken for its stabilization/modification: **1) novel nanodevices** were synthesised for its encapsulation and delivery, and **2) different enzymatic approaches** were applied for the synthesis of MTX-prodrugs.

In the first approach, new nanoemulsions were developed for its encapsulation and release profile study. Nanoemulsions are applied in many of our daily products, with known applications like food, drug delivery and cosmetic fields [4]. For this reason, we produced novel sugar-based nanoformulations, composed by synthesized hydrophobic compounds, like cyclo-oligosaccharides and palmitoyl chloride. The final nanoformulations were produced by emulsification of the lipophilic macromolecules using ultrasonic energy. MTX was successfully encapsulated for controlled release and stabilization.

The second approach here studied, was the production of MTX-prodrugs. A prodrug is a version of a known active agent, modified through chemical or enzymatic process [5]. This strategy is often applied by the pharmaceutical industry for the improvement of different properties of the drugs, and/or to overcome some limitations associated to their administration, like poor aqueous solubility, insufficient oral absorption, chemical instability, toxicity, fast metabolism, etc [5]. The most common strategy applied for prodrugs production, is the synthesis of esters, through the modification of carboxylic acids or alcohols.

Regarding the formation of MTX-prodrugs, different approaches were found in the literature describing the linkage of different compounds (ex. polyethylene glycol [6-8], dextran [9], albumin [10], proline [11]) to MTX. However, no reports were found employing enzymes as catalysts for their processing. Comparing with conventional chemical approaches, enzymatic catalysis offers many synthesis advantages, like mild reaction conditions, chemo-, enantio- and regioselectivity, increased kinetic speed, etc. [12]. Moreover, they are associated to suitable and green chemistry practices. Thus, different synthetic approaches were here investigated, aiming to produce MTX

prodrugs throughout enzymatic catalysis. For this purpose, lipases (from *Candida antarctica B* and *Thermomyces lanuginosus*) were firstly used to catalyse the reactions between MTX and different non-toxic triacylglycerols and cyclodextrins, to obtain new ester-derivatives of MTX. Afterwards, the presence of both amines and carboxylic acids in its structure, lead us to evaluate its self-polymerization by a protease, α -chymotrypsin. The purpose of the study was to produce a polymeric drug, by the formation of new peptide bonds among MTX units. The enzymatic approaches herein studied would represent suitable methodologies to produce MTX-prodrugs. Considering the high potential of enzymes as catalysts for different synthesis reactions, their chemical modification is often applied to enhance their catalytic properties [13]. Different strategies can be implemented for this purpose, such as the covalent bonding of polymers [14] and small molecules [15], or the immobilization onto solid supports [13]. In this thesis, the surface modification of enzymes with a polymer and small hydrophobic compounds was investigated to improve enzymes' stability and activity. Moreover, several enzyme properties can be enhanced throughout this strategy, like thermostability, organic solvent tolerance, enantioselectivity, etc [14, 15]. Considering this, we firstly studied the PEGylation of two lipases (from *Candida antarctica B* and *Thermomyces lanuginosus*) and of one cutinase (from *Fusarium solani pis*). Later, the chemical grafting of small hydrophobic compounds (aldehydes and isothiocyanates) to lipase from *Thermomyces lanuginosus*, was performed. Besides studying the impact of the modifications on their hydrolytic activity, a practical application for the modified enzymes was investigated. In literature, it is possible to find different strategies for the chemical modification of enzymes, however, their implementation for the synthesis of valued-industrial compounds is still poorly explored. Regarding this lacuna found, the synthesis of different ester compounds using the modified enzymes was here explored. The PEGylated enzymes were evaluated for the synthesis of a polyester, poly(ethylene glutarate), and lipase TL modified with the small molecules, for the synthesis of differentiated ester products, with diverse industrial applications.

The main points of this thesis are:

- ✓ Develop new nanodevices from non-toxic compounds, for the encapsulation and release of MTX.
- ✓ Use different enzymes for the modification of MTX.
- ✓ Chemically modify enzymes and evaluate their catalytic performance in the production of industrial valued products.

1.2. Thesis outline

This thesis is divided into 8 chapters presented according to the temporal order of execution of the works. Chapter 1 describes the layout adopted, as well as the motivations behind the investigation performed. Chapters 2 to 7 are dedicated to the experimental work performed. Chapter 8 is a detailed review, which summarizes the importance and the novelty of the works here presented, comparing our findings with the data from literature, in the same field of investigation. The purpose of this final chapter was to demonstrate the major achievements obtained, which fulfilled some identified literature gaps.

The content of each chapter is summarized below:

Chapter II. Oil-based cyclo-oligosaccharide nanodevices for drug encapsulation

This chapter was dedicated to the synthesis of new hydrophobic cyclo-oligosaccharides which demonstrated oily behaviour at low temperatures. This property was explored to produce new nanoemulsions. A full characterization of their physico-chemical properties was performed, as well as the capability to encapsulate MTX. A suitable release profile was observed, showing the promising properties of these novel nanoemulsions produced.

This chapter is based on the following publication:

Jennifer Noro, Ana Loureiro, Filipa Gonçalves, Nuno G. Azoia, Seunho Jung, Carla Silva, Artur Cavaco-Paulo, Oil-based cyclo-oligosaccharide nanodevices for drug encapsulation, *Colloids and Surfaces B: Biointerfaces*, 159 (2017) 259-267.

Chapter III. Ultrasound-assisted biosynthesis of novel methotrexate-conjugates

In this work, novel methotrexate (MTX) conjugates were biosynthesized, using two different lipases: lipase from *Thermomyces lanuginosus* and immobilized lipase from *Candida antarctica B*. The drug was covalently bonded to two different types of compounds: triacylglycerols and cyclodextrins. All reactions were performed in an ultrasonic bath, which was a key factor to obtain higher yields in the production of the conjugated compounds.

This chapter is based on the following publication:

Jennifer Noro, Rui L. Reis, Artur Cavaco-Paulo, Carla Silva, Ultrasound-assisted biosynthesis of novel methotrexate-conjugates, *Ultrasonics Sonochemistry*, 48 (2018) 51-56.

Chapter IV. α -Chymotrypsin catalyses the synthesis of methotrexate oligomers

A protease, α -chymotrypsin, was explored for the self-polymerization of methotrexate by the production of new peptide bonds among substrate units. The tested enzyme was able to form oligomers up to 6 units, demonstrating capacity to polymerize non-natural substrates.

This chapter is based on the following publication:

Jennifer Noro, Tarsila G. Castro, Artur Cavaco-Paulo, Carla Silva, α -chymotrypsin catalyses the synthesis of methotrexate oligomers, *Process Biochemistry*, 98 (2020) 193-201.

Chapter V. Catalytic activation of esterases by PEGylation for polyester synthesis

The effect of PEGylation on the catalytic properties of three enzymes was explored. Two lipases (from *Candida antarctica B* and *Thermomyces lanuginosus*) and one cutinase (from *Fusarium solani pisi*) were successfully PEGylated, and an improvement or preservation of their hydrolytic activity was observed. The main focus of the work was to explore their polymerase activity in the biosynthesis of a polyester, namely, poly(ethylene glutarate). It was observed that the PEGylation of lipase TL and of the cutinase enhanced their polymerase activity, comparing to their native forms.

This chapter is based on the following publication:

Jennifer Noro, Tarsila Castro, Filipa Gonçalves, Artur Ribeiro, Artur Cavaco-Paulo, Carla Silva, Catalytic activation of esterases by PEGylation for polyester synthesis, *ChemCatChem*, 11 (2019) 2490-2499.

Chapter VI. Substrate's hydrophobicity and enzyme's modifiers play a major role on the activity of lipase from *Thermomyces lanuginosus*

The chemical modification of lipase from *Thermomyces lanuginosus* with small hydrophobic compounds (isothiocyanates and aldehydes) was performed. The impact of the modification on the lipase's activity and enzyme's conformation was extensively studied. The chemical modification with aldehydes showed to improve their hydrolytic activity against differentiated size substrates and enhance their thermostability.

This chapter is based on the following publication:

Jennifer Noro, Tarsila G. Castro, Artur Cavaco-Paulo, Carla Silva, Substrate's hydrophobicity and enzyme's modifiers play a major role on the activity of lipase from *Thermomyces lanuginosus*, *Catalysis Science & Technology*, 10 (2020) 5913-5924.

Chapter VII. Chemical modification of lipase from *Thermomyces lanuginosus* enhances transesterification and esterification activity

In this chapter, a practical application of the most active modified lipase (grafted with 4 dodecyl chains) was evaluated on transesterification and esterification reactions. A range of linear alcohols differing in chain size (methanol to eicosanol) were studied, for the transesterification of *p*-nitrophenyl palmitate and the esterification of oleic acid. It was observed that the modified lipase showed higher activity for both transesterification and esterification reactions, than the native enzyme, being this increment more pronounced for the longer alcohols studied.

This chapter is based on the following publication:

Jennifer Noro, Artur Cavaco-Paulo, Carla Silva, Chemical modification of lipase from *Thermomyces lanuginosus* enhances transesterification and esterification activity, submitted to: ACS Catalysis.

Chapter VIII. Biotechnological approaches for the synthesis, modification and stabilization of hydrophobic compounds

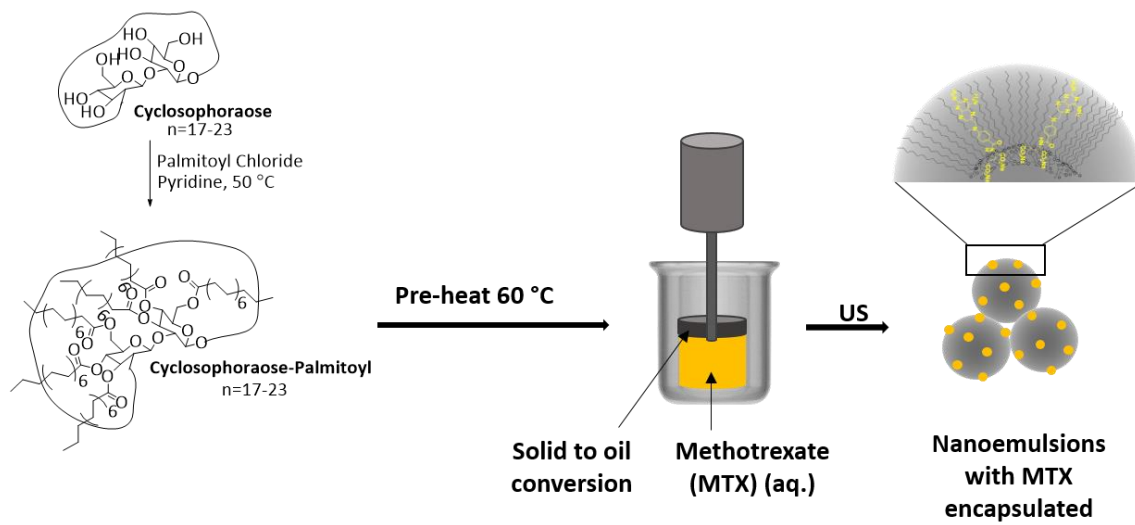
In this final chapter, a revision of the literature related with the research topics developed during the thesis were addressed. The results obtained were compared with the recent reports from literature, showing the direct impact on the investigation related with the stabilization and modification of hydrophobic compounds. The new compounds and techniques developed are beyond state-of-art, fulfilling the gaps identified in literature regarding the use of enzymes as catalysts for MTX-prodrugs and their practical application after chemical modification.

This chapter is based on the following publication:

Jennifer Noro, Artur Cavaco-Paulo, Carla Silva, Biotechnological approaches for the synthesis, modification and stabilization of hydrophobic compounds, submitted to: Critical Reviews in Biotechnology.

Chapter II

Oil-based cyclo-oligosaccharide nanodevices for drug encapsulation



Oil-based cyclo-oligosaccharide nanodevices for drug encapsulation

Abstract

New encapsulation nanodevices were synthesized by emulsification of cyclo-oligosaccharides fully substituted by hydrophobic palmitic chains. These highly hydrophobic compounds acquire oily-like behaviour at moderate temperatures (≈ 50 °C) and when submitted to ultrasounds (US) can undergo emulsification. The improved emulsifying properties of modified cyclo-oligosaccharides are suitable to produce small and narrow sized nanoemulsions with ability to encapsulate amphiphilic molecules. Both encapsulation and delivery of a therapeutic drug with amphiphilic character, methotrexate (MTX), were assessed. The physicochemical properties of the cyclo-oligosaccharide nanoemulsions containing MTX were investigated by nuclear magnetic resonance (NMR), scanning transmission electron microscopy (STEM) and dynamic light scattering (DLS). The results revealed that the modified cyclo-oligosaccharides are potential platforms for the encapsulation of bio compounds for cosmetic and pharmaceutical purposes.

This chapter is based on the following publication:

Jennifer Noro, Ana Loureiro, Filipa Gonçalves, Nuno G. Azoia, Seunho Jung, Carla Silva, Artur Cavaco-Paulo, Oil-based cyclo-oligosaccharide nanodevices for drug encapsulation, *Colloids and Surfaces B: Biointerfaces*, 159 (2017) 259-267.

2.1. Introduction

The administration of drugs with poor solubility and low rate of dissolution through different routes has been a major challenge for the pharmaceutical research. Several techniques have been attempted to drive drugs solubility, bioavailability, and dissolution properties, namely solubilisation [16, 17], cosolvency [18] and solid dispersions [19, 20]. The encapsulation of drugs into nanodevices has also been explored to overcome the unfavourable solubility and inappropriate interactions of drugs with other chemical compounds during delivery that are responsible by their toxicological characteristics [21]. Moreover, the nanodevices may protect the drug from degradation and increase selectivity of the drug modifying the pharmacokinetic and drug tissue distribution profile, which ensure a high safety and biocompatibility [21, 22]. Among various particulate systems, liposomes and nanoparticles have been applied for site specific delivery of drugs. However, they possess size dependent properties, stability, and scale-up problems. Lipid-based delivery systems and water-in-oil microemulsions have overcome the frequency of administration of certain drugs, e.g. MTX, by providing the control delivery to absorption sites but any of them was able to achieve the target or minimize the adverse side effects [23]. The encapsulation of drugs has been explored by using several other devices, namely micellar nano-networks [24], magnetic microcapsules [25], PLA-PEG-PLA nanoparticles [26], dendrimeric nanodevices [27], protein nanoemulsions [2, 28] among others. Still, some of them showed an almost completely release of the drug after one day [24, 25]. Cyclo-oligosaccharides complexation has been presented as a promising strategy to tackle the mentioned formulation issues. Their ability to form inclusion complexes with a wide variety of hydrophobic compounds provide significant advantages related with changes of the physicochemical and biological properties of the guest molecules. The complexation can also provide protection of the component against light and oxidation, its solubilisation, handling improvement and stability [29]. Cyclophoraoses (Cys) are unbranched cyclic β -1,2-D-glucans containing 17-23 glucose residues produced by *Rhizobium* and *Agrobacterium* species both intracellularly and extracellularly [30]. The targeting of non-polar chemicals like ergosterol, luteolin, vitamin D3 and naproxen has been reported as Cys complexation examples [31, 32]. A flexible backbone structure with doughnut-like ring shape is attributed to Cys and is responsible for the atypical induced-fit type complexation with hydrophobic molecules. Besides complexation systems, Cys can also be applied as a novel biosourced saccharide catalyst for chemical reactions as reported by Dindulkar *et al.* [33] They reported the use of microbial Cys for the synthesis of therapeutically important versatile indolyl 4*H*-chromenes

via a one pot three-component Knoevenagel–Michael addition–cyclization reaction of salicylaldehyde, 1,3-cyclohexanedione/dimedone, and indoles in water under neutral conditions. The chemical modification of Cys has been also assessed by Kim *et al.*, to increase its hydrophobicity [34]. Their studies revealed the improvement of the solubility of insoluble flavonoids, comparing with the non-modified Cys [34]. They also described a new pentacosadiynoyl cyclosophoraose (P-Cys) synthesized using a biosourced cyclo-oligosaccharide with intrinsic complexation capacity [30]. Their results indicated that P-Cys is a useful potential platform for the encapsulating emulsification of bioactive molecules for cosmetic and pharmaceutical applications. The main aims of this study were firstly to chemically modify the cyclo-oligosaccharides (Cys, β -cyclodextrin (CD) and γ -CD) by reaction of the hydroxyl groups with an hydrophobic compound, palmitoyl chloride (PAL-Cl), and to produce cyclo-oligosaccharide-PAL-based nanoemulsions via ultrasound-assisted methodology. This methodology has been previously exploited by Silva *et al.* [35] and Loureiro *et al.* [28]. Microspheres of bovine serum albumin (BSA) and silk fibroin were produced by applying ultrasound in a biphasic system consisting of an aqueous protein solution and an organic solvent. The protein microspheres were dispersed in an aqueous media where the protein remains at the interface covering the organic solvent. These nanodevices can improve the solubility of hydrophobic drugs encapsulated in the organic phase of the particles. The modified Cys hold typical fusion properties (melting point of around 50 °C) which it turns powder into a viscous liquid. Taking advantage of this phase-change, nanoemulsions of Cys-PAL and Cys-PAL/BSA were produced applying ultrasound in a biphasic system consisting of an aqueous solution (BSA/buffer) and an organic phase (Cys-PAL). The overall physicochemical and biological characterizations of developed nanoemulsions were assessed. A comparison with other cyclo-oligosaccharides, namely β - and γ -CD was performed. MTX was used as a model guest molecule to test the entrapment ability of the developed nanodevices. The efficiency of entrapment and the drug release over time were evaluated by fluorescence microscopy.

2.2. Materials and methods

2.2.1. Materials

All compounds were purchased from Sigma-Aldrich or TCI chemicals, and used without further purifications. Column chromatography was made using silica gel 60Å, with particle size of 70-200 μm as stationary phase, and ethyl acetate, chloroform or ethanol as mobile phase for the separation of the components. TLC plates (silica gel 60 F₂₅₄) were revealed under a UV lamp.

Human skin fibroblasts (BJ5ta cell line) (ATCC, CRL-4001) were obtained from American Type Culture Collection (LGC Standards, UK) and all culture media and supplements were purchased from Sigma-Aldrich. T75 flasks and 96-well tissue culture polystyrene plates were obtained from TPP, Switzerland. MTS assay was acquired from Promega, USA. MTX sodium salt was purchased from TevaGuard pharmaceutical.

2.2.2. Isolation of Cyclosophoraose

Cys (cyclic β -1,2 glucans) was isolated from *Rhizobium leguminosarum* biovar *viciae* VF39 following the procedures found in the literature [36, 37]. MALDI-TOF and NMR techniques were applied to confirm the structure and the average molecular weight.

2.2.3. Synthesis of modified cyclo-oligosaccharides

The modified cyclo-oligosaccharides were all synthesized using a similar procedure. Briefly, to a solution of cyclo-oligosaccharide (84-125 mg, 0.027-0.106 mmol) in dry pyridine (4-5 mL) under nitrogen atmosphere, was dropped the PAL-Cl (0.5-1.0 mL, 1.65-3.30 mmol) using a water bath at 50 °C. The mixture was stirred overnight at the same temperature. The solvent was removed by co-evaporation with toluene in a rotary evaporator. The formed solid was further purified by column chromatography to obtain the pure product (0.35-0.48 g, η = 60.4-74.9 %).

Cys (84 mg, 0.027 mmol); PAL-Cl (0.5 mL, 1.65 mmol); Dry pyridine (5 mL); 50 °C; overnight. Column chromatography 50 % CHCl₃/50 % AcOEt. Beige solid (0.35 g, 0.020 mmol, 74.9 %). Melting point= 48-50 °C (Gallenkamp apparatus). δ_H (CDCl₃): 0.88 (t, J = 6.8 Hz), 1.28 (br s), 1.63 (m), 2.35 (t, J = 7.6 Hz), 3.0-5.5 (br s) ppm. MALDI-TOF 20045 m/z.

β -CD (120 mg, 0.106 mmol); PAL-Cl (1 mL, 3.30 mmol); Dry pyridine (4 mL); 50 °C; overnight. Column chromatography CHCl₃/EtOH (6:1). Beige solid (0.392 g, 0.064 mmol, 60.4 %). Melting point= 44-46 °C (Gallenkamp apparatus). δ_H (CDCl₃): 0.88 (t, J = 6.8 Hz), 1.25 (br s), 1.62 (m), 2.34 (m), 3.49 (m), 3.97 (m), 4.10 (m), 4.51 (m), 4.95 (m) ppm.

γ -CD (125 mg, 0.096 mmol); PAL-Cl (0.9 mL, 2.31 mmol); Dry pyridine (5 mL); 50 °C; overnight. Column chromatography 50 % CHCl₃/50 % AcOEt. Beige solid (0.48 g, 0.068 mmol, 70.7 %). Melting point= 49-50 °C (Gallenkamp apparatus). δ_H (CDCl₃): 0.89 (t, J = 6.8 Hz), 1.31 (br s), 1.63 (m), 2.36 (m), 3.50 (m), 3.87 (m), 4.01 (m), 4.14 (m), 4.48 (m), 4.90 (m), 5.03 (m) ppm.

2.2.4. Nuclear Magnetic Resonance spectroscopy (NMR)

^1H and ^{13}C NMR spectroscopy were performed using a Bruker Avance III 400 (400 MHz for ^1H and 100 MHz for ^{13}C). CDCl_3 , DMSO-d_6 or D_2O were used as deuterated solvents, using the peak solvent as internal reference. Multiplicities are indicated as: t as triplet, br s as broad singlet and m as multiplet.

2.2.5. Matrix-Assisted Laser Desorption/Ionization Time-of-Flight (MALDI-TOF)

MALDI-TOF mass spectra were acquired on a Bruker Autoflex Speed instrument (Bruker Daltonics GmbH) equipped with a 337 nm nitrogen laser. The matrix solution for the measurements was prepared by dissolving a saturated solution of 2,5-dihydroxybenzoic acid (DHB) in 100 % ethanol. Samples were spotted onto a ground steel target plate (Bruker part n° 209519) and analysed in the linear positive mode using factory-configured instrument parameters suitable for a 10-30 kDa m/z range (ion source 1: 19,5kV; ion source 2: 18,3kV). Time delay between laser pulse and ion extraction was set to 130 ns, and the laser frequency was 25 Hz.

2.2.6. Cyclo-oligosaccharide-palmitoyl conjugate nanoemulsions

The nanoemulsions composed of cyclo-oligosaccharide (alone or in the presence of BSA) were produced by application of US. The mixtures containing the cyclo-oligosaccharide (alone or in presence of BSA) (4mL) in phosphate buffer saline (PBS) 10 mM at pH= 7.4 were previously submitted to a pre-heat at 60 °C for 10 min. Then, the mixture was subjected to US using a high-intensity ultrasonic horn (20 KHz Sonics & Materials Vibracell CV 33, 3 mm diameter titanium microtip) positioned at the middle of the mixture. The ultrasonication was performed at 60 °C for 3 min with an amplitude of 40 %. Control samples with unmodified oligosaccharides were also performed using the same conditions.

2.2.7. Dynamic Light Scattering (DLS)

The mean diameter (nm), polydispersity index (PDI) and zeta-potential (mV) of the nanoemulsions were measured in a Zetasizer Nano ZS (Malvern Instruments) at 25 °C. Prior to DLS measurements, the samples were diluted with PBS at pH 7.4 (for size) and with ultrapure water (for zeta-potential). In both cases, a dilution of 5x was made, followed by a filtration using 0.45 μm filters, (Spartan™ 30 RC, Whatman, GE Healthcare). All measurements were read in triplicate, being the results described as mean \pm standard deviation.

2.2.8. Nanoparticle Tracking Analysis (NTA)

NTA was used to access quantitatively the obtained nanoemulsions. The experiments were performed using a NanoSight NS500 instrument (Salisbury, UK). This system includes a charge coupled device camera that allows visualization and tracking Brownian motion of laser-illuminated particles in suspension. The measurements were made at room temperature and each video sequence was captured over 60 sec. The samples were 10x diluted with water and filtered (Millipore filters with pore size of 0.45 μm) and then injected into the system.

2.2.9. Differential Scanning Calorimetry (DSC)

All measurements were conducted on a power-compensated DSC instrument (DSC 6000 Perkin Elmer) with a nitrogen flux of 20 mL/min, using stainless steel capsules in the temperature range of 20-100 $^{\circ}\text{C}$ (heating rate: 10 $^{\circ}\text{C}/\text{min}$, powder sample weight: 3-7 mg). The DSC device was calibrated using indium and zinc, both of high purity. The samples were stored at selected levels of humidity (relative humidity of 45 %) and temperature (20–22 $^{\circ}\text{C}$) for 24 h prior to the analyses and each sample was measured at least two times, in order to validate the results.

2.2.10. Scanning Transmission Electron Microscopy (STEM)

STEM was performed with a NOVA Nano SEM 200 FEI microscope. The carbon coated copper grids (400 meshes, 3 mm diameter) were placed in contact with the nanoemulsions and the excess of solvent was instantly absorbed by a filter paper. Another set of samples was prepared by the same way with the addition of a final staining with uranyl acetate. For this, the grids were placed on the top of a drop of uranyl acetate (0.2 % v/w) for 5 min. The excess of the liquid was removed as described above and the grids were washed with water and dried at room temperature.

2.2.11. Molecular Dynamics Simulations

The simulations were performed with the software package GROMACS, using Martini force-field [38]. The system size was chosen according to the minimum image convention taking into account a cut-off of 1.2 nm. The bonds lengths were con-strained with LINCS [39]. Non-bonded interactions were calculated using a twin-range method, with short- and long-range cut-offs of 0.9–1.2 nm, respectively. Neighbour searching was carried out up to 1.2 nm and updated every ten steps. A time step of integration of 5 fs was used. A reaction field correction for the electrostatic interactions was applied using a dielectric constant of 15. Pressure control was implemented using the

Berendsen barostat [40], with a reference pressure of 1 bar, 3.0 ps of relaxation time and isothermal compressibility of $3.0 \times 10^{-5} \text{bar}^{-1}$. Temperature control was set using the Berendsen thermostat [40] at 520 K. Each component of the system was included in separated heat bath, with temperatures coupling constants of 0.30 ps. Two replica simulations of 15 ns in length were carried out using different initial velocities taken from a Maxwell–Boltzman distribution at 420 K. Initially the components were distributed uniformly through the simulation box and allowed to interact freely during the simulation.

2.2.12. Cellular viability assay

2.2.12.1. Cells and culture conditions

BJ5ta cell line, an adherent cell line, was grown in T75 flasks using a medium composed by 4 parts of Dulbecco's Modified Eagle's Medium and 1 part of M199 Medium supplemented with 2 mM L-glutamine; 4.5 g/L glucose; 1.5 g/L sodium bicarbonate; 10 % (v/v) of fetal bovine serum; 1 % (v/v) of penicillin/streptomycin solution; 10 µg/ml of hygromycin B. Exponentially growing culture was maintained in a humidified atmosphere of 5 % CO₂ in air at 37 °C.

2.2.12.2. Cell viability assay

Cell viability was studied using the Promega CellTiter 96[®] AQueous Non-Radioactive Cell Proliferation (MTS) assay. BJ5ta cells were seeded in 96-well tissue culture polystyrene plates at a density of 1×10^4 cells/well and incubated overnight to promote cell adhesion. The cells were incubated with different concentrations of nanoparticles (from 0.0625 mg/mL up to 1 mg/mL). The concentrations of nanoemulsions for the application in cells were calculated based in the concentration of cyclo-oligosaccharides in the initial formulations (5 mg/mL). The nanoemulsions were incubated with cells for 24, 48 and 72 h. A MTS mixture was then added and the cells were further incubated for 4 h at 37 °C. After this period, the plates were placed on Synergy Mx Multi-Mode Reader from BioTek (USA) and the absorbance of the formazan product was read at 490 nm. Cell viability was expressed as a percentage relative to the negative control (untreated control cells). Two independent experiments were made.

2.2.13. Stability of nanoemulsions in the presence of lipase

The disruption of the produced nanoemulsions was assessed by incubation with a lipase. For this, 1 mL of each sample was transferred to an assay tube and incubated with lipase from

Thermomyces Lanuginosus (activity: 407 $\mu\text{mol}/\text{mL}/\text{min}$) (50 μL) at 40 °C in a water bath at 60 rpm for 48 h. Aliquots were taken at different time points to measure the size of nanoemulsions and confirm disruption. Prior to DLS measurement the samples were diluted (5x) and filtered with 0.45 μm filter. The final disruption of nanoemulsions was evaluated after 48 h of incubation by extraction of the samples with CHCl_3 (3x10 mL). The organic layer was dried over MgSO_4 and filtered. The solution was evaporated using a rotary evaporator. The NMR spectra was acquired firstly in DMSO-d_6 , to detect the presence of palmitic acid. Afterwards, the NMR was acquired in CDCl_3 to evaluate the percentage of nanoemulsions ester cleavage.

2.2.14. Encapsulation and release of methotrexate

The ability of the developed nanoemulsions to encapsulate MTX was evaluated. The encapsulation was performed by including 10 mg/mL of MTX in the aqueous phase of nanoemulsions composition. The final nanodevices were produced as previously described in section 2.2.6. The encapsulation efficiency was verified by NMR spectroscopy by evaluation of the interaction between MTX and the modified cyclo-oligosaccharides. This evaluation was assessed by the chemical shift analysis comparing to the MTX in the free form. The MTX release profile was evaluated by placing the nanoemulsions containing MTX in mini dialysis tubes with 1 kDa cut-off (GE Healthcare) against PBS (1 mM). Aliquots were taken at different time points and read in a 96-quartz microplate at 303 nm for 72 h. After this period, the PBS was replaced, and the release proceed until no more MTX was detected (192 h).

2.3. Results and discussion

2.3.1. Synthesis of hydrophobic cyclo-oligosaccharides by conjugation with palmitoyl chloride

The synthesis of cyclo-oligosaccharides-PAL conjugates was carried out as previously described (**Figure 2.1**). A fully substitution of the hydroxyl groups of cyclo-oligosaccharides by palmitoyl (PAL) was accomplished by performing the reaction at 50 °C, overnight in the presence of pyridine. The isolation and purification of the final products was assessed using a chromatography column to separate the pyridinium chloride sub-product. High yields of product synthesis were obtained (η = 60.4-74.9 %).

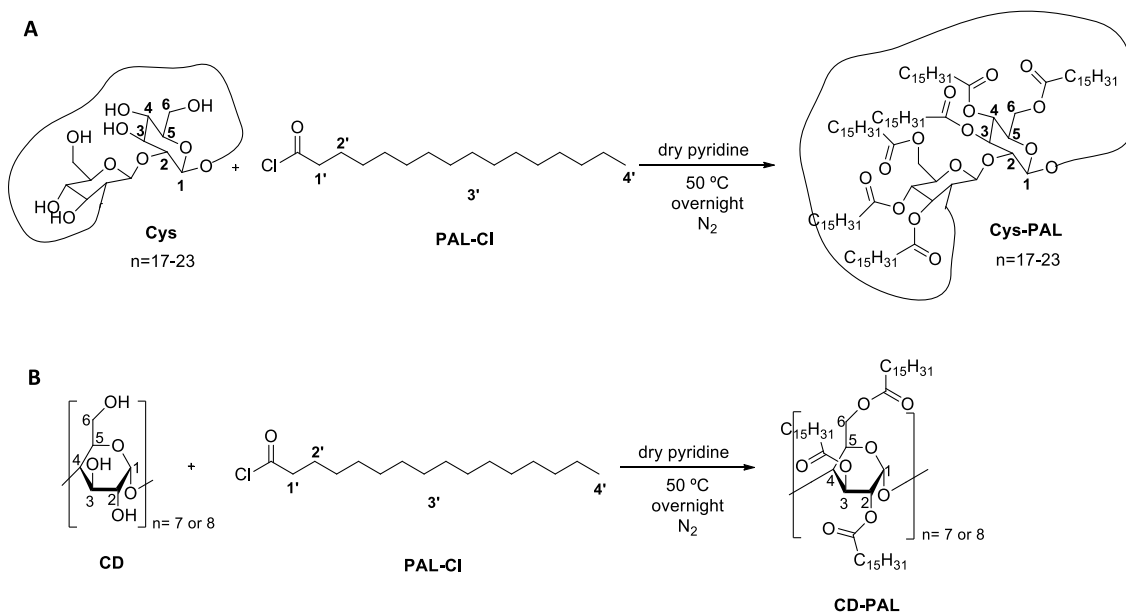


Figure 2.1. Synthesis of modified cyclo-oligosaccharides: **A)** reactional scheme of the conjugation of PAL-Cl with Cys; **B)** reactional scheme of the conjugation of PAL-Cl with β -CD ($n=7$) and γ -CD ($n=8$).

The molecular weight of modified cyclo-oligosaccharides was determined by MALDI-TOF mass spectrometry (**Figure 2.2**). Based on the degree of substitution (DS) of the cyclo-oligosaccharides, the ionization patterns of synthesized cyclo-oligosaccharides-PAL were determined. Cys has a number average molecular weight (M_n) of 3134 and Cys-PAL shows the substituted mass obtained according to the corresponding DS (23) conjugated with 68 PAL units. The molecular ions of β -CD-PAL were represented as [DS7 + 11 – 17 PAL], with signals at m/z 3799, 4016, 4253, 4493, 4733, 4963 and 5200. The representative ions of γ -CD-PAL were represented as [DS8 + 13–20 PAL], with signals at m/z 4422, 4660, 4900, 5138, 5378, 5614, 5853 and 6090. The mass difference between cyclo-oligosaccharides and cyclo-oligosaccharides-PAL was m/z 240 attributed to the palmitoyl chain.

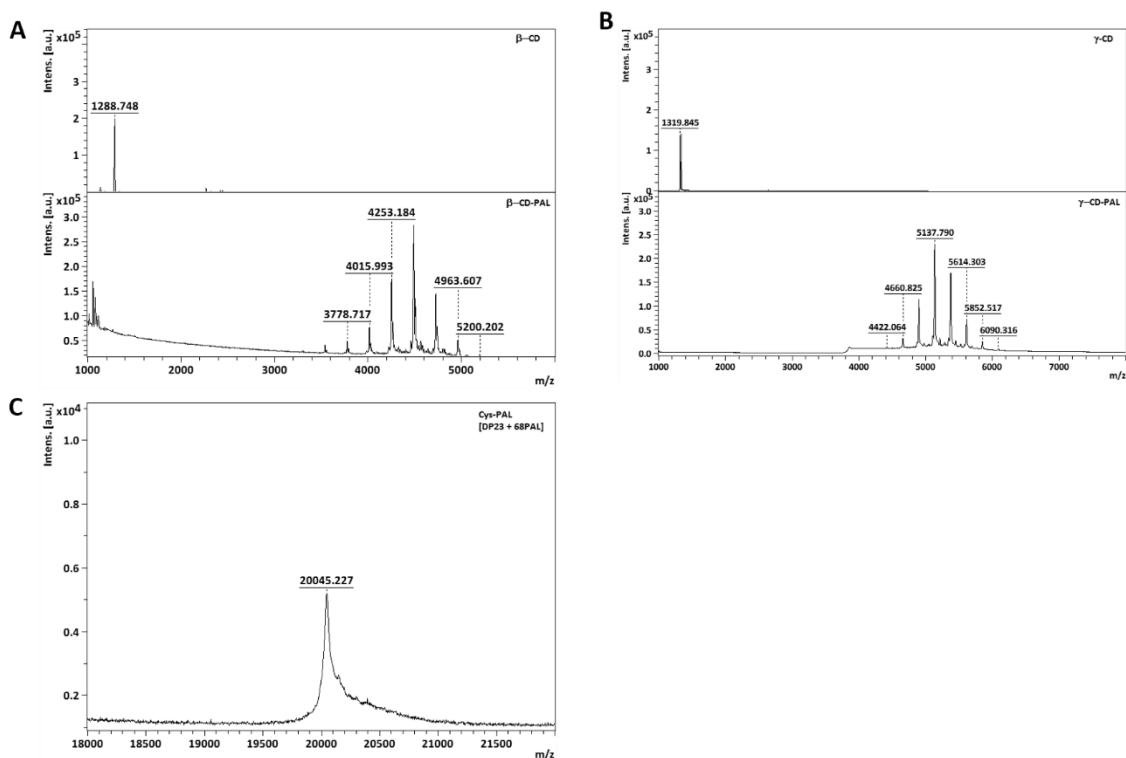


Figure 2.2. Positive ion MALDI-TOF spectrum of: **A)** β -CD-PAL, **B)** γ -CD-PAL and **C)** Cys-PAL on DHB.

The structures of the modified cyclo-oligosaccharides were elucidated recording the ^1H NMR in CDCl_3 (**Figure 2.3**).

The presence of the palmitic chain was confirmed by the peaks assigned as 1' to 4'. Peak 4' was attributed to the terminal CH_3 of the palmitic chain, arising as a triplet near δ_{H} 0.9 ppm in all cases. 1' and 2' were the CH_2 next the carbonyl group respectively, being 1' a triplet or multiplet (δ_{H} 2.34, 2.35 or 2.36 ppm), and 2' a multiplet (δ_{H} 1.62 or 1.63 ppm). The chain of palmitoyl appeared as a multiplet numbered as 3' (δ_{H} 1.25, 1.28 or 1.31 ppm). In the β -CD and γ -CD it was possible to calculate the degree of substitution regarding the relation between one of the peaks of the oligosaccharides and the CH_3 of the palmitoyl. This confirmed the full substitution of both compounds by palmitic chains. For Cys-PAL it was possible to observe that all C-H of the oligosaccharide scaffold appeared as a broad singlet between δ_{H} 3.0 and 5.5 ppm, hindering the calculation of the substitution degree. Considering β - and γ -CD, the C-H peaks of the oligosaccharide units were observed as multiplet signals in both cases (β -CD between δ_{H} 3.49 to 4.95 ppm; γ -CD between δ_{H} 3.50 to 5.03 ppm).

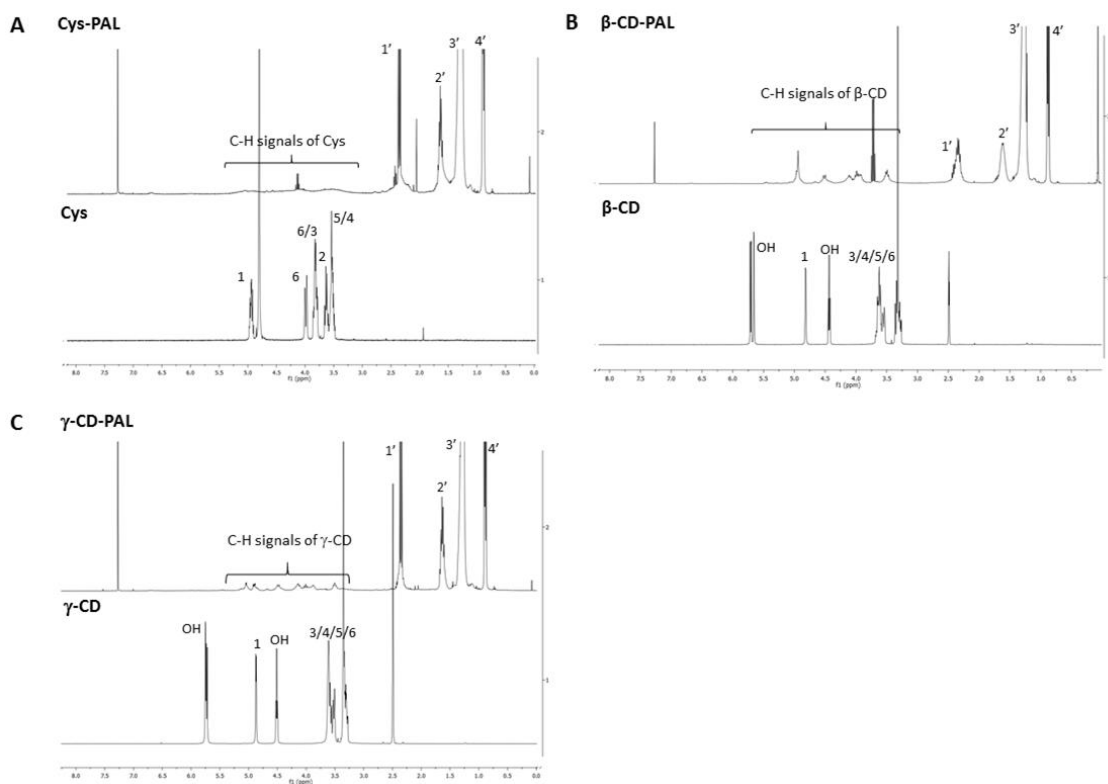


Figure 2.3. ^1H NMR spectra of: **A)** Cys and Cys-PAL; **B)** β -CD and β -CD-PAL and **C)** γ -CD and γ -CD-PAL.

2.3.2. Cyclo-oligosaccharides-palmitoyl emulsification ability

The formation of narrow sized and stable nanoemulsions containing BSA/*n*-dodecane by ultrasonication was previously investigated by Silva *et al.* [35]. They postulate that in an aqueous phase, proteins form stable 3D structures based on the balance between the outer hydrophilic segments covering the inner hydrophobic parts in a conformation of minimal energy. When high shear forces like US are applied to the biphasic system of water/oil, the proteins tend to adapt their structure and migrate to the interface. Depending on the protein structure, its adaptation may include its 3D modification [35]. In all cases, the protein seems to form a shell with hydrophobic characteristics near the organic solvent and hydrophilic properties near water. The protein microspheres were dispersed in the aqueous media whereas the protein remains at the interface covering the organic solvent [35]. Herein, we present a similar approach for the production of nanoemulsions of cyclo-oligosaccharides however excluding the organic solvent from the system. Experiments containing different concentrations of BSA on the nanoemulsions composition were also performed since this protein is a well-known material for nanoparticles production and drug encapsulation.

The emulsification ability of modified cyclo-oligosaccharides was investigated through the formation of emulsions in cyclo-oligosaccharide/water mixture systems. The modified cyclo-oligosaccharides were in a powder form and when heated at 60 °C (m.p.= 43-60 °C) acquire oily-like behaviour rendering to the system self-assembly capacity. We found that the oil-in-water nanoemulsions formed by cyclo-oligosaccharide/water mixtures exhibit remarkable stability against coalescence with the exception of β -CD-PAL (β -cyclodextrin-palmitoyl conjugate). All of these observations suggest an increased self-assembly ability of the cyclo-oligosaccharide containing more than 7 sugar units, which was incremented by the conjugation with the hydrophobic palmitoyl units. The self-assembly properties can be attributed to the characteristic flexible conformation of cyclo-oligosaccharides applied. It is noteworthy to highlight that with unmodified oligosaccharides no formation of nanoemulsions was observed (**Figure 2.4**). Their entrapment ability can be combined with the interaction of the conjugated hydrophobic tail, where the emulsification and encapsulation are differentiated depending on the host structures. The developed devices are good candidates for the encapsulation of amphiphilic substances.

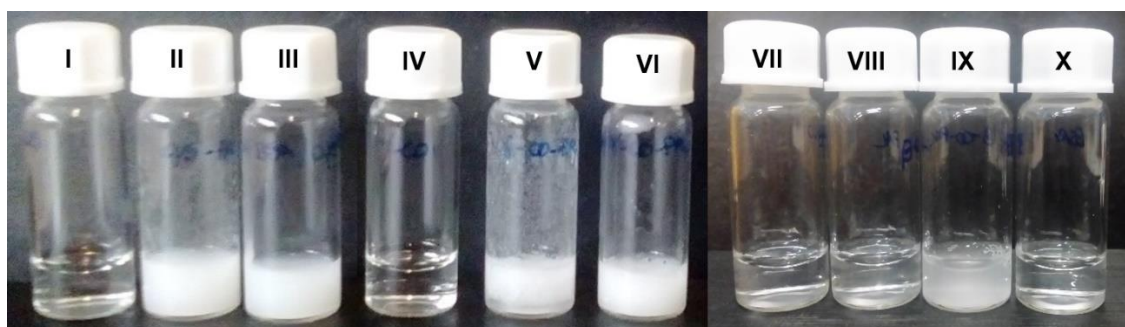


Figure 2.4. Formulations photographs after emulsification with US: I) Cys (5 mg/mL); II) Cys-PAL (5 mg/mL); III) BSA (10 mg/mL) + Cys-PAL (5 mg/mL); IV) γ -CD (5 mg/mL); V) γ -CD-PAL (5 mg/mL); VI) BSA (10 mg/mL) + γ -CD-PAL (5 mg/mL); VII) β -CD (5 mg/mL); VIII) β -CD-PAL (5 mg/mL); IX) BSA (10 mg/mL) + β -CD-PAL (5 mg/mL) and X) BSA (10 mg/mL).

Molecular dynamics simulations, used herein to better understand the interactions between all the components of the nanoemulsions, corroborate our assumptions confirming the ability of Cys-PAL and BSA-Cys-PAL to undergo emulsification. From the data obtained it was evident the interaction between the hydrophobic part of BSA and the oily-like phase of Cys-PAL, as it can be depicted in **Figure 2.5** (III and IV). These results also allow us to speculate that this behaviour would decrease the hydrophobic interactions between Cys-PAL and BSA, maybe contributing for the size reduction

when BSA was present in the nanoemulsions. The auto aggregation properties of Cys-PAL can justify the bigger sizes observed by DLS (**Figure 2.7**).

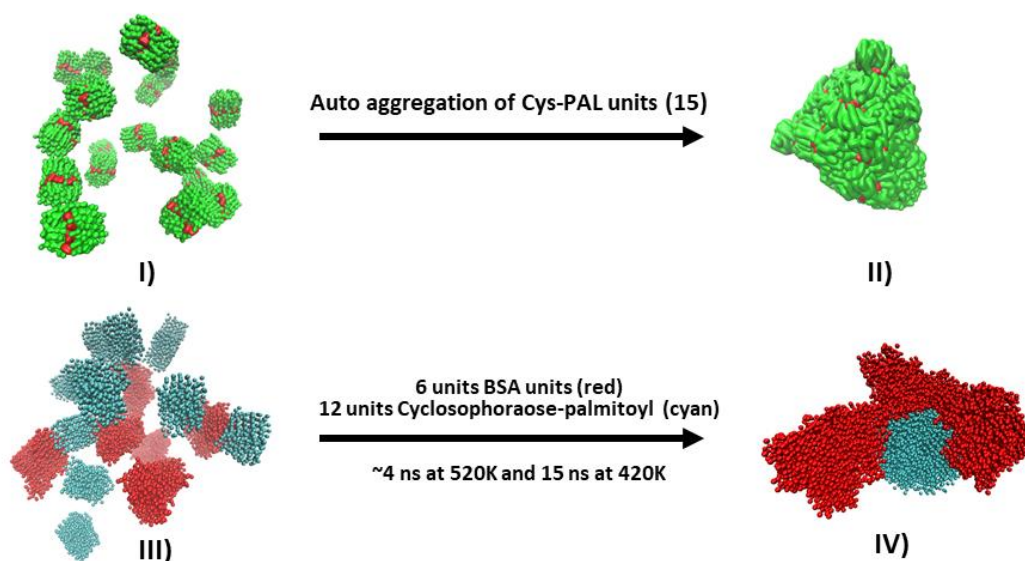


Figure 2.5. Molecular dynamic simulations of Cys-PAL auto aggregation: I) cyclophoraose (red) surrounded by covalently bonded palmitic chains (green), before aggregation, II) 15 units of Cys-PAL self-aggregated; and BSA-Cys-PAL aggregation: III) BSA-Cys-PAL before nanoemulsion simulation, showing 6 units of BSA (in red) and 12 units of Cys-PAL (in cyan), IV) BSA-Cys-PAL after nanoemulsion simulation (one unit of Cys-PAL surrounded by several units of BSA).

2.3.3. Microscopic observation

The morphology and structure of the developed nanoemulsions (Cys-PAL, β -CD-PAL, γ -CD-PAL, BSA-Cys-PAL, BSA- β -CD-PAL and BSA- γ -CD-PAL) were investigated by STEM to assess the form and size of emulsion droplets (**Figure 2.6**). All the nanoemulsions present homogeneous and regular aspect with particle size between 100-200 nm, with the exception of β -CD-PAL and BSA- β -CD-PAL (data not shown). These samples present much lower particle size compared to the others and by eye visualization a low stability against flocculation and coalescence was observed. The amount of sugar units played here a limiting role by hindering the nanoemulsions formation when β -CD (7 sugar units) was used. For further experiments, we excluded these samples from the studies. The results also demonstrate that Cys-PAL, γ -CD-PAL, BSA-Cys-PAL and BSA- γ -CD-PAL were successfully converted into spherical and smooth nanoemulsions by using high intensity ultrasound. This morphology is expected to offer high encapsulation potential as well as high

release performance and drug protection, providing the minimum contact with the aqueous environment [35].

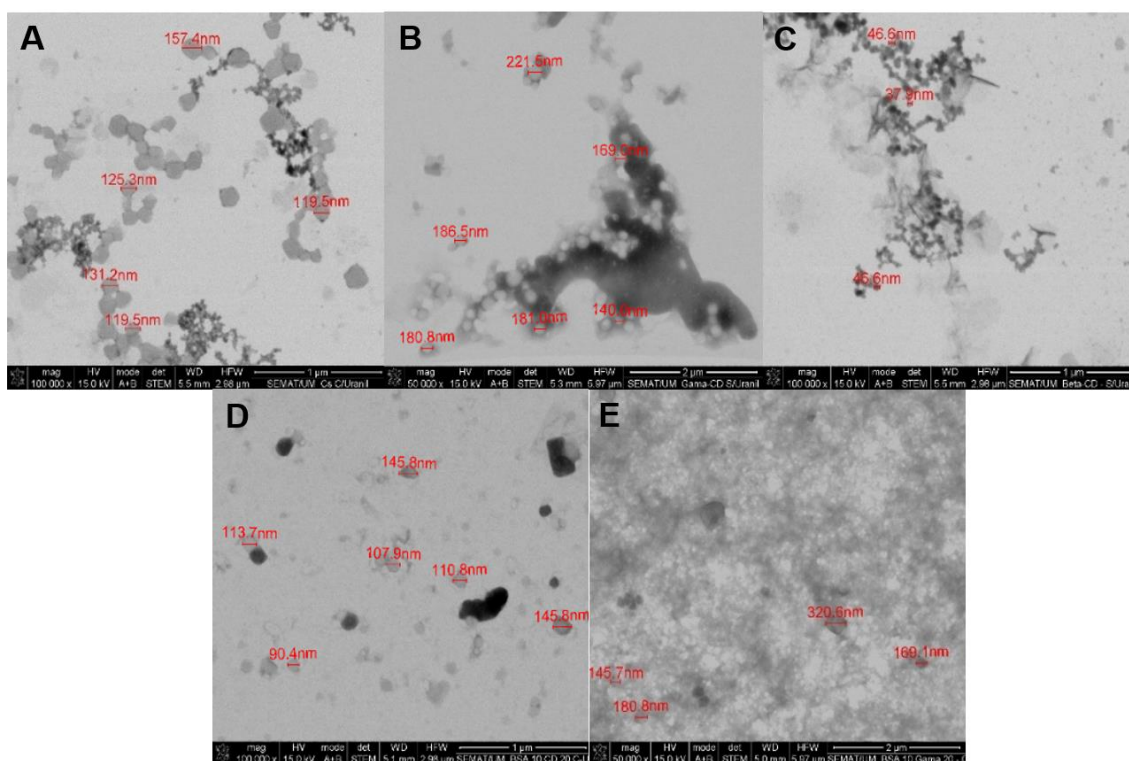


Figure 2.6. STEM images of nanoemulsions: **A)** Cys-PAL (5 mg/mL) (stained with uranyl acetate); **B)** γ -CD-PAL (5mg/mL); **C)** β -CD-PAL (5 mg/mL); **D)** BSA (10 mg/mL) + Cys-PAL (5 mg/mL) (stained with uranyl acetate); **E)** BSA (10 mg/mL) + γ -CD-PAL (5 mg/mL) (stained with uranyl acetate).

2.3.4. Nanoemulsions stability over time

The relative homogeneity of the developed nanoemulsions was further investigated by DLS analysis. **Figure 2.7** presents the mean size and PDI of samples at the first day of production and after 60 days of storage at 4 °C. All the formulations presented narrow sized distribution between 100-200 nm in diameter with low PDI (0.1-0.3) remaining stable in nanoemulsions state at least for 60 days of storage at 4 °C. Even though the values of size slightly changed along time, the PDI values remained highly stable, which is a good indicator for future applications. The zeta-potential is an important parameter in nanoemulsions characterization which allows to predict their stability over time. Long term stability of produced nanoemulsions has been verified, which was in accordance with the zeta-potential data obtained. The nanoparticles were highly negatively charged indicating high repulsive forces with low probability of agglomeration. Cys-PAL and γ -CD-PAL presented

similar zeta-potential values (≈ -40 mV) while BSA-Cys-PAL and BSA- γ -PAL showed zeta-values of around -20 mV attributed to the complexation of the cyclo-oligosaccharides with the protein. After storage for 60 days at 4 °C the surface charge of nanodroplets remained highly negative rendering high stability to the developed emulsions.

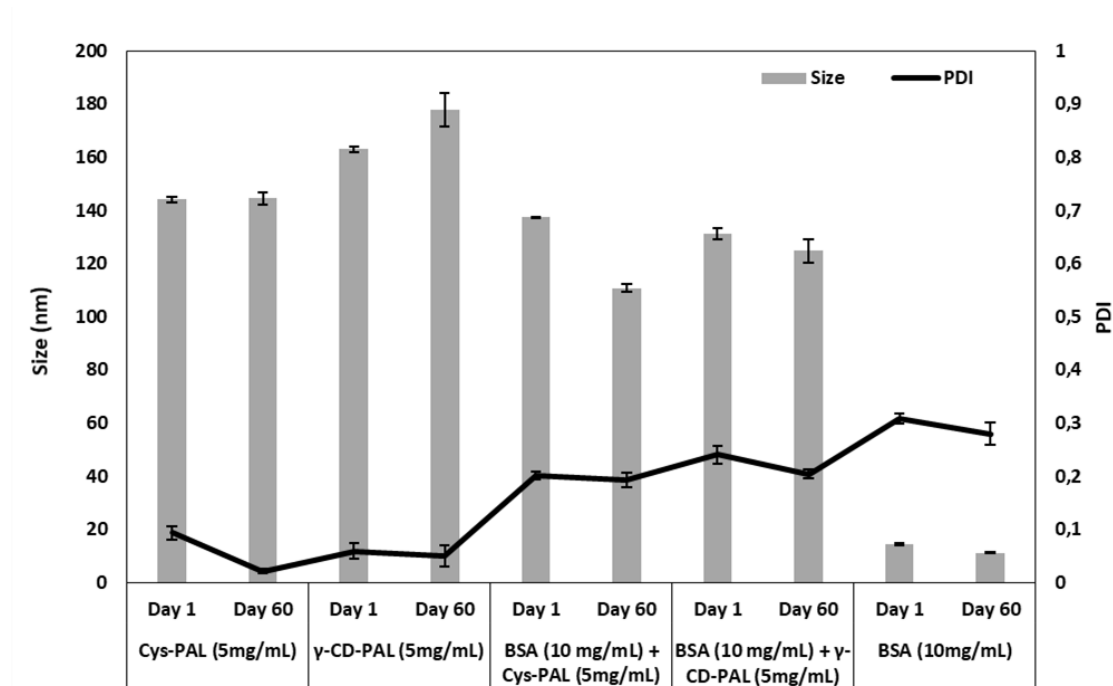


Figure 2.7. Stability (size and PDI) of nanoemulsions during storage at 4 °C for 60 days (values are the mean \pm SD of 3 independent experiments).

The formulations containing BSA in their composition presented the lowest size values and the highest PDI. The size observed might be explained by the presence of the protein which is believed to form a shell with hydrophobic characteristics near the oily-like cyclo-oligosaccharides and hydrophilic properties near water. The PDI observed might be related with the yield of nanoemulsions formation. While samples containing only cyclo-oligosaccharides present nanoemulsions formation yields very close to 100 %, samples containing BSA might contain protein that do not contribute to the nanodroplets formation, increasing the PDI measured by DLS. These results demonstrate that the cyclo-oligosaccharides-PAL seem to be an effective carbohydrate-based emulsifier. The high emulsion stability related with the low flocculation and/or coalescence obtained suggests many possibilities of uses as molecular devices for the development of cosmetic and/or pharmaceutical products with a long shelf life.

The size diameter of nanodroplets was also evaluated by NTA and the results were compared with the values obtained by DLS (**Table 2.1**). NTA, besides giving information about nanoemulsions concentration allowed us to eliminate the influence of small amounts of reagents that did not participate in the nanodroplets formation. The mean size diameter data obtained by both techniques follow the same tendency. Nanoemulsions containing only the modified cyclo-oligosaccharide show values of size diameter of 150-170 nm on both techniques. The same behaviour was observed for the samples containing BSA in their composition which demonstrate higher mean size values observed by NTA. Both techniques reveal only one peak, indicating the monodisperse behaviour. NTA analysis allowed to quantify the nanodroplets concentration on each sample. Similar concentration of particles per mL were measured for both Cys and γ -CD modified cyclo-oligosaccharides. From all the samples tested, the nanoemulsions containing BSA/Cys-PAL showed the highest concentration of particles after emulsification. The lowest particle concentration was observed for samples containing BSA- γ -CD-PAL.

Table 2.1. Mean size diameter (nm) and size distribution measured by DLS and NTA (values are the mean \pm SD of 3 independent experiments)

Nanoemulsions	DLS		NTA		
	Z-average (nm)	PDI	Mean (nm)	SD	Conc. particles (particles/mL)
Cys-PAL (5mg/mL)	144.1 \pm 1.05	0.093 \pm 0.01	151.5 \pm 0.71	52.5 \pm 3.5	6.29 \pm 6.3 (E9)
γ -CD-PAL (5mg/mL)	162.9 \pm 1.19	0.059 \pm 0.01	157 \pm 14.1	65 \pm 9.9	8.45 \pm 2.9 (E9)
BSA (10mg/mL)-Cys-PAL (5mg/mL)	137.4 \pm 0.23	0.201 \pm 0.01	173.5 \pm 3.5	52 \pm 4.2	11.3 \pm 0.02 (E9)
BSA (10mg/mL)- γ -CD-PAL (5mg/mL)	131.2 \pm 1.97	0.240 \pm 0.01	182 \pm 7.1	47.5 \pm 9.2	1.91 \pm 1.1 (E9)

2.3.5. Cytotoxicity of nanoemulsions

The effect of Cys-PAL (5 mg/mL), γ -CD-PAL (5 mg/mL), BSA (10 mg/mL)-Cys-PAL (5 mg/mL) and BSA (10 mg/mL)- γ -CD-PAL (5 mg/mL) on the viability of human BJ5ta cells was evaluated by the MTS assay. **Figure 2.8** shows BJ5ta cell viability in the presence of different concentrations of nanoemulsions and of DMSO at 30 % (v/v), as negative control. The results demonstrated that the nanoemulsions containing the modified cyclo-oligosaccharides do not induce cytotoxicity in cells after 72 h of contact even at the highest concentration (1 mg/mL). Nanoemulsions containing BSA induced some cytotoxicity, but only for the highest concentration tested (1 mg/mL). These results

indicate that modified cyclo-oligosaccharides have potential as biocompatible encapsulating emulsifiers for further applications in pharmaceuticals, foods or cosmetics.

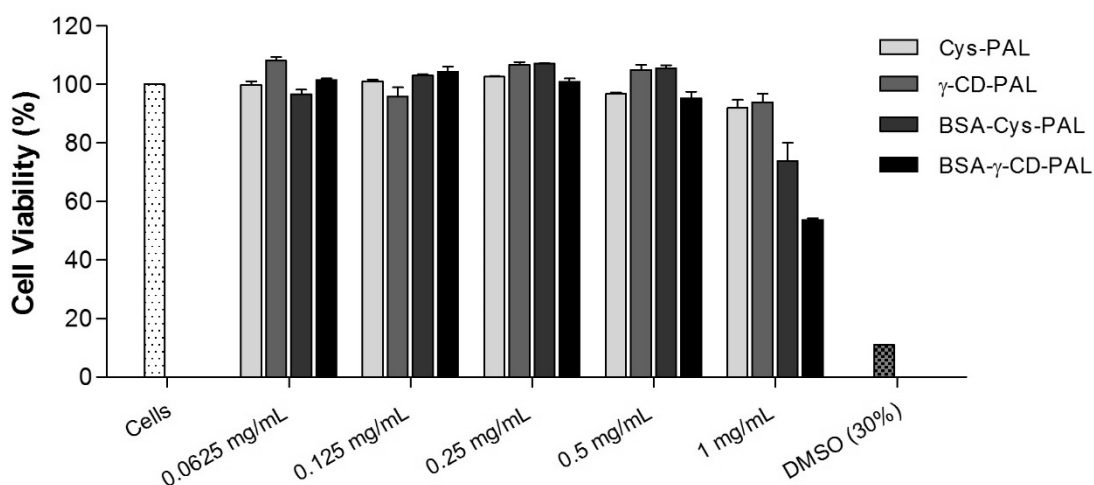


Figure 2.8. BJ5ta cell line viability after 72 h of contact with different concentrations (from 0.0625 mg/mL up to 1 mg/mL) of the four different nanoemulsion formulations, compared with cells (negative control) and cells incubated with 30 % (v/v) of DMSO (death control), determined by MTS assay. Values are the mean \pm SD of 2 independent experiments.

2.3.6. Stability of nanoemulsions in the presence of lipase

The stability of nanoemulsions *in vivo* is governed by several factors namely, pH, surface charge, concentration, salts and the presence of hydrolytic enzymes [41]. We have tested the stability of the developed nanoemulsions in the presence of lipase from *Thermomyces lanuginosus* (activity: 407 μ mol/mL/min). The enzyme remained active during all the incubation process time (lipase activity measured using the release of *p*-nitrophenol, from *p*-nitrophenyl butyrate, by absorbance at 400 nm) [42]. The stability of nanoemulsions was evaluated by particle size measurement at different time points of incubation and by quantification of palmitic acid concentration after hydrolysis. This quantification was performed separating the products of hydrolysis by liquid-liquid extraction with CHCl_3 , followed by NMR analysis (the isolated product was firstly dissolved in DMSO-d_6 to detect the presence of palmitic acid; then, to the same sample was added CDCl_3 , to calculate the percentage of palmitic acid cleavage from the nanoemulsions). **Table 2.2** presents the mean size diameter values of nanodroplets before and after enzymatic incubation for 48 h. It is noteworthy that the size of all the samples is influenced by the same amount of catalyst in solution. It can be depicted that nanoemulsions made-up of modified cyclo-oligosaccharides were not

disrupted by enzymatic action. This was confirmed by the vestigial amounts of palmitic acid (< 1%) detected by NMR (data not shown). Lipase catalyst was able to disrupt the nanoemulsions containing BSA as it can be observed by the results of size diameter. After incubation for 48 h the mean size and PDI increased indicating nanoemulsions destabilization and disruption. The characteristics of these nanoemulsions make them instable per se to time storage, as it can be depicted by the higher values of PDI obtained (**Figure 2.7**). The NMR analysis corroborate these findings. The percentages of palmitic acid cleavage were in the range of 20-55.7 % when lipase was applied (data not shown).

The self-aggregation ability of Cys-PAL gave rise to more robust nanoemulsions with high stability against hydrolysis.

Table 2.2. Particle size before ($t= 0$ h) and after 48 h in the presence of lipase (values are the mean \pm SD of 3 independent experiments)

	t_{0h}		t_{48h}	
	Before incubation		Lipase	
	Size (nm)	PDI	Size (nm)	PDI
Cys-PAL (5mg/mL)	146.0 \pm 1.2	0.134 \pm 0.02	152.2 \pm 8.7	0.118 \pm 0.02
BSA (10mg/mL)-Cys-PAL (5mg/mL)	106.0 \pm 0.6	0.385 \pm 0.06	134.4 \pm 7.1	0.283 \pm 0.00
γ -CD-PAL (5mg/mL)	172.7 \pm 2.1	0.087 \pm 0.02	144.5 \pm 13	0.286 \pm 0.11
BSA (10mg/mL)- γ -CD-PAL (5mg/mL)	129.7 \pm 3.6	0.289 \pm 0.00	128.7 \pm 12	0.437 \pm 0.08

2.3.7. Encapsulation and release of methotrexate

As previously reported by Kim *et al.* [30] we also studied herein the dual properties of modified cyclo-oligosaccharides, namely encapsulation and emulsifying ability using a model compound, MTX. In its native form MTX is an hydrophobic-like drug acquiring hydrophilic character when solubilized at high pH [43, 44].

Taking advantage of the phase-change phenomena (from solid to oily-like liquid) we could predict an efficient encapsulation of this drug at the moment of nanodroplets formation. The encapsulation take place by mixing 10 mg/mL of MTX, at the water phase, with the modified cyclo-oligosaccharides. The solution was heated at 60 °C and after ultrasonication the samples showed a milky-like emulsion with yellow colour indicating the encapsulation and/or emulsification of MTX into the cyclo-oligosaccharides [30]. The available ester groups of the cyclo-oligosaccharides are expected to interact with the hydrophilic groups of the drug, whereas the aromatic groups would

interact more easily with the hydrophobic palmitoyl chain introduced by synthesis with the cyclo-oligosaccharides.

By NMR spectroscopy it was possible to evaluate the molecular interactions between MTX and the cyclo-oligosaccharide nanoemulsions (**Figure 2.9**). The spectra of the commercial MTX evidence the aromatic peaks at δ_{H} 8.59, 7.72 and 6.89 ppm, which undergo chemical shifts when MTX was entrapped within nanoemulsions to δ_{H} 8.54, 7.66 and 6.79 ppm. The aliphatic peaks showed up at δ_{H} 4.79, 4.32, 3.18 and 2.32-2.02 ppm in the starting MTX, while in the nanodevices they appeared at δ_{H} 4.69, 4.32, 3.13 and 2.35-2.03 ppm. Considering the small chemical shifts observed, especially of the lipophilic part of the MTX (aromatic peaks), it was possible to predict that these groups preferentially interact with the hydrophobic palmitic chains of the cyclo-oligosaccharides leading to high MTX encapsulation yield. The small and narrow sized nanoemulsions containing MTX evaluated by DLS corroborate this assumption (**Table 2.3**). As we observed by NMR, MTX present in the solution was entrapped into nanoemulsions. We may speculate that this entrapment was near 100 %, since their physicochemical properties resemble the empty nanodevices and no free MTX was detected by DLS, and thus no additional step of separation was needed.

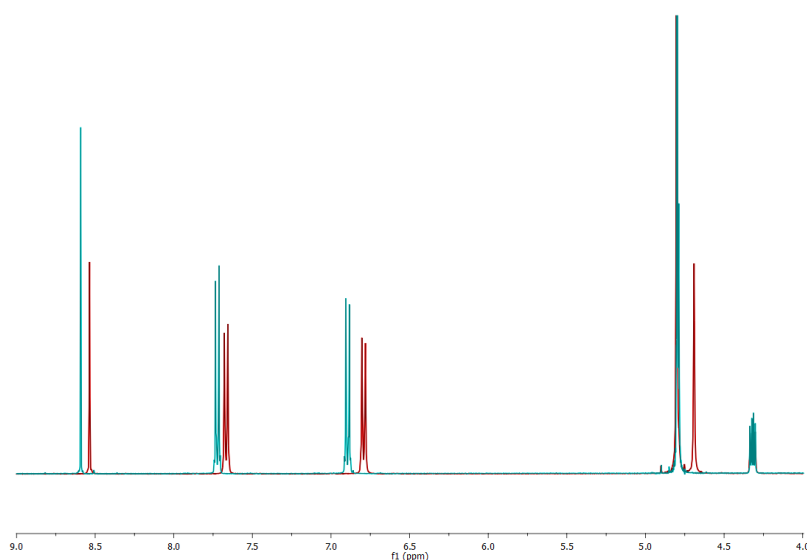


Figure 2.9. ^1H NMR (in D_2O) of MTX free (in blue) and encapsulated in $\gamma\text{-CD-PAL}$ nanoemulsions (in red).

Afterwards the release profile of the drug was traced by dialysis, until the amount of MTX released reached a plateau (**Figure 2.10**). Analysing the data obtained, we can observe a burst release in

the first 24 h of dialysis. It was also evident the release of almost 90 % of the drug after 7 days of dialysis, for all the cases studied. The observations suggest that the intrinsic entrapment ability of modified cyclo-oligosaccharides functioned herein as drug encapsulators and a similar behaviour has been observed for all the cyclo-oligosaccharides tested. The encapsulation and/or entrapment ability was not, in this case, size dependent, but related with the intrinsic phase-change properties of the cyclo-oligosaccharides and their ability to interact with amphiphilic-like compounds.

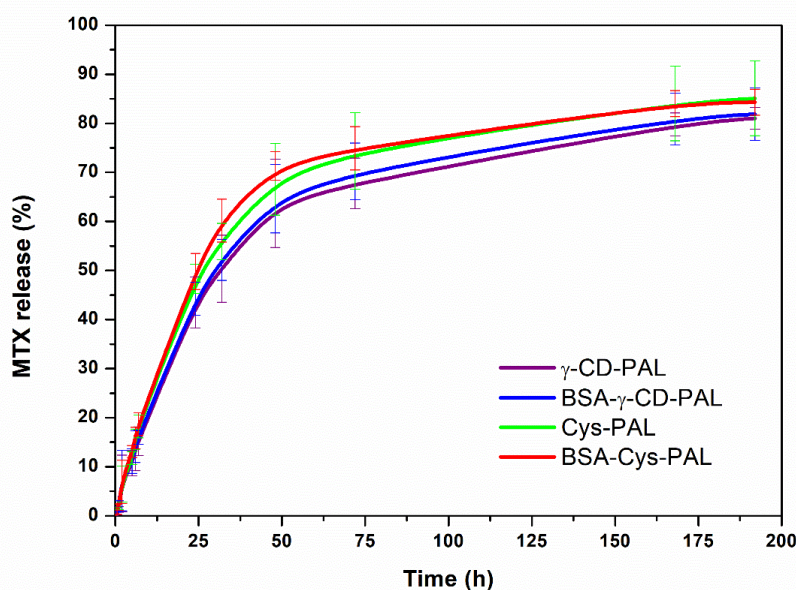


Figure 2.10. Release of MTX from the nanoemulsions over time (values are the mean \pm SD of 3 independent experiments).

In order to evaluate the structural stability of nanoemulsions after drug release, the size and PDI of the nanodroplets were evaluated by DLS. These parameters were measured immediately after nanoemulsions formation, when MTX encapsulation occurs, and after MTX release by dialysis. The nanoemulsions containing MTX revealed to be monodisperse with small and narrow sizes (**Table 2.3 and Figure 2.11**). After MTX release, the nanoemulsions maintained their mean size and PDI confirming their stability even after drug release.

Table 2.3. Size, PDI and surface charge of nanoemulsions, before and after MTX release

	Before MTX release			After MTX release		
	Size (nm)	PDI	Zeta-potential (mV)	Size (nm)	PDI	Zeta-potential (mV)
Cys-PAL	137.4 \pm 4.7	0.089 \pm 0.011	-41.3 \pm 6.4	131.0 \pm 4.6	0.081 \pm 0.024	-34.2 \pm 1.7
BSA-Cys-PAL	131.9 \pm 6.5	0.186 \pm 0.006	-21.7 \pm 0.6	127.4 \pm 10.3	0.205 \pm 0.035	-23.0 \pm 3.0
γ-CD-PAL	140.2 \pm 13.0	0.094 \pm 0.029	-36.3 \pm 2.9	147.2 \pm 3.22	0.087 \pm 0.018	-27.7 \pm 4.9
BSA-γ-CD-PAL	128.0 \pm 8.4	0.321 \pm 0.008	-20.9 \pm 2.0	128.1 \pm 2.31	0.269 \pm 0.014	-21.1 \pm 1.9

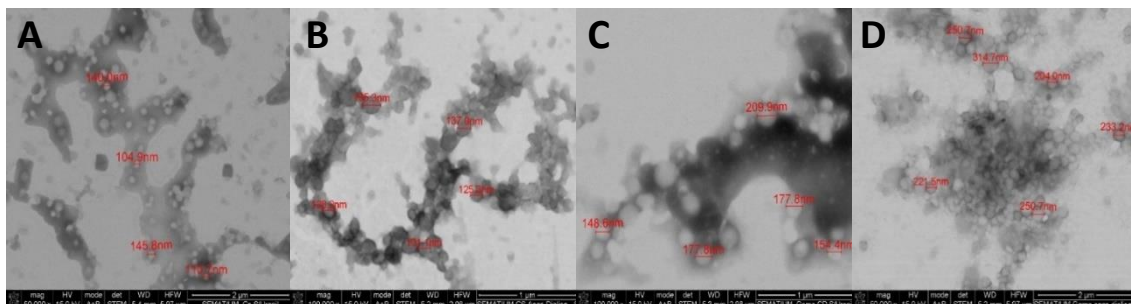


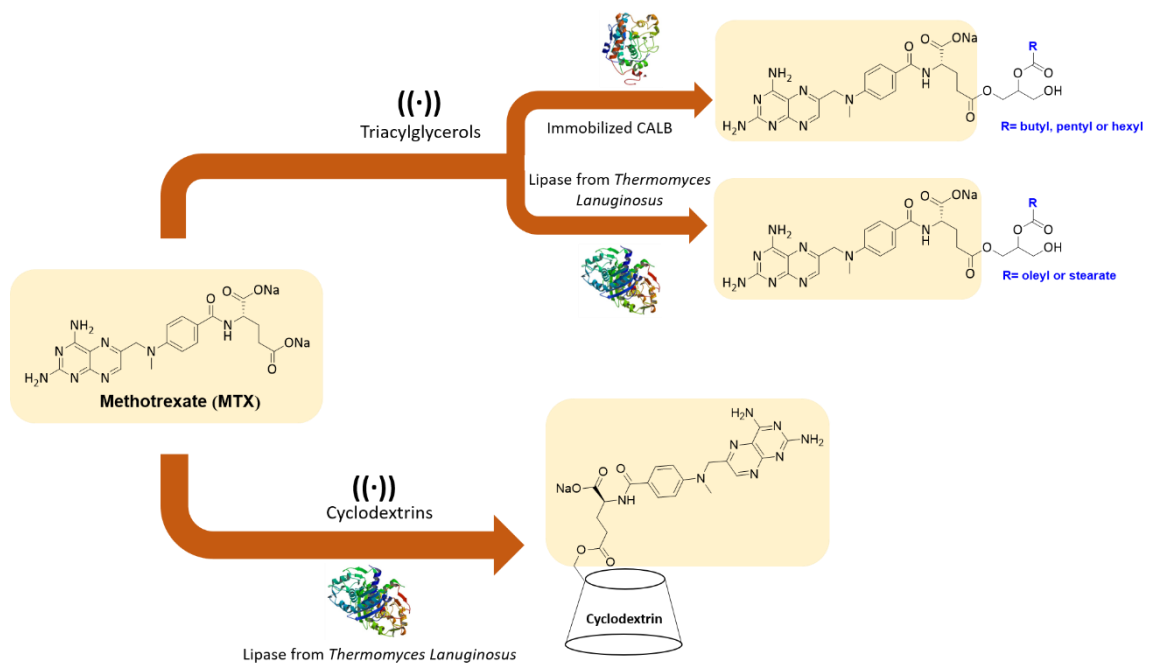
Figure 2.11. STEM microphotographs of nanoemulsions with MTX encapsulated: **A)** Cys-PAL-MTX before MTX release; **B)** Cys-PAL-MTX after MTX release; **C)** γ -CD-MTX before MTX release; **D)** γ -CD-MTX after MTX release.

2.4. Conclusions

Herein we report for the first time the synthesis of hydrophobic cyclo-oligosaccharides by fully substitution of the hydroxyl groups by an hydrophobic compound, a palmitic chain. The emulsifier properties of these hydrophobic cyclo-oligosaccharides made possible the development of stable nanoemulsions, as shown by DLS, NTA and STEM evaluations. Narrow sized, monodisperse and nontoxic nanoemulsions with great potential for amphiphilic drugs encapsulation were developed. The entrapment and delivery ability of these new hydrophobic compounds was evaluated by encapsulation of MTX. The results indicated that the intrinsic properties of modified cyclo-oligosaccharides were able to undergo emulsification in an hydrophobic environment due to their ability to acquire oily-like behaviour when heated. On the other hand, the water-soluble part of cyclo-oligosaccharides showed to be flexible and interact with the hydrophilic portion of the drug. The release of the drug revealed a sustained trend for 1 week of dialysis. Therefore, a step forward the fabrication of nanodevices for amphiphilic drugs encapsulation and delivery for cosmetic and pharmacological purposes was accomplished.

Chapter III

Ultrasound-assisted biosynthesis of novel methotrexate-conjugates



Ultrasound-assisted biosynthesis of novel methotrexate-conjugates

Abstract

New conjugates composed by methotrexate-acylglycerols and methotrexate-cyclodextrins (α , β and γ -CD) were obtained via esterification or transesterification reactions. All reactions were catalysed by esterases namely immobilized lipase from *Candida antarctica B* and lipase from *Thermomyces lanuginosus*. The use of ultrasound to assist the reactions revealed to be a key factor to obtain high conversion yields of both MTX conjugates. Transesterification reactions including long chain triacylglycerols were only successful when ultrasound was applied. In cyclodextrins esterification, a higher number of MTX molecules was also linked to cyclodextrins when ultrasound was applied. All the conjugates were characterized by MALDI-TOF and NMR spectroscopy.

This chapter is based on the following publication:

Jennifer Noro, Rui L. Reis, Artur Cavaco-Paulo, Carla Silva, Ultrasound-assisted biosynthesis of novel methotrexate-conjugates, *Ultrasonics Sonochemistry*, 48 (2018) 51-56.

3.1. Introduction

The production of drugs as esters derivatives is still the most common strategy used by the pharmaceutical industry to improve their physicochemical, pharmacokinetic or biopharmaceutical properties [5]. The synthesis of prodrugs can overcome problems related with chemical instability, rapid pre-systemic metabolism, toxicity, etc [5]. Moreover, the active principal of the drugs is not affected since it can be restored by esterases present in the blood, liver, and other tissues [45].

Methotrexate (MTX) is an anticancer drug, used in the treatment of choriocarcinoma, lymphocytic leukemia, lymphomas and some solid tumours [2]. It also presents therapeutic uses for rheumatoid arthritis and some autoimmune diseases [23]. Despite its relevant properties, this drug shows toxicity mainly related to dose side effects and drug resistance of the tumor cells [2]. The synthesis of methotrexate prodrugs has revealed to overcome some resistance problems associated to cancer cells [11]. Wu *et al.*, have synthesized methotrexate-proline prodrug by solid-phase peptide synthesis methodology. They were able to overcome the resistance of MDA-MB-231 cells, being the prodrug more active than methotrexate [11]. Kuznetsova *et al.*, produced methotrexate conjugated with a diglyceride unit as a prodrug. The conjugate was incorporated in the bilayer of a liposomal formulation. These liposomes bearing the methotrexate prodrug were able to overcome the resistance of human leukemia cells [46].

Lipases are well recognised efficient enzymes with high chemo, regio- and enantiospecific specificity and selectivity [47]. As catalysts of esterification and transesterification reactions, lipases can be applied in the presence of organic solvents [48], ionic liquids [49], aqueous medium [50-53], or in solvent free conditions [54], proving to be versatile assets. Nevertheless, any lipase-catalysed process is dependent on factors such as stability, mass transfer, selectivity, among others [55]. The enzymatic catalysis assisted by ultrasound has been proved to overcome some of the negative aspects associated with the reactional processes using lipases. The presence of ultrasound improves the enzymatic reactions comparing with the reactions performed in its absence, by improving the mass transfer, enhancing the substrate dissolution, minimizing the reactional time, increasing the reaction yield and the chemo-, regio- and stereo selectivity [56-58]. An example was reported by Gumel *et al.* [59], that used lipase from *Candida antarctica B* for the polymerization ϵ -caprolactone to poly(ϵ -caprolactone) by ring opening method. The ultrasound-assisted reaction showed to convert 75 % of the monomer while a conversion of only 16 % was observed with the conventional process [59].

Triacylglycerols are composed by a glycerol moiety, linked by ester bonds to three carbon chains. They are present in plants and in food, being essential to the human organism [60]. The formation of a prodrug containing an ester unit of a triacylglycerol can be considered as a novel methodology to produce non-toxic prodrugs.

Cyclodextrins are cyclic oligosaccharides commonly used for the solubilization of hydrophobic compounds in aqueous mediums by the formation of inclusion complexes. The complexation of a cyclodextrin with a drug is an interesting methodology, being already used by the pharmaceutical industry [29]. Cyclodextrins are nontoxic macromolecules, and after complexation with a drug, they improve its solubility and stability, increasing its bioavailability, and reducing its toxicity.

Shin and co-workers [61] reported other application for these cyclic oligosaccharides. They used lipase as catalysts for the esterification reaction of oleic acid with *n*-butanol by ultrasonication in buffer medium. They proved that the addition of cyclodextrins as emulsifier compounds allowed higher solubilization of the hydrophobic compounds affording excellent yields ($\eta = 80\%$) of the ester product [61].

The promising results obtained by Gumel *et al.* [59] and Shin *et al.* [61], regarding the green biosynthesis assisted by ultrasound lead us to explore similar conditions for the production of new MTX-acylglycerols and MTX-cyclodextrins conjugates, via transesterification and esterification reactions. The enzymatic catalysis was performed using two lipases, namely immobilized lipase from *Candida antarctica B* and lipase from *Thermomyces lanuginosus* (in free form). An aqueous/biphasic medium was used, enabling higher solubilization of the reagents and higher catalytic activity of the lipases. The transesterification reactions were performed using the following triacylglycerols: glycerol tributyrate (C₃), glycerol trivalerate (C₄), glycerol trihexanoate (C₅), glycerol tristearate (C₁₇) and triolein (C₁₇ with unsaturated bond at C₈). The esterification reactions were performed using cyclodextrins (α , β and γ -cyclodextrin). All the new conjugates were characterized by MALDI-TOF and ¹H and ¹³C NMR spectroscopy.

3.2. Materials and methods

3.2.1. Materials

Commercial lipase from *Candida antarctica B* (CALB), Fermase CALBTM 10,000, immobilized on glycidyl methacrylateter-divinylbenzene-ter-ethylene glycol dimethacrylate was obtained as a gift sample from Fermenta Biotech Ltd., Mumbai, India (activity of 8000 propyl laurate U/g). Lipase from *Thermomyces lanuginosus*, solution, $\geq 100\ 000$ U/g was purchased from Sigma-Aldrich. All

other compounds used in this work were purchased from TCI Chemicals or Sigma-Aldrich and used without any further purification. Ultrafiltration was performed with Ultracel 1 kDa ultrafiltration discs, composed of regenerated cellulose, 47 mm (Millipore) with ultrapure water (Milli-Q). Melting points were determined using a Gallenkamp apparatus.

3.2.2. General procedure

3.2.2.1. MTX-acylglycerol (small carbon chain) conjugates

In a flask with MTX (30 mg) was added 200 μ L of water, followed by the triacylglycerol (1 eq.). Immobilized CALB (3 mg, 10 % w/w) was added and the flask placed in an ultrasonic bath (USC600TH, VWR International Ltd., USA; frequency 45 kHz and power of 120 W) with duty cycles of 5 ON/5 OFF in a total time of 30 min. The enzyme was removed by filtration, and the water removed by lyophilization.

In the water bath approach, the same procedure was followed, but instead of ultrasound, the water bath (Grant, OLS Aqua Pro) operating at 40 °C, 100 rpm, was used in the same time that with US. Compound **2a** (yellow solid, η = 61 %). δ_{H} (DMSO- d_6): 0.83 (t, J = 7.2 Hz, 3H), 1.44 (sext, J = 7.2 Hz, 2H), 1.79 (m, 1H), 1.91 (m, 1H), 1.97 (t, J = 7.2 Hz, 2H), 2.09 (m, 1H), 2.18 (m, 1H), 3.17 (s, 3H), 3.28-3.42 (m, 5H), 4.15 (m, 1H), 4.75 (s, 2H), 6.59 (br s, 2H), 6.81 (d, J = 8.8 Hz, 2H), 7.41 (br s, 1H), 7.64 (d, J = 8.8 Hz, 3H), 7.80 (d, J = 4.0 Hz, 1H), 8.56 (s, 1H) ppm.

Compound **2b** (yellow solid, η = 64 %). δ_{H} (DMSO- d_6): 0.83 (t, J = 7.6 Hz, 3H), 1.24 (sext, J = 7.6 Hz, 2H), 1.43 (quint, J = 7.2 Hz, 2H), 1.78 (m, 1H), 1.90 (m, 1H), 2.03 (t, J = 7.2 Hz, 2H), 2.11 (m, 1H), 2.26 (m, 1H), 3.17 (s, 3H), 3.27 (dd, J = 10.8, 6 Hz, 2H), 3.35 (dd, J = 10.8, 5.2 Hz, 2H), 3.41 (quint, J = 6 Hz, 1H), 4.15 (quart, J = 7.6 Hz, 1H), 4.75 (s, 2H), 6.58 (br s, 2H), 6.81 (d, J = 9.2 Hz, 2H), 7.41 (br s, 1H), 7.64 (d, J = 8.8 Hz, 3H), 7.78 (d, J = 6.4 Hz, 1H), 8.56 (s, 1H) ppm. δ_{C} (DMSO- d_6): 13.8 (CH₃), 22.0 (CH₂), 27.6 (CH₂), 28.6 (CH₂), 33.1 (CH₂), 35.5 (CH₂), 39.0 (CH₃), 53.1 (CH), 54.9 (CH₂), 63.1 (CH₂), 72.5 (CH), 111.2 (CH), 121.4 (C_q), 122.0 (C_q), 128.4 (CH), 146.0 (C_q), 149.2 (CH), 150.8 (C_q), 155.2 (C_q), 162.7 (C_q), 164.9 (C=O), 173.9 (C=O), 175.4 (C=O), 175.7 (C=O) ppm.

Compound **2c** (yellow solid, η = 58 %). δ_{H} (DMSO- d_6): 0.83 (t, J = 7.2 Hz, 3H), 1.22 (m, 4H), 1.41 (quint, J = 7.6 Hz, 2H), 1.79 (m, 1H), 1.88 (t, J = 7.2 Hz, 2H), 2.05 (m, 2H), 3.16 (s, 3H), 3.28-3.42 (m, 5H), 4.07 (s, 1H), 4.75 (s, 2H), 6.58 (br s, 2H), 6.81 (d, J = 9.2 Hz, 2H), 7.40 (br s, 1H), 7.63 (d, J = 8.8 Hz, 3H), 7.87 (br s, 1H), 8.56 (s, 1H) ppm.

3.2.2.2. MTX-acylglycerol (long carbon chain) conjugates

In a flask with MTX (30 mg) was added the triacylglycerol (1 eq.) followed by 500 μ L of lipase from *Thermomyces lanuginosus*. The flask was placed in an ultrasonic bath with duty cycles of 5 ON/5 OFF in a total time of 30 min. The suspension was extracted with CHCl_3 (3x) for the removal of unreacted triacylglycerol, and the aqueous phase centrifugated using vivaspin 10 kDa (Sartorius) for the removal of the lipase. After freeze-dried an orange oil/solid product was obtained.

In the water bath approach, the same procedure was followed, but instead of ultrasound, the water bath operating at 40 $^{\circ}\text{C}$, 100 rpm, was used in the same time that with US.

Compound **2d** (orange solid/oil, η = 63 %). δ_{H} (DMSO- d_6): 0.85 (t, J = 6.8 Hz, 3H), 1.23 (m, 20H), 1.46 (m, 2H), 1.81 (m, 2H), 1.97 (m, 4H), 2.15 (t, J = 7.6 Hz, 2H), 2.23 (m, 2H), 3.14-3.58 (m, 5H), 3.16 (s, 3H), 4.22 (s, 1H), 4.76 (s, 2H), 5.32 (m, 2H), 6.60 (br s, 2H), 6.80 (br s, 2H), 7.20 (br s, 1H), 7.43 (s, 1H), 7.67 (br s, 3H), 7.80 (br s, 1H), 8.56 (s, 1H) ppm. δ_{C} (DMSO- d_6): 13.9 (CH₃), 22.1 (CH₂), 24.9 (CH₂), 26.5 (CH₂), 26.6 (CH₂), 28.5 (CH₂), 28.6 (CH₂), 28.7 (CH₂), 28.8 (CH₂), 29.1 (CH₂), 31.3 (CH₂), 34.6 (CH₂), 39.8 (CH₃), 54.9 (CH₂), 63.1 (CH₂), 72.5 (CH), 111.2 (CH), 121.5 (C_q), 122.0 (C_q), 128.5 (CH), 129.7 (CH), 146.1 (C_q), 149.2 (C_q), 150.8 (C_q), 155.2 (C_q), 162.7 (C=O), 162.8 (C=O), 165.2 (C=O), 175.5 (C=O) ppm.

Compound **2e** (orange solid/oil, η = 64 %). δ_{H} (DMSO- d_6): 0.83 (t, J = 7.2 Hz, 3H), 1.21 (m, 24H), 1.47 (m, 2H), 1.83 (m, 1H), 1.90 (m, 1H), 2.11 (m, 1H), 2.14 (t, J = 7.6 Hz, 2H), 2.21 (m, 1H), 2.23 (m, 2H), 3.12-3.57 (m, 5H), 3.16 (s, 3H), 4.18 (s, 1H), 4.74 (s, 2H), 6.60 (br s, 2H), 6.78 (br s, 2H), 7.20 (br s, 1H), 7.41 (s, 1H), 7.65 (br s, 3H), 7.77 (br s, 1H), 8.54 (s, 1H) ppm.

3.2.2.3. MTX-cyclodextrin conjugates

In a flask with MTX (3 eq.) was added the cyclodextrin (30 mg) followed by 500 μ L of lipase from *Thermomyces lanuginosus*. The flask was placed in an ultrasonic bath with duty cycles of 15 ON/5 OFF in a total time of 2 h. The enzyme was removed by centrifugation using vivaspin 10 kDa. The separation of unreacted MTX was performed by ultrafiltration (membrane disc of 1 kDa). The solution was freeze-dried to obtain the yellow solid products.

In the water bath approach, the same procedure was followed, but instead of ultrasound, the water bath operating at 40 $^{\circ}\text{C}$, 100 rpm, was used in the same time that with US.

Compound **3a** (yellow solid, η = 17 %). δ_{H} (DMSO- d_6): 1.86 (m, 2H), 2.07 (m, 2H), 3.16 (s, 3H), 3.19-3.22 (m, glucose unit), 3.56-3.67 (m, glucose unit), 3.83 (t, J = 9.2 Hz, 2H), 4.08 (d, J = 6.0 Hz, 1H), 4.43 (br s, 2H), 4.76 (m, 5H), 6.03 (br s, 2H), 6.42 (br s, 2H), 6.58 (br s, 2H), 6.81 (d,

δ_{H} (DMSO- d_6): 9.2 Hz, 2H), 7.38 (br s, 2H), 7.65 (br s, 1H), 7.67 (d, $J = 8.8$ Hz, 2H), 7.78 (m, 1H), 8.56 (s, 2H) ppm. δ_{C} (DMSO- d_6): 29.3 (CH₂), 34.1 (CH₂), 38.9 (CH₃), 54.0 (CH), 54.9 (CH₂), 60.0 (CH₂), 72.0 (CH), 72.4 (CH), 72.8 (CH), 79.2 (CH), 81.9 (CH), 102.1 (CH), 111.2 (CH), 121.4 (C_q), 122.4 (C_q), 128.4 (CH), 146.0 (C_q), 149.2 (CH), 150.6 (C_q), 155.2 (C_q), 162.7 (C=O), 162.8 (C=O), 164.8 (C=O) ppm.

Compound **3b** (yellow solid, $\eta = 19$ %). δ_{H} (DMSO- d_6): 1.85 (m, 2H), 2.03 (m, 2H), 3.16 (s, 3H), 3.22-3.27 (m, glucose unit), 3.52-3.72 (m, glucose unit), 4.11 (d, $J = 7.2$ Hz, 2H), 4.43 (br s, 4H), 4.74 (s, 2H), 4.81 (d, $J = 3.6$ Hz, 3H), 6.24 (br s, 2H), 6.42 (br s, 3H), 6.58 (br s, 2H), 6.81 (d, $J = 8.4$ Hz, 1H), 7.40 (br s, 1H), 7.61 (br s, 1H), 7.66 (d, $J = 8.8$ Hz, 2H), 7.78 (m, 1H), 8.56 (s, 1H) ppm. δ_{C} (DMSO- d_6): 29.1 (CH₂), 33.9 (CH₂), 38.9 (CH₃), 54.9 (CH₂), 59.9 (CH₂), 67.2 (CH), 67.3 (CH₂), 72.0 (CH), 72.7 (CH), 81.1 (CH), 101.8 (CH), 111.2 (CH), 121.4 (C_q), 122.3 (C_q), 123.9 (C_q), 128.4 (CH), 146.0 (C_q), 149.2 (CH), 150.7 (C_q), 155.2 (C_q), 162.7 (C=O), 162.8 (C=O), 164.9 (C=O) ppm.

Compound **3c** (yellow solid, $\eta = 22$ %). δ_{H} (DMSO- d_6): 1.85 (m, 2H), 2.05 (m, 2H), 3.16 (s, 3H), 3.33-3.61 (m, glucose unit), 4.07 (m, 1H), 4.30-4.50 (m, 3H), 4.74 (s, 2H), 4.88 (m, 1H), 4.98 (m, 1H), 6.38 (br s, 1H), 6.58 (br s, 2H), 6.69 (br s, 1H), 6.81 (d, $J = 8.4$ Hz, 2H), 7.40 (br s, 2H), 7.64 (d, $J = 8.8$ Hz, 2H), 7.88 (m, 1H), 8.56 (s, 1H) ppm.

3.2.3. Nuclear Magnetic Resonance spectroscopy (NMR)

^1H and ^{13}C NMR spectroscopy was performed using a Bruker Avance III 400 (400 MHz for ^1H and 100 MHz for ^{13}C). DMSO- d_6 (Cortecnet) was used as deuteride solvent, and the peak solvent was used as internal reference.

3.2.4. Matrix-Assisted Laser Desorption/Ionization Time-of-Flight (MALDI-TOF)

MALDI-TOF mass spectra were acquired on a Bruker Autoflex Speed instrument (Bruker Daltonics GmbH) equipped with a 337 nm nitrogen laser. The matrix solution for the measurements was prepared by dissolving a saturated solution of 2,5-dihydroxybenzoic acid (DHB) or α -cyano-4-hydroxycinnamic acid (CHCA) in an aqueous solution of 0.1 % trifluoroacetic acid (70 %) and acetonitrile (30 %). Samples were spotted onto a ground steel target plate (Bruker part n° 209519) and analysed in the linear positive or linear negative modes using factory-configured instrument parameters suitable for a 0-5 kDa m/z range (ion source 1: 19.5kV; ion source 2: 18.3kV). Time

delay between laser pulse and ion extraction was set to 130 ns, and the laser frequency was 25 Hz.

3.2.5. Electrospray Ionization (ESI)

Electro spray ionization was performed in a mass detector Thermo Finnigan LxQ (Linear Ion Trap). Mass detector susceptible of analysis in full scan mode, SIM and MS/MS with positive ionization. Mass spectra range was between 50 and 2000. Capillary voltage was used as 29 V.

3.3. Results and discussion

3.3.1. Methotrexate-acylglycerol conjugates

The catalytic activity of both, immobilized CALB and free form lipase from *Thermomyces lanuginosus*, against different triacylglycerols (carbon chain length between C3 and C17) was investigated using a water and an ultrasonic bath. The immobilized form was chosen for comparison due to its higher thermal stability and catalytic activity comparing with the free form. Moreover, the purification steps can be simplified using this enzyme form since a simple paper filtration removes the enzyme from the reactional medium [56].

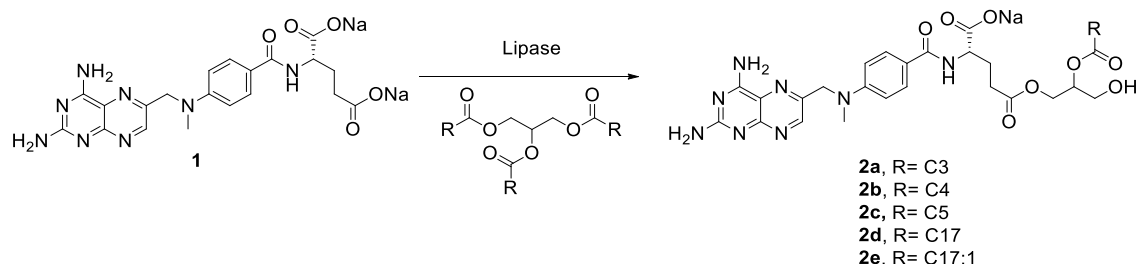
The transesterification reactions were conducted herein using a green methodology, with water as solely solvent. MTX is poorly soluble in almost all the solvents, namely DMSO which does not allow the fully solubilization of the reactants disabling the hydrolytic activity of the esterases. The addition of the triacylglycerol to the MTX solution, formed as expected, an immiscible biphasic system, being the powder enzyme suspended at the soluble phase.

After reaction we observed that for longer triacylglycerols, namely triolein (C_{17:1}) and glycerol tristearate (C₁₇), immobilized CALB did not presented any hydrolytic activity (**Table 3.1**). After removal of the reactional mixture from the US, followed by a liquid-liquid extraction of the unreacted triacylglycerols, only free MTX was recovered in the aqueous phase. This result was expectable since recently, Chiplunkar *et al.* reported that immobilized CALB did not hydrolyse triolein in organic medium [62]. For the short triacylglycerols used, glycerol tributyrate (C₃), glycerol trivalerate (C₄) and glycerol trihexanoate (C₅), after 30 min under ultrasonication, we observed the disappearance of the biphasic system formed initially, and the precipitation of a solid that turns into soluble when more water was added to the reactional flask. The different catalytic behaviour of immobilized CALB depending on the size of the triacylglycerols may be justified by the poor mobility of the immobilized enzyme form hindering the catalysis of longer substrates. Considering this enzyme drawback, we

replaced the immobilized CALB by a liquid lipase from *Thermomyces lanuginosus* in the free form and use it without the addition of any other solvent. After reaction, it was possible to observe the hydrolysis of the longer triacylglycerols and the formation of the MTX-acylglycerol conjugates. Our data corroborate previous findings which highlighted an high activity of this lipase for long triacylglycerols, such as triolein [63].

The reactional scheme proposed for the conjugation of MTX with triacylglycerols is presented in **Scheme 3.1**. We proposed that the enzyme starts the hydrolysis of the triacylglycerol, forming an intermediate in the active site, with the final release of a fatty acid chain. This reaction occurs twice, which in turns the glycerol unit with only one side chain available. Then, the MTX binds to the active site of the enzyme, by the carboxylic group, forming an ester intermediate. The glycerol can undergo a nucleophilic attack, which led to the formation of the final conjugates.

¹H NMR data did not allow us to ensure which carbonyl group was involved on the reaction, thus we therefore propose the γ -position carbonyl group, since it is the most reactive carboxyl group of the glutamic acid portion [64].



Scheme 3.1. Reactional scheme of methotrexate-acylglycerols conjugates synthesis. Compound **1**, methotrexate; Compounds **2a-2c** were produced using US in the presence of immobilized CALB. Compounds **2d** and **2e** were produced using US and lipase from *Thermomyces lanuginosus*. **2a** was produced using glycerol tributyrate, **2b** using glycerol trivalerate, **2c** using glycerol trihexanoate, **2d** using glycerol tristearate and **2e** using triolein.

From ¹H NMR data we can infer that both lipases hydrolysed two of the three fatty acid chains of the triacylglycerols. Works reported have been recognising that some lipases can own 1,3-selectivities against triacylglycerols [65]. Taking into account this enzyme property and considering that only one carbon chain remained attached to the glycerol moiety, we propose that the carbon chain remains in the second position (**Scheme 3.1**).

The use of ultrasound to assist the enzymatic reactions, due to emulsifying events, allowed to obtain higher conversion rates comparing with the results using a water bath. As can be depicted in **Table 3.1**, high yields of crude products were obtained as solids or oils after freeze-drying. The role of ultrasound on enzymatic reactions enhancement has been described as due to several reasons. One of them are the mechanical effects of ultrasound which promote mass transfer from the bulk solution to the enzyme. The collision of substrate molecules and the enzyme promote the reaction rate increment and the miscibility of the two reactional initial phases. Another reason relies on the steady cavitation corrosion of ultrasound which might cause the enzyme molecule or cell granulation around it to be shared by microstreaming [55], improving the mass transfer inside or outside of the enzyme. The final reason is related with the enzyme structure, which in the presence of ultrasound, become more flexible, and thus, may shift into its active configuration [58]. Considering that different enzymes own different stereo-configurations, for the same ultrasonic parameters adopted, different enzyme behaviour was observed for both immobilized CALB and free liquid lipase. This distinct behaviour is determined by several factors including the bulk of ultrasonic energy, the adaptability of the enzyme, and the micro-conditions around the enzyme. Analysing the entries 1 to 6 of **Table 3.1**, it is possible to observe that lipase from *Thermomyces lanuginosus* was able to hydrolyse the short triacylglycerols in a low extent. The reaction yields calculated by ^1H NMR data were low, revealing that this enzyme was only able to hydrolyse part of the carbon chains available. Only a vestigial amount of product was detected by the unfolding of the triacylglycerols peaks on ^1H NMR. High conversion yields were obtained on the conjugation of methotrexate with longer acylglycerols using the free liquid enzyme form in the presence of ultrasound. In both cases only vestigial amounts of product were detected after incubation in the water bath. Herein, the use of ultrasound to assist the synthesis reactions was again crucial for an effective conjugation.

Table 3.1. Experimental conditions and conversion yields for methotrexate-acylglycerol conjugates using immobilized CALB and free lipase from *Thermomyces lanuginosus* (TL) (results with standard deviation from at least 2 independent experiments)

Entry	Triacylglycerol	Carbon Chain Length	Reaction Conditions	Yield (%)**	
				Immobilized CALB	Lipase TL
1	Glycerol Tributyrate	C3	WB (40°C, 30 min)	–*	–*
2			US (5min ON/5min OFF; 30 min)	61.4 ± 4.0	–*
3	Glycerol Trivalerate	C4	WB (40°C, 30 min)	–*	–*
4			US (5min ON/5min OFF; 30 min)	64.1 ± 0.4	–*
5	Glycerol Hexanoate	C5	WB (40°C, 30 min)	45.8 ± 1.7	–*
6			US (5min ON/5min OFF; 30 min)	58.0 ± 7.6	–*
7	Triolein	C17:1	WB (40°C, 30 min)	– ^a	–*
8			US (5min ON/5min OFF; 30 min)	– ^a	62.6 ± 4.3
9	Glycerol Tristearate	C17	WB (40°C, 30 min)	– ^a	–*
10			US (5min ON/5min OFF; 30 min)	– ^a	63.7 ± 6.4

^ano reaction occurred;

*only vestigial amount of conjugate product was detected by ¹H NMR;

** the yield was calculated based on the initial number of moles and the moles of the product.

To confirm the conjugation, we also evaluated the melting point of the conjugates produced. The melting point of methotrexate disodium salt is reported to be between 212-216 °C. For the conjugates produced we observed a different behaviour, they do not display a melting point, starting to decompose at around 250 °C. The conjugate composed by a hexanoate carbon chain was the most stable, starting to decompose at temperatures above 280 °C. The conjugate composed by a valerate chain (C₄) was fully decomposed at 250 °C. The melting behaviour was not evaluated for the conjugates with longer carbon chains since they were isolated as a mixture of oil/solids.

¹H NMR spectra of conjugates **2a-e** (see **Scheme 3.1**) showed a unique set of peaks of MTX protons, meaning that the transesterification reaction occurred in only one of the carbonyl groups (**Figure 3.1**). The hydrolysed chains were eliminated during the liquid-liquid extraction (longer triacylglycerols) or during the freeze-drying process, in the case of short triacylglycerols. **Figure 3.1** shows the ¹H NMR of methotrexate-hexanoate conjugate and of free MTX. Significant chemical shifts were observed on the protons of methotrexate, mainly on the protons of the glutamic portion of the MTX. The amine proton signals remained untouched confirming that the conjugation occurred at one of the carboxylic groups.

The amide proton (**g**) suffered a chemical shift from δ_{H} 8.14 to 7.85 ppm. Proton **h** appeared at δ_{H} 4.08 instead of 3.85 ppm. The aliphatic protons of the glutamic portion unfolded in two: proton **j** appeared at a higher chemical shift δ_{H} 2.12 and 2.06 instead of 1.89 ppm; protons **i** stayed in a

similar place: from δ_H 1.79 to 1.82 ppm. Glycerol moiety was observed under the HDO peak, between δ_H 3.25-3.50 ppm.

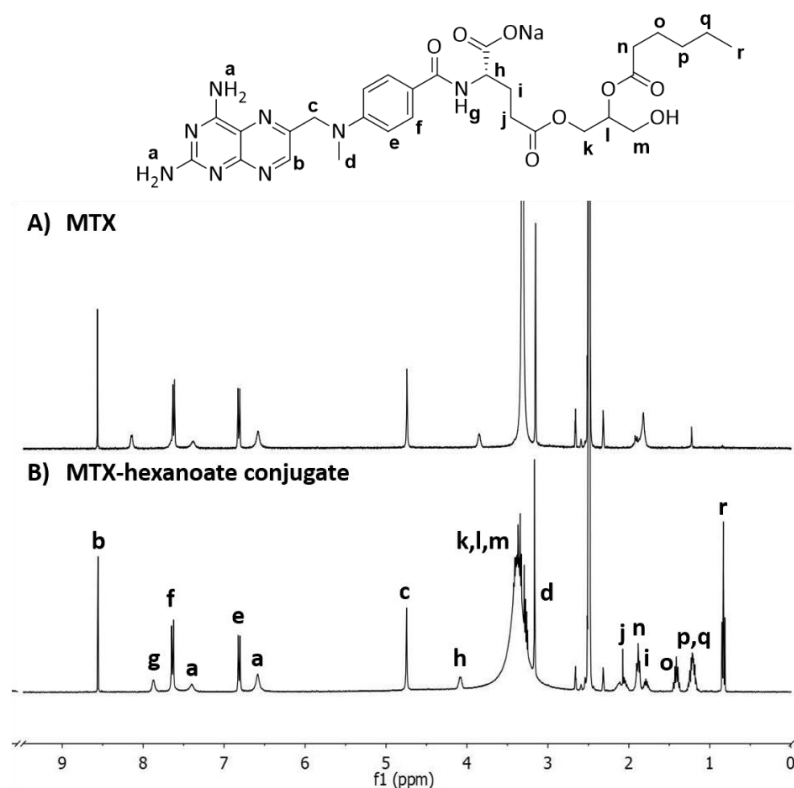


Figure 3.1. ^1H NMR spectra of **A)** free MTX and **B)** methotrexate-hexanoate conjugate (DMSO-d_6).

Electrospray ionization (ESI) and MALDI-TOF techniques were also assessed to confirm the formation of the conjugates (**Table 3.2**). The masses obtained either by ESI or MALDI-TOF were very similar to the theoretical values calculated, confirming the formation of conjugates between MTX and the acylglycerols.

Table 3.2. Values of theoretical and experimental mass obtained by ESI and MALDI-TOF

	Theoretical mass	Mass obtained by ESI	Mass obtained by MALDI-TOF
MTX-butyrate	620.6	666.6 (620.6 + 2Na ⁺)	625.4
MTX-valerate	634.2	625.5	631.4
MTX-hexanoate	648.6	659.2	671.1 (648.6 + Na ⁺)
MTX-oleate	814.9	823.2	815.7
MTX-stearate	816.9	833.6	816.5

3.3.2. Methotrexate-cyclodextrin conjugates

Cyclodextrins (CD) are cyclic sugars used as devices for the solubilization of hydrophobic compounds by formation of inclusion-complexes in aqueous medium. Considering their non-toxic properties, the covalent bonding of molecules to these devices can also be assessed as an effective strategy to produce pro-drugs [66].

We studied the biosynthesis of methotrexate-cyclodextrin conjugates using a similar methodology described previously for the triacylglycerols. The reactions were carried out without addition of solvents, using the free liquid lipase from *Thermomyces lanuginosus* as reactional medium to ensure the solubilisation of all reactants. Immobilized CALB was also tested, however due to its difficulty to access and accommodate longer substrates, an extremely low yield (around $\eta = 1\%$) was obtained after reaction.

The effect of ultrasound on the formation of the conjugates was also evaluated. The reactions were performed using an US bath, for 2 h with duty cycles of ultrasound of 15 minutes ON followed by 5 minutes OFF. The same reaction time was used for the reactions performed in a water bath (WB). Comparing with MTX-acylglycerol conjugates, the total time of the reactions was extended considering the size of the cyclodextrin substrates. As previously reported for MTX-acylglycerol conjugates, the use of US led to high yields of MTX-CD conjugates, and a higher number of MTX units linked to the macromolecules.

The amount of MTX equivalents used was also incremented but the findings revealed that it does not lead to higher degrees of modification or conversion yield.

In **Table 3.3** are depicted the results obtained after MTX-CD conjugation. Observing the data, we found that the degree of modification of the cyclodextrins was size dependent and greatly influenced by stereochemical impediments. The larger the size of the cyclodextrin molecule, higher was the number of MTX molecules bound. The smaller cyclodextrin used, α -CD composed by 6 glucose units, was only conjugated to one molecule of MTX, while the longer, γ -CD with 8 glucose units, was conjugated to a maximum of 3 units of MTX.

Table 3.3. Reaction conditions and conversion yields obtained after conjugation of methotrexate with cyclodextrins using liquid lipase from *Thermomyces lanuginosus* (TL) (results with standard deviation from at least 2 independent experiments)

Entry	Cyclodextrin	Reaction Conditions	Lipase TL	
			Max. degree of modification	Conversion Yield
1	α -CD	WB (40 °C, 2h)	1	8.9 \pm 3.4 %
2	α -CD	US (15 min ON/5 min OFF) x 6 cycles	1	16.8 \pm 1.8 %
3	β -CD	WB (40 °C, 2h)	1	14.8 \pm 3.4 %
4	β -CD	US (15 min ON/5 min OFF) x 6 cycles	2	19.0 \pm 0.4 %
5	γ -CD	WB (40 °C, 2h)	1	3.0 \pm 4.2 %
6	γ -CD	US (15 min ON/5 min OFF) x 6 cycles	3	22.0 \pm 2.8 %

By ^1H NMR spectroscopy, it was possible to observe significant differences between the spectra of the starting reactants and of the final conjugates. The decrease and change in the chemical shift of the OH protons of the cyclodextrins were the most evident alteration. As starting materials, the OH peaks of the CD appeared between δ_{H} 5.75 and 4.43 ppm. When conjugated, these peaks were observed between δ_{H} 6.58 and 4.45 ppm. Differences in the glycosyl peaks of the CD, mainly in the chemical shifts and pattern, were also detected. The pattern of the MTX in all the cyclodextrins remains very similar in all the conjugates obtained.

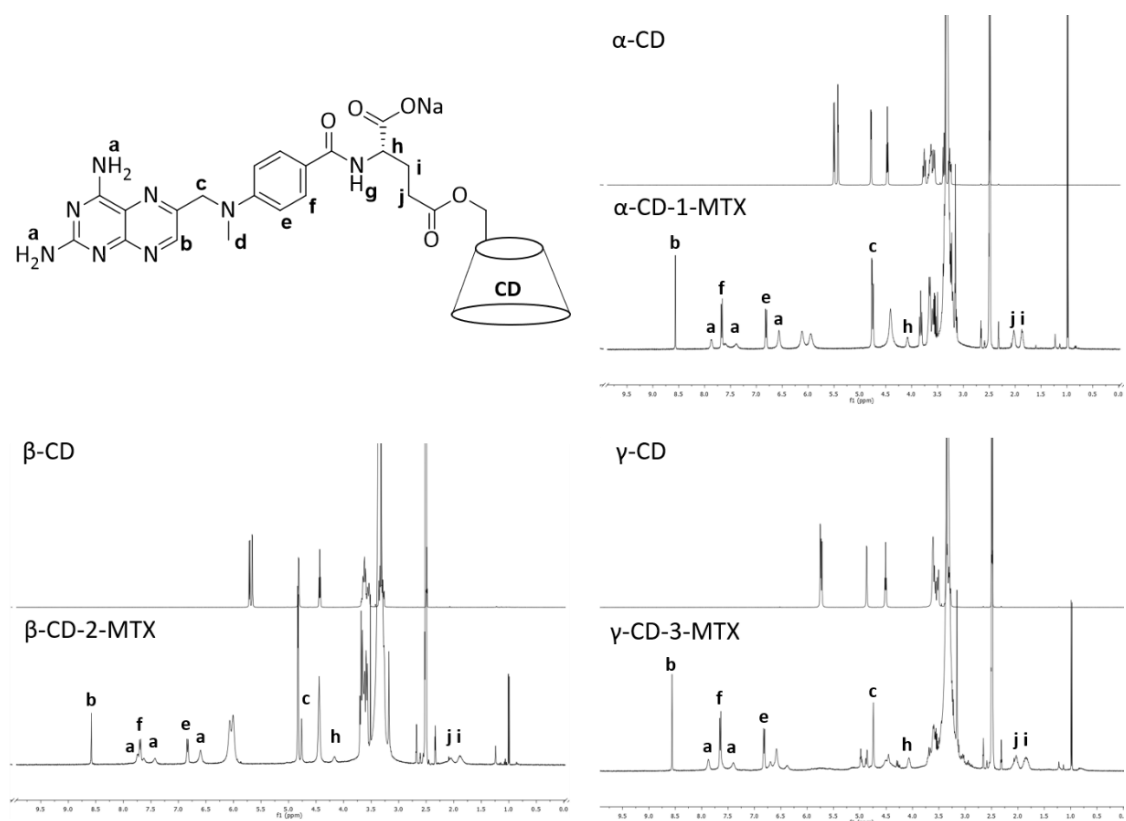


Figure 3.2. ^1H NMR of MTX-CD (α , β and γ)-conjugates in DMSO-d_6 using lipase from *Thermomyces lanuginosus* in the US.

MALDI-TOF analysis allowed us to calculate the degree of modification of the cyclodextrins with methotrexate (**Figure 3.3**). We confirmed a direct correlation between the size of the cyclodextrin and the degree of modification. α -CD presented the lowest modification, with only one MTX unit ($m/z = 1478$) (**Figure 3.3A**), β -CD was conjugated with 2 units of MTX ($m/z = 2128$) (**Figure 3.3B**), and γ -CD was conjugated to 3 MTX units ($m/z = 2692$) (**Figure 3.3C**). Glycosyl cleavage can be observed in the MALDI-TOF spectra, with values around $m/z \approx 170$. Based on the ^1H NMR and MALDI-TOF data we propose in **Figure 3.3** the structure of the final MTX-CD conjugates.

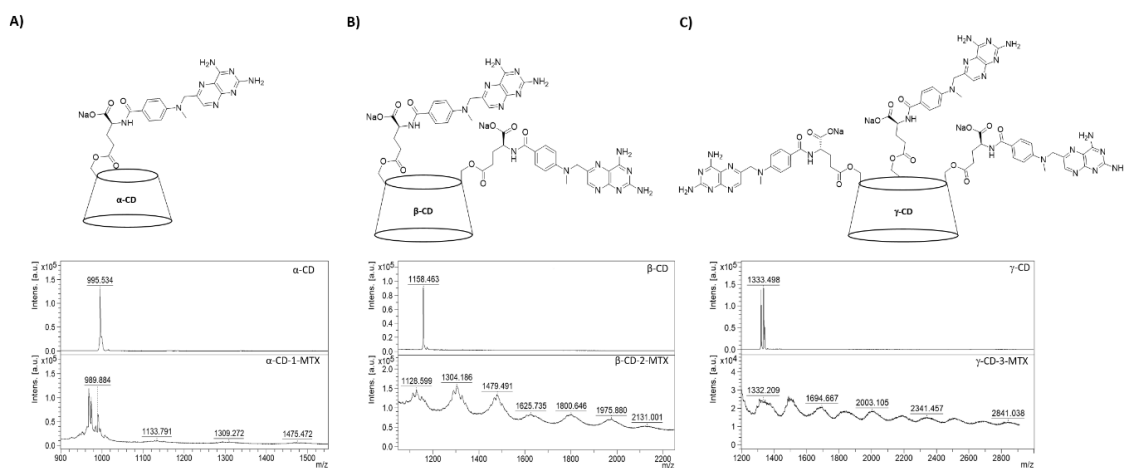


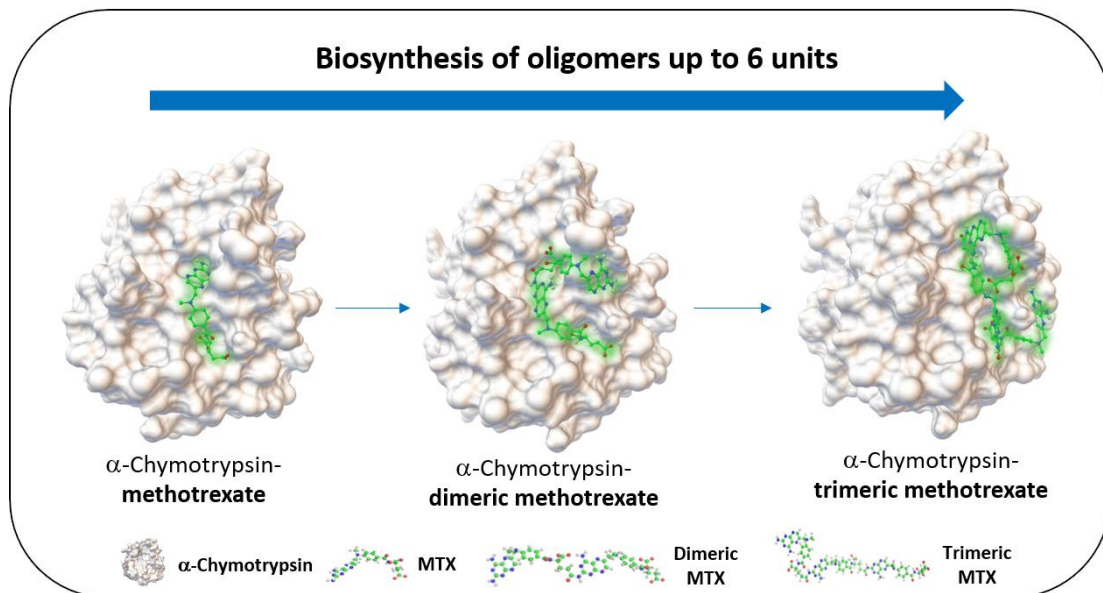
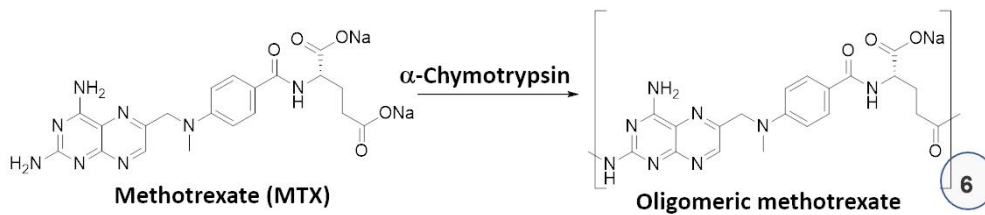
Figure 3.3. MALDI-TOF of MTX-CD conjugates: **A)** α -CD conjugated with 1 MTX unit, **B)** β -CD conjugated with 2 MTX units, **C)** γ -CD conjugated with 3 MTX units; the upper image shows the proposed MTX-CD conjugates; all conjugates were obtained after reaction using lipase from *Thermomyces lanuginosus* in ultrasound.

3.4. Conclusions

In the present study we developed new methotrexate-acylglycerols and methotrexate-cyclodextrin (α , β and γ -CD) conjugates via enzymatic transesterification or esterification reaction assisted by ultrasound. We verified that ultrasound played a crucial role on the final conversion yields and degree of modification. The ultrasonic system was not only advantageous over the traditional water bath (WB) in terms of reaction rates, but was also responsible for the products purity and selectivity, namely for the isolation of cyclodextrins with high amount of MTX units conjugated. The therapeutic association of non-toxic triacylglycerols and cyclodextrins, are herein presented as promising therapeutic compounds since they may prevent the development of transport resistance of the drug, which is often observed during the clinical use of methotrexate.

Chapter IV

α -Chymotrypsin catalyses the synthesis of methotrexate oligomers



α -Chymotrypsin catalyses the synthesis of methotrexate oligomers

Abstract

The enzymatic synthesis of methotrexate (MTX) catalysed by α -chymotrypsin was studied for the first time. The proteolytic enzyme displayed activity for the synthesis of MTX oligomers composed by 6 repeating units ($DP_{avg} = 1.5$). For longer oligomers, molecular dynamics simulations confirmed that as the oligomeric chain grows its accommodation in the enzymes' active site was hindered, which was evidenced by a decrease of the binding energy associated. The full characterization of the oligomers produced was performed by nuclear magnetic resonance (NMR, 1H and ^{13}C), matrix-assisted laser desorption/ionization-time of flight (MALDI-TOF), electrospray ionization (ESI) and differential scanning calorimetry (DSC).

This chapter is based on the following publication:

Jennifer Noro, Tarsila G. Castro, Artur Cavaco-Paulo, Carla Silva, α -chymotrypsin catalyses the synthesis of methotrexate oligomers, *Process Biochemistry*, 98 (2020) 193-201.

4.1. Introduction

The synthesis of polymeric drugs is an area with increasing interest for the pharmaceutical industry that aims to improve their pharmaceutical performance mainly for applications requiring a drug-controlled delivery. The controlled release, the improvement of safety and the biodistribution profile, are some of the benefits associated to the application of polymeric drugs [67]. The promising results obtained so far in clinical trials using polymer-anticancer drug conjugates have been raising the interest in the development of these type of drugs [68]. The conjugation of poly(ethylene glycol) (PEG) with drugs is one of the most studied strategies for the synthesis of polymer-drug conjugates, being that some of the developed products have already reached the market [69]. Recently, Suksiriworapong *et al.* [70], synthesized a methotrexate-poly(glycerol adipate) conjugate, with improved toxicity for Saos-2 cells than the unmodified methotrexate.

The polymer-drug conjugates or polymeric drugs are expected to be easily hydrolysed *in vivo*, depending on the type of bond established between the polymer and the drug or among the drug monomer units. Prodrugs containing amide bonds are highly stable *in vivo*, being hydrolysed by carboxylesterases [71], peptidases, or proteases [72]. Proteases are enzymes commonly used for the hydrolysis of amide bonds between two amino acids. Despite their hydrolytic activity, they are also able to catalyse the inverse reaction, e.g., the formation of amide bonds (peptides) [73]. The chemoenzymatic peptide synthesis is considered as a green chemistry practice to replace the typical methods, liquid, or solid phase peptide synthesis [74], taking advantage of the low costs associated with the use of proteases as catalysts [75]. Enzymes like papain, chymotrypsin, bromelain, trypsin and even lipase can be used as catalysts of these type of reactions [73]. Qin *et al.* [75] studied the use of papain for the biosynthesis of perfectly alternating oligopeptides. They started by the synthesis of the dipeptide AG-OEt, followed by the addition of papain and a short incubation period, isolating a peptide with a maximum of 21 AG units. The authors mentioned that an accurate choice of the ideal protease is crucial to afford oligomerization. This selection is essential to avoid hydrolysis and/or transamidation reactions during the process. The protease selection should rely on the specificity of the enzyme, determined by its specific hydrolytic properties between two amino acids. Following the same approach, the authors [76] studied the ability of α -chymotrypsin on the oligomerization between dipeptide KL-OEt. The selection of the protease relied on its high specificity for the hydrolysis between -LK- residues. After synthesis of the dipeptide KL-OEt, the α -chymotrypsin was added, forming the expected oligomer. At a specific pH the enzyme triggered the formation of an hydrogel due to the spontaneous self-assembling of

the KL chains into β -sheets. When papain was used for the same purpose, no hydrogel was formed, and a random sequence of oligopeptides was produced. The low selectivity of papain for the hydrolysis of -LK- bonds was responsible for the low reactional outcome.

Methotrexate is a commercially available drug for the treatment of several cancers, auto-immune diseases, and rheumatoid arthritis [1]. However, this drug presents several limitations, such as poor solubility in water, low resistance, high toxicity, and diverse side-effects associated to its administration [77]. Due to the presence of both amine and carboxylic acid groups in its structure, this compound represents an excellent template for peptide bond formation. The conjugation of MTX with polymers is a well explored strategy [9, 70, 78], however, as far as we know, its self-polymerization has never been explored. The practical application of an oligomeric MTX is envisaged to decrease several adverse side effects associated to its administration like its toxicity and cell resistance [79].

In this work, we explored for the first time the ability of α -chymotrypsin to catalyse the oligomerization of methotrexate. The main goal was to produce an oligomeric drug with improved properties in comparison to the monomeric commercial alternative. Molecular dynamics simulations were performed to evaluate the affinity of methotrexate monomer, dimer and trimer, to the protease active site. The resulting oligomers were fully characterized by NMR (^1H and ^{13}C), MALDI-TOF, ESI and DSC.

4.2. Materials and methods

4.2.1. Materials

All compounds were purchase from Sigma-Aldrich or TCI chemicals, and used without further purifications. α -chymotrypsin from *bovine pancreas* type II, was purchase from Sigma-Aldrich, and used without any further treatment.

4.2.2. General procedure for the synthesis of oligomeric methotrexate.

To a solution of MTX di-sodium salt (10 mg) in distillate water (1 mL) was added NaOH until pH= 9-10. α -chymotrypsin was then added to the reaction (1 mg) suspended in 200 μL of water. The solution was placed in a water bath at 50 $^{\circ}\text{C}$, 100 rpm for 7 days. After this time, the enzyme was removed by centrifugation at 2500 g using vivaspin 10 kDa (Sartorius).

4.2.3. Activity of α -chymotrypsin

The activity of α -chymotrypsin was measured using the universal protease activity assay, with casein as substrate [80]. The activity was calculated by the tyrosine units hydrolysed by the protease, detected at 660 nm after colorimetric reaction with Folin & Ciocalteu's phenol reagent. Value of activity obtained: 0.61 U/mg. The values of the activity were given as Units (U) of tyrosine per milligram of protease. The activity of the α -chymotrypsin in the medium along time was evaluated by incubating the enzyme under the same reactional conditions for the synthesis of the oligomers, without addition of the methotrexate. At different periods of time, an aliquot of the solution was removed, and the activity was measured as mentioned.

4.2.4. Nuclear Magnetic Resonance spectroscopy (NMR)

^1H and ^{13}C NMR spectroscopy were performed using a Bruker Avance III 400 (400 MHz for ^1H , 100 MHz for ^{13}C), using DMSO-d_6 or D_2O (Cortecnet, France) as deuteride solvent and the peak solvent used as internal reference. Heteronuclear single quantum coherence spectroscopy (HSQC) and heteronuclear multiple bond correlation (HMBC) were also performed for an accurate signal assignment. Signal multiplicity was given as: s (singlet), d (doublet), dd (doublet of doublets), t (triplet) and m (multiplet).

NMR characterization of the isolated oligomeric methotrexate: ^1H NMR (D_2O): δ_{H} 1.98-2.08 (m, 1H), 2.13-2.21 (m, 1H), 2.32 (t, $J = 8.0$ Hz, 2H), 3.21 (s, 3H), 4.31 (dd, $J = 8.8, 4.4$ Hz, 1H), 4.83 (s, 2H), 6.92 (d, $J = 9.2$ Hz, 2H), 7.75 (d, $J = 8.8$ Hz, 2H) and 8.42 (s, 1H) ppm.

^{13}C NMR (D_2O): δ_{C} 28.5 (CH_2), 34.3 (CH_2), 38.5 (CH_3), 55.4 (CH_2), 55.9 (CH), 111.9 (CH), 120.7 (C_q), 128.4 (C_q), 129.0 (CH), 146.9 (CH), 147.7 (C_q), 151.9 (C_q), 155.6 (C_q), 163.7 (C_q), 169.7 ($\text{C}=\text{O}$), 172.7 (C_q), 179.3 ($\text{C}=\text{O}$) and 182.4 ($\text{C}=\text{O}$) ppm.

4.2.5. Matrix-Assisted Laser Desorption/Ionization Time-of-Flight (MALDI-TOF)

MALDI-TOF mass spectra were acquired on a Bruker Autoflex Speed instrument (Bruker Daltonics GmbH) equipped with a 1 kHz solid-state smartbeam laser. The samples were prepared as reported [79] using 2,5-dihydroxybenzoic acid (DHB) as matrix, and analysed in the linear negative mode. The number average molecular weight (M_n), weight average molecular weight (M_w), polydispersity ($\text{PDI} = M_w/M_n$) and average and maximum degree of polymerization (DP_{avg} and DP_{max}) were calculated using the data obtained from the MALDI spectra [81].

The conversion rate (p) was calculated based on Carothers equation, using the DP_{avg} value obtained by MALDI-TOF.

$$\text{Carothers equation: } DP_{avg} = \frac{1}{1-p}$$

4.2.6. Electrospray Ionization (ESI)

Electrospray ionization was performed in a mass detector Thermo Finnigan LxQ (Linear Ion Trap). The analysis was made using a mass detector susceptible of analysis in full scan mode with negative ionization. The mass spectra range was between m/z 50 and 2000 and a capillary voltage of 29 V was used. Samples were prepared using ultrapure water (Milli-Q) and methanol (HPLC grade, Fisher Chemical). Prior to analysis, the sample was filtrated using a 0.2 μm filter (Whatman).

4.2.7. Differential Scanning Calorimetry (DSC)

All measurements were conducted on a power-compensated DSC instrument (DSC 6000 Perkin Elmer) with a nitrogen flux of 20 mL/min, using stainless steel capsules in the temperature range of 20-300 °C (heating rate: 10 °C/min, sample weight: 1-2 mg). The DSC device was calibrated using indium and zinc, both of high purity. The samples were freeze-dried for 24 h prior to the analyses and each sample was measured at least three times, in order to validate the results.

4.2.8. Molecular Dynamics Simulations and docking

Bovine α -chymotrypsin, PDB ID: 1OYG [82], with 2.2 Å resolution, comprising residues 1-245, was chosen for the modelling experiments in this work.

PROPKA (built-in PDB2PQR server) [83] was used to assign the amino acids protonation states at pH 9.5. GROMACS tool pdb2gmx permits to set the protonation state for titratable amino acids. At pH 7 the default protonation distribution was used and at pH 9.5 we modify the protonation of N -terminal and residues LYS, ARG and HIS, making them neutral, according to PROPKA prediction. Wild type α -chymotrypsin was modelled in water with the simple point charge water model in a cubic box with a hydration layer of at least 1.5 nm between the peptide and the walls. At pH 7, we added Cl^- ions to neutralize the simulation box. At pH 9.5, we also added Na^+ to mimic the experimental environment, in which the basic pH was obtained by the addition of NaOH.

One stage of energy minimization was performed using a maximum of 10000 steps with steepest descent algorithm. The systems were initialized in a NVT ensemble, using V-rescale algorithm [84], with the coupling constant $\tau_T = 0.10$ ps, to control temperature at 310 K in pH 7 and 323 K at pH 9.5. After that, an NPT initialization step was performed, with V-rescale [84] and Parrinello-Rahman barostat [85] algorithms to couple temperature and pressure at 310 K or 323 K and 1 atm, respectively, with the following coupling constants: $\tau_T = 0.10$ ps and $\tau_P = 2.0$ ps. 50 ns of Molecular Dynamics Simulation was performed for α -chymotrypsin at both temperatures and pHs, to investigate the conditions that stabilize better this enzyme. All simulations were performed using the GROMACS 5.1.5 version [86], within the GROMOS 54a7 force field (FF) [87, 88]. The Lennard-Jones interactions were truncated at 1.4 nm and using particle-mesh Ewald (PME) [89] method for electrostatic interactions, also with a cut-off of 1.4 nm. The algorithm LINCS [90] was used to constrain the chemical bonds of the enzyme and the algorithm SETTLE [91] in the case of water. Optimized 3D-structure and charges for MTX monomer, dimer and trimer were achieved with gaussian 09 [92], through semi-empirical PM6 [93] calculations. These quantum parameters obtained for MTX monomer and oligomers, with gaussian, were sufficient to generate *pdbqt* files required for docking calculations.

From MD simulations, the trajectories were analysed looking at the RMSD (Root Mean Square Deviation) to understand the stability of α -chymotrypsin in both conditions of temperature and pH. We also look at the electrostatic surface potential generate with PDB2PQR server and APBS plugin for PyMOL, to perceive the positive and negative areas that can interfere in MTX binding.

One-to-one binding model was considered to evaluate individually each MTX molecule to the target α -chymotrypsin.

Docking experiments were performed with AutoDock 4.0 [94] and prepared with the AutoDock Tools Software [94]. The middle structure obtained for the native α -chymotrypsin, from the MD simulation at pH 9.5 and 323 K, were used as target macromolecule for the docking experiments. A grid box was set according to the size of the oligomer, ranging from 50x50x50 to 80x80x100 in the case of trimer, with a resolution of 0.375 Å. The grid box was centered in the active site - catalytic triad - and grid potential maps were calculated using AutoGrid 4.0. We chose Lamarckian Genetic Algorithm (LGA) [94, 95] as search algorithm. Each docking consisted of 150 independent runs, with a population of 150 individuals, a maximum number of 25×10^5 energy evaluations for MTX monomer and 25×10^6 energy evaluations for dimer and trimer (due the torsions of the

oligomers), and a maximum number of 27,000 generations. Additionally, the binding site preference and interactions were identified through the AutoDock tools.

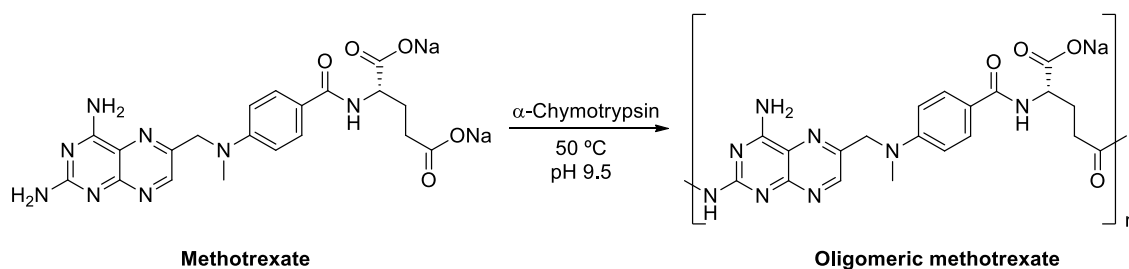
We analysed docking results looking at the binding energy and the Ligand Efficiency (LE), which measures the binding energy per ligand heavy-atom (kcal/HA) to understand how the increase in the oligomer size contributes to the binding.

4.3. Results and discussion

4.3.1. α -Chymotrypsin-catalysed synthesis of oligomeric MTX

The use of proteases as polymerization tools for the synthesis of peptides is being explored by several researchers [75, 76]. Considering the chemical structure of methotrexate, composed by two carboxylic acids and two primary aromatic amines, we considered it as a promising template to evaluate the polymerase activity of α -chymotrypsin (**Scheme 4.1**). Moreover, the production of a polymeric drug would represent a promising strategy for the pharmaceutical industry regarding its increased interest in the commercialization of these type of drugs [96]. As an amide prodrug, the oligomeric MTX is expected to have higher stability in the human body than the monomeric structure. Moreover, the amide linkages of the oligomeric units, being more prone to hydrolysis by enzymatic action, would improve drug metabolism and decrease dosage administration [97, 98]. The improved metabolism is expected to result in a less toxic drug with lower side effects than the commercial monomeric specie [97, 98].

Methotrexate di-sodium salt was used as starting material to ensure water solubility and provide hydrophilic character to the produced oligomers.



Scheme 4.1. Reactional scheme for the oligomerization of methotrexate.

α -Chymotrypsin was chosen for the MTX oligomerization based on its well-known ability to polymerize peptides [76], and its high selectivity for the hydrolysis of aromatic amino-acids, such

as tyrosine, phenylalanine, and tryptophan [99]. The reactional conditions, namely temperature, pH, and time, were optimized to achieve the maximum oligomerization degree (**Table 4.1**).

Table 4.1. Reactional conditions tested for the α -chymotrypsin-assisted synthesis of methotrexate oligomers

Entry	Temperature	pH	Time ^[a]	Methotrexate oligomers ^[b,c]
1	RT	7	1 week	1
2	50 °C	7	1 week	1
3	50 °C	7.8	1 week	1
4	50 °C	9.5	48 h	3
5	50 °C	9.5	72 h	3
6	50 °C	9.5	96 h	5
7	50 °C	9.5	1 week	6
8	50 °C	9.5	2 weeks	6
9	50 °C	9.5	1 week	1 ^[d]

^[a]Maximum time tested.

^[b]Detected by MALDI-TOF, where 1 unit corresponds to the monomer.

^[c]Maximum oligomeric units detected.

^[d]Control reaction without enzyme.

Most of the proteases have an optimum working pH between 7.0-9.0. Based on this feature, on the low basicity of the aromatic amines and on the lack of reactivity of the pteridine ring, the reactions were conducted under basic medium. Similarly to the previously observed by Qin and co-workers [76] for the synthesis of $-(KL)_x-$ peptides catalysed by α -chymotrypsin, we confirmed that no oligomers were produced when the reactions were carried out at neutral pH (**Table 4.1**, entries 1-3). For an efficient reaction synthesis, it was critical to perform the reactions at alkaline pH, using NaOH as base (≈ 9.5 , **Table 4.1**, entries 4-8). The best reactional outcomes were obtained herein when performing the reactions at 50 °C, which is in accordance with the optimum temperature postulated by other authors for the same protein [100].

During reaction, samples were withdrawn, and continuously monitored by MALDI-TOF, until 2 weeks of reaction (**Table 4.1**, entries 4-8). The best reactional outcome was achieved after 1 week of reaction with the formation of oligomers composed by 6 monomeric units (DP_{max}). Longer reactional times led to the recovery of similar-sized MTX oligomers, however in lower amount. The DP average calculated (1.5) indicates that the most abundant specie in the reactional medium was the methotrexate dimer, confirmed by MALDI-TOF and ESI (**Table 4.2**). After one week of reaction, the enzyme converted 33 % of the monomer molecules into oligomers, while the reaction carried

out in the absence of enzyme did not lead to the formation of any oligomeric species (**Table 4.1**, entry 9 and **Table 4.2**).

Table 4.2. Conversion rate (%), average and maximum degree of polymerization (DP_{avg} and DP_{max}) analysed by MALDI-TOF and electrospray ionization (ESI), for the oligomerization of methotrexate, with and without α -chymotrypsin

	With α -chymotrypsin	Control (without enzyme)
Conversion rate ^[a]	33.4 %	0 %
DP_{avg} ^[b]	1.5	1
DP_{max} ^[b]	6	1
ESI	975.4 g/mol ^[c]	453.28 g/mol ^[d]

^[a]Calculated by the Carothers equation.

^[b]Calculated by MALDI-TOF.

^[c]Most abundant specie, corresponding to the dimer. MW dimer= 956.8, where in ESI: 975= 956 + Na⁺ - 4H⁺.

^[d]Monomer MW= 454 g/mol or 498 g/mol (di-sodium form), where in ESI: 453= 454 - 1H⁺.

In order to ensure an efficient oligomerization, it was imperative to infer the maintenance of the basic pH during reaction. For this, the pH was continuously monitored and after 1 week of reaction, one observed a pH decrease from 9.5 to 8, and to 7.5, after 2 weeks. We may assume that as the reaction occurs, the NaOH was consumed by the low basic amines in the pteridine ring, which were deprotonated, leading to a pH decrease. The addition of NaOH was crucial to increase the amines reactivity and proceed with the oligomerization.

It was noteworthy that the activity of α -chymotrypsin remained almost unaltered during the first week of reaction (activity of 0.61 U/mg), decreasing only 15 % after 2 weeks (activity of 0.52 U/mg). The high stability of the catalyst ensured the efficient catalysis for longer periods of incubation.

4.3.2. Synthesis of dimeric MTX – proposed mechanism

Methotrexate, mainly composed by aromatic rings, is presented herein as a suitable substrate for α -chymotrypsin. Based on the data obtained, we have proposed a mechanism for the synthesis of a dimeric unit of methotrexate catalysed by α -chymotrypsin (**Figure 4.1**). The reaction is predicted to start by the nucleophilic attack of the OH terminal group of the serine, in the catalytic triad, to one of the carboxylic groups of MTX (step 1), leading to the formation of the tetrahedral

intermediate (step 2). The carboxylic group in the glutamic moiety, which suffers the nucleophilic attack as depicted in **Figure 4.1**, is reported as the most reactive [79]. This carboxylic group is also less sterically precluded, which is an important feature to afford oligomerization and an effective catalysis by the protease. After release of a water molecule, an MTX-enzyme complex is formed, through the formation of an ester bond between MTX and the serine residue of the catalytic triad. This reactive bond easily suffers a nucleophilic attack by one of the amines in the pteridine ring of another MTX unit (step 3). The dimeric MTX is then formed and released from the enzyme, where the catalytic triad of α -chymotrypsin is restored (step 4).

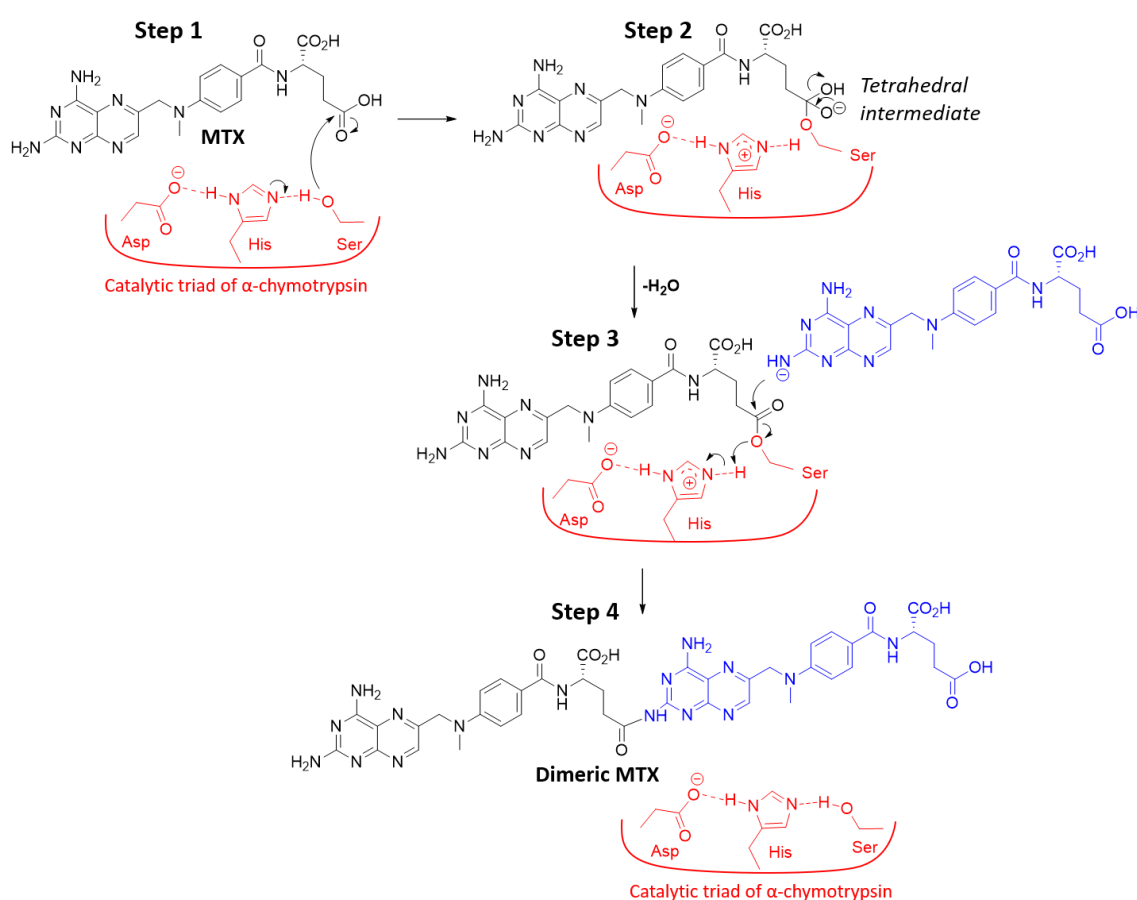


Figure 4.1. Proposed mechanism for the synthesis of a dimeric unit of methotrexate catalysed by α -chymotrypsin.

Considering the data previously described, we may predict that the reaction was not restricted to the synthesis of dimeric units, but it can go further to longer species ($DP_{max}=6$). The size of the oligomers was however dependent on the affinity of MTX oligomers to the enzyme' active site. Regarding the data obtained, we may infer that α -chymotrypsin was able to synthesize species until

a maximum of 6 MTX units. However, longer species were hampered to be synthesized due to stereochemical constraints resulting from the molecular weight of MTX (498 g/mol), which is comparably higher than the natural substrates of this enzyme (amino acids, peptides).

For a better understanding of these findings, molecular dynamics simulations were performed to evaluate the affinity of MTX and oligomeric MTX to the active site of the enzyme and evaluate the role of the substrate size on the enzyme activity.

4.3.3. Molecular Dynamics Simulations

Bovine α -chymotrypsin (PDB ID: 1OXG) [82] was evaluated under different conditions of temperature and pH during Molecular Dynamics (MD) Simulations. Firstly, the enzyme was evaluated at 310 K and physiological pH, then at 323 K and pH 9.5; this second simulation was performed to mimic the experimental conditions used. RMSD results (**Figure 4.2A**), indicate that the experimental conditions established are the ideal to study the enzyme behaviour, since the enzyme demonstrates to be more stable at the higher temperature and pH. **Figure 4.2B** shows the α -chymotrypsin crystallographic structure (**I**) highlighting the active site, where the catalytic triad composed by His57, Asp102 and Ser195 takes place, and the electrostatic distribution for this enzyme (**II**).

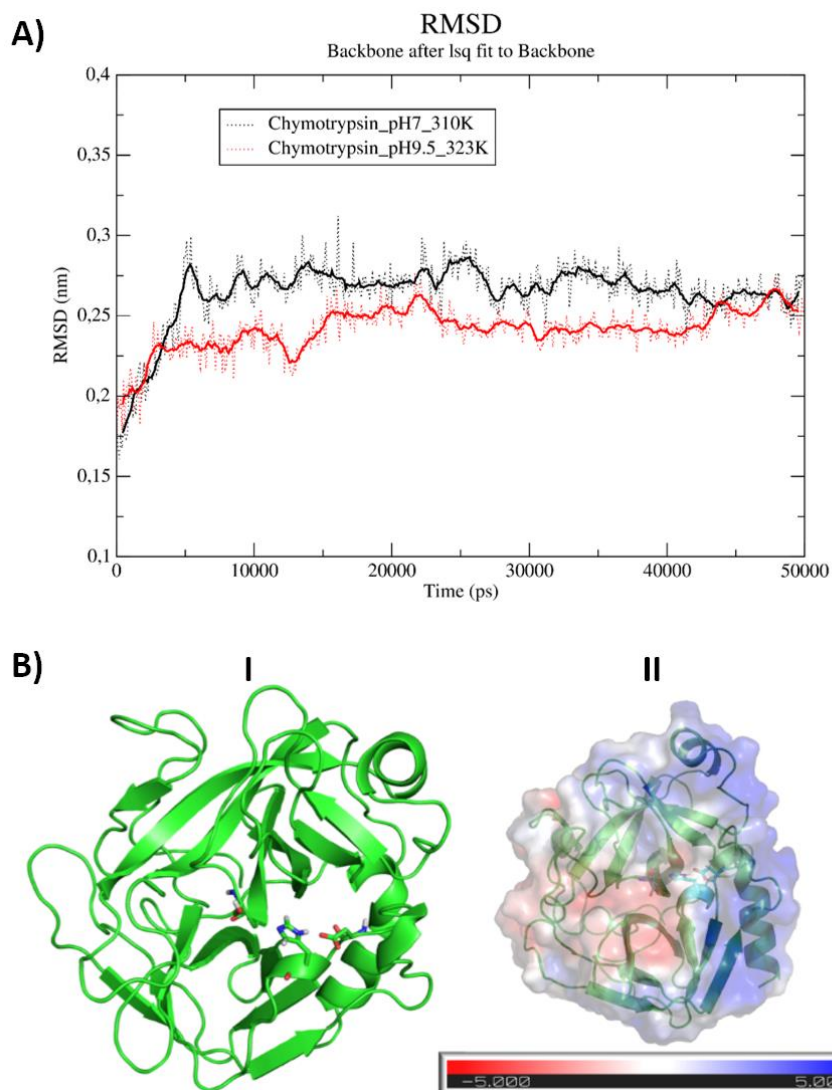


Figure 4.2. **A)** Backbone RMSD of α -chymotrypsin, simulated at 310 K and physiological pH (black trace), and at 323 K and pH 9.5 (red trace), from the initial 3D structure (10XG); **B)** 3-D structure of bovine α -chymotrypsin (PDB ID: 10XG), from X-ray diffraction (**I**), highlighting in stick representation the catalytic triad: His57, Asp102 and Ser195. Green for carbon, blue for nitrogen, red for oxygen and white for hydrogens; (**II**) shows the electrostatic distribution, where blue corresponds to positive areas and red to negative ones.

MTX and MTX oligomeric structures were predicted at PM6 level [93], a semi-empirical method that performs geometry optimization and charge distribution, making the structures suitable to be used for molecular docking. In the case of MTX, the neutral and negative forms (at pH 9.5) were evaluated. The structures presented in **Figure 4.3** were used in Molecular Docking experiments.

Overall, monomer (MTX), dimer and trimer have an increasing flexibility due to the increasing number of torsions. Dimer and trimer (**Figure 4.3**, C-D) optimized with PM6, can undergo more "bent" conformations when submitted to docking, due to the higher number of torsions.

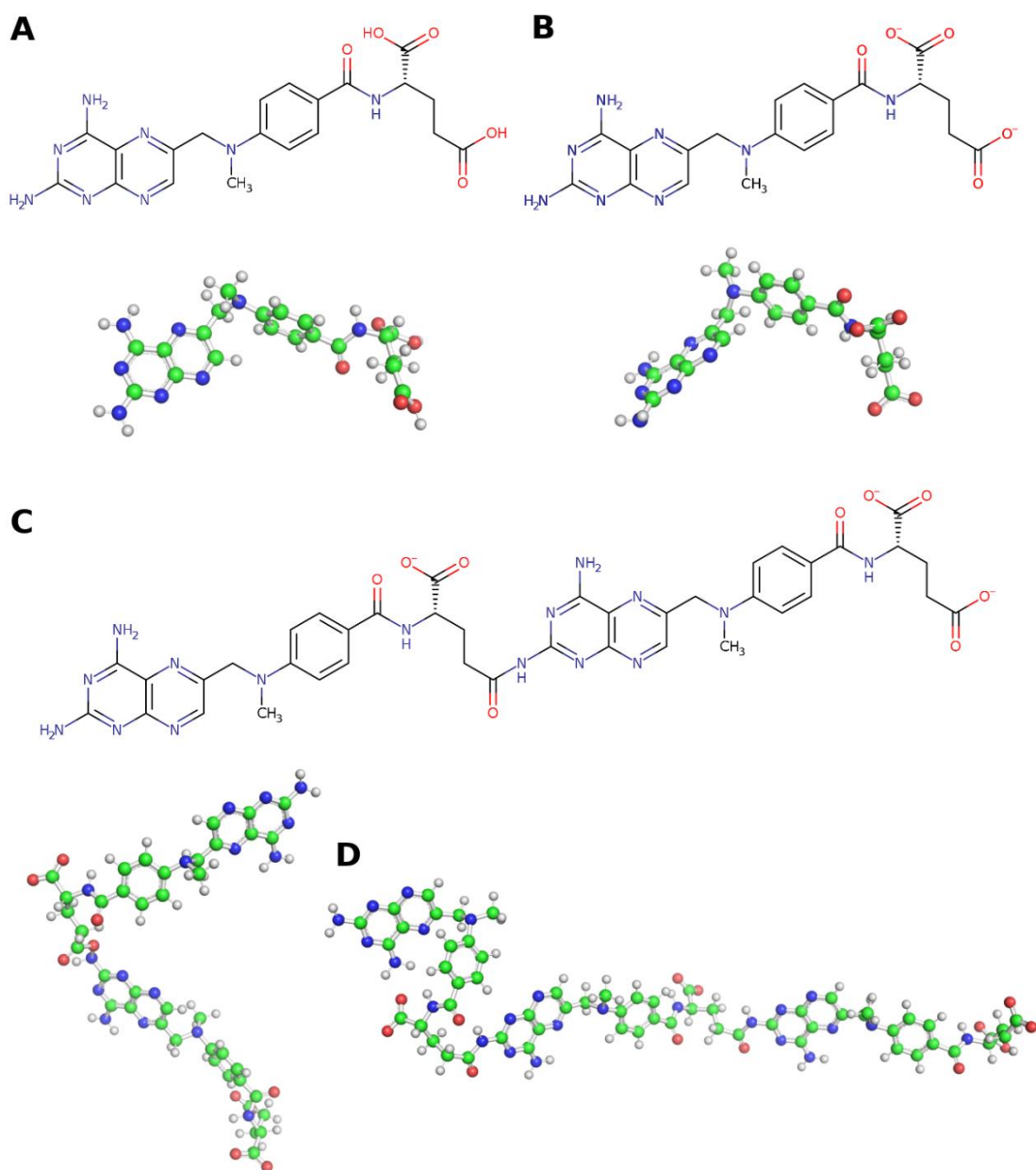


Figure 4.3. A) Skeletal and 3-D methotrexate (MTX) structures at pH 7.0 and B) the deprotonated forms at pH 9.5. C) skeletal and 3-D structures of MTX dimer, at pH 9.5 and D) shows the trimer 3-D representation. The colour scheme use green for carbon, blue for nitrogen, red for oxygen and white for hydrogen.

Docking experiments were conducted in order to understand the interactions between MTX and α -chymotrypsin, and the role of this enzyme in the synthesis process. We selected an area that enwrap the active site with enough space to comprise the MTX units (monomer, dimer or trimer) to dock. **Figure 4.4** shows the correlation between the MTX and the enzyme, and the binding energy involved for each case studied.

MTX complexed with α -chymotrypsin, presented a binding energy of -6.94 kcal/mol (-29.04 kJ/mol) and a Ligand Efficiency (LE) of -0.19 kcal/HA (-0.79 kJ/HA). The monomer has hydrogen bonds with Ala56, Gly59, Ser96, Tyr94 and Thr104, and van der Waals interactions were found with His57 and Asp102. For dimeric MTX, Gly59 and Tyr94 were also involved in hydrogen bonds, as well as Lys90 and Asn95. The binding energy was -6.35 kcal/mol (-26.61 kJ/mol) in this case, and a LE of -0.1 kcal/HA (-0.42 kJ/HA). His57 was still a close contact for MTX dimer.

The trimer binds to the enzyme with -5.45 kcal/mol (-22.80 kJ/mol) and LE of -0.06 kcal/HA (-0.25 kJ/mol). Similarly, His57 and Asp102 interact with the trimer. In addition, five hydrogen bonds were found, two with Ser96 and the others with Leu97, Asn91, and Thr104. In all the three cases, electrostatics interactions were also present, between the carboxylic acids of MTX and the positive region observed in **Figure 4.2B II**.

Farhadian and co-workers recently reported docking experiments with α -chymotrypsin [101, 102]. However, the complexes were not formed in the active site, where the catalytic triad take place. Some other works addressing the docking near the catalytic site do not reveal the complex binding energy for the association of a molecule to the protein [103, 104]. Other larger molecules have been described to efficiently bind to α -chymotrypsin, however these molecules are used as inhibitors, and therefore cannot be compared to our work [104]. The lack of similar docking approaches makes it difficult to compare our binding preferences and energies with other studies. Moreover, the conversion of the binding energy to association constants is also hard to obtain. In docking experiments, the protein is static, the whole long-range electrostatics is not considered, and no water molecule is present. Therefore, the use of the equation $\Delta G = -RT \ln K_a$, would lead to a rough approximation.

All these interactions demonstrate the ability of MTX to bind to the protease active site, leading to the formation of oligomeric MTX. Even though being possible more interactions of longer MTX forms with the protease, the binding energy decreases discretely as well as the LE per heavy-atom. One may infer that this was due to the energy penalties resulting from the increased number of torsions and desolvation of the bulky forms of MTX (dimer and trimer), since they can undergo

more conformations, as previously observed during docking experiments. The results indicated a decrease of the binding energy as the oligomer chain grows, justifying that only a maximum of 6 units of MTX could be biosynthesized by α -chymotrypsin.

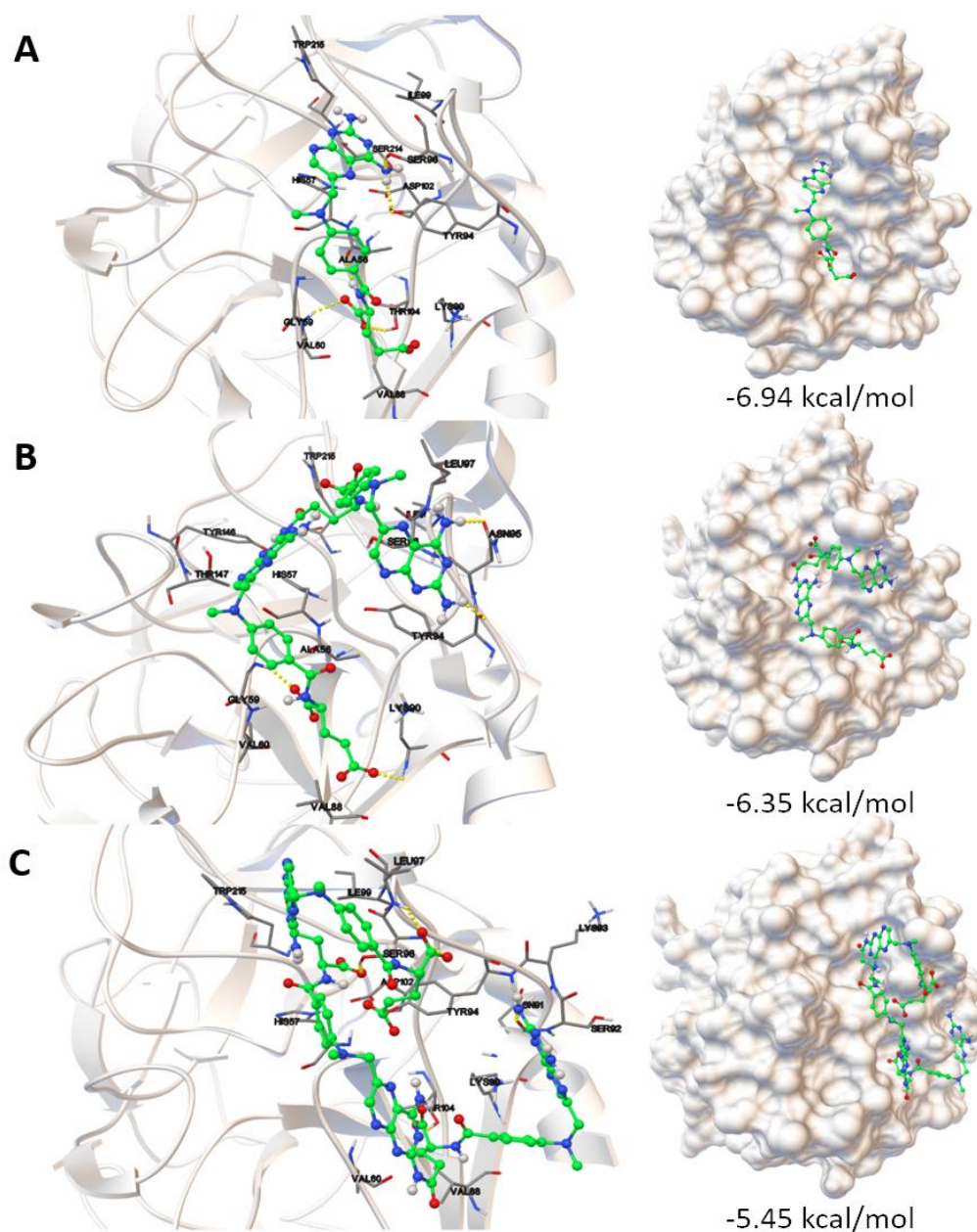


Figure 4.4. Docking poses showing the interaction of α -chymotrypsin with the different methotrexate species, and the respective binding energies obtained using AutoDock 4.0: **A)** α -chymotrypsin with methotrexate; **B)** α -chymotrypsin with dimeric methotrexate and **C)** α -chymotrypsin with trimeric methotrexate. Surface/cavities representation are in the right panel. Enzyme is represented in light grey, hydrogen bonds in yellow dashes and methotrexates following the scheme previous described in Figure 4.3.

4.3.3.1. NMR Spectroscopy

By ^1H NMR spectroscopy, it was possible to identify differences between MTX oligomers and the starting material (monomer). In the spectra of free MTX, the signals appeared at δ_{H} 8.56, 8.13 (NH), 7.62, 7.38 (NH), 6.81, 6.58 ppm (NH_2), in the aromatic region (**Figure 4.5A**). The spectra of oligomeric MTX (**Figure 4.5B**) show significant chemical shifts in the pteridine ring, δ_{H} 8.15 (**b**), 8.14 (NH), 7.62, 6.78 ppm. The pattern of the signals remained the same as in the monomer MTX, confirming that the amide bond (near proton **g**) was not hydrolysed by the protease during the oligomerization reaction.

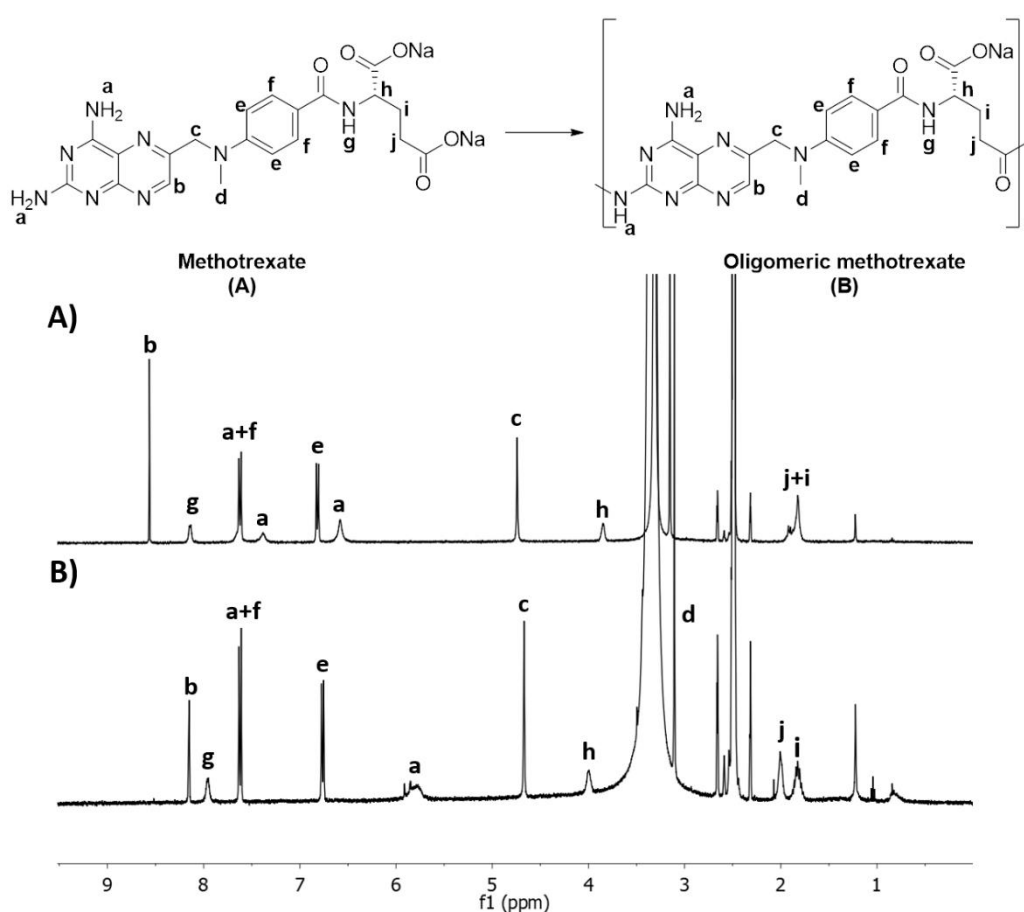


Figure 4.5. ^1H NMR ($\text{DMSO-}d_6$) spectra of **A)** methotrexate and **B)** oligomeric methotrexate synthesized by α -chymotrypsin.

4.3.3.2. MALDI-TOF and ESI

MALDI-TOF spectra displays the pattern of MTX oligomers, catalysed by α -chymotrypsin (**Figure 4.6B**), and of the control reaction without enzyme, showing the peak of the monomer below m/z 500 (**Figure 4.6A**). By ESI the ion peak corresponding to the monomer was observed at m/z 453

(Figure 4.6 C) and no fragmentation was detected. The most abundant specie detected by ESI on the samples catalysed by α -chymotrypsin is a dimer (Figure 4.6 D).

Regarding the oligomer spectrum (Figure 4.6B), (MTX)₁ was observed at 475 Da [498-Na⁺], whereas a repetitive pattern of m/z of \approx 521 Da was detected. This behaviour was observed until a maximum m/z of 3106.45 Da, attributed to the longest oligomer obtained composed by 6 MTX units. The repeating unit between species (\approx 521 Da) corresponds to the tri-sodium methotrexate, most probably resulting from the presence of the NaOH on the reactional medium, which may be linked to more than one amine in the pteridine ring. Additional sodium was also found on the recorded ESI spectra of the oligomer. In Table 4.3 are summarized the results expressed in terms of number average molecular weight (M_n), weight average molecular weight (M_w) and PDI (M_w/M_n). The oligomers produced by the protease showed a M_n value of 724.8 g/mol and a M_w of 1225.7 g/mol. The polydispersity index obtained was 1.69, showing some sample heterogeneity.

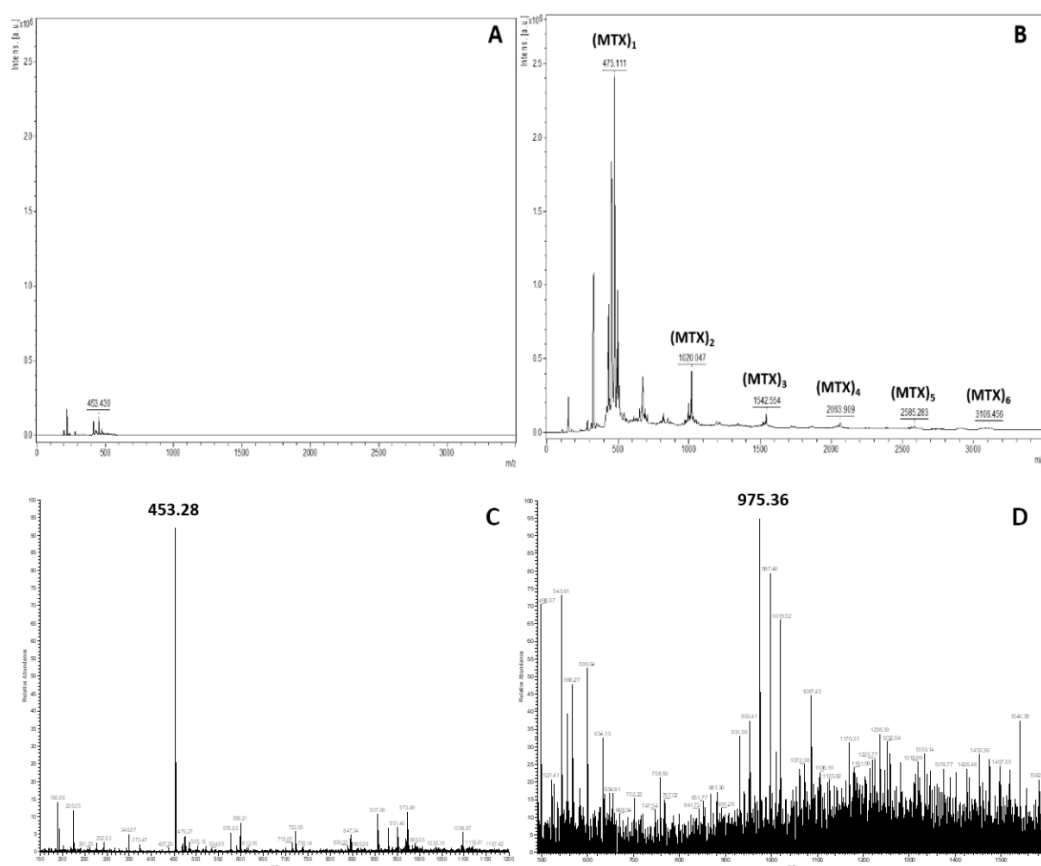


Figure 4.6. MALDI-TOF spectra of: **A)** control reaction carried without enzyme, and **B)** oligomeric methotrexate synthesized by α -chymotrypsin, and ESI spectra of: **C)** monomeric methotrexate and **D)** oligomeric methotrexate where the most abundant specie (100 %) is observed at m/z 975.36 corresponding to the dimeric MTX.

Table 4.3. Number average molecular weight (M_n), weight average molecular weight (M_w), polydispersity (PDI), average and maximum degree of polymerization (DP_{avg} and DP_{max}) of the obtained oligomeric methotrexate catalysed by α -chymotrypsin at 50 °C after 1 week

	Oligomeric methotrexate
DP_{avg}	1.5
DP_{max}	6
M_n	724.8
M_w	1225.7
PDI	1.69

4.3.3.3. DSC

The DSC analysis highlights differentiated thermal behaviour depending on the size of the MTX oligomers (**Figure 4.7**). The monomeric MTX showed a melting point at 139 °C (black line) and no other thermal events were observed at higher temperatures. As the chain length grows, higher melting points were expected. The oligomers synthesized by the protease (grey line), showed a melting point at 184 °C.

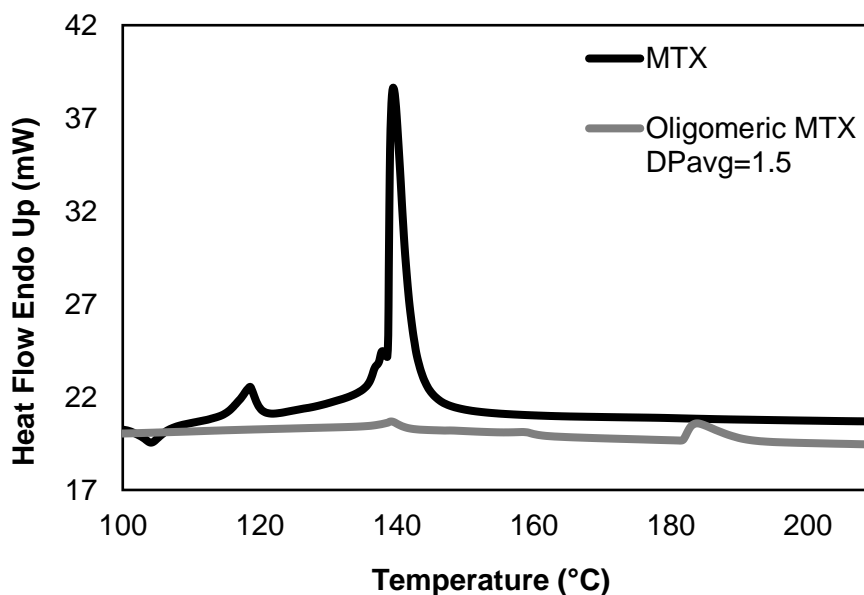


Figure 4.7. Differential scanning calorimetry (DSC) curves of methotrexate (MTX) and oligomeric methotrexate; the black line corresponds to the monomer; the grey line corresponds to oligomeric MTX synthesized by α -chymotrypsin.

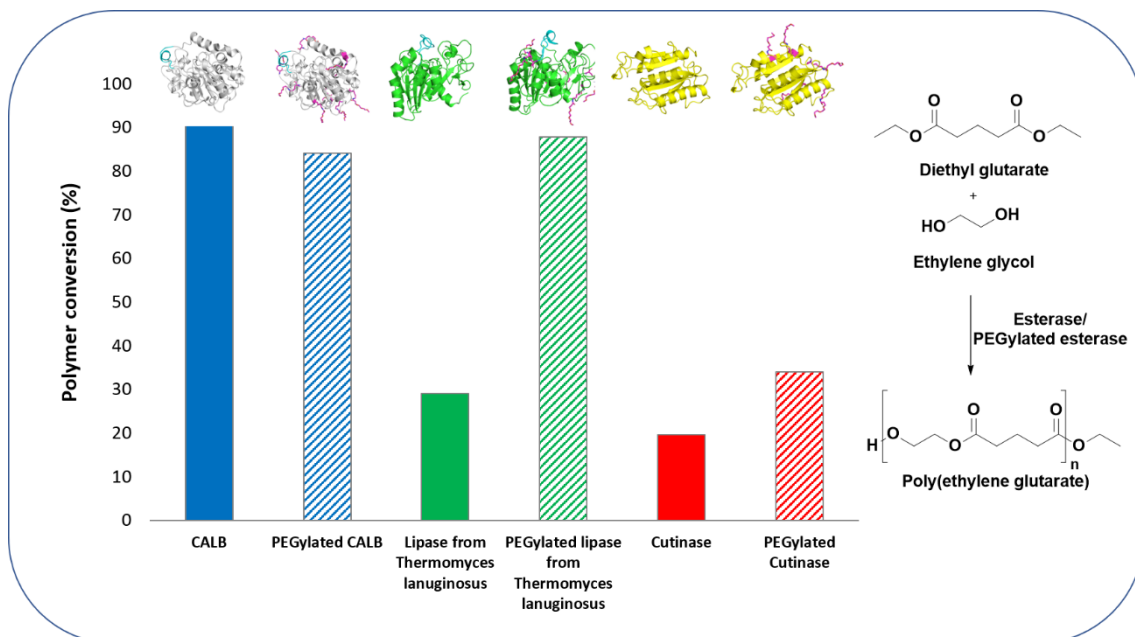
4.4. Conclusions

In this work the synthesis of MTX oligomers assisted by α -chymotrypsin was explored for the first time. The oligomeric species obtained were predominantly small (dimers) due to the size of the monomer (MTX, MW= 498 g/mol), which imparted stereochemical impediments to the active site. Operational conditions like temperature (50 °C) and pH (9-10) were found critical for the efficient oligomerization. Molecular dynamics simulations confirmed that as the oligomeric chain grows, its accommodation in the active site was hindered, which was evidenced by a decrease of the binding energy associated (-6.94 kcal/mol for the monomer and -5.45 kcal/mol for the trimer). The data also revealed that α -chymotrypsin was able to synthesize oligomeric species with 6 units, however in a lower extent (33 %).

α -chymotrypsin is presented herein as a versatile catalyst for oligomer synthesis, even for substrates that are not naturally catalysed by it, like methotrexate. Moreover, the oligomerization of this drug would represent an alternative route for the treatment of many diseases, by reducing some side effects associated to the monomer administration.

Chapter V

Catalytic activation of esterases by PEGylation for polyester synthesis



Catalytic activation of esterases by PEGylation for polyester synthesis

Abstract

In this work we explored PEGylation as an efficient strategy to improve esterase's catalytic performance. For this, we PEGylated three esterases, namely lipase from *Candida antarctica B* (CALB), lipase from *Thermomyces lanuginosus* (TL) and cutinase from *Fusarium solani pisi* (CUT) and evaluated their catalytic performance by using the biosynthesis of poly(ethylene glutarate) as model reaction. After PEGylation with a 5 kDa aldehyde-PEG, CALB and cutinase revealed an increase of activity against *p*-nitrophenyl butyrate hydrolysis (2-fold of increase for CALB and 4-fold of increase for cutinase). Unmodified and PEGylated lipase TL displayed however similar activity results. The polymerase activity of native and PEGylated esterases was also assessed. The data revealed a higher polymerase activity for the lipase TL and cutinase PEGylated forms (88 % conversion for PEG-lipase TL and 34 % for PEG-cutinase). Molecular dynamics simulations were used to evaluate the effect of PEG on the geometry of the active site of enzymes with lid domain (TL and CALB). These studies corroborate the experimental data revealing a more open active site cavity for the PEGylated catalysts, which favours the catalysis.

This chapter is based on the following publication:

Jennifer Noro, Tarsila Castro, Filipa Gonçalves, Artur Ribeiro, Artur Cavaco-Paulo, Carla Silva, Catalytic activation of esterases by PEGylation for polyester synthesis, ChemCatChem, 11 (2019) 2490-2499.

5.1. Introduction

Protein PEGylation is the term attributed to the covalent bond formed between a protein and a unit of polyethylene glycol (PEG) [105, 106]. In the recent years, the PEGylation of proteins is being widely explored for many applications, due to their associated advantages. PEG is a nontoxic and nonimmunogenic polymer [107] already approved by FDA and classified as generally safe [108]. The attachment of PEG to the surface of a protein or enzyme is a strategy often applied to improve its pharmacokinetic behaviour [109, 110]. This modification results in several physical and chemical changes being the protein's size, the electrostatic binding, the conformation and hydrophobicity the main alterations associated [107]. It has been also described that PEGylation of enzymes may render them soluble in organic solvents maintaining however their catalytic activity [111]. Aiming to increase their stability, the PEGylation of proteins/enzymes is a current practice in the pharmaceutical industry, being some PEGylated-proteins currently available on the market [105].

Despite the improvement of protein's stability, PEGylation is commonly associated to a loss of activity. However, some contradictory examples are also possible to find in the literature. Vandertol-Vanier *et al.* observed that laccase from *Corioloopsis gallica* showed a higher catalytic activity than its native form when conjugated with mPEG [112]. Lee *et al.* PEGylated the interferon Beta-1b by site-specific PEGylation technology and increased their pharmacokinetic and antitumor activities [113]. Su *et al.* studied the effect of PEGylation of laccase from *Myceliophthora thermophila*. The authors observed an increment of the conversion and degree of polymerization when the PEGylated laccase was applied for catechol polymerization [114].

The use of lipases for the catalysis of polyesters has been presented as an excellent alternative to the chemical approaches, generally involving the use of high temperatures and/or expensive and non-environmentally friendly metal catalysts [115]. Lipases are most often not expensive, reusable, and are associated to green chemistry practices [116]. Lipase from *Candida antarctica B* (CALB) is one of the most explored enzymes for the biosynthesis of polyesters due to its unique specificities [117-119]. The lack of need of interfacial activation and the diversity of solvent mediums in which reactions can be performed, are some of the most attractive properties associated.

Despite the broaden applications on several fields, the effect of PEGylation on esterase's activity and stability is still unexplored for synthetic purposes.

In this work, and for the first time, we PEGylated three esterases, namely lipase from *Candida antarctica B*, lipase from *Thermomyces lanuginosus* and cutinase from *Fusarium solani pisi*, and

evaluate their catalytic performance on the biosynthesis of poly(ethylene glutarate), from diethyl glutarate and ethylene glycol. The reactions were carried out in the absence of water using the substrates as reactional medium. Molecular dynamics simulations in organic (reactant mixture) and aqueous medium were assessed in order to study the effect of PEGylation on the lipase's conformation and on the access of the substrates to the active site cavity. A complete characterization of the synthesized oligomers was performed by proton and carbon nuclear magnetic resonance spectroscopy (^1H and ^{13}C NMR), matrix-assisted laser desorption/ionization-time of flight (MALDI-TOF), Fourier-transform infrared spectroscopy (FTIR), differential scanning calorimetry (DSC) and thermogravimetric analysis (TGA).

5.2. Materials and methods

5.2.1. Materials

Lipase from *Thermomyces lanuginosus* (solution, $\geq 100,000$ U/g), lipase from *Candida antarctica* B (0.3 U/mg), *O*-[2-(6-Oxocaproylamino)ethyl]-*O*-methylpolyethylene glycol (PEG, MW 5000 Da), ethylene glycol ($\geq 99\%$), diethyl glutarate ($\geq 99\%$), 2,4,6-trinitrobenzene sulfonic acid (5% (w/v) in H_2O), *p*-nitrophenyl butyrate (*p*-NPB, $\geq 98\%$) and sodium cyanoborohydride (95%) were purchased from Sigma-Aldrich. Tetrahydrofuran (HPLC grade, Fisher Chemical) was used without further purification. Ultrafiltration was performed with Ultracel 10 kDa regenerated cellulose ultrafiltration discs, 47 mm (Millipore) with ultrapure water (Milli-Q). The expression and production of cutinase from *Fusarium solani pisi* (EC 3.1.1.74) was performed following the procedure reported by Araújo *et al.* [120].

5.2.2. Synthesis

5.2.2.1. General procedure for the PEGylation of esterases

The PEGylation of the esterases was performed using the procedure reported by Mayolo-Deloya *et al.* [121]. Briefly, the esterase (12 mg/mL) was solubilized in phosphate (100 mM) and NaBH_3CN (20 mM) buffer (pH= 5.1) followed by the addition of the PEG-aldehyde (esterase 1:4 PEG w/w). The reactional mixture was placed at 4 °C, overnight, under stirring. The separation of the unreacted PEG and buffer was carried out by ultrafiltration using a 10 kDa regenerated cellulose membrane housed in an ultrafiltration device using ultrapure water. The PEGylated esterase was obtained as a white solid after freeze-drying for 2 days.

5.2.2.2. General procedure for synthesis of poly(ethylene glutarate)

Ethylene glycol was added to a 50 mL round-bottom flask, followed by the addition of the diethyl glutarate (equimolar amount) forming a biphasic mixture. The esterase was added, and the suspension was placed in an ultrasonic bath (USC600TH, VWR International Ltd., USA; frequency 45 kHz and power of 120 W) programmed to not exceed the 45 °C. After sonication for 2 hours, the round-bottom flask was transferred to a rotary evaporator (Heidolph, Germany) at 40 °C, 120 rpm, to complete 7 hours of total reactional time. Tetrahydrofuran was added to the reactional mixture and the enzyme was removed by filtration. The solvent was removed in the rotary evaporator and the final solution formed a colourless oil.

¹H NMR (CDCl₃): δ_H 1.23 (t, *J* = 6.8 Hz, CH₃), 1.91-1.96 (m, CH₂), 2.37-2.42 (m, CH₂), 3.78-3.81 (m, CH₂), 4.10 (q, *J* = 7.2 Hz, CH₂), 4.18-4.20 (m, CH₂) and 4.28 (s, CH₂) ppm.

¹³C NMR (CDCl₃): δ_C 14.1 (CH₃), 19.8 (CH₂), 19.9 (CH₂), 20.0 (CH₂), 20.3 (CH₂), 32.7 (CH₂), 32.8 (CH₂), 32.9 (CH₂), 33.0 (CH₂), 33.1 (CH₂), 33.2 (CH₂), 33.3 (CH₂), 60.4 (CH₂), 60.9 (CH₂), 61.9 (CH₂), 62.1 (CH₂), 65.9 (CH₂), 172.5 (C=O), 172.6 (C=O), 172.7 (C=O), 172.8 (C=O), 173.0 (C=O), 173.1 (C=O), 173.2 (C=O), 173.3 (C=O), 176.5 (C=O), 176.7 (C=O) and 176.9 (C=O) ppm.

5.2.3. Enzyme characterization

5.2.3.1. SDS-PAGE

SDS-PAGE electrophoresis of lyophilized esterases was performed by solubilize them in water and the samples were loaded on polyacrylamide Gel Electrophoresis (SDS-PAGE) gel 12.5 %. The gel was stained with Coomassie brilliant blue solution to analyse size and purity.

5.2.3.2. Esterase activity

The activity of all the esterases used was determined by a continuous spectrophotometric assay using *p*-nitrophenyl butyrate (*p*-NPB) as substrate. One unit of enzyme activity was defined as the amount of enzyme which catalyses the production of 1 μmol *p*-nitrophenol per minute. The standard assay was performed at 37 °C in a final volume of 4 mL containing *p*-NPB (6 mM), the enzyme and the assay buffer (K₂HPO₄ buffer, pH 7.8, 50 mM). The reaction was initiated by the addition of the enzyme. The hydrolysis of *p*-NPB was monitored by the formation of the *p*-nitrophenol at 400 nm [122]. The measurements were conducted in a Synergy Mx Multi-Mode Reader from BioTek (USA).

5.2.3.3. Protein quantification

The quantification of the protein concentration was performed by using the DC protein assay (BIO-RAD).

5.2.3.4. Degree of PEGylation

The degree of enzyme PEGylation was indirectly evaluated by colorimetric titration. This methodology occurs by the reaction of 2,4,6-trinitrobenzene sulfonic acid (TNBSA) with the free amine residues at the surface of the enzymes. Knowing the total amount of amine residues available in each protein, this quantification allowed us to calculate the amount of PEG chains coupled to each esterase. The procedure was followed as reported by Castillo *et al.* [123].

5.2.3.5. Molecular Dynamics Simulations

Molecular Dynamics (MD) simulations were performed on lipase from *Thermomyces lanuginosus* (lipase TL, PDB ID: 1TIB) [124], on lipase B from *Candida antarctica* (CALB, PDB ID: 1TCA) [125], and on its PEGylated forms, to understand the role of the lid and active site cavity in different environments.

Lipases were modelled in the simple point charge water model, for control, and in a mixture of diethyl glutarate and ethylene glycol, respecting the same experimental proportion. In both cases, a cubic box with an approximate volume of 530 nm³ was used, with the enzyme centralized and Na⁺ ions to neutralize the system. One stage of energy minimization was performed using a maximum of 50,000 steps with steepest descent algorithm. Position restraints (with force constant of 1000 kJ·mol⁻¹·nm⁻²) were applied to all heavy atoms at the initialization steps, the first using an NVT ensemble and the second, with NPT. The temperature was maintained constant with V-rescale algorithm [84] and the pressure, was regulated at 1 atm, with the Parrinello-Rahman barostat [85]. In the control situation (enzyme in water), a temperature of 310 K was used, but for the second situation, enzymes in the mix of substrates, a temperature of 313 K was chosen to mimic exactly the experimental procedure. The following coupling constants were considered: $\tau_T=0.10$ ps and $\tau_P=2.0$ ps. After that, all systems were submitted to MD simulations during 40 ns, in an NPT ensemble, without position restraints.

All simulations were performed using the GROMACS 5.1.4 version [86, 126], within the GROMOS 54a7 force field (FF) [87, 88]. The Lennard-Jones interactions were truncated at 1.4 nm and we use particle-mesh Ewald (PME) [89] method for electrostatic interactions, also with a cut-off of 1.4

nm. The algorithm LINCS [90] was used to constrain the chemical bonds of the proteins and the algorithm SETTLE [127] in the case of water.

To design and simulate the box containing the substrates diethyl glutarate and ethylene glycol as solvents, we had to optimize and parameterize these molecules. For this we run a PM6 calculation [93] with Gaussian09 software [92] followed by submission of the resulting optimized structures at ATB server (Automated Force Field Topology Builder) [128, 129]. As result, we obtained optimized structures with a GROMOS 54a7 FF parameter associated to each one.

The PEGylated systems were designed replacing Lysine (Lys) residues to a new type of Lysine, named as LYP, where a PEG chain was linked. To prevent high computational costs, we connect only three PEG units to each chosen lysine side chain. The GROMOS topology necessary for this new residue, LYP, was also obtained using ATB server. In the case of lipase TL, 5 types of PEGylation took place until the limit of 5 of 7 Lys PEGylated: the analogue LP1 has LYP only in position 98, LP2 has LYP98 and the Lys PEGylated in β -sheets (positions 74, 223 and 237), LP3 has LYP98 and the Lys PEGylated in α -helices (positions 24, 46 and 127), LP4 present LYP98 and 4 random Lys PEGylated (positions 24, 46, 223 and 237) and LP5 is the only case where Lys98 was not PEGylated, but 5 random Lys were replaced by LYP (positions 46, 74, 127, 223 and 237). For CALB, an analogue with all Lys PEGylated was designed. This was done to correspond to the results obtained experimentally.

From MD simulations, we computed a cluster analysis from GROMACS package, with the single-linkage method, to determine the middle structure of each enzyme, i.e., this technique adds structures that are below a RMSD cut-off, generating more or less populated clusters and, within the largest cluster, it finds a middle structure that is the most representative of the whole simulation. We also follow the changes in the lid conformation and in the region involving the catalytic triad through visualization analysis with PyMOL [130].

5.2.4. Polymer characterization

5.2.4.1. Nuclear Magnetic Resonance spectroscopy (NMR)

All NMR spectra, namely ^1H NMR, ^{13}C NMR, Distortionless Enhancement by Polarization Transfer (DEPT), ^1H - ^{13}C Heteronuclear Single Quantum Coherence (HSQC) and ^1H - ^{13}C Heteronuclear Multiple Bond Correlation (HMBC) were carried out on a Bruker Avance III 400 spectrometer (400 MHz for ^1H and 100 MHz for ^{13}C). Deuterated chloroform (CDCl_3 , Cortecnet, France) was used as

NMR solvent, and the peak solvent used as internal reference. Signal multiplicity was given as: s (singlet), t (triplet), q (quartet) and m (multiplet).

5.2.4.2. Matrix-Assisted Laser Desorption/Ionization Time-of-Flight (MALDI-TOF)

MALDI-TOF mass spectra were acquired on a Bruker Autoflex Speed instrument (Bruker Daltonics GmbH) equipped with a 337 nm nitrogen laser. The procedure was followed as previously reported [79, 131]. 2,5-dihydroxybenzoic acid (DHB) or α -cyano-4-hydroxycinnamic acid (CHCA) were used as matrix. Samples were analysed in the linear positive or negative mode.

The number average (M_n) and weight average molecular weight (M_w), the polydispersity index (PDI= (M_w/M_n)), the average and maximum degree of polymerization (DP_{avg} , DP_{max}) (DP_{avg} = M_n /repeating unit of the oligomer) were calculated based on the MALDI-TOF spectra obtained, based on the m/z values and intensity, following the equations:

$$1) \quad M_n = \frac{\sum ni M_i}{\sum ni}$$

$$2) \quad M_w = \frac{\sum ni M_i^2}{\sum ni M_i}$$

Where ni is the relative abundance of each peak in the MALDI-TOF spectra and M_i is the m/z corresponding to each peak.

5.2.4.3. Fourier-transform infrared spectroscopy (FTIR)

Infrared spectra were recorded on a FTIR Bomem MB using NaCl cells. The samples were analysed over the range 500-4000 cm^{-1} , with a spectral resolution of 4 cm^{-1} . All spectra were an average of over 20 scans.

5.2.4.4. Differential Scanning Calorimetry (DSC)

DSC measurements were conducted on a power-compensated DSC instrument (DSC 6000 Perkin Elmer) with a nitrogen flux of 20 mL/min, using stainless steel capsules in the temperature range of 20-250 $^{\circ}\text{C}$ (heating rate: 20 $^{\circ}\text{C}/\text{min}$, sample weight: 2-3 mg). The DSC device was calibrated

using indium and zinc, both of high purity. The samples were freeze-dried, prior to the analyses and the sample was measured at least six times, to validate the results.

5.2.4.5. Thermogravimetric Analysis (TGA)

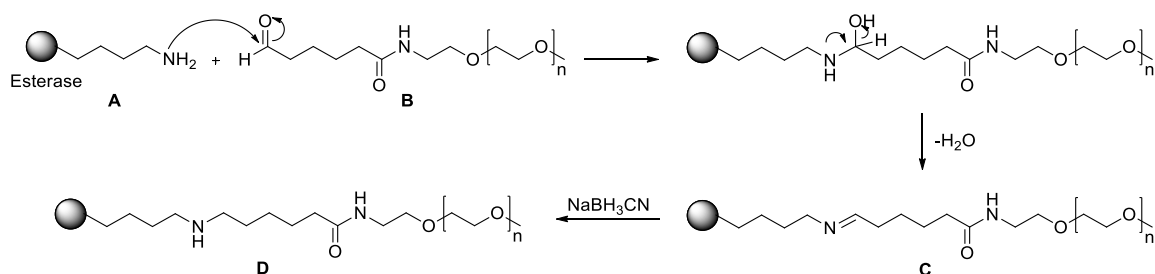
TGA analysis was performed in a Perkin Elmer TGA 4000. The calibration was performed with metals, such as Nickel, Alumel and Perkalloy, based on their Curie Point Reference. The temperature range was 30-800 °C (heating rate 20 °C/min, sample weight: 12-16 mg) and the nitrogen flow rate was 20 mL/min (3 bar).

5.3. Results and discussion

5.3.1. PEGylation and catalytic properties of PEGylated esterases

Most of the soluble enzymes are highly stabilized in the presence of high concentrations of polyethylene glycol. The presence of a medium with a high viscosity is expected to prevent the undesired changes in enzyme structure promoted by denaturing agents (e.g., high temperatures, strong basic conditions, extreme pH values) and, therefore, the stability of the soluble enzymes greatly increases. Based on these observations, our approach was to build such a layer around the enzyme to stabilize it, by PEGylation of the primary amine groups available.

The PEGylation of lipase from *Thermomyces lanuginosus* (lipase TL), lipase from *Candida antarctica B* (CALB) and cutinase from *Fusarium solani pisi* (CUT) was performed as reported in the literature, using a monofunctional PEG with an aldehyde group (MW 5000 Da) [121]. The reaction occurred at acidic pH (5.1) in the presence of a reducing agent, sodium cyanoborohydride, as proposed in **Scheme 5.1**.



Scheme 5.1. Proposed mechanism for the PEGylation of esterases; **A)** Lysine residue of an esterase; **B)** PEG-Aldehyde; **C)** Esterase-lysine-PEG as imine intermediate; **D)** Esterase-lysine-PEG.

The TNBSA assay allowed the quantification of the free amine residues at the surface of the esterases which were not modified by PEGylation. Indirectly, we were able to infer that, under the conditions described, the PEGylation of CALB resulted in a protein with 100 % of the exposed amines linked to PEG. After modification of lipase TL and cutinase, only 59 and 78 % of the amino groups were linked to PEG, respectively (**Table 5.1**). Depending on the position of the amine residues at the enzyme's surface, stereo-chemical impediments might influence the degree of PEGylation. More exposed amines are more prone to covalently react with the PEG available chains [132]. Regarding the methodology used to PEGylate, it is likely that the amine residue of the *N*-terminus had been also PEGylated. This assumption is based on the use of acidic pH during the reaction, which led to the activation of the *N*-terminus [121].

Table 5.1. Percentage of amine residues modified by PEGylation and activity of esterases, before and after PEGylation

Esterase	Amine modification^[a]	Activity^[b] (U/mg_{protein})
CALB	—	60
PEGylated-CALB	100 %	132
Lipase TL	—	26
PEGylated-Lipase TL	59 %	27
Cutinase	—	260
PEGylated-Cutinase	78 %	1061

^[a]obtained by TNBSA assay.

^[b]calculated by the hydrolysis of *p*-nitrophenyl butyrate over 1 min and considering the same initial amount of protein; 1 U of enzyme activity was defined as the amount of enzyme required to convert the substrate (*p*-nitrophenyl butyrate) into *p*-nitrophenol in 1 min.

The PEGylation was also ascertained by SDS-PAGE electrophoresis as a complementary methodology (**Figure 5.1**).

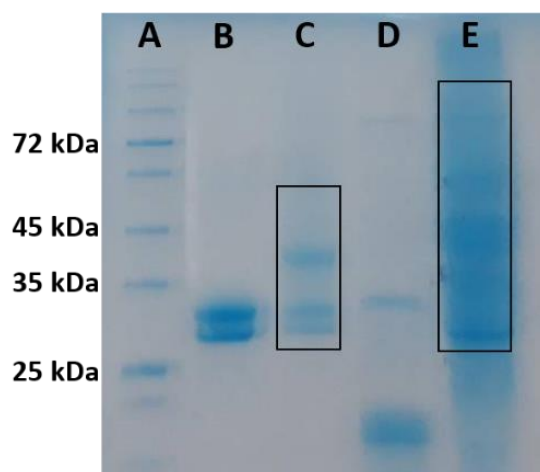


Figure 5.1. SDS-PAGE gel of native and PEGylated esterases stained with Coomassie brilliant blue; **A)** GRS Protein Marker Blue (from Grisp, Portugal), **B)** Lipase from *Thermomyces lanuginosus*; **C)** PEGylated lipase from *Thermomyces lanuginosus*; **D)** Cutinase from *Fusarium solani pisi*; **E)** PEGylated cutinase from *Fusarium solani pisi*.

Lipase from *Thermomyces lanuginosus* has a typical visible band at 30 kDa and when PEGylated a new band appears at around 40 kDa (corresponding to 2 units of PEG covalently bond to the protein). Cutinase display a representative band at 22 kDa, while its PEGylated form shows an intense smear with two pronounced bands in the range of 25 and 45 kDa. The PEGylated forms present also an evident smear suggestive of an increase of the molecular weight incremented by PEGylation. As a consequence of the reduction in the number of free amino groups, the enzyme derivatives (PEGylated forms) showed a smaller electrophoretic mobility toward the cathode than the unmodified esterase.

Due to the presence of stabilizers in the medium, the native and PEGylated CALB were not successfully revealed by SDS-PAGE electrophoresis.

The activity of enzymes is a parameter greatly influenced by the PEGylation procedure. Thus, the hydrolytic activity of the esterases against *p*-nitrophenyl butyrate was evaluated, before and after PEGylation, and the results obtained reveal a different catalytic behaviour of the catalysts after the chemical modification. We have found that PEGylation greatly enhanced the CALB and CUT catalytic activities comparing to their native state. This was a surprising result since only few examples of increased activity after PEGylation can be found in the literature, as previously mentioned [112]. Comparing to their native forms, the activities of PEGylated CALB and CUT increased 2-fold and 4-fold after PEGylation, respectively. According to our data, the PEGylation of

lipase TL did not influence its catalytic activity which remained unaltered after chemical modification.

The addition of free PEG to the native enzymes' medium was also evaluated and the results revealed no effect of the stabilizer on their hydrolytic activity (data not shown).

It was noteworthy that all PEGylated catalysts remained stable for at least six months of storage at room temperature.

To evaluate their stability under processing conditions, we incubated the enzymes at 40 °C and measured the activity over time (activity measured using *p*-NPB as substrate). From the results obtained one might infer that PEGylation conferred stabilizing effects to the modified esterases. We observe that both native and PEGylated enzyme forms, remained active for more than 50 days under the same storage conditions, with minimal activity loss. During all the reactional process at 40 °C, no loss of activity was registered based on the results obtained after 8 h of incubation (**Figure 5.2**). The temperature of incubation has been described in literature as a differential factor for PEG stabilization performance. The high thermal stability achieved herein at 40 °C might be explained by the high viscosity of PEG layers surrounding the enzymes.

Although PEGylation is being described as a methodology prone to inactivate some proteins [133], the results obtained clearly demonstrate that this methodology allows to improve esterase's activity and stability.

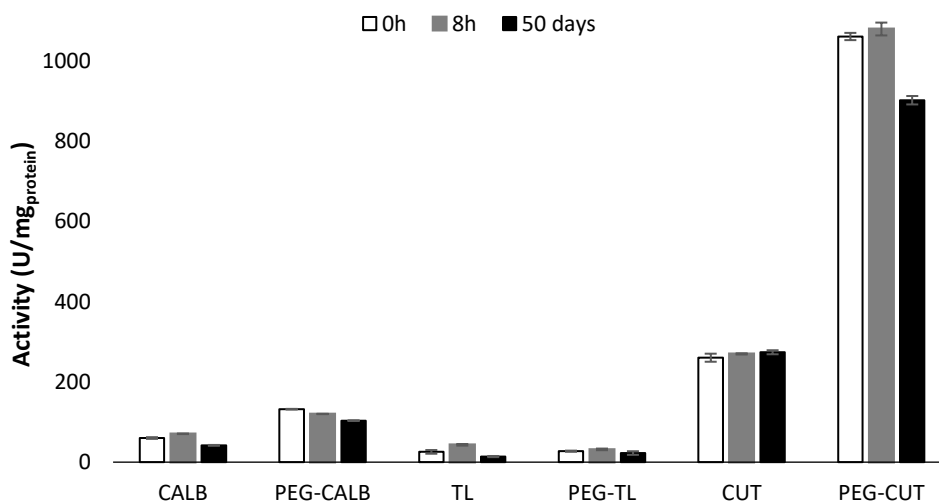
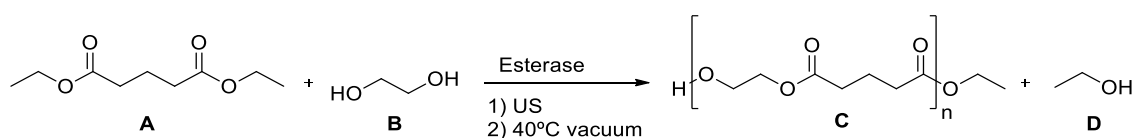


Figure 5.2. Absolute activity of esterases (native and PEGylated forms), at time zero, after 8 h, and after 50 days of incubation at 40 °C in phosphate buffer (pH 7.8). The activity was measured against *p*-NPB over 1 min and considering the same initial amount of protein; 1 U of enzyme activity was defined as the amount of enzyme required to convert the substrate (*p*-nitrophenyl butyrate) into *p*-nitrophenol in 1 min.

5.3.2. Effect of PEGylation on the polymerase activity of esterases

The synthesis of poly(ethylene glutarate) catalysed by immobilized CALB was previously investigated by us [54], using diethyl glutarate and ethylene glycol diacetate as starting reagents. Herein, we replace the ethylene glycol diacetate by ethylene glycol, which would allow to obtain a greener sub-product, ethanol, instead of ethyl acetate. A greener and environmentally friendly methodology is also associated with the proposed method due to the absence of solvents on the reactional mixture, being all the reactions carried out in bulk. Moreover, mild reaction conditions of temperature (40 °C) and short reactional times were used, reducing therefore the energy costs associated to the process.

Regarding the previous results published [54] we proceed with the processing optimizations (data not shown) and established the best reactional conditions for the polymerization of the proposed polyester: 2 h under US followed by 5 h under vacuum at 40 °C, following the reaction presented in **Scheme 5.2**.



Scheme 5.2. Reactional scheme for the synthesis of poly(ethylene glutarate) catalysed by esterase; **A)** diethyl glutarate; **B)** ethylene glycol; **C)** poly(ethylene glutarate); **D)** ethanol.

Taking into account the best reactional procedure established, the enzyme loading (2 to 130 U/mg) was tested to evaluate the best conditions to attain the highest synthesis conversion (**Figure 5.3**). Results from **Figure 5.3** reveal that, when comparing to their native forms, the highest product conversion was obtained when using both PEGylated-lipase TL and PEGylated-CUT enzymes. CALB display however an opposite behaviour after PEGylation, giving rise to slightly lower conversion levels. One can also observe that all enzymes tested showed a similar trend between 2 and 130 U/mg of enzyme loading, reaching however different levels of conversion, depending on the enzyme form and source. At the maximum enzyme loading, PEGylated lipase TL revealed the highest polymerase performance comparing to its native form, reaching levels of conversion of around 90 % whereas PEGylated-CUT converts only 60 % of the monomers. The reactions were also carried out with native enzymes in the presence of free PEG in the reactional medium. The data obtained at these conditions showed lower conversions than compared with native enzymes

without additive (data not shown). In this case, the free PEG can saturate the medium, hindering the access of the substrate to the enzymes' active site, while when PEG is attached to the enzymes, it induces an opposite effect, contributing to the improvement of their activity and stability.

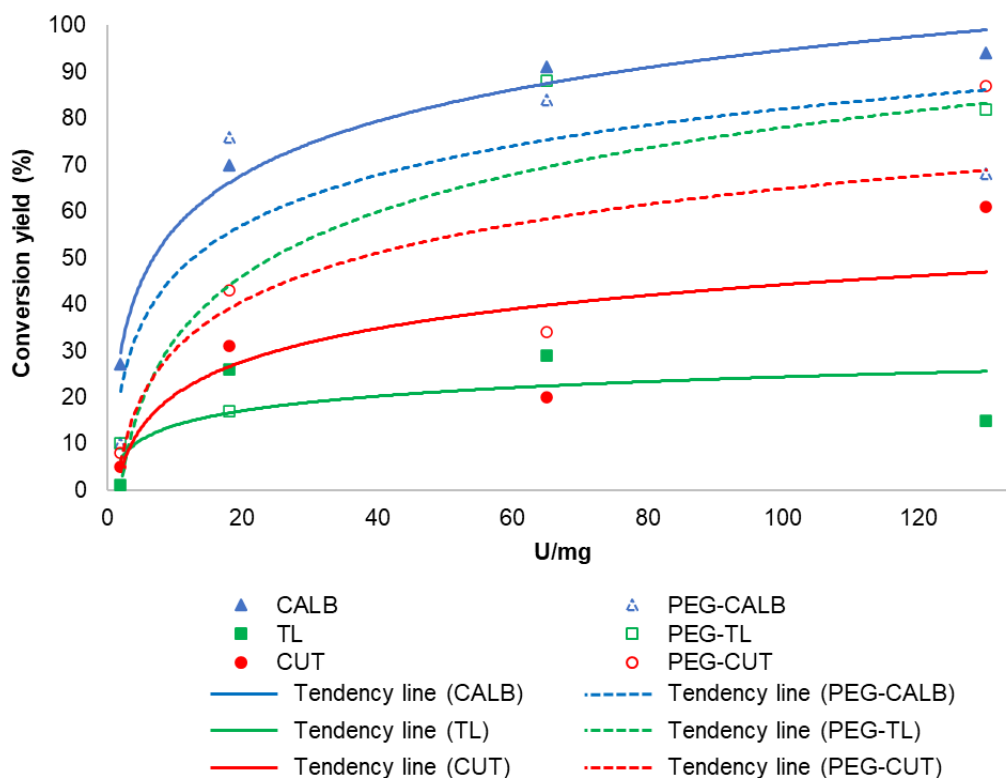


Figure 5.3. Conversion (%) *vs* enzyme loading (U/mg) after synthesis of poly(ethylene glutarate).

Comparing both polymerase and hydrolytic activities, the findings indicate that for lipase TL the presence of PEG chains on the macromolecular surface somewhat maintain unaltered the binding of *p*-NPB, a more hydrophilic substrate, however increasing considerably the binding of the hydrophobic starting reactants. Apparently, PEG modification improved the relative selectivity of the enzyme towards different substrates. For a better understanding of the role of PEG on the performance of the modified esterases, we calculated the degree of polymerization (DP) and oligomer conversion when using a fixed enzyme loading (65 U/mg) (**Figure 5.4**).

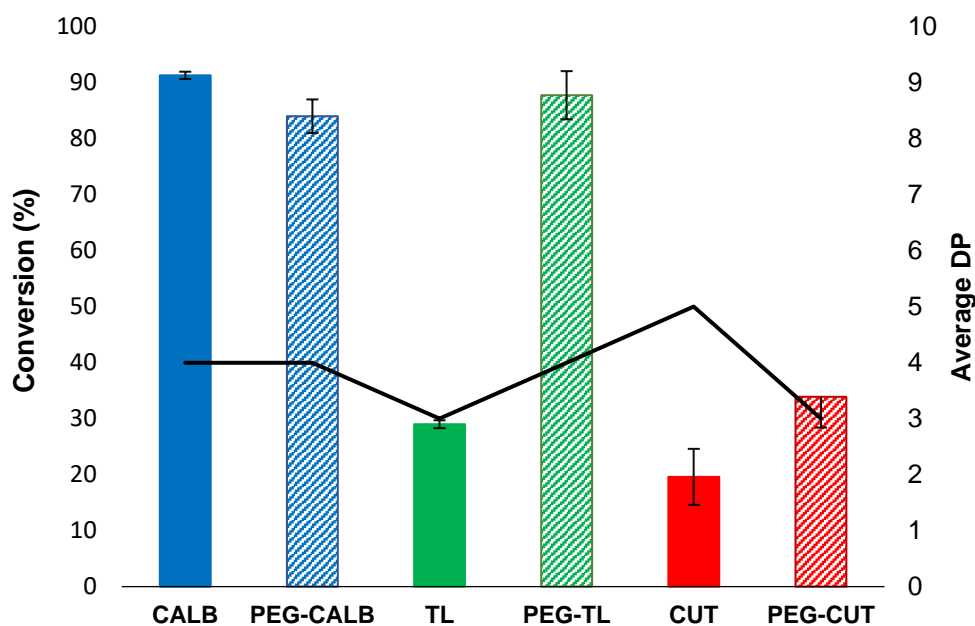


Figure 5.4. Conversion (%) and degree of polymerization (DP) for all the tested esterases under the optimized conditions: 2 h under US followed by 5 h under vacuum, at 40 °C; 65 U/mg. The graph bar corresponds to the conversion (%) and the graph line to the average DP.

Comparing to its native form, PEGylated-TL showed the highest biosynthesis activity (60 % of improvement) evaluated in terms of average DP (conversion 88 %; DP_{avg} : 4 units). Both CALB forms, native and PEGylated, converted similar amount of starting reagents into poly(ethylene glutarate) with similar DP. The PEGylated form of cutinase was more prone to catalyse the polyester synthesis than its native form (20 % conversion) however with a lower corresponding DP.

Many reports using CALB as catalyst for the polyester synthesis are found in literature, however the use of native lipase TL for this purpose is still poorly explored. Zhao *et al.* [134], reported the *in situ* coating of cotton with polyesters synthesised by lipase TL and CALB. In their work the polyester synthesis was carried out using different amounts of each enzyme, and for this reason it was hard to distinguish their catalytic behaviour for the same substrate. Nevertheless, the findings suggested lower catalytic performance of lipase TL regarding polyester biosynthesis.

Naik *et al.* [135], studied the specificity of different ester groups for different lipases. Their findings recognized a different catalytic behaviour for CALB and lipase TL. While CALB had a large acyl and narrow alcohol, binding cleft, lipase TL presented a wide alcohol and narrow acyl, binding cleft. These assumptions suggest that the use of a large acyl compound (like diethyl glutarate) might favour the reaction when CALB is applied. Moreover, being ethylene glycol a small molecule, more

easily gets into the enzyme's alcohol cleft. These findings are in accordance with the high conversion obtained for either native and PEGylated CALB (> 80 %).

For lipase TL, the opposite was expected to occur. The large alcohol and the narrow acyl cleft may justify the low conversion obtained for the native form (< 30 %). The size of the starting reagents may hinder the access to the respective enzyme clefts, which is mitigated by the presence of PEG on the PEGylated enzyme form, which in turned higher polymerase conversion.

From all the esterases tested, cutinase presented the lowest catalytic performance for the polyester biosynthesis, giving rise to conversions below 33 %. Despite the low conversion, this esterase was able to catalyse the synthesis of larger oligomers, evidenced by the highest oligomer DP observed (DP_{avg} : 5 units). The studies of Naik *et al.* [135], revealed that cutinase from *Fusarium solani pisi* have both clefts larger, which may justify the higher DP obtained when this catalyst was used.

Both, lipase and cutinase, belong to the same family of α/β hydrolases, but display different affinities to the substrates [136]. While the activity of lipase is greatly enhanced at lipid-water interface, needing interfacial activation, cutinase lack this need of activation [136]. This phenomenon is crucial for lipases to exhibit activity, since they possess a hydrophobic flap in their structure which overlies the active site and changes in this flap are related to the interfacial activation [137]. In lipase TL the need for this activation is reported, while CALB only needs little or even no activation [135]. Considering these assumptions, one might infer that on the presented experiments the need of interfacial activation of native lipase TL might led to a lower polyester biosynthesis performance, when compared with CALB.

We believe that the higher polymerase activity observed for PEGylated lipase TL might be attributed to the PEG linked to the enzyme's surface. The polyethylene glycol chains can change the structure of the flap or of the global enzyme conformation. The linked PEG may enlarge the active site or create a larger opening for an easier access of the substrates. Moreover, the results obtained can also be explained by entropic stabilization by PEG conjugation due to the restricted motion of some surface amino acid side chains, resulting in a more stable active site. Thus, in order to better understand the role of PEG on the improvement of the catalytic performance of lipase TL and CALB, molecular dynamics (MD) simulations were conducted.

5.3.3. Molecular Dynamics Simulations

MD simulations were carried out for lipase TL, CALB and all analogues (**Figure 5.5**) to examine their behaviour near the active site and lid, when in an aqueous medium or in substrates medium,

before and after PEGylation. Regarding the similar conversion levels obtained for both native and PEGylated cutinase and the lack of interfacial activation, no MD simulations were conducted. The small differences obtained experimentally are easily explained by the enzyme large clefts which did not favour the synthesis when either native or PEGylated forms were used.

In the case of lipase TL, PEGylation was thought to replace up to 5 Lys per LYP (PEGylated Lys), as it was experimentally confirmed by the TNBSA assay an average of 5 PEGylated Lysines. The PEGylation of Lys98, which is placed in one of the enzyme's arms that can move the lid, was also assessed. For PEGylated-CALB, and since experimentally all the Lys were PEGylated, all the 9 lysines were replaced by LYP.

The lid of lipase TL comprises the amino acids 82-98, presenting an α -helix (residues 86-91) and two hinge domains (anterior and posterior). The catalytic triad is composed of Ser146, His258, and Asp201 residues, and as this lipase approaches a lipid interface, the lid moves, clearing the access to the catalytic triad and allowing catalysis [138]. In the case of CALB, the catalytic triad is formed by the Ser146, His224 and Asp187 residues and, similarly to lipase TL, there is an α -helix situated above the cavity that encompasses the triad (residues 139-148). However, in this lipase the access to the active site is not hampered as in the case of lipase TL. In fact, several authors do not consider this helix as a lid, and therefore the catalytic mechanism is not dependent on the displacement of this structure [139, 140].

Despite the mechanistic differences already established for both lipases, these assumptions were not sufficient to explain the differentiated results obtained experimentally, especially for the PEGylated enzyme forms. The modelling studies aimed, in the case of CALB, to understand the role of the medium and PEGylation, on the triad cavity and on the lid or lid-like structure.

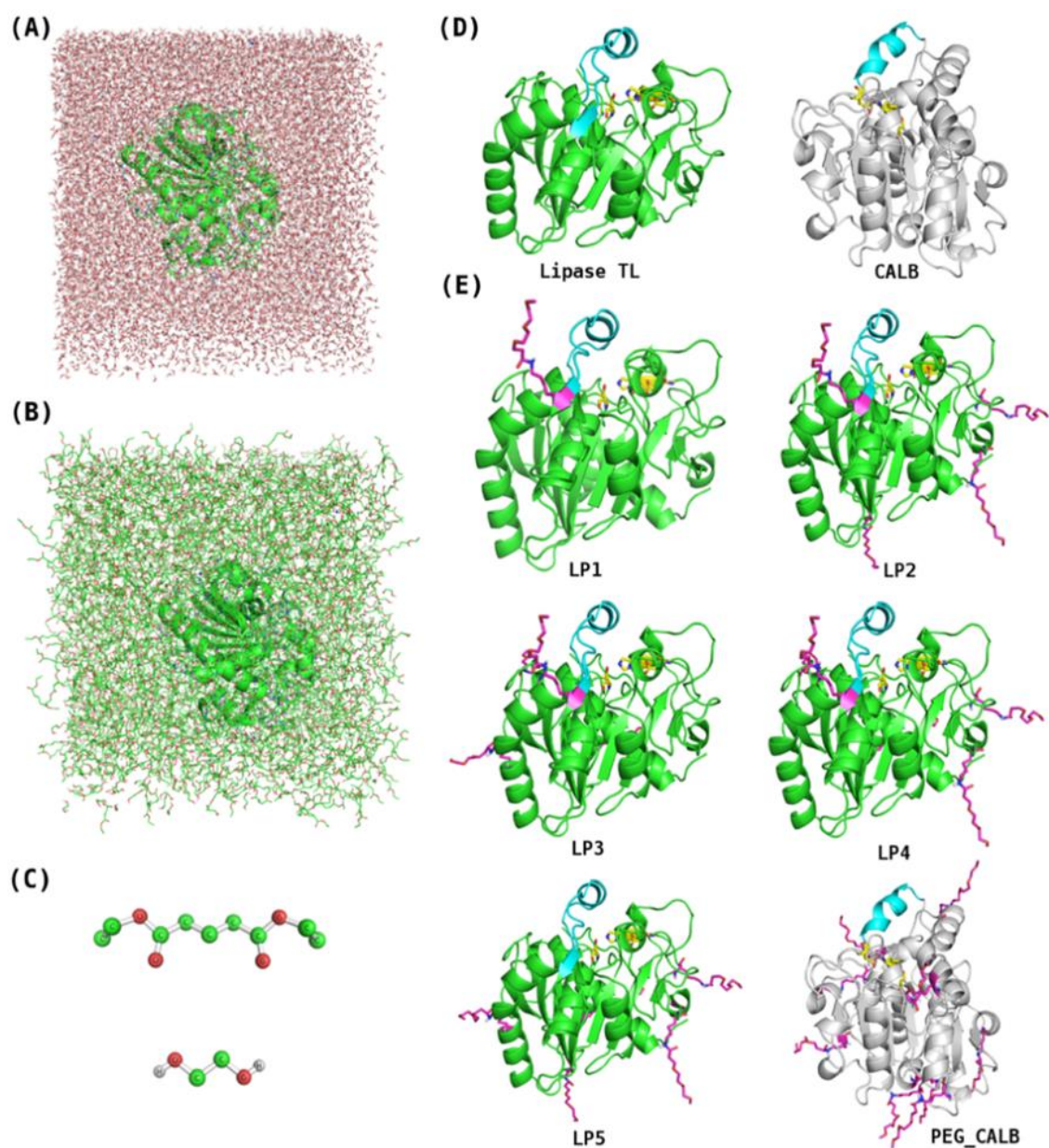


Figure 5.5. Lipase TL in water medium (A) and in substrates mixture medium (B). Optimized structures of diethyl glutarate and ethylene glycol in united-atom GROMOS 54a7 FF representation (C). Initial structures of lipase TL (green, 1TIB) and CALB (grey, 1TCA) (D). PEGylated structures based on lipase TL and CALB: LP1 (LYP98), LP2 (LYP98, LYP74, LYP223 and LYP237), LP3 (LYP98, LYP24, LYP46, LYP127), LP4 (LYP98, LYP24, LYP46, LYP223, LYP237), LP5 (LYP46, LYP74, LYP127, LYP223, LYP237) and PEG-CALB (all Lys replaced by LYP). Lipases are represented in cartoon, with the lid region highlighted in cyan, the catalytic triad in yellow, and LYP residues in magenta.

RMSD results (Figure 5.6) demonstrated that in both medium (water or reactants) lipase TL and analogues were very stable, varying only 0.15-0.4 nm from the initial X-ray structure. For CALB systems, a smaller deviation was observed, ranging from 0.1-0.3 nm. However, it was noteworthy that the PEG stabilizing effect was only observed when the systems were in the solvent-reactants mixture, being much less pronounced in water.

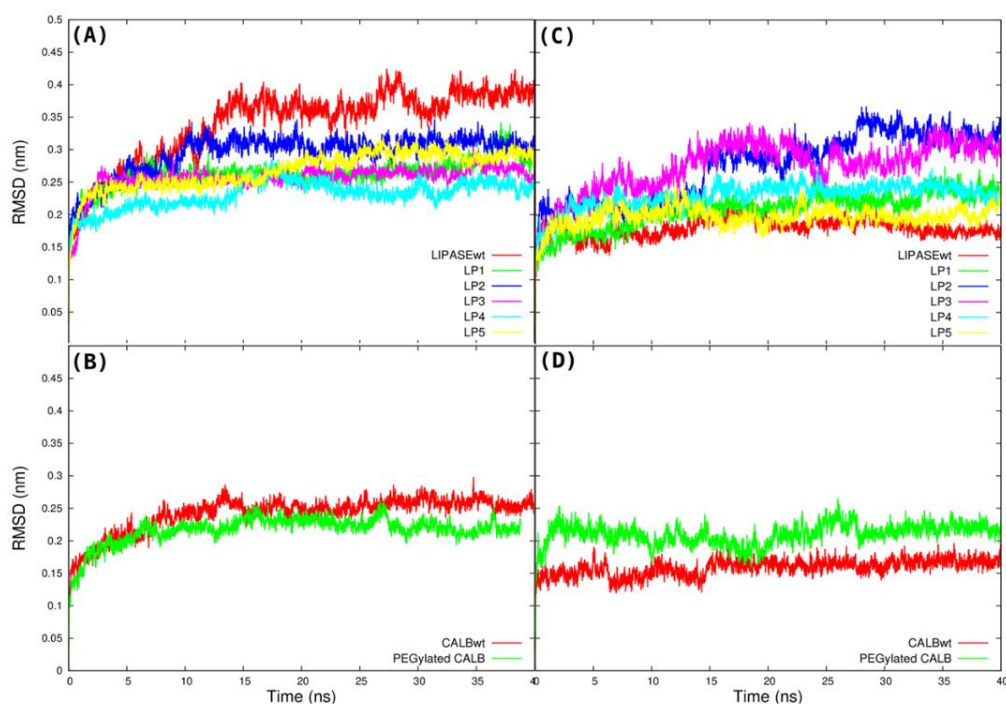


Figure 5.6. Backbone RMSD of lipase TL, CALB and PEGylated analogues in solvent (A-B) and in water (C-D).

After simulation, the middle conformation was determined for each case-studies, to evaluate the effects of the medium and PEGylation on the global width of the cavity that encompasses the catalytic triad. Although these lipases are globally stable structures, when looking to the central structures (Figure 5.7), the most significant deviations observed were in the region of the lid structure.

The effect of medium and PEGylation is exemplified in Figure 5.7, by lipase TL and LP1 analogue (LYP in position 98), where it is perceptible that wild type lipase TL and the analogue, in reactants mixture, present a larger cavity in comparison with the same systems in water. Also, this example indicates that the PEGylation of the Lys98 favours the enlargement of the enzyme's active site. A larger cavity can result in a larger acyl cleft, which led to a better accommodation of diethyl

glutarate. This is evident in **Figure 5.7 (A)**, which highlights the active site of lipase TL and LP1 in reactant mixture.

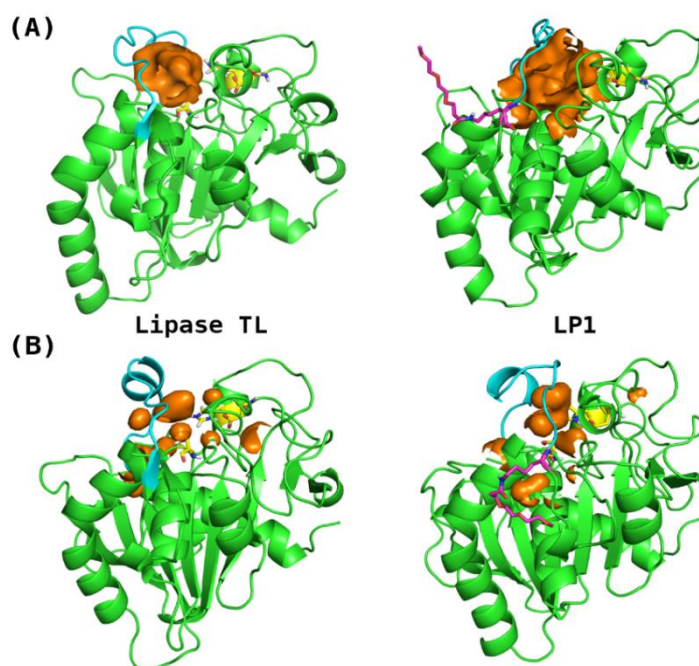


Figure 5.7. Middle conformations of lipase TL and PEGylated analogue LP1, in reactant mixture **(A)** and in water **(B)**, highlighting the interior cavities and pockets surrounding the catalytic triad and lid regions.

The CALB middle structures demonstrate that the medium has a similar impact on the enzyme's cavity region. In water, the PEGylation seems to not disturb the structure and the active site cavity which remains unaltered. In the reactant mixture (**Figure 5.8**), although PEG stabilizes CALB, it does not generate a great enlargement of the cavity, promoting a more discrete effect on this enzyme, when compared with the effect towards TL. Regarding the similar conversion yield and DP obtained experimentally for both CALB forms, a negligible effect of PEG on the CALB structure was expected. CALB owns a large acyl and small alcohol, clefts, ideal for the polymerization of the substrates tested. MD studies reveal that PEG did not disturb the active site of the enzyme, thus maintaining the size of both clefts which resulted in similar polymer conversion, independently on the enzyme form used.

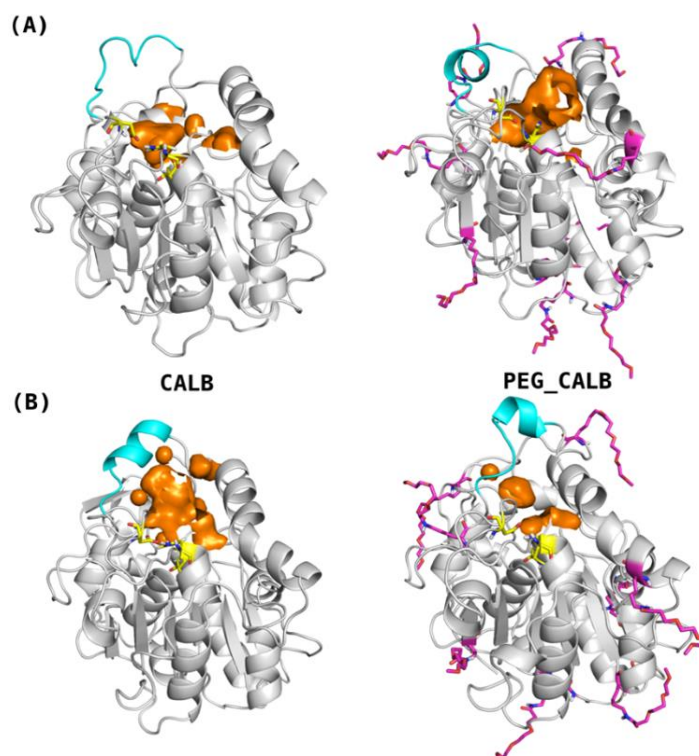


Figure 5.8. Middle conformations of CALB and PEGylated CALB, in reactant mixture **(A)** and in water **(B)**, highlighting the cavities and pockets surrounding the catalytic triad and lid regions. Cartoon in grey, catalytic triad in yellow, lid-like region in cyan, LYP residues in magenta and the orange spheres represent the empty space (cavity or pocket) on each structure.

Recently, MD studies and other modelling techniques have been used to understand the mechanisms of interfacial activation in lipase TL, CALB and other lipases [141-143]. However, these studies were in general performed using water as medium, or a water-lipid/water-oil interface. We show herein an innovative approach to demonstrate the contribution of PEGylation on the final enzyme arrangement. By comparing simulations in water and in the reactant mixture, we were able to confirm that the starting organic reactants, diethyl glutarate and ethylene glycol, create the best environment to enhance the catalytic properties of lipase, i.e., an open access to the catalytic triad.

5.3.4. Poly(ethylene glutarate) characterization

The results of the biosynthesis are summarized in **Table 5.2**, including the number average molecular weight (M_n), the weight average molecular weight (M_w), the polydispersity index ($(M_w)/M_n$) and the average and maximum degree of polymerization, for all the reactions performed.

The synthesized polymers displayed M_n values between 415.97 and 799.99 g/mol, and M_w values between 527.03 and 1031.61 g/mol. All reactions gave rise to polymers with good polydispersity, whereas PEGylated-CALB displayed the more homogeneous (1.04) and PEGylated-TL the more heterogeneous (1.48).

As previously stated, PEGylated-lipase TL showed higher DP than its native form. This PEGylated esterase, also showed the highest maximum degree of polymerization (16 units). Both forms of CALB have the same average and maximum DP. The native form of cutinase showed better performance than its PEGylated form. A possible explanation for all these results was already discussed elsewhere in this chapter.

Table 5.2. Number average molecular weight (M_n), weight average molecular weight (M_w), polydispersity (PDI), average degree of polymerization (DP_{avg}), maximum degree of polymerization (DP_{max}) (calculated by MALDI-TOF) and conversion rate, after poly(ethylene glutarate) biosynthesis (2 h under US followed by 5 h under vacuum at 40 °C with the 65 U/mg of enzyme)

Esterase	M_n	M_w	M_w / M_n	DP_{avg}	DP_{max}	Conversion rate (by 1H NMR)
CALB	580.89	625.18	1.08	4	8	91.3 ± 1.3 %
PEGylated-CALB	597.91	624.32	1.04	4	8	84.0 ± 5.9 %
Lipase TL	415.97	590.78	1.42	3	10	29.0 ± 1.4 %
PEGylated-Lipase TL	691.49	1021.40	1.48	4	16	87.8 ± 8.7 %
Cutinase	799.99	1031.61	1.29	5	15	19.6 ± 16 %
PEGylated-Cutinase	428.02	527.03	1.23	3	8	33.9 ± 13 %

5.3.4.1. NMR

1H NMR spectra of the new polymers formed have a similar pattern independently on the enzyme used and the degree of polymerization obtained. In **Figure 5.9A** is represented the 1H NMR spectra of poly(ethylene glutarate). The monomer, ethylene glycol, presented only one peak in the spectrum which appeared at δ_H 3.73 ppm. These protons, suffered a significant chemical shift when the synthesis occurred, appearing as a singlet at δ_H 4.30 ppm (**e**). The terminal ethylene glycol unit (protons **a** and **b**) appeared as two distinct peaks, one at δ_H 3.82 ppm (protons **a**) and the other at δ_H 4.21 ppm (protons **b**), both as multiplets. The glutarate moiety in the polymer do not showed significant changes comparing with the same protons in the monomer. Only the terminal part

(protons **h** and **i**) showed a decrease in the signal intensity depending on the degree of polymerization.

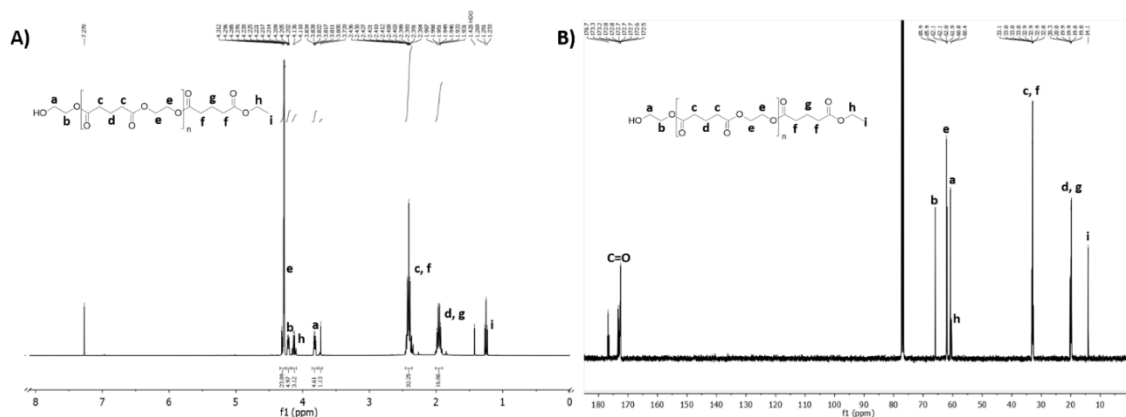


Figure 5.9. ^1H (A) and ^{13}C (B) NMR spectra of poly(ethylene glutarate) recorded in CDCl_3 .

In the ^{13}C NMR spectra (**Figure 5.9 B**) the expected peaks related with the new polymer were observed. The C=O were observed between δ_{C} 172.5 and 176.9 ppm. The terminal CH_3 (**i**) appeared at δ_{C} 14.1 ppm and CH_2 (**h**) at δ_{C} 60.4 ppm, while the other carbons of the glutarate (**c, d, f, g**) moiety were observed between δ_{C} 19.8-20.3 and 32.7-33.3 ppm. The ethylene glycol moiety (**e**) appeared at δ_{C} 61.9 and 62.1 ppm. The terminal **a** and **b** carbons were observed at δ_{C} 60.9 and 65.9 ppm, respectively.

The pattern obtained was in accordance to the previous poly(ethylene glutarate) reported [54], and the chemical shifts in the ^{13}C NMR are typical of polyesters [144].

5.3.4.2. MALDI-TOF

The MALDI-TOF mass spectrum of the formed poly(ethylene glutarate), recorded in linear positive mode, displays a typical isotopic distribution between 500 and 2500 m/z (**Figure 5.10**). From the spectra one can depict a repetition unit mass between each two peaks, corresponding to the monomeric repeating unit ($[M]= 158$). This confirmed the presence of the monomeric repeating unit in the polymer main chain. Similar spectra were obtained for the polyester synthesized by the other esterases studied, showing different DPs (data not shown). These results are in agreement with the formation of the proposed polymer, with $\text{DP}_{\text{avg}}= 5$, as suggested by ^1H NMR and ^{13}C NMR data. The pattern obtained for the polyester is in accordance with similar polyesters described in the literature [145].

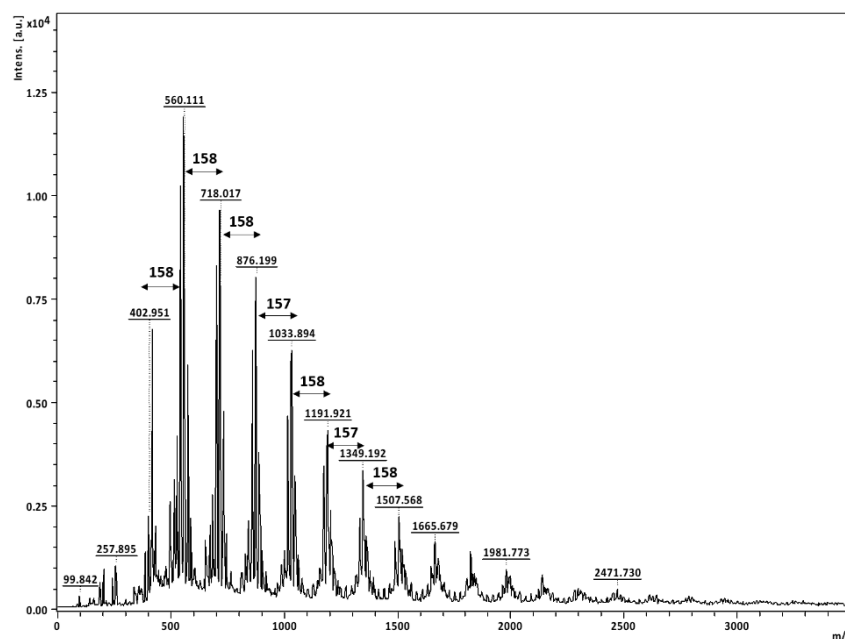


Figure 5.10. Positive ion MALDI-TOF spectra of poly(ethylene glycol) ($DP_{max}=16$ and $DP_{avg}=5$).

5.3.4.3. FTIR, DSC and TGA

FTIR analysis was also conducted to evaluate the chemical changes after enzymatic synthesis. From the data obtained (Figure 5.11), as expected, one can observe that the stretch of the OH terminal group was more pronounced for low degrees of polymerization. Also, the OH appeared in the polymer at ν 3500 cm^{-1} while in the monomer was observed at ν 3300 cm^{-1} . Regarding the C=O bond, it was observed at ν 1700 cm^{-1} for monomers and polymers.

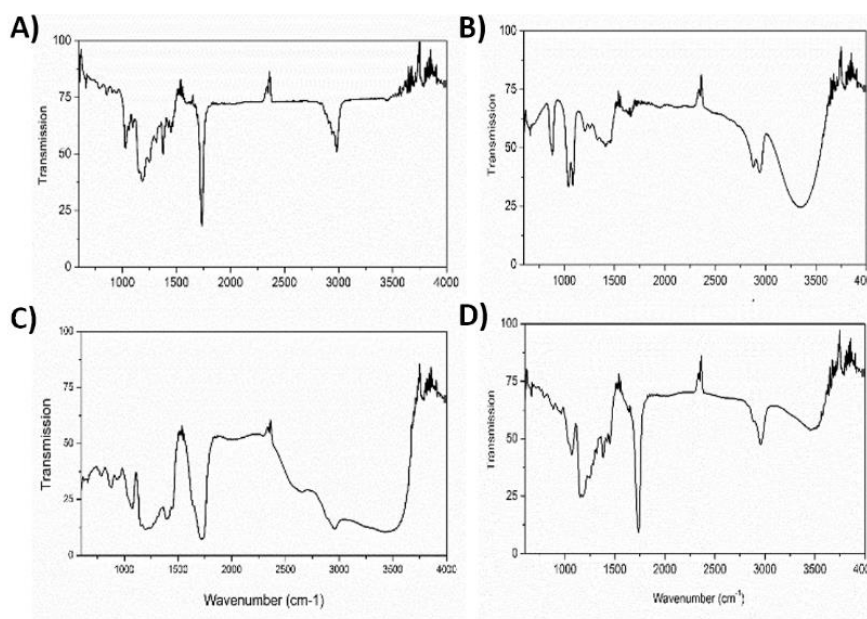


Figure 5.11. FTIR spectra of **A)** diethyl glutarate; **B)** ethylene glycol; **C)** poly(ethylene glutarate) with a $DP_{avg}=3$; **D)** poly(ethylene glutarate) with a $DP_{avg}=5$.

The glass transition temperature (T_g) of the polymer was determined by DSC analysis. Poly(ethylene glutarate) showed a value of $T_g = 77.29 \pm 1.21$ °C with an energy of $\Delta C_p = 0.228 \pm 0.095$ J/g $^{\circ}\text{C}^{-1}$ (Figure 5.12A). A melting point (T_m) was observed at $T_m = 195.7$ °C with an associated enthalpy of $\Delta H_m = 19.967$ J/g. The pattern here obtained is very similar to the DSC analysis of polyesters reported in literature [144].

The thermal properties of the synthesized polyester were investigated by thermogravimetric analysis scanned between 30-800 °C (Figure 5.12B). Both monomers present a one-step decomposition, losing all weight at around 180 °C. The polyester presented two distinct stages of weight loss: one at around 220 °C, corresponding to 10 % of weight loss; and another at 400 °C, corresponding to 50 % of weight loss. The total material decomposition was observed near 500 °C. The thermal behaviour observed, typical for this type of polymers [146], confirms the polyester biosynthesis.

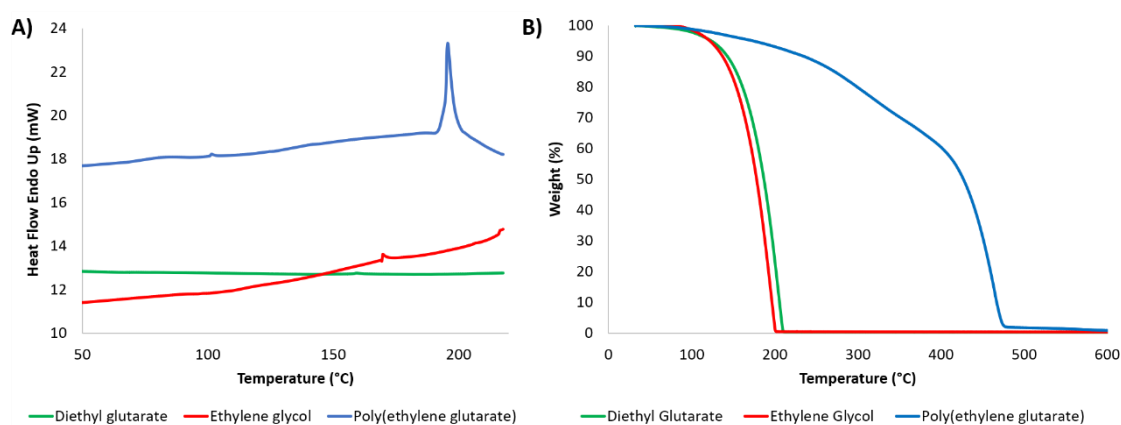


Figure 5.12. Graphics of **A)** DSC curve of poly(ethylene glutarate) with $T_g = 77.29 \pm 1.21$ °C and $T_m = 195.7$ °C, and the respective monomers and **B)** TGA curves of the starting materials (diethyl glutarate and ethylene glycol) and the formed poly(ethylene glutarate).

5.4. Conclusions

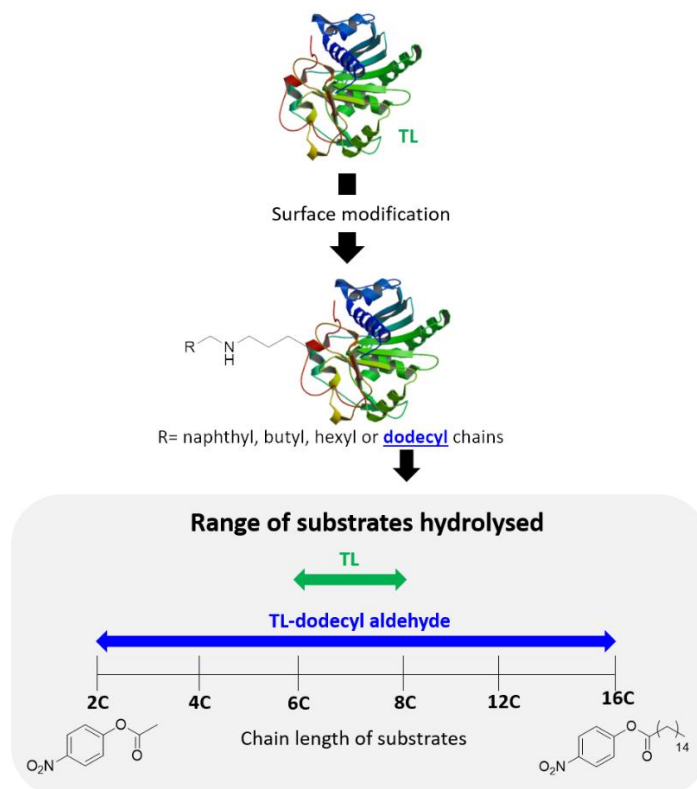
In this work we PEGylated three esterases (lipase from *Candida antarctica B*, lipase from *Thermomyces lanuginosus* and cutinase from *Fusarium solani pisi*) and compared their catalytic performance for the biosynthesis of poly(ethylene glutarate). All the enzymes were successfully PEGylated, and their hydrolytic activity, with exception of lipase TL, was improved comparing to their native form. Regarding their polymerase activity, we observed a similar performance for native and PEGylated CALB, explained mainly by their large acyl cleft. On the other hand, lipase TL

presented an improved performance when PEGylated. Molecular dynamics simulations, performed on lipase TL and CALB, support that the PEGylation of the lysine at the enzyme's lid had a positive effect on the substrate accessibility to the active site. The simulations conducted in the reactant mixture medium confirm the stabilization of the enzyme by PEG in a more organic environment. The entropic stabilization by PEG conjugation also caused the motion restriction of some surface amino acid side chains, resulting in a more stable active site.

The PEGylation of esterases demonstrated to be an easy, not expensive, and timeless methodology to enhance enzyme's performance on the biosynthesis of polyesters, envisaging a diverse range of applications.

Chapter VI

Substrate's hydrophobicity and enzyme's modifiers play a major role on the activity of lipase from *Thermomyces lanuginosus*



Substrate's hydrophobicity and enzyme's modifiers play a major role on the activity of lipase from *Thermomyces lanuginosus*

Abstract

Lipase from *Thermomyces lanuginosus* (TL) displays high affinity for long-chain substrates, such as triolein and other long-chain triacylglycerols. Aiming to broaden the substrate chain-length specificity, different aldehydes (naphthaldehyde, butyraldehyde, hexyl aldehyde and dodecyl aldehyde) and naphthyl isothiocyanate were grafted onto lipase TL, through lysine coupling. The catalytic activity of the modified lipases was investigated by reaction with substrates differing in the aliphatic chain size (*p*-nitrophenyl benzoate, *p*-nitrophenyl acetate, *p*-nitrophenyl butyrate, *p*-nitrophenyl hexanoate, *p*-nitrophenyl octanoate, *p*-nitrophenyl laurate and *p*-nitrophenyl palmitate). The enzymes modified with aldehydes displayed higher activity than the enzymes modified with the isothiocyanate. The most notable results were achieved for lipase TL, grafted with 4 units of a dodecyl chain (TL5), which displayed the highest activity against all the tested substrates, being 10-fold more active than the native enzyme for smaller substrates (acetate and butyrate chains), and 2-fold for longer (laurate and palmitate chains). The kinetic parameters evaluated (V_{\max} , K_M and k_{cat}/K_M) also confirmed the significant catalytic performance of TL5 comparing to the native form. The increased activity, revealed by the modified lipases, was directly proportional to the size and hydrophobicity of the linkers' aliphatic chain. Small conformational changes, either on the enzymes' lid as on the cavity of the active site were suggested by Molecular Dynamics simulations, Circular Dichroism and Fluorescence spectroscopy. Moreover, the grafting with aldehydes or with the isothiocyanate, conferred higher thermostability to the lipase. The chemical surface modification developed efficiently improved the activity of lipase TL, broadening the substrates chain-length specificity, incrementing thereafter the substrate possibilities for industrial reactions.

This chapter is based on the following publication:

Jennifer Noro, Tarsila G. Castro, Artur Cavaco-Paulo, Carla Silva, Substrate's hydrophobicity and enzyme's modifiers play a major role on the activity of lipase from *Thermomyces lanuginosus*, *Catalysis Science & Technology*, 10 (2020) 5913-5924.

6.1. Introduction

Lipase from *Thermomyces lanuginosus* (EC 3.1.1.3) was firstly isolated from compost medium containing, among other components, long-chain esters like soybean oil, corn steep liquor and starch [147]. The natural function of lipase from *Thermomyces lanuginosus* is described in literature as the degradation of the long chain triacylglycerols present in the compost medium [147-149].

Nowadays, this lipase is produced using a recombinant strain of *Aspergillus oryzae*, a filamentous fungus often used for enzyme production [150], and the isolated enzyme is responsible for the lipolytic activity of Lipolase[®], used for many applications like the production of flavours, biodiesel, and fine chemicals [151]. It is also commonly used for the hydrolysis of substrates such as triolein [142] and other long-chain triacylglycerols [151, 152]. This enzyme owns 1,3-stereospecificity, meaning that it specifically hydrolyses the ester group of triacylglycerols in the position 1 and 3. The hydrolysis of the position 2 occurs by migration of the acyl group to the position 1, and further hydrolysis by the enzyme.

The surface modification of enzymes is a strategy often applied to improve their global properties, mainly the thermostability. The immobilization of enzymes onto solid supports, is the strategy mostly studied, with diverse associated advantages, such as easy recovery, increase of resistance and robustness, among others [153].

Lipase from *Thermomyces lanuginosus* is mainly used in its immobilized form, as reported by several authors, due to the higher catalytic performance acquired in the immobilized form, comparing to the free form. Cipolatti and co-workers [154], studied the adsorption of lipase TL onto PEGylated polyurethane particles, and confirmed the improvement in the production of ethyl esters, comparing to the free native enzyme. Vasconcellos *et al.* [155], reported the immobilization of lipase TL on nanozeolites. They observed an increase on the production yield of biodiesel using this novel nanozeolite-enzyme complex.

Despite the promising results reported so far, the use of solid supports for enzyme immobilization often reduces its catalytic activity resulting from the reduced mobility imposed by the immobilization. A strategy to overcome this limitation and, at the same time, increment their catalytic activity, is the surface modification of the enzyme with small molecules like imidazolium or alkylated ammonium salts. However limited number of works have been reported in literature so far about this topic [156].

Jia and co-workers performed the chemical binding of ionic liquids to the surface of lipase from *porcine pancreas* [157]. They observed that the lipase modification, bearing kosmotropic cations and chaotropic anions, increased the enzymes' thermostability and enantioselectivity against the hydrolysis of racemic 1-phenethyl acetate.

The same strategy was applied to lipase from *Candida antarctica* B which revealed, after modification, a higher catalytic efficiency for the hydrolysis of *p*-nitrophenyl palmitate in aqueous medium. The thermostability and tolerance in organic media was also significantly improved by chemical modification of the enzymes' surface [158].

We have previously demonstrated in chapter 5 the positive effect of lipase TL PEGylation, on the lid destabilisation, which allowed an easier access of the substrates to the active site, when synthesizing polyesters. The PEGylated form allowed to produce a higher amount of polymer with a higher degree of polymerization in comparison with its native form [81].

Herein we aim to broaden the substrate chain-length specificity that lipase from *Thermomyces lanuginosus* can efficiently catalyse. Given that this lipase is used, in nature and in industry, for the hydrolysis of long-chain substrates, improving its catalytic performance for other substrates, would increment its range of applications in diverse fields. The degradation of fats in detergency or the chiral organic synthesis [159] are some of the applications that would benefit from this improvement. Thus, we chemically modify, for the first time, the surface of lipase TL by attaching linkers with differentiated chain length and hydrophobicity (naphthyl isothiocyanate, naphthaldehyde, butyraldehyde, hexyl aldehyde and dodecyl aldehyde) to the surface lysines and evaluated its activity and stability after modification.

A range of long-chain differentiated substrates were used for the evaluation of the modified enzyme's activity, following by the calculation of the kinetic parameters. Molecular dynamics simulations were performed to evaluate the impact of the modifications on the global conformation of the enzyme. Docking experiments were used to calculate the binding energies between the substrates and the native and modified lipases.

6.2. Materials and methods

6.2.1. Materials

Lipase from *Thermomyces lanuginosus* (solution, $\geq 100,000$ U/g), dodecyl aldehyde, naphthyl isothiocyanate, octyl isothiocyanate, phenethyl isothiocyanate, sodium cyanoborohydride, *p*-nitrophenyl butyrate, *p*-nitrophenyl laurate, *p*-nitrophenyl palmitate, *p*-nitrophenol and 2,4,6-

trinitrobenzene sulfonic acid (5 % (w/v) in H₂O) were purchased from Merck. Naphthaldehyde, butyraldehyde, hexyl aldehyde, benzoyl chloride, *p*-nitrophenyl acetate and *p*-nitrophenyl hexanoate were obtained from TCI Chemicals and *p*-nitrophenyl octanoate from Alfa Aesar. All compounds were obtained with high purity and used without further purification. Prior to use, the native lipase was ultrafiltrate for the removal of any additives present. Ultrafiltration was performed with ultracel 10 kDa ultrafiltration discs composed of regenerated cellulose, 47 mm (Millipore) with ultrapure water (Milli-Q).

6.2.2. Synthesis

6.2.2.1. Chemical modification of lipase from *Thermomyces lanuginosus*

With isothiocyanates: The enzyme (2 mL) was added to 5 mL of sodium carbonate buffer (pH 9, 0.1 M), followed by the addition of the isothiocyanate (10 μL, or 5 mg in 50 μL of DMSO). The solution was kept at 4 °C overnight with vigorous stirring. The precipitates were then removed by filtration, followed by ultrafiltration (10 kDa). The modified enzymes were recovered after 48 h of freeze-drying.

With aldehydes: The enzyme (2 mL) was added to 5 mL of phosphate/NaBH₃CN buffer (pH 5.1, 0.1 M sodium phosphate, 0.02 M NaBH₃CN), followed by addition of the aldehyde (4:1 w/w aldehyde: lipase). The solution was kept at 4 °C overnight with vigorous stirring [121]. The precipitates were removed by filtration, followed by ultrafiltration (10 kDa). The modified enzymes were recovered after 48 h of freeze-drying.

6.2.2.2. Synthesis of *p*-nitrophenyl benzoate

To a solution containing *p*-nitrophenol (100 mg, 0.72 mmol) in dry pyridine (2 mL) was added the benzoyl chloride (108 μL, 0.94 mmol) in an ice bath. The solution remained with stirring at 0 °C for 1 h, under nitrogen atmosphere, followed by rt overnight. The reaction was then stopped with the addition of water, and then the pyridine was removed using a rotary evaporator (Heidolph, Germany). Chloroform was then added, and the solution washed with NaHCO₃ (5x). The organic layer was dried over MgSO₄, filtered and the solvent removed in the rotary evaporator, affording the product as a white solid (quantitative yield). ¹H NMR (DMSO-d₆) δ_H: 7.62 (t, *J* = 7.6 Hz, 2H), 7.62 (d, *J* = 8.8, 2H), 7.77 (tt, *J* = 7.2, 1.2 Hz, 1H), 8.15 (dd, *J* = 8.4, 1.2 Hz, 2H), 8.35 (d, *J* = 9.2 Hz, 2H) ppm.

6.2.3. Enzyme characterization

6.2.3.1. Modification efficiency

The modification of the lipases was evaluated by reaction with 2,4,6-trinitrobenzene sulfonic acid (TNBSA), following the procedure reported by Castillo *et al.* [123].

6.2.3.2. Matrix-Assisted Laser Desorption/Ionization Time-of-Flight (MALDI-TOF)

MALDI-TOF mass spectra were acquired on a Bruker Autoflex Speed instrument (Bruker Daltonics GmbH), as reported by Noro *et al.* [79]. Sinapic acid was used as matrix, and the samples analysed in the linear positive mode, between 0-35 kDa m/z range.

6.2.3.3. Protein modification and SDS-PAGE

The quantification of the protein concentration and SDS-PAGE electrophoresis of all lipases were performed as described previously by Noro *et al.* [81]

6.2.3.4. Enzyme activity

Small length substrates (*p*-nitrophenyl acetate to *p*-nitrophenyl octanoate): The activity was measured at 37 °C, in a final volume of 4 mL, containing the desired substrate (*p*-NPAcetate, *p*-NPButyrate, *p*-NPHexanoate or *p*-NPOctanoate at 6 mM), the enzyme (1 mg of protein) and the assay buffer (K₂HPO₄ buffer, pH 7.8, 50 mM). The reaction was initiated by the addition of the enzyme and stopped with the addition of acetone. The hydrolysis of the substrate was monitored by the formation of the *p*-nitrophenol at 400 nm. The measurements were conducted in a Synergy Mx Multi-Mode Reader from BioTek (USA) in a 96 well plates. One unit of enzyme activity was defined as the amount of enzyme which catalyses the production of 1 μmol *p*-nitrophenol from the initial substrate per minute. All substrates were clear solutions at the concentration used.

Large length substrates (*p*-nitrophenyl laurate and *p*-nitrophenyl palmitate): For large length substrates, the activity was measured in the same conditions that previously detailed but using the following assay buffer: K₂HPO₄ 50 mM, pH 7.8, containing 0.5 mM of deoxycholic acid and 0.05 % w/v of gum arabic. After the reaction was stopped with acetone, the suspensions were filtered, followed by measuring the *p*-nitrophenol formed at 400 nm. All substrates were clear solutions at the concentration used.

6.2.3.5. Kinetic parameters

The enzymes' activity was measured following the procedure described previously. A range between 1 to 350 mM of *p*-NPAcetate, *p*-NPButyrate and *p*-NPOctanoate as substrates were used. The enzyme concentration was kept constant in all assays (1 mg/mL), performed at 37 °C. The maximum rate (V_{max}), the Michaelis-Menten constant (K_M), the turnover number (k_{cat}) and the catalytic efficiency (η) were determined after plotting the Michaelis-Menten curve. All calculations were obtained resorting to GraphPad Prism 5.0 software (La Jolla, CA, USA), with at least 3 independent experiments performed.

6.2.3.6. Molecular Dynamics Simulations

Molecular Dynamics (MD) simulations were performed on lipase from *Thermomyces lanuginosus* (lipase TL, PDB ID: 1TIB) [124] and on its modified form, with a dodecyl chain in position 98 (TL5), to understand the role of this linker on the lid and active site cavity. Previous work indicated that the lysine in position 98 directly interferes with the activity pocket and lid configuration [81]. TL5 structure were optimized and GROMOS parameters generated, using ATB server (Automated Force Field Topology Builder) [128, 129]. Modified TL was designed using PyMOL [130]. The lipase with the linker (TL5) was then simulated in the simple point charge water model, at 310 K, during 60 ns. The simulations options and algorithms are described in chapter 5, as well as the simulation performed for the native TL. All simulations were performed using the GROMACS 5.1.4 version [126, 160], within the GROMOS 54a7 force field (FF) [87, 88]. From MD simulations, we computed a cluster analysis from GROMACS package, with the single-linkage method, to determine the middle structure of each lipase (TL and TL5). These representative structures were used for docking experiment. Electrostatic potential surfaces were calculated using the PDB2PQR server [83] and images generated in PyMOL, with the APBS plugin [161].

6.2.3.7. Molecular docking and complexes simulations

The substrates used for the hydrolytic activity, *p*-nitrophenyl butyrate and *p*-nitrophenyl octanoate were optimized using Gaussian09 software [92], through a DFT calculation with B3LYP/6-31+G(d,p) basis set [162]. The optimized structures were transferred to *pdbqt* format (atomic coordinates, partial charges and AutoDock atom types) for the use on docking protocol. Docking experiments were performed with AutoDock 4.0 [94, 95] and prepared with the AutoDock Tools Software [94, 163]. The middle structures from TL and TL5 MD simulations were used as

macromolecules and the substrates used as ligands. Lamarckian Genetic Algorithm (LGA) was chosen as search algorithm [164]. A grid box was created and centered at the activity site, in a resolution of 0.375 Å, with the necessary size to involve all catalytic triad and the different substrates. Grid potential maps were calculated using AutoGrid 4.0. Each docking consisted of 100 independent runs, with a maximum number of 25×10^5 energy evaluations and a maximum number of 27,000 generations. Complexes simulations were performed using the best docking pose for each case, i.e. when the substrate was more internalized in the cavity and interacting with the catalytic triad. To simulate the complex, we also generated GROMOS parameters for the substrates using ATB. The complexes were minimized and equilibrated using the same options above described. MD simulations were carried out during 10 ns for each enzyme-substrate complex; the sufficient to perceive the spontaneous tendency of the substrate to remain or leave the active site. The interactions and distances between the substrates and the catalytic triad were followed.

6.2.3.8. Linkers simulations

The linkers used to obtain TL1 to TL5 were designed, optimized, and simulated in water, to understand which characteristics could have a role on enzyme activity, by changing the lipase and the environment. These 5 linkers were designed without the Lys core (see **Table 6.1**) and optimized using DFT calculations and Gaussian 09 [92]. After this procedure, the linkers were submitted to ATB to generate GROMOS topologies and MD simulations were carried out during 10 ns, using the protocol previously described. From MD simulations trajectories, we computed the solvent accessible surface area (SASA), to determine the percentage of hydrophobic area of the linkers used to modify TL1 to TL5. This percentage correspond to the hydrophobic area divided by the total area of each linker, to enable a direct comparison between all cases. This information combined with experimental results revealed a tendency on activity accordingly to the linker profile.

6.2.3.9. Half-life time ($T_{1/2}$)

The $T_{1/2}$ of each enzyme was performed by incubating the lipase solution in a water bath at 60 °C (1 mg/mL, pH 7.8). The activity was then calculated as previously described [165]. The stability of the enzymes in solution at 4 °C and 37 °C through the months was also evaluated. Both assays were evaluated by measuring the hydrolytic activity of *p*-nitrophenyl butyrate at 37 °C, as mentioned before.

6.2.3.10. Effect of the pH on the activity

The enzymes were incubated in the respective pH (range of pH 1.81 to 10.5) under universal buffer (Britton-Robinson buffer [166]) at 37 °C. After incubation for 10 min at the respective pH, the activity of the enzyme was measured at 37 °C in phosphate buffer (pH 7.8) as mentioned above, using *p*-nitrophenyl butyrate, *p*-nitrophenyl octanoate or *p*-nitrophenyl palmitate as substrates.

6.2.3.11. Effect of the temperature on the activity

The enzymes were incubated in the respective temperature (range of 10 °C to 70 °C) in a Thermal Shaker like (VWR) with phosphate buffer (pH 7.8). After incubation for 10 min at the desired temperature, the activity of the enzyme was measured at 37 °C using *p*-nitrophenyl butyrate, *p*-nitrophenyl octanoate or *p*-nitrophenyl palmitate as substrates.

6.2.3.12. Circular Dichroism (CD)

The native and modified lipases from *Thermomyces lanuginosus* were studied by CD spectroscopy, using a Jasco J-1500 spectropolarimeter. The sample preparation and parameters used were followed as reported by Noro *et al.* [81].

6.2.3.13. Fluorescence measurements

The intrinsic fluorescence of all lipases was conducted by their excitation at 280 nm. The emission spectra were set between 300 and 600 nm. All enzymes were analysed with a final concentration of 0.2 µM, dissolved in phosphate buffer (K₂HPO₄ buffer, pH 7.8, 50 mM).

6.3. Results and discussion

The covalent modification of enzymes modulates their function and properties, being their catalytic performance greatly influenced by the properties of the modifiers. The nature, size and hydrophobicity of the linkers is expected to alter the enzyme performance at different levels depending also on the degree of modification.

6.3.1. Chemical modification of lipase from *Thermomyces lanuginosus*

Herein lipase from *Thermomyces lanuginosus* (TL) was firstly reacted with compounds (linkers) from two different classes: isothiocyanates and aldehydes, with different chain length and

hydrophobicity. The linkers were chosen based on their high reactivity and ability to covalently bond to the primary amines of the exposed lysine residues of the enzyme (total of 7 residues observed by molecular dynamics). The proposed scheme for the reactions between the enzyme and the tested linkers is represented in **Figure 6.1**.

The degree of modification was assessed by the TNBSA assay and by MALDI-TOF spectrometry (**Table 6.1**).

After product isolation and evaluation (MALDI-TOF and TNBSA) the data revealed that all aldehyde compounds tested were successfully linked to the enzyme, with modification of at least one lysine available (**Table 6.1**).

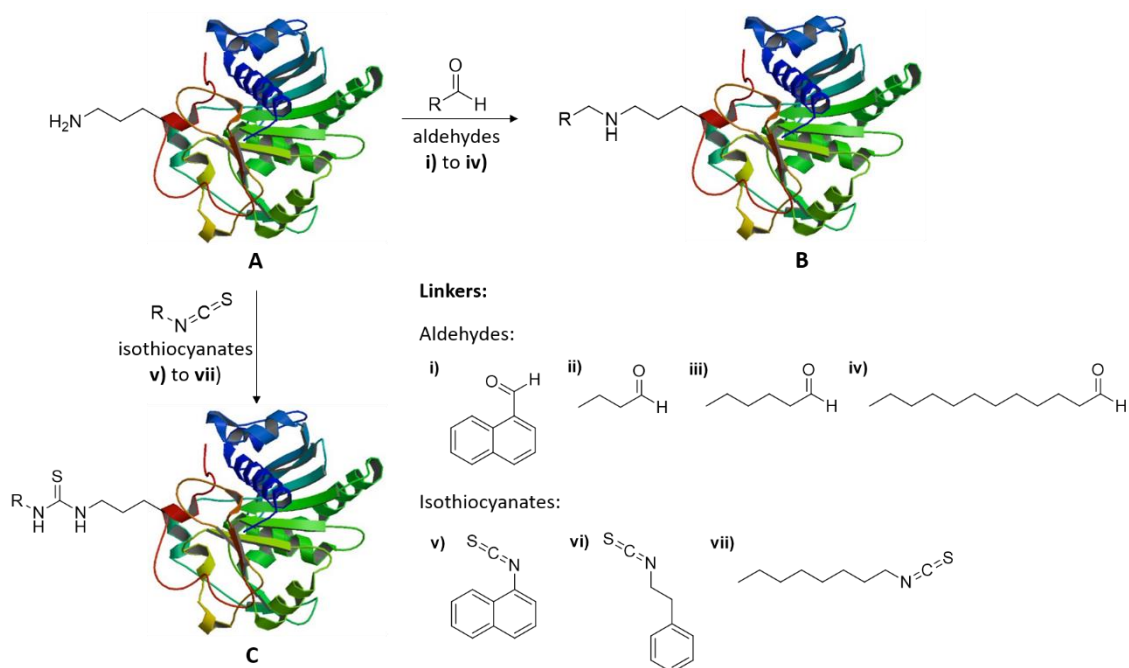
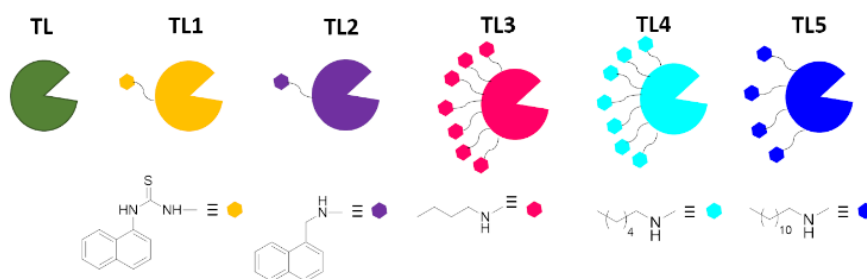


Figure 6.1. Proposed reactional scheme for the enzyme modification: **A)** native enzyme with an exposed lysine residue represented; **B)** enzyme modified with an aldehyde in the lysine residue, leading to a secondary amine; **C)** enzyme modified with an isothiocyanate in the lysine residue, leading to a thiourea; linkers used for lipase modification: **i)** naphthaldehyde; **ii)** butyraldehyde; **iii)** hexyl aldehyde; **iv)** dodecyl aldehyde; **v)** naphthyl isothiocyanate; **vi)** phenethyl isothiocyanate; **vii)** octyl isothiocyanate.

The aliphatic isothiocyanates (**Figure 6.1**, **vi** and **vii**) displayed the lowest reactivity, confirmed by the isolation of non-modified lipase. One unit of a more reactive aromatic isothiocyanate (**Figure 6.1**, **v**) was grafted onto lipase enzyme's surface. We can assume, as it is postulated, that isothiocyanate compounds, when linked to the amine group of the lysine residue, give rise to

thioureas, whereas aldehydes give rise to secondary amines [81, 167]. Lysine residues are the most nucleophilic amines present in enzymes [168]. The chosen class of compounds (aldehydes and isothiocyanates) are described to be preferentially linked to this residue instead to other reactive amino acids [168]. Different reactivities between linkers might explain the differentiated modification degrees obtained experimentally.

Table 6.1. Modification degree and number of modified residues evaluated by MALDI-TOF and TNBSA assay, being TL the native enzyme, and the modified enzymes: TL1 modified with naphthyl isothiocyanate, TL2 modified with naphthyl aldehyde, TL3 modified with butyraldehyde, TL4 modified with hexyl aldehyde and TL5 modified with dodecyl aldehyde



	MALDI-TOF (values in Da)	N ^o of residues modified by MALDI-TOF	% of modification (by TNBSA assay)	N ^o of residues modified by TNBSA
TL	29620	-	-	-
TL1	29771	1	8	1
TL2	29826	1	15	1
TL3	30283	7	93	7
TL4	30392	7	97	7
TL5	30270	4	49	3-4

MALDI-TOF results revealed, in comparison with the non-modified lipase (29620 Da), an increase of the molecular weight of the enzyme after modification with all the compounds used. In all cases, the results of MALDI-TOF and TNBSA were in accordance, revealing a direct relation between the degree of modification with the number of residues modified (**Table 6.1**).

The lipases modified with a naphthyl moiety (TL1 and TL2) revealed only one modified residue, probably due to their poor solubility and/or low reactivity of the starting material. TL3 and TL4 (with butyl and hexyl chains, respectively) were modified in all the 7 available lysines, while TL5 (with dodecyl chains) was only modified in 4 of the 7 available lysines. The length of the chains may induce a steric effect, which might explain the different modification degree obtained for the tested

linkers. Lysines located at positions surrounded by larger amino acids, are less prone of being modified by larger linkers. One may predict that, in the case of aldehydes, the degree of enzyme modification was inversely proportional to the size of the linker chain.

The modified lipases were also analysed by SDS-PAGE to evaluate size and purity (**Figure 6.2**). All enzymes were obtained pure, displaying only one visible band at around 30 kDa. The small molecular weight of the linkers was not detectable by SDS-PAGE and thus no significant differences between modified lipases were observed.

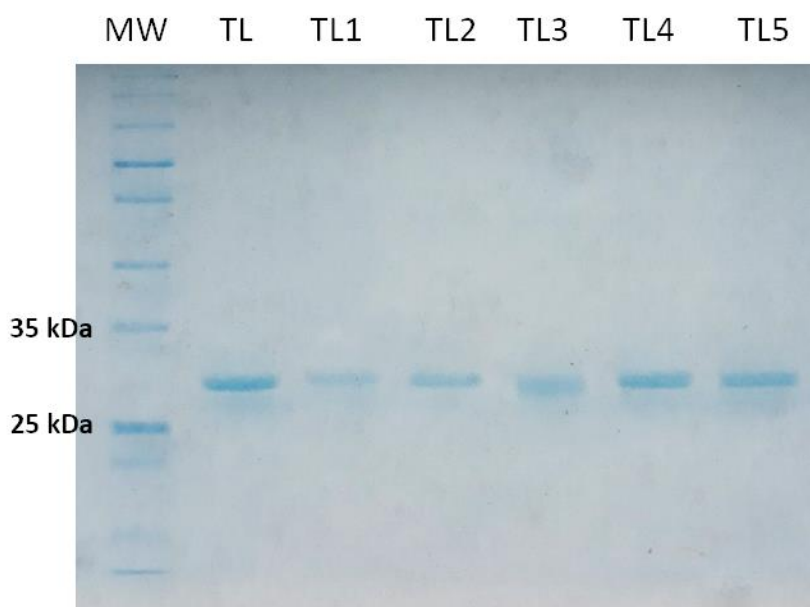


Figure 6.2. SDS-PAGE of native lipase from *Thermomyces lanuginosus* and modified lipases (TL1-TL5).

6.3.2. Hydrolytic activity

6.3.2.1. Absolute activity

The hydrolytic activity of a fixed amount of lipase (1 mg) was evaluated against seven substrates, differing in the size of the aliphatic chain (from 0 to 16 carbons) (**Figure 6.3A**). The results are expressed in U/mg, after incubation at 37 °C for 1 min (**Figure 6.3B** and **6.3C**).

From the results depicted in **Figure 6.3**, it is possible to perceive that the modification of lipase with the different linkers induced the improvement of the hydrolytic activity against substrates with differentiated chain-length, which are not normally hydrolysed by the native enzyme form. One may observe that for all the enzymes tested, the highest hydrolytic activity was achieved against the

medium-length chain substrates, *p*-nitrophenyl hexanoate (*p*-NPH, 6C) and *p*-nitrophenyl octanoate (*p*-NPO, 8C). Activity values higher than 100 U/mg were reached for all the lipases.

An exception was observed for the enzyme TL5. This enzyme, modified with four dodecyl chains, displayed higher activity against all the substrates tested, comparing with the native lipase. For the small chain-length substrates, *p*-nitrophenyl acetate (*p*-NPAc, 2C) and *p*-nitrophenyl butyrate (*p*-NPB, 4C), the hydrolytic activity obtained was at least 3-fold higher than obtained with the native enzyme. For these two substrates, all other modified enzymes showed activity values similar to the native enzyme. It is also worth mentioning that this modified lipase (TL5) also displayed activity (13 U/mg) against a synthetic substrate (*p*-nitrophenyl benzoate, 0C). For higher chain-length substrates (*p*-NPL and *p*-NPP), from all the tested enzymes, TL5 displayed also the highest hydrolytic activity (2-fold). For *p*-NPL, TL2, TL3 and TL4 revealed higher activity than native lipase (2-fold of activity increase). These three enzymes displayed activity values of ≥ 100 U/mg, for substrates containing 6, 8 and 12 carbons in the aliphatic chain, while the native enzyme only reached this activity for *p*-NPH (6C) and *p*-NPO (8C).

Lipase from *Thermomyces lanuginosus* is an enzyme composed by a lid over its active site, requiring interfacial activation. Moreover, the active site is surrounded by hydrophobic residues, which hinders its activity against small hydrophilic substrates. These features make lipase TL more able to hydrolyse longer substrates [151].

This lipase has a lysine residue near the lid (residue number 98 of the enzymes' sequence), which is a plausible position for modification with the tested linkers. Given the linkers' hydrophobicity, possible Van der Waals interactions with the lid and/or the hydrophobic surface surrounding the active site can occur, leading to different activity performances depending on the linker used. In this way, molecular dynamics tools were applied herein to infer the hydrophobicity of the linkers and correlate this parameter with the hydrolytic activity displayed by the modified lipases.

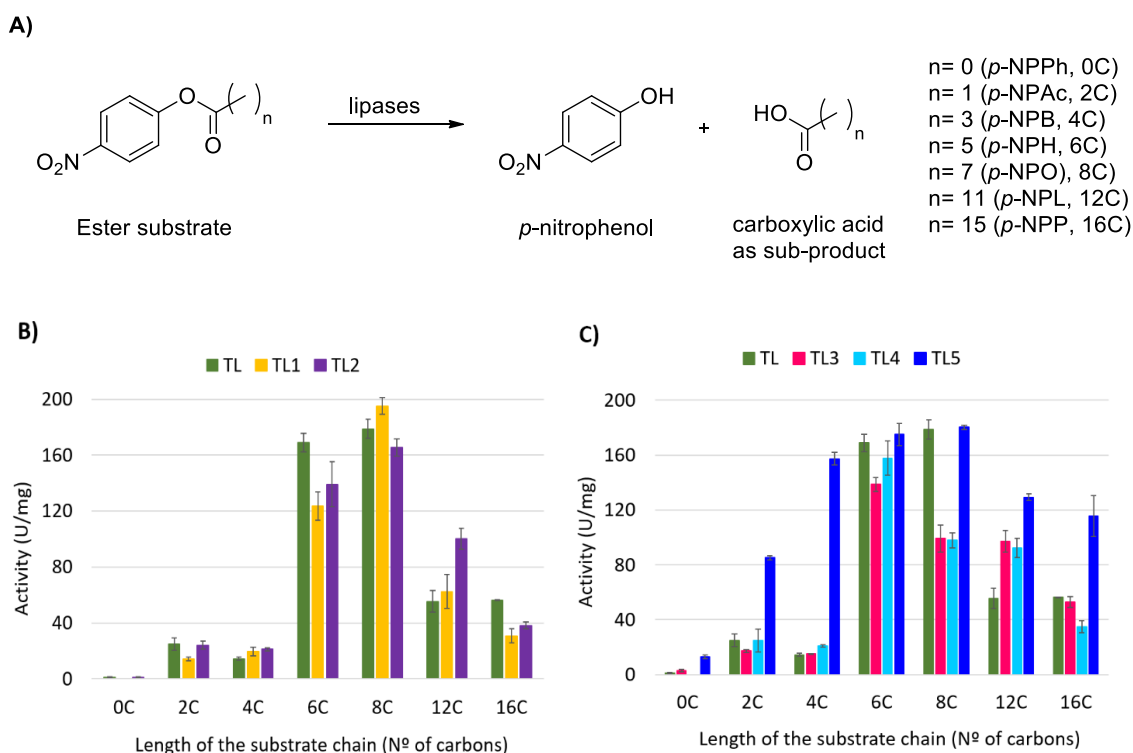


Figure 6.3. A) Proposed reactional scheme representing the hydrolysis of the ester substrates and the designation of each substrate according to the number of carbons in the aliphatic chain; **B)** Absolute hydrolytic activity of native lipase (TL) and of modified lipases with aromatic linkers (TL1 and TL2), and **C)** with aliphatic linkers (TL3-TL5), measured against different substrates: *p*-nitrophenyl benzoate (*p*-NPPH, 0C), *p*-nitrophenyl acetate (*p*-NPAC, 2C), *p*-nitrophenyl butyrate (*p*-NPB, 4C), *p*-nitrophenyl hexanoate (*p*-NPH, 6C), *p*-nitrophenyl octanoate (*p*-NPO, 8C), *p*-nitrophenyl laurate (*p*-NPL, 12C) and *p*-nitrophenyl palmitate (*p*-NPP, 16C).

Figure 6.4 depicts the hydrophobic area of the linker versus the hydrolytic activity of the modified lipases against three different substrates, representative of short, medium, and long chain-length: *p*-nitrophenyl acetate (*p*-NPAC), *p*-nitrophenyl hexanoate (*p*-NPH) and *p*-nitrophenyl laurate (*p*-NPL). From the data obtained it can be perceived that the hydrolytic activity of the enzyme modified with a specific linker was directly related with the percentage of its hydrophobic area. The highest overall activity was obtained for the lipase TL5, modified with the highly hydrophobic linker, 4 dodecyl chains (hydrophobic area higher than 70 %). We may assume that this linker can interact more favourably with the lid and/or with the hydrophobic residues surrounding the active site, eliminating the need for interfacial activation. These findings might explain the excellent catalytic performance of TL5 for all substrates, especially for the short-chain substrates. Together with an easier access

of the small substrates, a slight increase of the active site size may also occur, so that longer substrates can be better accommodate and further hydrolysed.

All other linkers tested are less hydrophobic than the dodecyl chain differing in their hydrophobic area in about 10 % (between 55-65 %). TL3 (butyl chains) and TL4 (hexyl chains) were completely modified, which indicates that the lysine near the lid was alkylated. However, these linkers are less hydrophobic than the dodecyl chain (TL5) which can consequentially lead to a weaker interaction with the hydrophobic environment around the active site. We may infer that these modified enzymes still required interfacial activation, given that vestigial activities were achieved when used against the shorter chain substrates. The same assumption might be valid for TL1 and TL2 (both with a naphthyl moiety), in which only one lysine residue was modified.

Comparing with native lipase the most pronounced activity differences regarding TL2, TL3 and TL4, were observed for *p*-NPL. For this substrate, the three enzymes showed activity values 2-fold higher than native enzyme. It was predicted that the modification of these lipases induced a slight change in the size cavity of the active site, which might explain the highest activity measured. Nevertheless, the effect of the cavity size was still less pronounced than the observed for TL5 when tested against longer substrates (*p*-NPP, 16C).

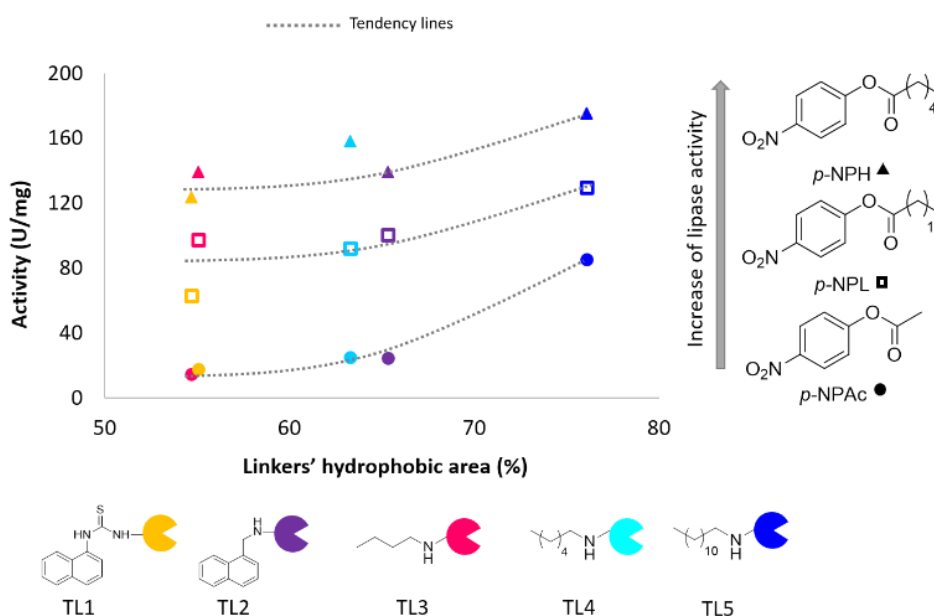


Figure 6.4. Activity of the modified lipases versus hydrophobic area of the linkers; activity measured against *p*-nitrophenyl acetate (*p*-NPAc, ●), *p*-nitrophenyl hexanoate (*p*-NPH, ▲) and *p*-nitrophenyl laurate (*p*-NPL, □). The colour of the symbols in the graphs corresponds to the colour of each modified enzyme represented below the graph.

TL1 did not displayed superior activity than the native enzyme in neither of the tested substrates. This modified lipase was only mono substituted with an isothiocyanate group, in a lysine placed away from the active site enabling any destabilization of the lid nor of the active site cavity.

It is important to state that the presence of the free aldehyde or isothiocyanate in the medium did not induced any alteration on the enzymes' activity, confirming that the performance differences observed are induced by the surface modifications undertaken. In chapter 5, we PEGylated lipase TL, through modification of the surface lysines with a monofunctional aldehyde-PEG (5000 Da). The modified lipase displayed a higher polymerase activity for the synthesis of a polyester, poly(ethylene glutarate), comparing to the native form. However, the hydrolytic activity of the modified lipase against *p*-nitrophenyl butyrate, remained similar to the native enzyme [81]. The surrounding PEG allowed an easier access of the monomers to the active site, nevertheless, the substrate used for hydrolytic activity evaluation revealed similar accommodation in the active site for both native and PEGylated form. Contrarily to PEG, which is an hydrophilic macromolecule, the linkers herein studied are small hydrophobic compounds which, depending on their size, may influence the enzyme conformation and therefore its hydrolytic activity.

As postulated by some authors, a proportional increment of the enzymes' activity with the degree of modification would be expected [157]. However, for the lipase studied, this behaviour was not observed, since higher levels of modification did not correspond to the best performance results (comparing TL5 with TL3 and TL4). One may assume that the activity was not only dependent on the level of modification but was extremely influenced by the linker type, chain size, hydrophobicity, and positioning at the enzyme's spatial.

6.3.2.2. Kinetic parameters

The kinetic parameters of the lipase modified with the different linkers were evaluated against different substrates: *p*-nitrophenyl acetate, *p*-nitrophenyl butyrate and *p*-nitrophenyl octanoate (Table 6.2). The substrates were chosen based on the preliminary activity results obtained for the modified lipase, where an increase of the enzymes' activity over the grown of the substrate chain length was observed.

Given the data obtained from Table 6.2, and as expected, the best kinetic parameters were obtained for *p*-NPO. For this substrate, the highest V_{max} was achieved with TL1, however, with a low K_M and catalytic turnover, revealing that this enzyme displayed the lowest catalytic performance for *p*-NPO, comparing to all other enzymes tested. The K_M values of TL2, TL3, TL4

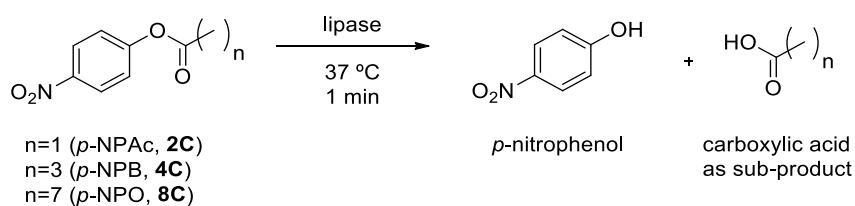
and TL5 are similar to the values of the native enzyme, being the catalytic turnover similar or lower after modification.

For the shorter substrates, TL5 displayed the best catalytic performance. The lowest K_M value (23 mM) was obtained for *p*-NPB, being 5-fold lower than the K_M value obtained for the native enzyme (110 mM). Moreover, the highest catalytic turnover (**Figure 6.5**) was observed for this modified enzyme against *p*-NPB ($\eta = 23364 \text{ M}^{-1} \text{ s}^{-1}$), which was 9-fold higher than the value obtained for the native enzyme ($\eta = 2552 \text{ M}^{-1} \text{ s}^{-1}$). All other modified enzymes showed a catalytic turnover similar to the native lipase.

For *p*-NPAC, the K_M value of TL5 (128 mM) was half of the K_M value of the native enzyme (245 mM). This modified enzyme revealed a catalytic turnover 6-fold higher than TL, whereas no significant alterations of the kinetic values were verified for the other modified enzymes.

As previously stated, lipase from *Thermomyces lanuginosus* is usually used for hydrolytic purposes in its immobilized form. The immobilization strategy increases its specific activity comparing to its free form, however some kinetic parameters are negatively affected [169, 170]. The strategy here applied does not restrict the enzymes' conformation and, in some cases, even improves its kinetic parameters (TL5).

Table 6.2. Kinetic parameters of native and modified lipases (V_{\max} ($\mu\text{mol}/\text{mg}/\text{min}$), K_M (mM) and $\eta = k_{\text{cat}}/K_M$ ($\text{M}^{-1} \text{ s}^{-1}$)) calculated for the hydrolysis of *p*-nitrophenyl acetate (*p*-NPAC), *p*-nitrophenyl butyrate (*p*-NPB) and *p*-nitrophenyl octanoate (*p*-NPO) under the conditions: substrate concentration varied between 1 and 350 mM, enzyme content (1 mg), performed at 37 °C for 1 min



Enzyme	<i>p</i> -nitrophenyl acetate (<i>p</i> -NPAC)			<i>p</i> -nitrophenyl butyrate (<i>p</i> -NPB)			<i>p</i> -nitrophenyl octanoate (<i>p</i> -NPO)		
	V_{\max}	K_M (mM)	η ($\text{M}^{-1} \text{ s}^{-1}$)	V_{\max}	K_M (mM)	η ($\text{M}^{-1} \text{ s}^{-1}$)	V_{\max}	K_M (mM)	η ($\text{M}^{-1} \text{ s}^{-1}$)
TL	752	245	1517	566	110	2552	1426	56	12482
TL1	610	214	1412	626	129	2402	1671	125	6612
TL2	680	223	1516	335	63	2656	1022	45	11340
TL3	780	299	1316	554	126	2218	701	42	8439
TL4	503	253	1005	708	229	1563	610	34	9018
TL5	2535	128	9828	1061	23	23364	1391	53	12979

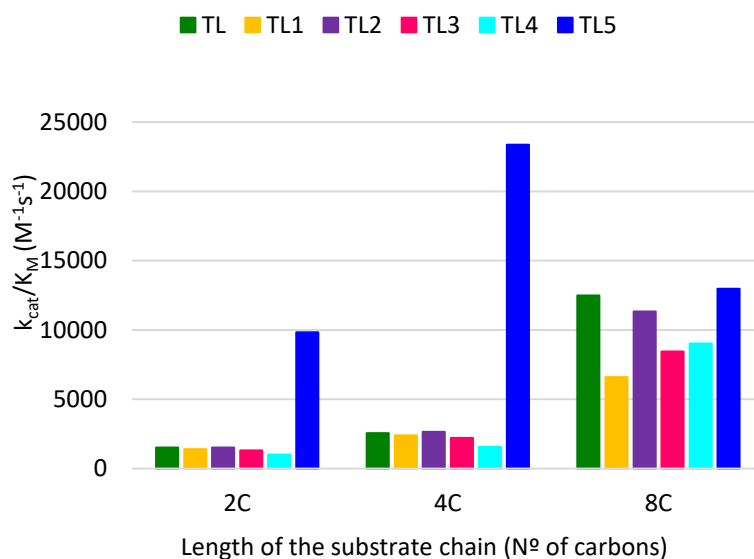


Figure 6.5. Catalytic turnover ($\eta = k_{cat}/K_M$) of the native and modified enzymes calculated for the hydrolysis of *p*-nitrophenyl acetate (*p*-NPAc, 2C), *p*-nitrophenyl butyrate (*p*-NPB, 4C) and *p*-nitrophenyl octanoate (*p*-NPO, 8C).

The kinetic profile of lipase TL is described to be improved as the chain-length of the substrates grows [171], as we also confirmed. Moreover, the modified enzymes obtained, revealed better kinetic performance than the native enzyme, mainly for the shorter substrates.

The kinetic parameters of the modified lipases are, as mentioned previously, greatly influenced by the type of linker attached and its positioning at the enzymes' surface. The activity data also indicated that the lack of hydrophobicity of the small substrates seems to be counterbalanced by the hydrophobic character of the linker, as the highest activity differences were observed for smaller and less hydrophobic substrates. For longer and hydrophobic substrates, the impact of the enzyme modification (TL5) seems to be irrelevant since the access to the enzymes' active site was always ensured (Figure 6.5).

In order to predict the enzyme performance and better understand the conformational changes induced by the modifications, molecular dynamics simulations were performed on TL and TL5.

6.3.3. Molecular Dynamics Simulations

MD simulations were carried out using a similar strategy applied on a previous work using the same enzyme [81]. During simulations, no modifications were carried out for native TL (PDB ID: 1TIB), whereas for TL5, the enzyme was modified at Lys98 with a dodecyl chain (Figure 6.6A and

C, respectively). This specific lysine is in one of the lid arms and any modification may cause important alterations of the lid arrangement or of the size/opening of the active site, which is crucial for the enzymes' activity.

Figure 6.6 highlights the lid, the catalytic triad, and the linker in the case of TL5 (**Figure 6.6C**). In these middle structures we observe that the helical lid undergoes some unfolding on its structure in both enzymes, nevertheless leading to a larger cavity for TL5 (yellow filling), in which the amino acids side chain positioning also contributes to a well-defined cavity. This conformational change was followed through RMSD and RMSF analysis (**Figure 6.7**), where a RMSF peak is seen around the residue 98 in TL5. Globally, the two lipases are stable in aqueous medium.

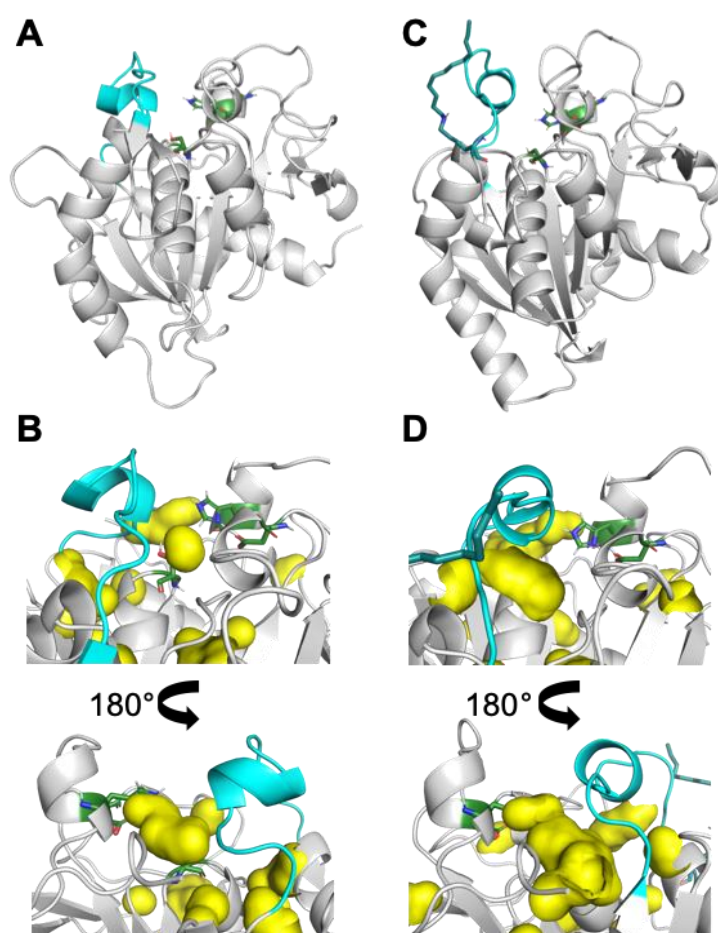


Figure 6.6. Middle structures characterized for lipase TL (**A**) and TL5 (**C**); Lid is highlighted in cyan, catalytic triad with the residues in green sticks and TL5 in blue sticks (**C**); (**B**) and (**D**) zoom in the active site, showing the pockets/cavities in yellow surface.

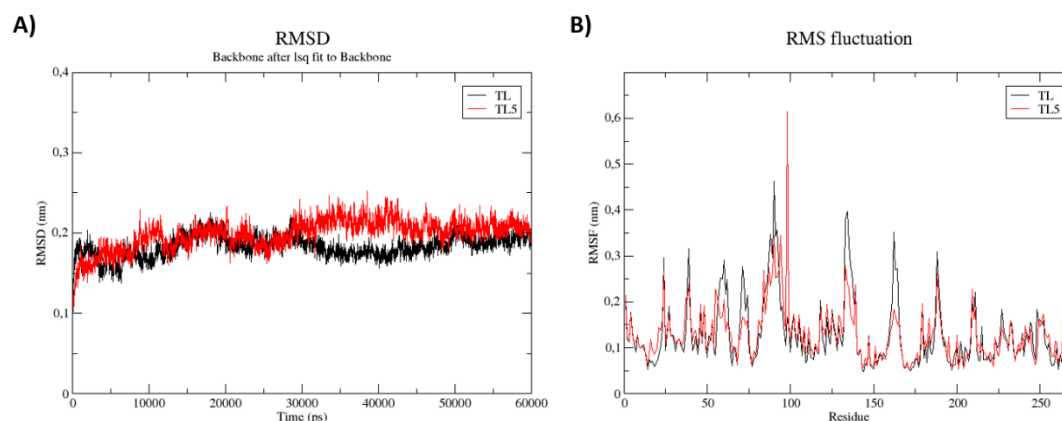


Figure 6.7. A) Backbone RMSD of lipase TL and TL5 in water; **B)** amino acids RMSF.

The larger cavity obtained for TL5 may be responsible for the increase of the activity for longer substrates (p -NPL and p -NPP), since a better accommodation of the long aliphatic chain can occur. The same can be stipulated for TL2, TL3 and TL4, which were more active than the native TL for p -NPL. However, the increase of the cavity size of TL2, TL3 and TL4 was not so pronounced than for TL5, explaining the lower activity of these enzymes for the longer substrate tested (p -NPP).

Noteworthy is that the change in the cavity size and conformation of TL5, might induced the great increase of its activity against small substrates (p -NPAC and p -NPB), resulting from an easier access of these substrates and a higher affinity to the active site.

Using PyMOL two possible accesses to the active site were found, one from the top and another from the left lateral side, under the lid. To monitor the possibilities of binding and the dynamics, the molecular docking of the substrates to the lipases was performed, followed by the simulation of the resulting complexes.

Docking experiments were carried using two substrates: p -NPB (4 carbons) and p -NPO (8 carbons). The obtained results agree with the experimental data, revealing a higher affinity of both substrates with the active site of TL5 (- 7.7 kcal/mol), where a stronger interaction takes place (**Figure 6.8, C-D**), while the native enzyme presented lower binding energies (< 3 kcal/mol). Furthermore, native TL also showed lower values of energy for p -NPB (-4.36 kcal/mol) than for p -NPO (-5.47 kcal/mol), as expected, given the activity values observed experimentally (14.4 U/mg and 175 U/mg, respectively).

During simulations, one can observe that p -NPB was more unstable in TL, leaving rapidly from the active pocket, remaining stable in TL5. The p -NPO substrate remains stable in the pocket in both cases.

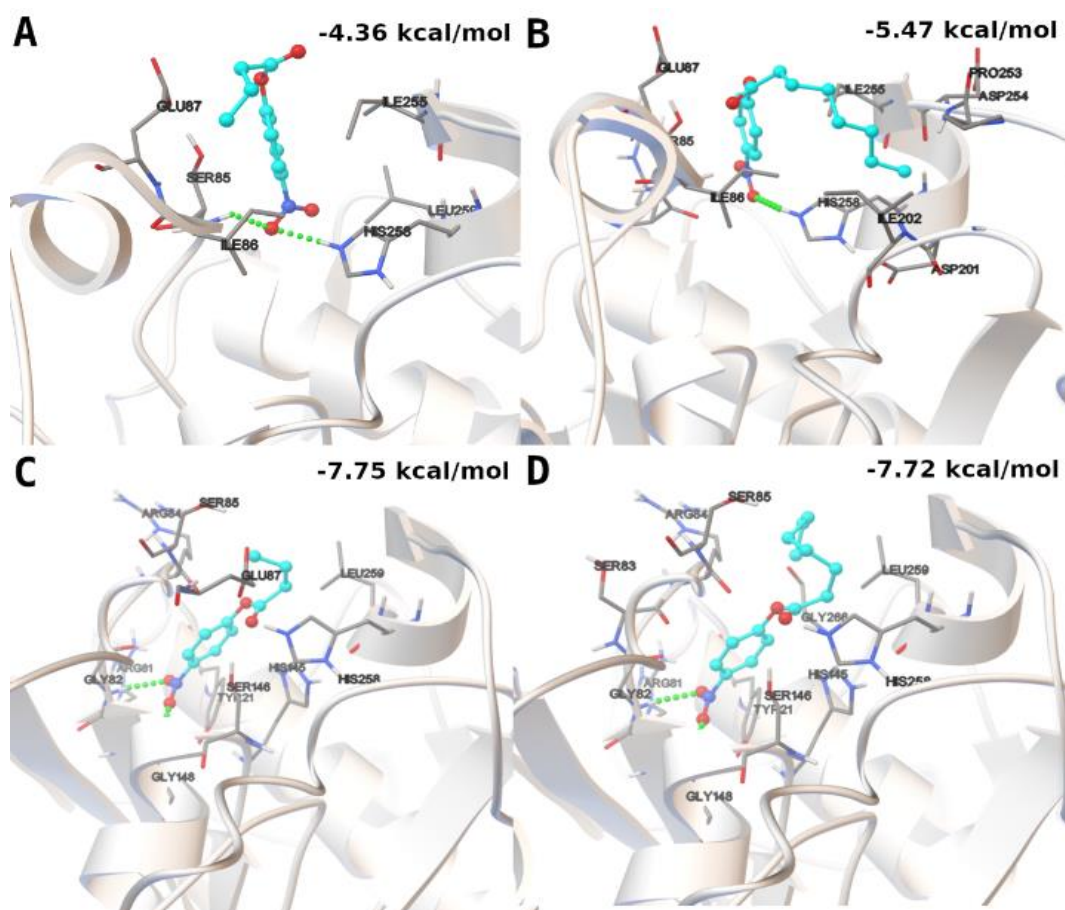


Figure 6.8. Representation of the best docking poses, interactions and $\Delta G_{\text{binding}}$ between *p*-nitrophenyl butyrate with native TL (A) and with TL5 (C); *p*-nitrophenyl octanoate with native TL (B) and with TL5 (D). Enzymes are represented in grey cartoon, sticks to highlight the amino acids residues participating in the binding, substrate in cyan ball and sticks, and hydrogen bonds in green dashed.

The distance between the substrates and the Ser146 residue of to the catalytic triad, was measured along time (Figure 6.9). The results confirmed what was observed visually following the simulation trajectories in PyMOL, i.e., the spontaneous unbinding of *p*-NPB in TL (purple line), indicating a weaker interaction than with TL5 (blue line). For *p*-NPO, similar results were obtained.

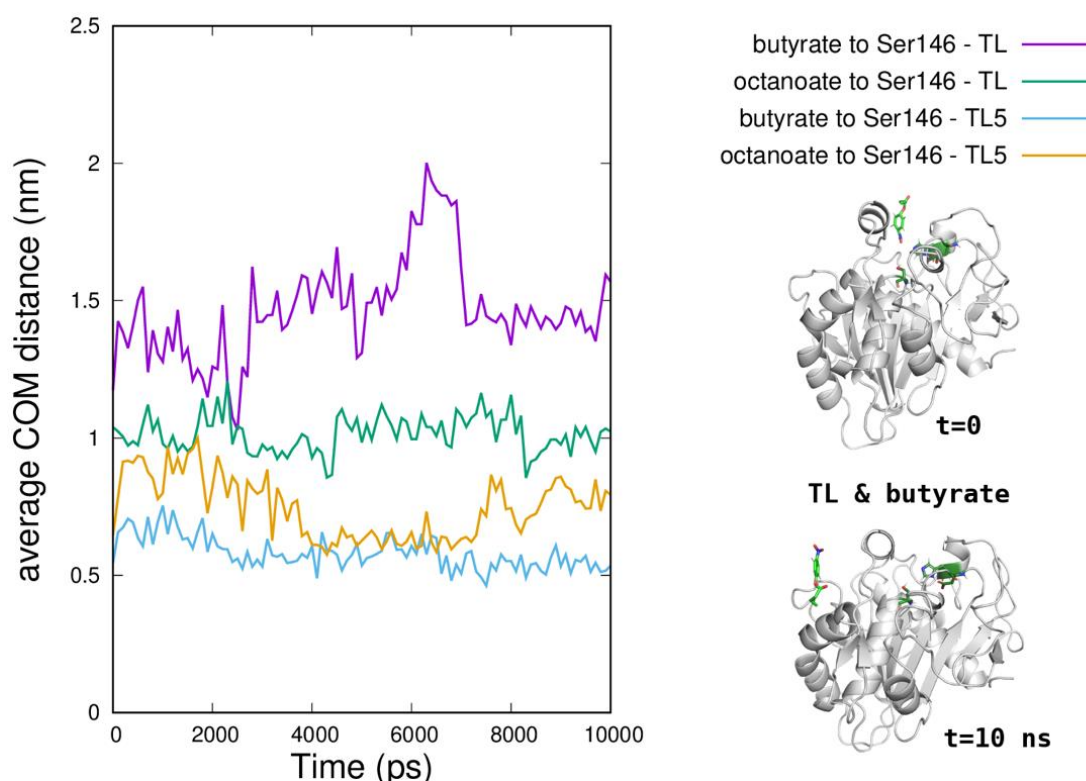


Figure 6.9. Distance (nm) along simulation time from *p*-nitrophenyl butyrate or *p*-nitrophenyl octanoate to the Ser146 in catalytic triad.

6.3.4. Stability of TL and modified lipases

The stability over time of TL and modified lipases was firstly evaluated at different temperatures: 4 °C, 37 °C and 60 °C. All enzymes revealed remarkable stability in solution at 4 °C, with minimum activity lost after 4 months (**Figure 6.10A**). At 37 °C, after 4 months, at least 20 % of their initial activity endures. Despite a similar hydrolytic activity and kinetic profile, TL2 showed a higher thermostability compared with native enzyme. After 4 months at 37 °C, the activity of this enzyme was still almost 2-fold higher than the native enzyme. All enzymes modified with an aromatic or aliphatic aldehyde revealed higher thermostability than the native lipase.

At 60 °C, the activity lost was more pronounced, allowing to calculate the half-life time of the enzymes (**Figure 6.10B**). With exception of TL5, all lipases revealed higher half-life time than native TL. Despite the lower half-life time obtained for TL5, the specific activity of this modified form was still higher than native (30 U/mg vs 6 U/mg).

Lipase from *Thermomyces lanuginosus* is known by its broad range of optimum pHs, from 7 to 10, with an optimum temperature at around 40 °C.

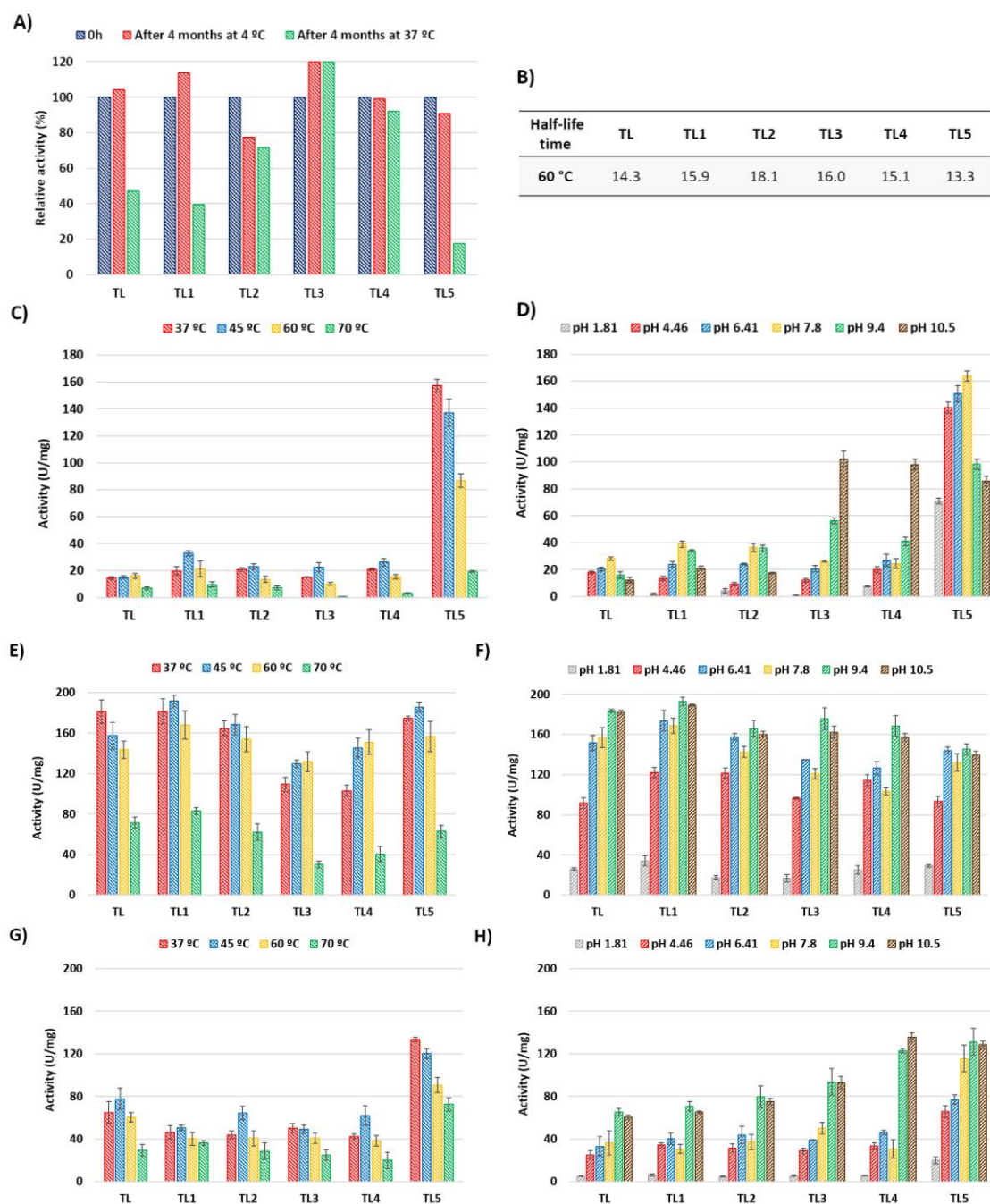


Figure 6.10. Stability of native and modified enzymes: **A)** Relative activity (%) at time zero, and after 4 months in solution at 4 °C and 37 °C; **B)** Half-life time (in hours) of the enzymes at 60 °C; **C)** Effect of temperature in the enzymes' activity after 10 min incubated at the respective temperatures (37 °C, 45 °C, 60 °C and 70 °C); **D)** Effect of pH in the enzymes' activity after 10 min incubated at the respective pH (1.81, 4.46, 6.41, 7.80, 9.40 and 10.5). The results presented were obtained using *p*-nitrophenyl butyrate as substrate. **E)** and **G)** same as **C)** but using *p*-nitrophenyl octanoate or *p*-nitrophenyl palmitate as substrate, respectively; **F)** and **H)** same as **D)** but using *p*-nitrophenyl octanoate or *p*-nitrophenyl palmitate as substrate, respectively.

The effect of temperature (10-70 °C) and pH (1.8-10.5) in the lipases' activity was investigated (**Figure 6.10C** and **6.10D**) both using *p*-nitrophenyl butyrate as substrate. From the data obtained it was possible to perceive a similar activity trend for all the enzymes tested.

Regarding temperature, all enzymes showed similar activity against *p*-nitrophenyl butyrate between 37 °C and 45 °C, presenting only residual activity at 70 °C. These results agree with the thermal stability associated with lipase TL. A similar trend was observed when other differentiated chain-length substrates were used, such as *p*-nitrophenyl octanoate (8C, *p*-NPO) and *p*-nitrophenyl palmitate (16C, *p*-NPP) (**Figure 6.10E** and **G**, respectively).

Regarding pH, TL was completely inactive while all modified enzymes showed some residual activity against *p*-nitrophenyl butyrate at the lowest pH tested (pH 1.81). At this pH, TL1, TL2, TL3 and TL4 showed activity values below 6 U/mg, while TL5 maintained remarkable activity (70 U/mg). These findings agree with the literature reports, which describe that the chemical modification of enzymes improve their stability. A similar tendency among native and modified lipases (TL1-TL4) was observed when a larger substrate (*p*-NPP) was used at the lowest pH. The activity of TL5 was still 4-fold higher than TL (**Figure 6.10**). All enzymes revealed similar activity values against *p*-NPO at pH 1.81.

The most surprising result was the activity obtained for TL3 (butyl linkers) and TL4 (hexyl linkers) at the highest pH tested (9.4 and 10.5). The hydrolytic activity of these lipases increased 4-fold compared to the activity obtained at standard pH (7.8). In both enzymes all the lysines were modified, and the buffer pH change would drastically affect their total charge, inducing therefore alterations on the activity. Circular dichroism was applied to study this behaviour. From the results obtained one may observe that the increase of pH does not lead to any significant change in the enzymes' conformation (data not shown), which keep a profile similar to the native lipase. Moreover, lipase from *Thermomyces lanuginosus* is known for its broad range of activity until pH 10, indicating that no denaturation should occur at higher pHs. Regarding this, the increase in the hydrolytic activity of TL3 and TL4 at higher pH values, may be caused by the different charge acquired upon modification.

The pKa value of the lysine residue is reported to be around 10.4 [172]. Also, the pKa of the lysines are highly influenced by many factors, such as position, surrounded amino acids, etc [173]. After alkylation, pKa values are expected to be different, and therefore, different charges are estimated.

In order to confirm these allegations, we used molecular dynamics simulations (**Figure 6.11**) to evaluate the effect of the enzymes' total charge on their hydrolytic activity, by calculating the pKa by Poisson-Boltzmann electrostatics.

This tool allowed to infer the positioning of the most significant charge variations on the lipase's structure. From **Figure 6.11**, we may observe that when the lysines were alkylated, the most affected area was the surrounding active site. TL3 and TL4 showed an increase in their activity at higher pH for all the substrates tested (4C, 8C and 16C). These results may indicate that at higher pH, the alkylation of the lysines, together with an enlargement of the active site and/or an easier access of the substrates, might occur, and thus the interfacial activation may no longer be necessary. We may assume that the similar phenomenon previously postulated for TL5 may occur for TL3 and TL4, however, with greater influence of the different charge acquisition induced by pH fluctuations. It is well known that the secondary structure of the proteins is ensured by the hydrogen bonds between amino acids. Amine residues are crucial in this phenomenon [174]. It is possible that small structural changes might occur near the active site due to changes in the residues' charge, improving the access of the substrate to the active site, therefore enhancing the enzymes' activity.

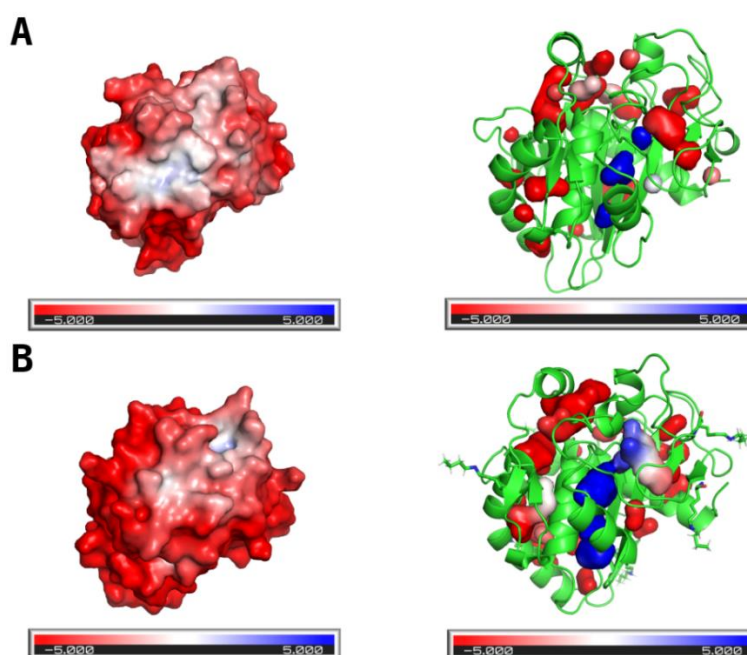


Figure 6.11. Electrostatic potential surface ($k_b T e_c^{-1}$) generated with PDB2PQR server and APBS plugin in PyMOL, at pH 10.5, for: **A**) TL with all Lys side chain protonated, and **B**) TL3 with all Lys converted to TL3 linker. On the left exterior surface and on the right the cavities/pocket representation.

6.3.5. Circular dichroism

Circular dichroism (CD) was undertaken to evaluate the effect of the modifications performed, on the conformational structure of the enzymes (**Figure 6.12**). The CD spectra of the native enzyme showed the expected behaviour, described in literature [175]. Lipase TL is structurally composed by a central eight-stranded, mostly by parallel beta-sheets and five interconnecting alpha helices [151]. All modified enzymes (TL1 to TL4) revealed a profile similar to the native TL, with no significant modifications in the number of α -helices and β -sheets. Given the experimental results obtained for these enzymes, these results were expectable.

TL5 revealed the most discrepant profile, displaying the lowest intensity. The decrease in the intensity can be related to a slight unfolding of the protein's structure. Considering the experimental activity results, one may infer that the access of the active site, was facilitated by the modification with the dodecyl chain at the enzymes' lid, which enhanced its activity for short and long substrates. This behaviour was also observed by molecular dynamics simulation that confirmed the active site enlargement and a consequent easy access of the substrates.

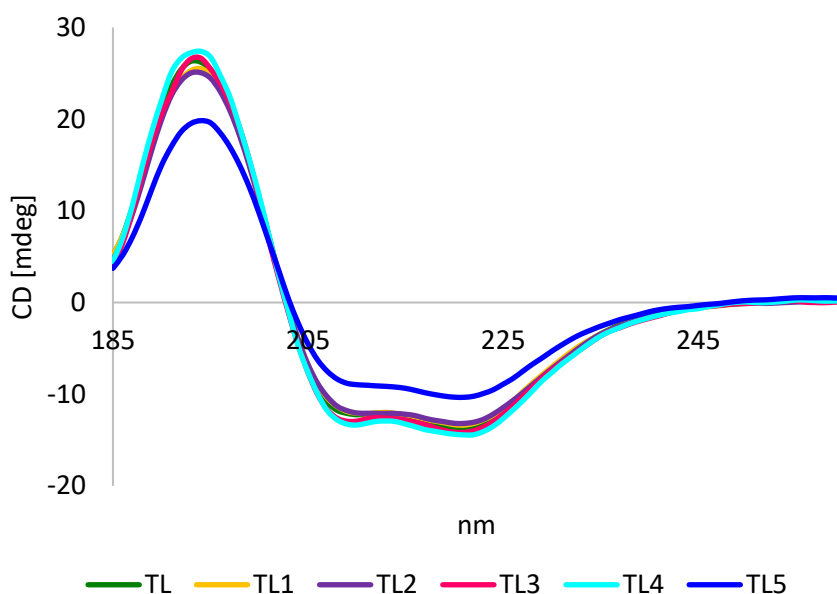


Figure 6.12. Circular dichroism of native lipase (TL) and modified lipases (TL1 to TL5).

6.3.6. Fluorescence analysis

The intrinsic fluorescence of the lipases, related to the presence of fluorophore residues, was considered, as a strategy to observe conformational fluctuations [176] induced by the compounds grafted to the lysine residues (**Figure 6.13**). Comparatively to native lipase, all the modified lipases

showed a decrease of the fluorescence intensity, which is usually associated to an unfolding of the protein. However, the fluorescence intensity can be also affected by other factors, such as morphology, protein size and protein aggregation [177]. By circular dichroism it was only possible to observe a slight unfolding of TL5, indicating that the decrease of fluorescence that was observed for all other modified lipases (comparing to the native form), might be related to other factors.

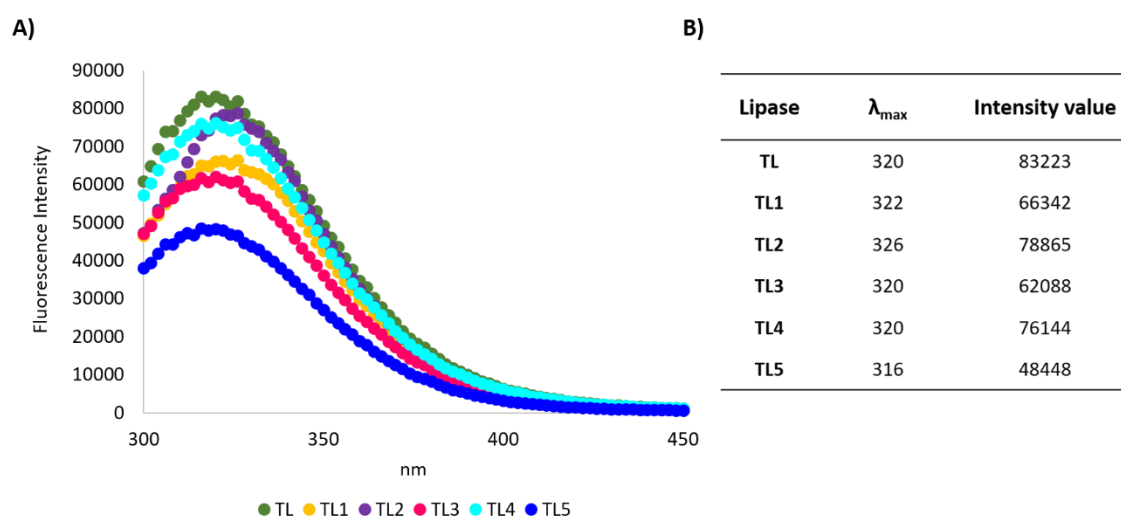


Figure 6.13. A) Fluorescence spectra of native (TL) and modified lipases (TL1-TL5) after excitation at 280 nm. **B)** Table of the maximum wavelength with the respective intensity value.

A hypochromic blue shift (from 320 to 316 nm) was observed for TL5, while TL3 and TL4 showed their maximum intensity at the same wavelength as the native enzyme, or at a higher wavelength (TL1 and TL2). The blue shift is frequently associated to the exposure of the amino acids to a more hydrophobic microenvironment, in which the fluorophore residues are more internalized [178]. The tryptophan residue at the lid of lipase TL is one of the amino-acids responsible for the enzymes' fluorescence [138]. Changes in the microenvironment of this residue may influence the fluorescence, which given the differences obtained in terms of activity, might indicate that the lid of the enzyme was modified. Since TL5 is modified with the most hydrophobic linker, its fluorescence decreases greatly, induced by a more hydrophobic microenvironment.

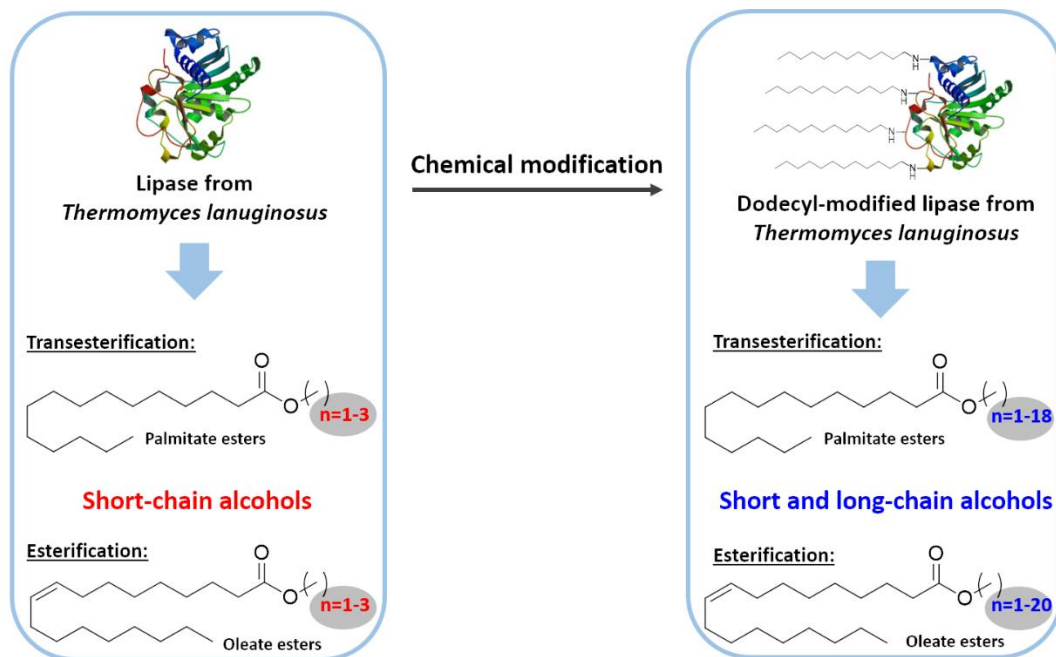
6.4. Conclusions

In this work, chemical modifications of lipase from *Thermomyces lanuginosus* with different linkers (isothiocyanates and aldehydes) were for the first time explored to improve activity, stability, and affinity to differentiated substrates. The results showed that aldehyde linkers were more prone to modify the lysines of lipase comparing with the isothiocyanates. One concluded that the size and hydrophobic character of the linkers influenced greatly the enzyme activity. The longer and hydrophobic is the linker, the stronger is its interaction with the hydrophobic amino acid residues near the active site, conducting to a destabilization of the lid and to an enlargement of the active site's cavity. This is expected to induce an improvement of the lipase performance.

The implementation of the easy methodology developed, broadening the substrates chain-length specificity, increments thereafter the range of substrate possibilities that can be hydrolysed by this lipase, paving the way to the establishment of new industrial applications.

Chapter VII

Chemical modification of lipase from *Thermomyces lanuginosus* enhances transesterification and esterification activity



Chemical modification of lipase from *Thermomyces lanuginosus* enhances transesterification and esterification activity**Abstract**

Lipase from *Thermomyces lanuginosus* is one of the most explored enzymes for the esterification of several added-value industrial compounds. The modified form (grafted with 4 dodecyl chains, TL5) revealed previously higher hydrolytic activity against size-differentiated substrates, compared with the native enzyme. In this work, we evaluated the transesterification and esterification activity of native and modified lipase, using *p*-nitrophenyl palmitate and oleic acid as model compounds, respectively. Linear size-differentiated alcohols (from 1 to 20 carbons in the aliphatic chain) were used to explore for the first time the effect of the chain length in both transesterification and esterification reactions. The chemically modified lipase showed greater catalytic performance, than the native enzyme, being this increase directly proportional to the size of the alcohols chain used as substrates. The enormous potential and remarkable versatility of this chemically modified lipase was here demonstrated, where diverse types of esters, differing in their potential applications, were efficiently synthesized. The produced esters were fully characterized by ¹H NMR, GC-MS, and FTIR.

This chapter is based on the following publication:

Jennifer Noro, Artur Cavaco-Paulo, Carla Silva, Chemical modification of lipase from *Thermomyces lanuginosus* enhances transesterification and esterification activity, submitted to: ACS Catalysis.

7.1. Introduction

Lipase from *Thermomyces lanuginosus* (TL) was the first recombinant lipase produced [179], and nowadays, it remains one of the most explored enzymes for the synthesis of compounds with industrial value. Besides their natural triacylglycerols hydrolysis function, it also demonstrates esterification and transesterification activity [151]. Ester compounds are present in many daily products, being the major components of flavours, fragrances, polymers, fats, among others [180]. The use of lipases for their synthesis is considered a green and environmentally friendly practice, regarding the high reactional yields and the mild reaction conditions associated [181].

Among the different lipases, lipase TL is one of the most explored for transesterification and esterification reactions. Ashrafuzzaman and co-workers observed that immobilized lipase TL demonstrated the highest regioselectivity in the acylation of sucrose esters comparing to other lipases [182]. The transesterification reaction was carried out using divinyl esters. A similar approach was undertaken by Chávez-Flores *et al.* [183], in the regioselective transesterification of vinyl laurate with a probiotic sugar, lactulose, using the same form of enzyme. Corrêa and co-workers [184] studied the esterification of the flavours, geraniol and citronellol, promoted by immobilized lipase TL. The reactions were carried out by coupling oleic, lauric, and stearic acid, being the produced esters isolated in good yields (>60 %) [184].

The esterification of oleic acid with isoamyl alcohol was performed by Lage *et al.* [185]. The authors used lipase TL immobilized onto polymethacrylate particles as reaction catalyst. The ester, isoamyl oleate, which can be used as a biolubricant, was successfully synthesized with high conversion (85 %).

Another major field of application of this lipase is in the production of biodiesel. The extensive investigation reported in this area stems from the world demand to find green and renewable sources of fuels [186]. Biodiesel can be manufactured through enzymatic catalysis, by the transesterification or esterification of oils/fats with small-length alcohols, such as methanol or ethanol. Countless sources of oils/fats can be used for this purpose. Sunflower, coconut, soybean, palm, and cotton seed oils or even wastes from the food industry, with varied composition, are some of the potential sources [187-189].

As described previously, most reports regarding transesterification and esterification reactions describe the use of lipase TL in its immobilized form. The immobilization of enzymes presents several advantages, in comparison to other methodologies, including reusability, thermostability, and others [190]. However, immobilization techniques, besides being a more expensive strategy,

it reduces the enzyme mobility and consequently, its catalytic performance [191]. Many reports from literature have been describing the chemical modification of lipases as an efficient methodology to overcome the limitations associated to the immobilization methodologies [157, 158, 192]. However, a lack of practical examples regarding its implementation on the synthesis of industrial added-value products can be found. In chapter 5, we have reported that the PEGylation of lipase TL improved its polymerase activity comparing with the native enzyme. Higher degree of polymerization and conversion yield were obtained in the biosynthesis of a polyester, poly(ethylene glutarate) [81].

Previously, in chapter 6, we performed the chemical modification of lipase TL by grafting small hydrophobic aldehydes and isothiocyanates to the exposed lysine residues at the enzymes' surface. Besides increasing their thermostability, the modification of the enzyme with aliphatic aldehydes showed to improve their activity in the hydrolysis of differentiated chain-length substrates [192]. Lipases displaying both esterification and transesterification selectivities for short and long alcohols are difficult to found, especially to obtain high reactional yields.

In this work, the transesterification and esterification activity of the native and modified (grafted with four dodecyl chains, TL5) lipase TL were explored by investigation of their activity towards differentiated chain-length alcohols. *p*-Nitrophenyl palmitate and oleic acid were used as model lipids for the transesterification and esterification reactions, respectively. A broad range of alcohols (from methanol to eicosanol, in a total of 11 alcohols) were used as substrates for the evaluation of the activity of both enzyme forms (native *vs* modified).

7.2. Materials and methods

7.2.1. Materials

Lipase from *Thermomyces lanuginosus*, butanol, hexanol, oleyl alcohol, *p*-nitrophenol, molecular sieves 4 Å pellets (1.6 mm diameter), were purchased from Merck. *p*-nitrophenyl palmitate was obtained from Santa Cruz Biotechnology. Oleic acid, methanol, ethanol, propanol, pentanol, heptanol, decanol, dodecanol and eicosanol were purchased from TCI Chemicals. *n*-Heptane was acquired from Fischer Chemicals (HPLC grade) and dried over molecular sieves prior to usage.

7.2.2. Chemical modification of lipase TL

The chemical modification of the lipase was performed as previously described in chapter 6 [192]. The modified lipase TL (TL5) was isolated with four grafted dodecyl chains. Native lipase TL was used after ultrafiltration for the removed of any additives. Both enzymes were used in their lyophilized form.

7.2.3. Half-life time of the enzymes ($T_{1/2}$)

The half-life time of the lipases (native and modified) was evaluated at different temperatures (25, 37 and 50 °C). Prior to the evaluation of the transesterification/esterification activity, the $T_{1/2}$ of the enzymes was accessed to ensure that no significant loss of activity occurred at the different temperatures tested. For this, the lipases (1 mg/mL), dissolved in phosphate buffer (pH 7.8, 50 mM), were placed in a water bath, under different temperatures (25, 37 and 50 °C). At different time intervals, the hydrolytic activity was measured against *p*-nitrophenyl hexanoate. The assay was executed as previously described [192]. Afterwards, the $T_{1/2}$ was calculated as reported [165]. The measurements were performed in a Synergy Mx Multi-Mode Reader from BioTek (USA) in a 96 well plates. One unit of enzyme activity was defined as the amount of enzyme which catalyses the production of 1 μ mol *p*-nitrophenol from the initial substrate per minute.

7.2.4. Transesterification activity

The transesterification activity of both enzymes (native and grafted with four dodecyl units) was measured using different alcohols, to evaluate the effect of the chain length on the final activity of the enzymes. The reactions were performed following the procedure reported by Teng and Xu [193]. Briefly, the enzymes (10 mg), were added to a flask containing 10 mL of a 10 mM solution of *p*-nitrophenyl palmitate in dry *n*-heptane. Then, 60 μ L of 1 M of the respective alcohol was added to the flask and placed in a water bath at 37 °C, under stirring (150 rpm). Aliquots of 30 μ L were withdrawn at different time intervals and quenched with 1 mL of NaOH (0.1 M). Then, 200 μ L were placed in a 96-well plate and the *p*-nitrophenol released was read at 400 nm. The enzymes activity was then calculated by plotting the *p*-NP released over time.

7.2.5. Esterification activity

In a flask containing the enzyme (native or modified, 0.08, 0.17 or 0.25 % w/v) was added the oleic acid (300 μ L) and the respective alcohol (1 equivalent) in 3 mL of *n*-heptane. The suspension was placed at the desired temperature (25, 37 or 50 $^{\circ}$ C) under stirring. At different time intervals, 100 μ L of the solution was taken, and the volume made up until 5 mL with a solution of ethanol/acetone 1:1. This solution was then titrated with NaOH 20 mM, using phenolphthalein 0.5 % w/v as indicator.

K values were then calculated for both reactions, regarding the following equation:

$$K = \frac{[\text{Ester product}]}{[\text{Starting material}]}$$

7.2.6. Products characterization

7.2.6.1. Nuclear Magnetic Resonance spectroscopy (NMR)

After both transesterification and esterification reactions, the *n*-heptane and the volatile alcohols were completely removed in the rotary evaporator (Heidolph, Germany). Chloroform was added, and the solution washed with 5 % NaHCO₃ solution (3x) followed by water (2x). The organic layer was dried over MgSO₄, filtered and the solvent removed in the rotary evaporator to afford the pure product as a white solid (palmitate esters) and colourless oil (oleate esters). ¹H NMR (400 MHz) was then performed dissolving the products in deuterated chloroform (CDCl₃), and the samples analysed in a Bruker Avance III.

7.2.6.2. Gas Chromatography – Mass Spectrometry (GC-MS)

GC was performed using a Bruker SCION 436 system with a split/splitless injector coupled to a mass spectrometer (MS). Injections were carried at 250 $^{\circ}$ C in the split mode 1:10 using a Rxi-5Sil MS (Restek) column (30 m \times 0.25 mm, and 0.25 μ m film thickness), with a column-head pressure of 7.3 psi using helium as carrier gas. The oven temperature started at 150 $^{\circ}$ C and was held for 3 min, and the temperature increased until 280 $^{\circ}$ C at a rate of 7 $^{\circ}$ C/min. A full scan mode (50–600 *m/z*) was applied for the identification of the target compound. The mass spectrometer (MS) was operated in electron ionization (EI) mode at 70 eV with total ion chromatogram detection mode for quantitative determination and *S/N* ratio of 5.

7.2.6.3. Fourier-transform infrared spectroscopy (FTIR)

Infrared spectra were recorded on a FTIR Platinum-ATR Bruker Alpha II. The samples were analysed over the range 400-4000 cm^{-1} , with a spectral resolution of 4 cm^{-1} . All spectra were an average of over 24 scans.

7.3. Results and discussion

7.3.1. Chemical modification of lipase TL

Lipases are ubiquitous enzymes with outstanding catalytic properties. Besides their natural function for the hydrolysis of triacylglycerols into glycerol and fatty acids, they can perform the opposite reaction, the biosynthesis of esters. Esters are found in countless type of compounds, and are of great importance in the food industry, cosmetics, pharmaceuticals, etc [184, 194].

In chapter 6, we reported the modification of lipase TL with different aliphatic/aromatic aldehydes and isothiocyanates and tested their hydrolytic activity against 7 differentiated chain-length *p*-nitrophenyl substrates [192]. It was observed that the lipase modified with four dodecyl chains (TL5) (**Figure 7.1A II**) showed an improved hydrolytic activity for all tested substrates (up to 2-fold), comparing to the native enzyme. The degree of modification was accessed through MALDI-TOF analysis (**Figure 7.1B**) and the TNBSA assay. Given the promising results obtained, herein we aim to explore the catalytic activity of this modified enzyme for the production of industrial added-value esters.

Prior to the evaluation of the transesterification and esterification activity of both enzymes, their half-life time at different temperatures was assessed (25, 37 and 50 °C) (**Figure 7.1C**). The temperatures were chosen according to the optimum temperature range of activity of the studied lipases and considering the typical array of temperatures reported for the evaluation of esterification reactions.

The data revealed that at 25 and 37 °C, both enzymes showed remarkable stability until 2 months of incubation. At 50 °C both enzymes displayed high stability, with half-life times near 200 h. In this way, both lipases showed to be suitable catalysts for longer reactional times.

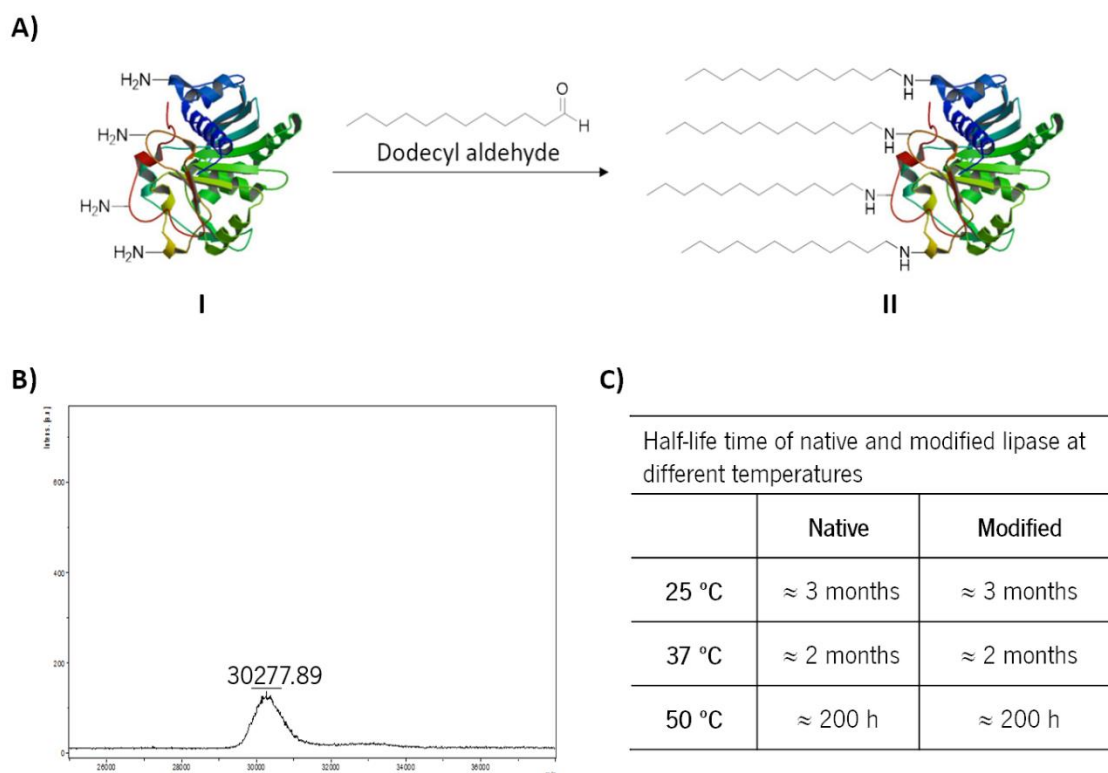


Figure 7.1. A) Representative scheme for the modification of (I) native lipase from *Thermomyces lanuginosus* with dodecyl aldehyde to produce (II) modified lipase TL with 4 dodecyl chains; **B)** MALDI-TOF of the modified lipase, confirming the grafting of 4 dodecyl chains (MW of native=29620.3) [192]; **C)** Half-life time of both enzymes at different temperatures.

7.3.2. Transesterification activity

The transesterification activity of both native and modified lipase TL was assessed using the standard procedure of the literature [193]. The colorimetric assay allows to observe the activity by the release of *p*-NP after transesterification of *p*-nitrophenyl palmitate with an alcohol.

Typically, this assay is only performed using ethanol, as alcohol source. No data regarding its execution using differentiated alcohols were found. For this reason, three different alcohols were tested: methanol, pentanol and decanol, representatives of small, medium, and long aliphatic chains, respectively (**Figure 7.2A**).

In **Figure 7.2B** is depicted the ester formation using native and modified lipase TL, regarding the transesterification of *p*-NPP with the mentioned alcohols. Given the known selectivity of lipase TL, the best results were achieved when the shorter alcohol tested, methanol, was applied. An activity decreasing tendency was observe as the chain length of the alcohols increased. Despite this trend, the modified enzyme showed superior transesterification activity comparing with the native form,

for all the alcohols tested. We may infer from **Figure 7.2B**, the increment of ester formation, proportional to the *p*-NPP transesterification. Comparatively to the native form, the activity of the modified lipase for the transesterification with methanol increased 26 %, whereas for pentanol increased 86 % and for decanol an increment of 103 % was achieved.

For an accurate comparison of the transesterification activity of both lipases, a constant value (K) was calculated ($K=[\text{ester product}]/[\text{starting material}]$) after reaction. This value is directly proportional to the amount of product formed. From **Figure 7.2B** it can be perceived that a higher K value was obtained for the modified lipase, corresponding to an higher amount of product formed. GC-MS was performed to validate this assay after 7 h of reaction (**Figure 7.2C**). The chromatogram showed two major peaks, one corresponding to the unreacted *p*-NPP (23 min), and the other to the transesterified ester product (methyl ester at 11.2 min, pentyl ester at 15.9 min and decyl ester at 21.3 min.).

Figure 7.2C depicts the GC chromatograms of the products after reactions with both lipases (native in black, and modified in red), using methanol as alcohol substrate. The peak intensity differences obtained for native and modified lipase was rather evident. The peak intensity of the methyl ester was more pronounced when the modified lipase was used as transesterification catalyst, confirming an higher amount of ester efficiently synthesized. The same trend was observed for the other alcohols tested, pentanol and decanol (data not shown), as previously observed by the colorimetric assay (release of *p*-NP).

The impact of the chemical modification on the lipases' structure was previously carried out using molecular dynamics simulations. The data revealed an enlargement of the active site, ensuring an easier access of the substrates. Moreover, the hydrophobic character of the linker (dodecyl aldehyde) could decrease the need of interfacial activation [192].

Considering these previous findings, we may predict that the enlargement of the active pocket promoted by the chemical modification had also a positive effect towards the transesterification activity of the enzyme.

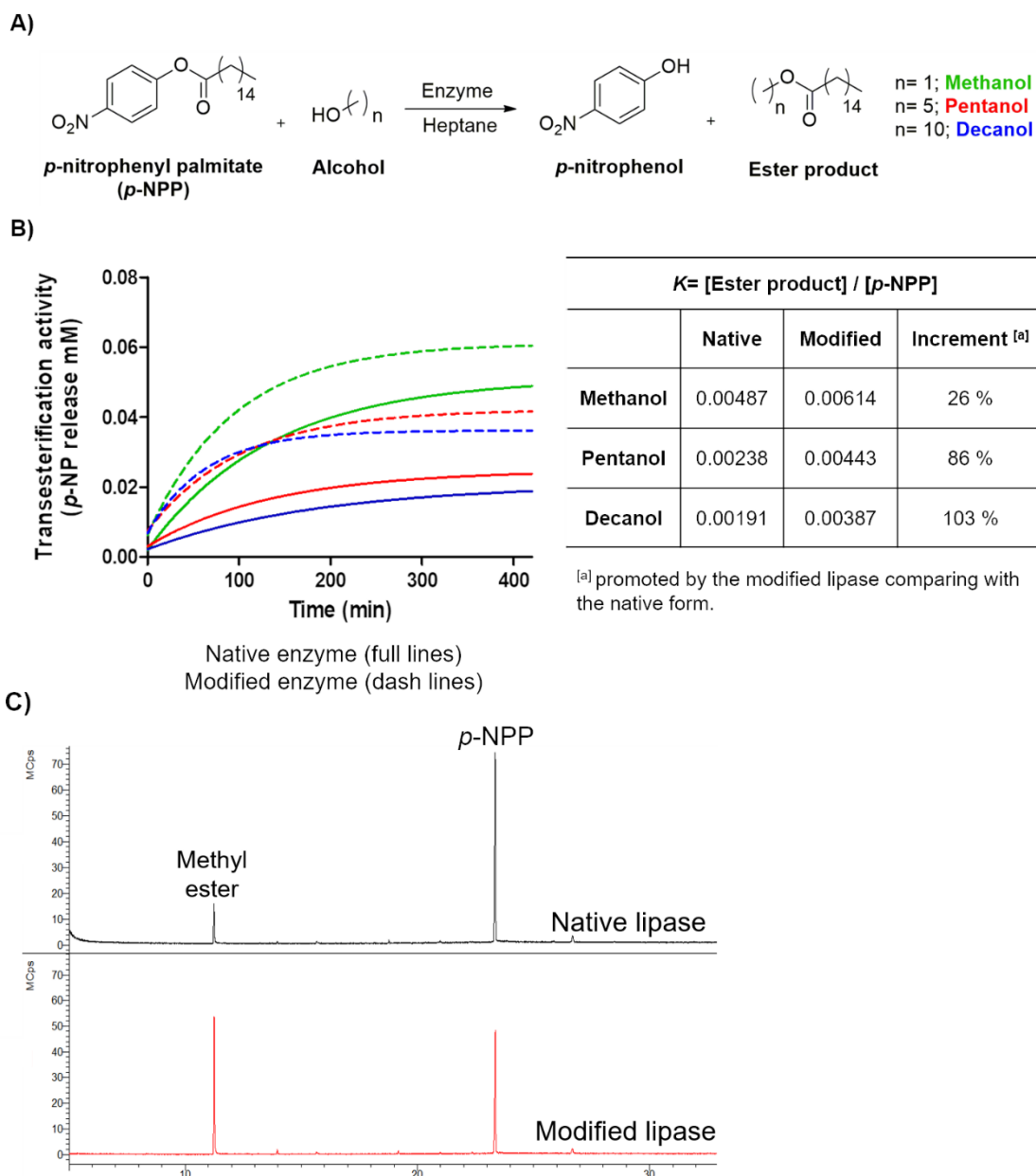


Figure 7.2. A) Reactional scheme for the transesterification reaction of *p*-nitrophenyl palmitate (*p*-NPP) with differentiated size-alcohols (methanol, pentanol and decanol), to produce *p*-nitrophenol and an aliphatic ester; **B)** Transesterification activity of native (full lines) and modified lipase (dash lines), using methanol (green), pentanol (red) and decanol (blue) as alcohol substrates. *K* values calculated after 7 h of reaction; **C)** GC-MS chromatograms of the products of the transesterification of *p*-NPP with methanol, catalysed by native and modified lipase (after 7 h of reaction).

7.3.3. Esterification activity

7.3.3.1. Effect of alcohol's chain-size

Oleic acid is a lipophilic compound well explored to test the esterification activity of many lipases, broadening their application for biodiesel production, when esterified with small alcohols [195, 196], or for lubricants or cosmetical purposes when esterified with longer alcohols [197, 198].

Besides the many applications reported for lipase TL, most of them describe its use in the immobilized form. Moreover, as far as we know, the effect of the alcohol chain-length on the lipase esterification activity was only recently explored using an immobilized form [199]. For this reason, this subject was herein extensively explored for the first time, using both forms of the enzyme (native and chemically modified), envisaging to open up new routes for the development of new industrial products where the ester compounds play a crucial role. Furthermore, the lack of practical examples regarding the production of industrial products by chemically modified lipases inspired us to deepen the knowledge about this issue.

In this way, a total of 11 linear alcohols were tested, varying from 1 carbon (methanol) to 20 carbons (eicosanol) in the aliphatic chain, for the esterification of oleic acid (**Figure 7.3A**).

From the data obtained (**Figure 7.3B**), we may observe that both enzyme forms showed similar catalytic performances for the shorter chain alcohols, containing until 3 carbons (from methanol to propanol), being the esters isolated with excellent yields ($\approx 80\%$). For the longer chain alcohols, with more than 3 carbons, a remarkable difference of the catalytic behaviour was observed between native and modified enzyme. While reactional yields below 40 % were obtained when catalysis was performed by the native form, the reactional yields obtained when using the modified form were superior for all the longer alcohols tested. The limited size of the native enzymes' active site may be associated to the activity loss when longer alcohols were used as substrates. Moreover, the alcohol, when in contact with the enzyme, may induce an inhibitory effect [200]. Nonetheless, reactional yields up to 56 % were obtained when using modified lipase regardless the alcohol used. Apart from the easier access to the active site, resulting from the enlargement promoted by the grafting with dodecyl chains [192], the greater stability acquired against increasing chain-length alcohols may be the differentiating factor for the higher ester production yields achieved. Moreover, the highly hydrophobic linker (dodecyl) may strongly interact with the organic solvent (*n*-heptane) and the substrates used. This feature may improve the catalytic activity of modified lipase at the solid-liquid interface. Additionally, favourable interactions between the dodecyl chain, located at the

lipases' lid, and the longer alcohols may occur, driving the substrate closely to the active site for further synthesis.

Kovalenko *et al.* [199] performed a similar study but using an immobilized form of the enzyme, and no comparison with the free enzyme form was reported. The results showed that the highest reactional rate was achieved when heptanoic acid (7C) and butanol (4C) were used as starting materials. In this work, a much longer acid was used as starting material (oleic acid C18:1), and therefore, due to constraints related with the active site access, it may be expected that only small alcohols, like methanol or ethanol, would be efficiently synthesized by the native enzyme.

The chemically modified form of this lipase, revealed to have higher catalytic activity against longer alcohols, demonstrating high potential for industrial applications.

We previously performed other chemical modifications of lipase TL [192]. This enzyme was also grafted with naphthyl isothiocyanate, naphthaldehyde, butyraldehyde or hexyl aldehyde. However, the esterification activity after these modifications, did not display different values than observed for native enzyme form (data not shown).

7.3.3.2. Enzyme dosage vs temperature of reaction

The reaction temperature, alongside with the amount of catalyst are key factors to control in esterification reactions. The optimum hydrolytic temperature of lipases is 37 °C, being also commonly used for the esterification reactions. Considering that, lower or higher temperatures may also be applied on these types of reactions. Herein the studies were also carried out at room temperature (25 °C) and at 50 °C, given the great stability of the lipases, previously observed (**Figure 7.1C**). Higher temperatures were not considered in this study, given the low stability of the enzymes previously reported by us [192].

In **Figure 7.3C** are depicted the *K* values obtained after esterification reaction with the lowest enzyme dosage tested (0.08 % w/v) at different temperatures (25, 37 and 50 °C). To simplify, only the results of three alcohols, representing a small, medium, and longer alcohol (methanol, 1C, decanol, 10C, and eicosanol, 20C) are presented.

For the lowest temperature tested (25 °C), the native enzyme showed only great catalytic activity when methanol was used as substrate. For the longer alcohols (decanol and eicosanol), no esterification was observed (results similar to the control experiments). At this temperature, the modified lipase revealed considerably higher esterification conversion (higher *K* values) than the native enzyme, regardless the substrate used. The esterification activity of the native form at 37 °C

was superior than at 25 °C, especially for eicosanol. The reactional conditions using the optimal temperature of the enzyme may be responsible for this increase. The same trend was observed for the modified enzyme. Low reactional outcomes were observed at 50 °C for the native enzyme, using the longer alcohol substrates (decanol e eicosanol). This activity loss was probably due to some inactivation of the enzyme when exposed to high temperatures.

The modified lipase showed similar K values for the reactions carried out at 37 and 50 °C, confirming the thermostability acquired by chemical modification with the dodecyl chains. Given the known selectivity of the native form for shorter alcohols, such as methanol, the esterification conversion increased only 1.2-fold when this substrate was applied. The increment observed for the longer alcohols was remarkably higher, 5.5-fold for decanol and 3.7-fold for eicosanol. The higher stability of the modified enzyme in an hydrophobic environment (*n*-heptane) may contribute for the enhancement of the esterification activity. Moreover, the hydrophobic grafted dodecyl chains around the lipase, in particular the chain located at the lid, may drive the substrates to the active site, favouring the esterification reaction.

Regarding the effect of the enzyme dosage, we observe that, for both enzyme forms, the esterification activity was directly proportional to the amount of enzyme used (data not shown). It was also noteworthy that the performance of the modified lipase, for the lowest enzyme dosage (0.08 %), surpassed the native outcome for the highest enzyme concentration (0.25 %) (data not shown).

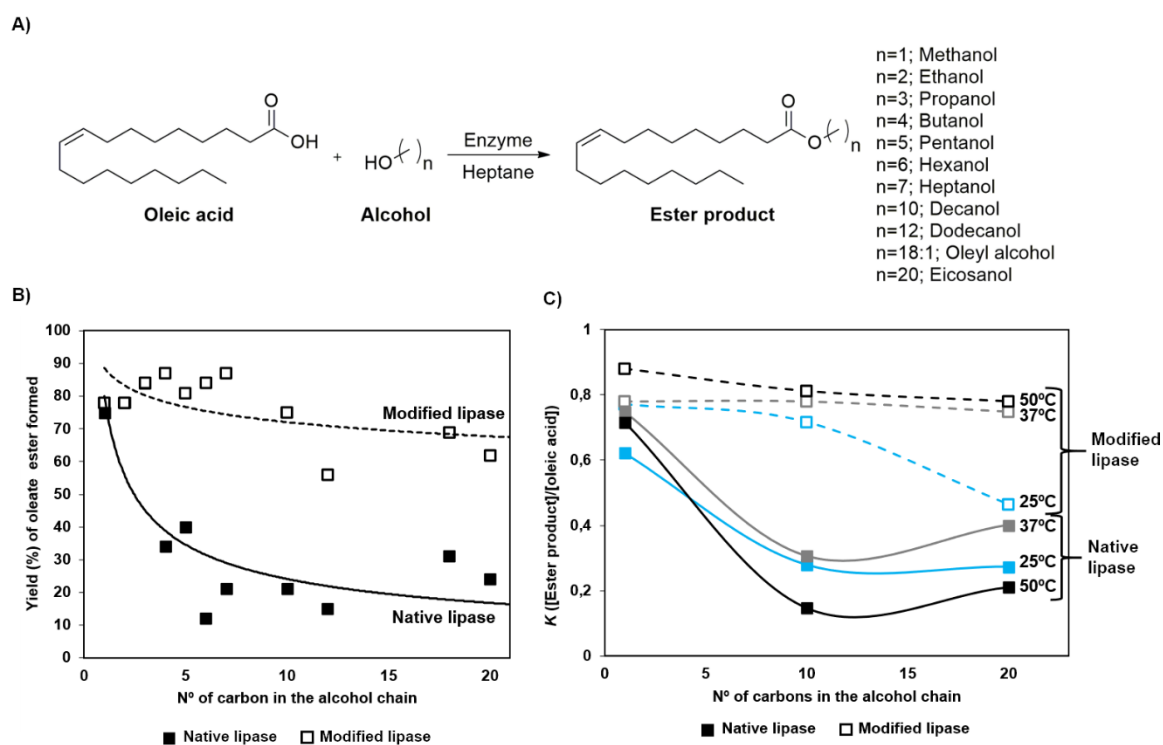


Figure 7.3. A) Reactional scheme for the esterification of oleic acid with differentiated chain-size alcohols; B) Reactional yield (%) of the esterification reaction of oleic acid with different alcohols catalysed by native and modified lipase TL (0.08 % w/v). Results obtained after 24 h of reaction, with the reactions performed at 37 °C; C) *K* values ($K = [\text{ester product}]/[\text{oleic acid}]$) regarding the effect of temperature (25, 37 and 50 °C), in the esterification of oleic acid with alcohols (methanol, decanol and eicosanol), using native *vs* modified lipase (0.08 % w/v) after 30 h of reaction.

7.3.4. Products characterization

^1H NMR spectroscopy was accessed for the characterization of all the biosynthesized esters. The spectra of the esters showed a similar profile, where the differences relied on the presence of the peaks of the introduced alcohols. Considering this, **Figure 7.4A** depicts, as example, the ^1H NMR spectrum of propyl oleate, the ester produced in the reaction between oleic acid and propanol.

Regarding the oleate moiety, the protons of the double bond (**d**) were generally observed at δ_{H} 5.3 ppm as a multiplet. The protons adjacent to the allenic bond (**c**) were detected at $\delta_{\text{H}} \approx 2.0$ ppm, in the same signal multiplicity. At δ_{H} 2.2 ppm was observed a triplet, attributed to the protons near the carbonyl bond (**f**). All other signals of the oleate unit were observed below 2 ppm.

A triplet at δ_{H} 4.0 ppm was detected in all compounds, which corresponds to the protons located near the oxygen atom (**g**). This signal confirms the occurrence of the esterification since it was not

present in the spectrum of oleic acid. The remaining protons belonging to the alcohol moiety were also observed below 2.0 ppm, which in most cases, appeared overlapped by the oleate peaks.

Gas chromatography was also carried out to confirm the synthesis of the esters through their mass fragmentation. In **Figure 7.4B** are described the retention time of each ester, their m/z after analysis, and their theoretical molecular weight. From the data obtained, we may assert that all expected esters were successfully obtained.

FTIR analysis was also conducted for the analysis of the ester products. All the biosynthesised compounds showed a similar profile. In **Figure 7.4C** is depicted the spectra of oleic acid and propyl oleate. In the spectrum of the starting material, oleic acid, it was possible to observe a broad stretching band between ν 2500 and 3200 cm^{-1} which corresponds to C-H stretching vibration and to the OH group of the carboxylic acid. The carbonyl group (C=O) was observed at 1706 cm^{-1} in the oleic acid, and at 1738 cm^{-1} in the ester. A strong stretching C-O band at 1177 cm^{-1} was observed in all biosynthesized product, which corresponds to the C-O band of the ester bond. From the data obtained, we may conclude that the FTIR analysis clearly indicate the formation of the respective ester compound.

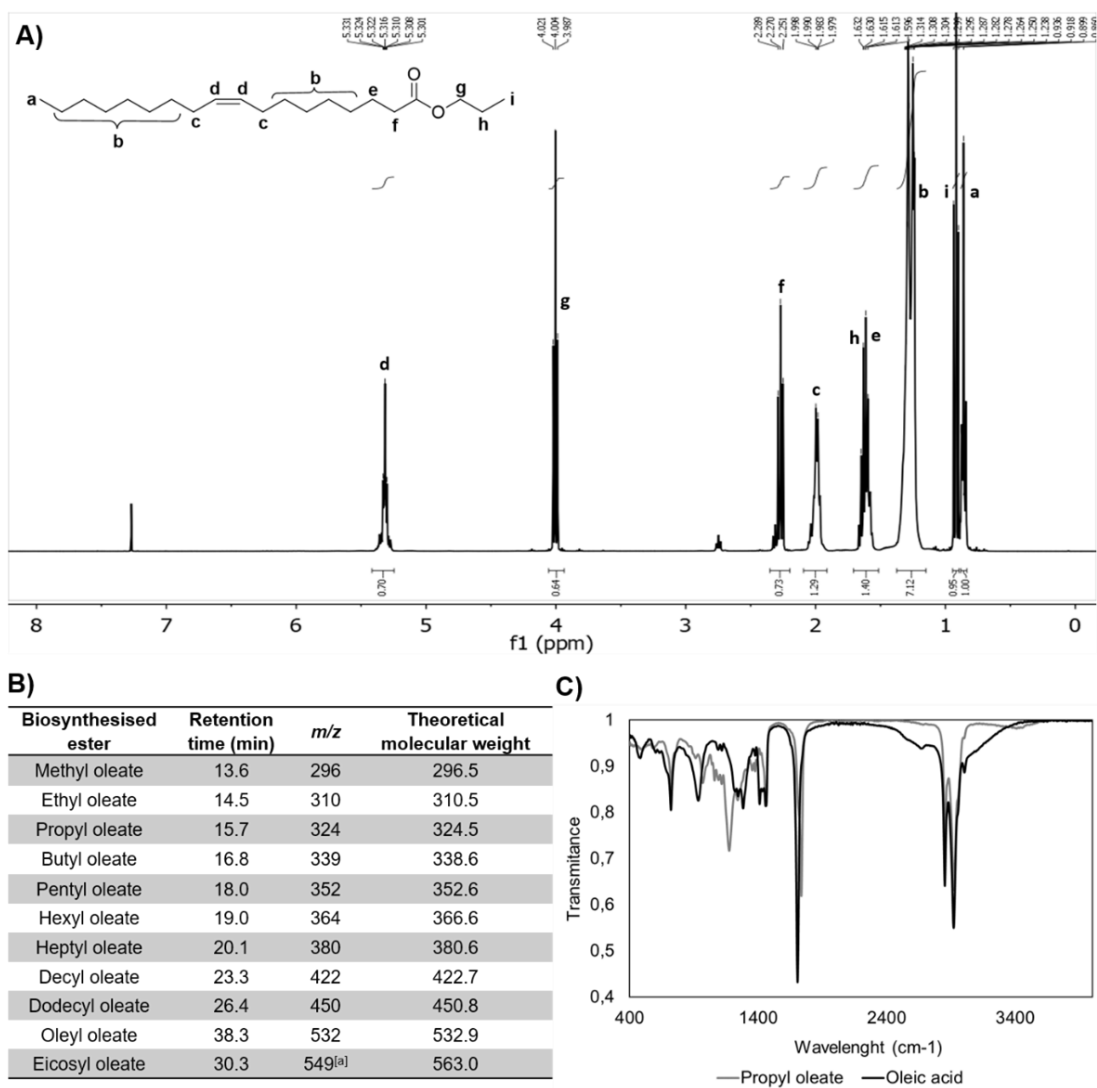


Figure 7.4. A) ^1H NMR spectrum of propyl oleate, synthesized by reaction between oleic acid and propanol catalysed by the modified lipase; **B)** Retention time, m/z obtained after GC-MS analysis and theoretical molecular weight of all biosynthesised esters; **C)** FTIR spectra of oleic acid (black) and of propyl oleate (grey) synthesized by the modified lipase.

7.4. Conclusions

The chemical modification of lipase TL by grafting with four dodecyl chains revealed an outstanding improvement of the enzymes' stability and activity toward transesterification and esterification reactions. In both reactions, the increment of the ester synthesized was directly proportional to the size of the alcohol aliphatic chain. A large panoply of esters differing in the final application, from biodiesel to cosmeceutical, revealed to be efficiently biosynthesized using a single enzyme. These results underline the potentiality of the chemical modification approach as a cheap, versatile, and efficient technique for the synthesis of many value-added industrial products.

Chapter VIII

Biotechnological approaches for the synthesis, modification and stabilization of hydrophobic compounds

Biotechnological approaches for the synthesis, modification and stabilization of hydrophobic compounds**Abstract**

Hydrophobic compounds are present in many daily products compositions, being of great importance in numerous fields of applications. Their synthesis, modification and delivery are factors to be considered by the scientific and industrial communities at the moment of development and application. Considering their outstanding catalytic properties, enzymes have been applied as catalysts to produce a panoply of value-added hydrophobic products. Their performance can be improved by chemical modification, aiming to increment the solvent tolerance, activity, and stability, under differentiated conditions. Among the different enzymes applied for synthesis purposes, lipases, are the most studied and explored catalysts. In this chapter, the potential of different enzymes in the production or modification of hydrophobic compounds will be assessed, especially focusing on the lipases' application. The most recent strategies developed for the synthesis/modification of hydrophobic compounds are described, as well as different strategies to chemically modified lipases and their outcoming applications. The use of nanoemulsions as a stabilization strategy to encapsulate hydrophobic compounds is also addressed.

This chapter is based on the following publication:

Jennifer Noro, Artur Cavaco-Paulo, Carla Silva, Biotechnological approaches for the synthesis, modification and stabilization of hydrophobic compounds, submitted to: *Critical Reviews in Biotechnology*.

8.1. Introduction

Hydrophobic compounds, like therapeutic drugs, small esters, and polyesters, are the main components of industrial products applied in a vast variety of applications. The improvement of their structure, function and delivery approach is of extreme importance to obtain products with differentiated functions. From the chemical modification, synthesis of analogs, encapsulation and enzymatic catalysis, different strategies have been presented in literature aiming to modify these compounds and increment their industrial potential application. Enzymes as green catalysts for biotechnological processes have been applied for the modification/production of hydrophobic compounds. The chemical modification of enzymes, aiming the improvement of their catalytic performance is of great interest considering their potential to synthesize and modify specific hydrophobic compounds, like ester-based compounds or therapeutic drugs. Together with immobilization, different strategies have been developed to produce catalysts with higher activity and stability. These methodologies, based on the chemical modification with small or macromolecules, allow to enhance the catalytic properties of enzymes, like lipases, incrementing the diversity of products that can be catalysed and the final industrial products obtained.

Other approach commonly used for a suitable delivery of hydrophobic compounds, is their encapsulation in nanoemulsions. This stabilization methodology is the most explored for biotechnological applications, being implemented in numerous industrial fields.

The propose of this chapter is to describe the practical insights regarding the different strategies developed in the last years for the synthesis or modification of hydrophobic compounds, e.g., hydrophobic drugs, ester-based compounds (like flavors, fragrances, biodiesel), and others, highlighting case studies in a biotechnological point of view. The chapter will also include a compilation of the strategies for the chemical modification of enzymes, with special focus on lipases, and its effect on their catalytic performance. From a stabilization point of view, the encapsulation of hydrophobic molecules into differentiated nanoemulsions will also be presented.

8.2. Enzymes for the synthesis or modification of hydrophobic compounds

Greener, environmentally friendly, and proficient practices are increasingly requested for suitable synthetic procedures. Among different strategies, the use of enzymes as biocatalyst is the approach that stands out. Nature provides a broad range of enzymes with diverse properties that can be implemented in almost all known chemical reactions [191]. Currently, many synthetic processes already used enzymes in important reactional steps, where an accurate management of the

chemo-, enantio- and regioselectivity of the reaction is required. Their use to replace high cost and pollutants metals, or to avoid the use of high temperatures/pressures is also undertaken. Moreover, biocatalysis also increases the kinetics speed of a reaction, comparing to the chemical traditional approach [12].

Many distinct enzymes, differing in their catalytic properties, are used in the synthesis or modification of different types of hydrophobic compounds. Additionally, they can be implemented in diverse fields of applications, such as, pharmaceuticals, cosmetics, biofuels, paper, pulp, detergent and food [201, 202] (**Figure 8.1**). The importance of the use of enzymes for the synthesis or modification of compounds is demonstrated by numerous patents filled in the area, for academic or industrial purposes [203, 204].

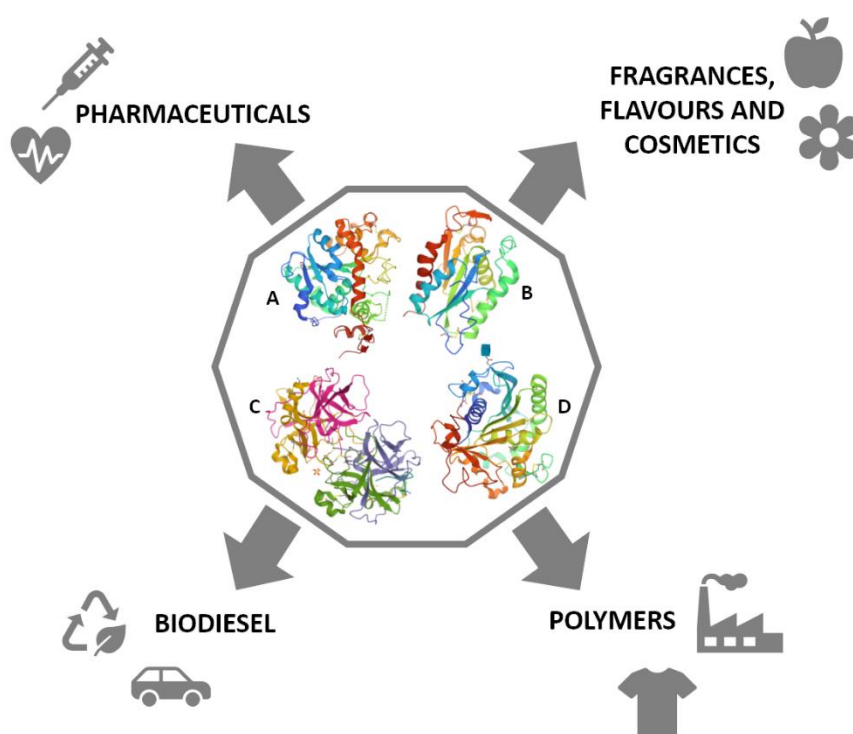


Figure 8.1. Different fields of application where enzymes can be incorporated for the synthesis or modification of hydrophobic compounds (enzymes represented: **A**) lipase from *Candida antarctica* B PDB ID: 4K6G; **B**) cutinase from *Fusarium solani* PDB ID: 1CUS; **C**) α -chymotrypsin from *bovine pancreas* PDB ID: 1YPH; **D**) lipase from *Thermomyces lanuginosus* PDB ID: 5AP9).

8.2.1. Synthesis and/or modification of hydrophobic drugs: practical applications

The pharmaceutical industry is the sector where enzymes display a more crucial role. Most drugs have chiral centers in their structure, which are synthetically difficult to manage. Moreover, the

chirality of a compound is an important factor to ensure their efficacy and safety [205]. Due to the special demand of conferring chemo-, enantio- and regioselectivity to a certain drug or their intermediate, is in this reactional step that different enzymes are frequently implemented [205]. In **Table 8.1** are described some examples of enzymes used in the synthesis or modification of drugs over the past 5 years.

Table 8.1. Examples of enzymes applied for the synthesis or modification of drugs

Class of enzyme	Enzyme(s)	Drug synthesized/ modified	References
<i>Oxireductases</i> (EC 1)	Ketoreductase-EW124 and -P3-G09	LNPO23	[206]
	Laccase CgL1 from <i>Corynebacterium glutamicum</i> and vanillyl-alcohol oxidase	Pinoresinol	[207]
<i>Transferases</i> (EC 2)	Transaminase	Strictosidine	[208]
<i>Hydrolases</i> (EC 3)	Immobilized lipases from <i>Thermomyces lanuginosus</i> and from <i>Candida antarctica B</i>	(<i>R</i>)-Luliconazole	[209]
	Lipase from <i>Candida antarctica B</i>	Crizotinib	[210]
	Immobilized lipase from <i>Candida antarctica B</i>	Buprenorphine	[211]
	Lipase from <i>Thermomyces lanuginosus</i> and immobilized lipase from <i>Candida antarctica B</i>	Methotrexate	[79]
	Lipases from <i>Pseudomonas fluorescens</i> and <i>Candida rugosa</i>	Pindolol	[212]
	Lipase from <i>Candida rugosa</i>	Propranolol	[213]
	α -Chymotrypsin from <i>Bovine pancreas</i>	Methotrexate	[214]
	Phosphotriesterase from <i>Pseudomonas diminuta</i>	(<i>Rp</i>)-Remdesivir	[215]
<i>Lyases</i> (EC 4)	Amorphadiene synthase	Artemisinin	[216]
	Strictosidine synthase	Strictosidine	[208]

Depending on the type of reaction, different classes of enzymes can be employed. Lipases, proteases, ketoreductates, nitrilases, transamidases, alcohol oxidases, etc., are only a few examples [217].

Fischereder and coworkers [208] used two different class of enzymes for the synthesis of the alkaloid Strictosidine. The enzymatic reactions were performed simultaneously, and the desired product was obtained diastereomerically pure (> 98 %) [208].

The pharmaceutical industry Novartis is currently using different ketoreductases for the synthesis of a novel drug, LNP023 [206]. The enzymes are used in the reduction of a ketone group to ensure the desired enantioselective compound [206].

Noro *et al.* used two different strategies for the modification of methotrexate (MTX). A protease (α -chymotrypsin from *Bovine pancreas*) [214] and two lipases (from *Candida antarctica B* and from *Thermomyces lanuginosus*) [79] were studied for this purpose. MTX is a pharmaceutical drug, available in the market, with many therapeutical applications. However, the associated side-effects make imperative its modification. One strategy based on the attachment of triacylglycerols and cyclodextrin to MTX via lipase catalysis was proposed by Noro *et al.* [79]. MTX prodrugs were thus efficiently produced by the attachment of non-toxic compounds. The other approach developed included the use of α -chymotrypsin as catalyst. For the first time, a polymeric structure composed exclusively by MTX units was biosynthesized. Oligomers composed up to 6 MTX units were obtained with 30 % of conversion. This strategy showed a novel route for a potential controlled drug delivery system [214].

Lima *et al.* [212] used two different lipases, differing in their selectivity, for the synthesis of Pindolol, a nonselective β -blocker. Firstly, lipase from *Pseudomonas fluorescens* was applied on the kinetic resolution of one of the drug intermediates, followed by the hydrolysis of the other intermediate by lipase from *Candida rugosa*. The final drug was isolated in quantitative yield with excellent enantiomeric excess (*ee* 97 %) [212].

Luhavaya and coworkers [218], proposed for the first time a biosynthetic pathway for the synthesis of L-4-chlorokynurenine. Four different enzymes (flavin-dependent tryptophan chlorinase, flavin reductase, tryptophan 2,3-dioxygenase and kynurenine formamidase) were explored to produce this prodrug candidate, which it is being studied for the treatment of depressive disorders.

Peet and Kavarana [219] patented the biosynthesis of several cannabinoid prodrugs through catalysis with cannabionoid acid synthase enzymes. The numerous therapeutic applications associated to these compounds have triggered their investigation.

A cascade reaction for the synthesis of islatravir was reported by Huffman *et al.* [220]. Nine enzymes were employed in the synthesis of this potential drug for the treatment of HIV. The

compound was isolated with an overall yield of 51 %, and the data revealed that the enzymatic route reduced the time and reactional steps necessary, comparing to the conventional synthesis.

8.2.2. Polyester synthesis by enzymes

Polyesters are one of the major classes of natural macromolecules. These polymers are composed by ester groups between repeating units and can be classified as aromatic, semi-aromatic, or aliphatic [221]. Their importance relies on their use on many daily products, such as textiles, food packaging, microelectronics, but also in biomedical applications: control drug delivery, orthopedic devices, sutures, tissue engineering, among others [222]. An alternative to their chemical synthesis is a crucial demand, given that high temperatures, pressure, and/or hazardous compounds are usually used in their synthesis. Moreover, being petrol-based materials, these products are associated a non-environmentally friendly processes [223].

Enzymes, more precisely lipases, are the most viable and suitable options, being the most explored enzymes for the synthesis of polyesters [224]. Several examples of their implementation as catalysts for polyester synthesis can be found in literature [221, 223, 225, 226].

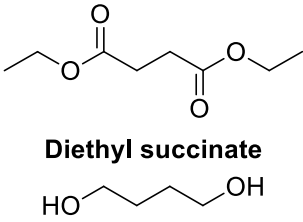
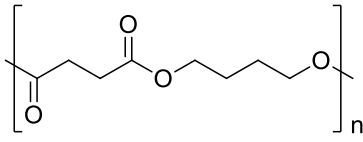
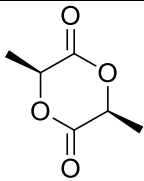
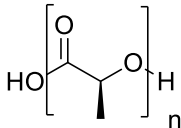
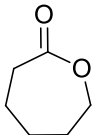
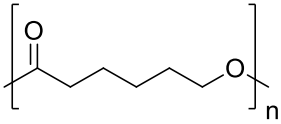
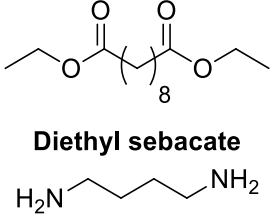
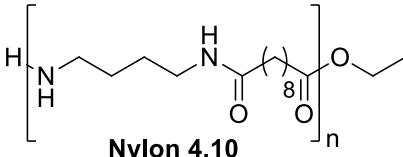
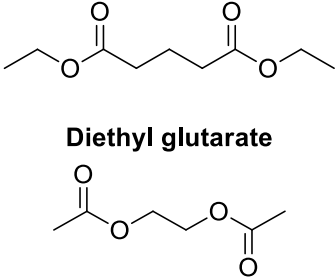
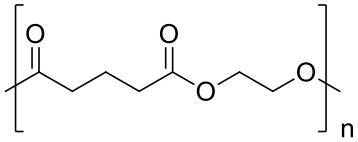
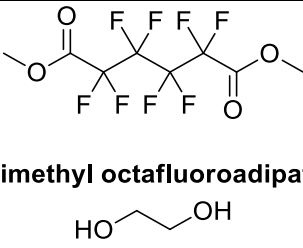
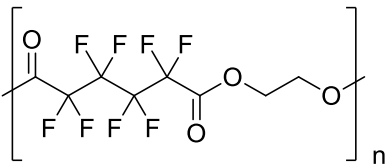
The most explored polyesters are poly(butylene succinate), poly(lactic acid), poly(ethylene terephthalate), poly(caprolactone) and poly(butylene terephthalate), which are already present in many of our daily products [222] (**Table 8.2**). However, due to their huge importance, the pursuit for the discovery of novel polyesters catalysed by lipases remains a challenge.

Zhao *et al.* [54], used an immobilized lipase from *Candida antarctica B* (CALB) for the biosynthesis of poly(ethylene glutarate). This enzymatic reaction led to the isolation of the polyester with excellent yield (96 %). A similar approach was later performed by Tomke and coworkers [227], wherein the same polymer was synthesized by the same lipase, as well as poly(ethylene malonate) and poly(ethylene phthalate) [227].

Highly hydrophobic polyesters were recently synthesized by Zhao *et al.* [228], using fluorinated compounds. The produced polymers, poly(ethylene tetrafluorosuccinate), poly(ethylene hexafluoroglutarate) and poly(ethylene octafluoroadipate) were isolated with higher yield when immobilized CALB was used as reactional catalyst [228].

The versatility of enzymes for polymerization reactions is not confined to polyester synthesis, but can also be implemented to produce polyamides, as exemplified in **Table 8.2** [221, 229].

Table 8.2. Synthetic approaches for the biosynthesis of polyesters/polyamides

Starting materials	Polymer formed	Enzymes used
 <p>Diethyl succinate HO-CH₂-CH₂-CH₂-CH₂-OH</p> <p>Butanediol</p>	 <p>Poly(butylene succinate)</p>	CALB [221, 230]
 <p>L-Lactide</p>	 <p>Poly(L-lactide)</p>	CALB [221, 231]
 <p>ε-caprolactone</p>	 <p>Poly(ε-caprolactone)</p>	Lipase from <i>Trichosporon laibacchii</i> [232]
 <p>Diethyl sebacate H₂N-CH₂-CH₂-CH₂-CH₂-NH₂</p> <p>1,4-diaminobutane</p>	 <p>Nylon 4,10</p>	Cutinase [233]
 <p>Diethyl glutarate Ethylene glycol diacetate</p>	 <p>Poly(ethylene glutarate)</p>	CALB [54]
 <p>Dimethyl octafluoroadipate HO-CH₂-CH₂-OH</p> <p>Ethylene glycol</p>	 <p>Poly(ethylene octafluoroadipate)</p>	CALB [228]

8.2.3. Other synthesis applications: cosmetic, food, biofuels, etc.

Due to the high versatility of enzymes, many other biotechnological applications can be found. Besides the synthesis of pharmaceuticals and polymers for the textile industry, they can be implemented in the synthesis of flavors and fragrances for the food industry, novel biofuels, among others [234]. The food and cosmeceutical industries rely on the usage of many hydrophobic ester compounds, either as food additives, fragrances, or wax esters. These last ones are applied for cosmetic purposes, as emollients, cleaners, and conditioning esters [235].

Khan *et al.* [236] used immobilized lipase from *Candida antarctica B* for the synthesis of a novel emollient ester for cosmetic applications. The product, cetyl oleate, was obtained with excellent yield (96 %), after 30 min of reaction [236].

Ungcharoenwiwat and H-Kittikun [237] biosynthesized wax esters from coconut oil and oleyl alcohol. Two immobilized lipases were used as catalyst (lipases from *Rhizomucor miehei* and from *Burkholderia sp. EQ3*). The products were obtained with excellent yield (88 %), and are potential components for applications in cosmetics and skin care products [237]. Terpenic esters of geraniol and citronellol were produced through catalysis by immobilized lipases from *Thermomyces lanuginosus* and *Candida antarctica B*. The coupling of the fragrances with oleic, lauric, and stearic acids were successfully accomplished by the lipases [238]. Bayout *et al.* [194] used different lipases for the synthesis of three flavor esters: *cis*-3-hexen-1-yl acetate, 2-phenylethyl acetate, and methyl phenylacetate. The biosynthesized esters were isolated in good yields (up to 90 %) [194]. Different lipases from *Aspergillus niger* were expressed by Cong and co-workers [239], for the synthesis of diverse flavour esters (ethyl lactate, butyl butyrate and ethyl caprylate) [239]. Many other enzymes have shown potential for the synthesis of bioactive compounds for cosmeceutical applications [240].

Another field of application of enzymes is on the synthesis or modification of hydrophobic compounds for the production of biofuels. Fossil fuels are a non-renewable source being highly pollutant for the environment. The use of biodiesel has gained much attention in the past years, given its many advantages, like biodegradable, non-toxicity, renewability, and for being environmentally friendly [241]. The use fatty acids to produce suitable biofuels is a common practice in this research area. Enzymes play herein a crucial role in comparison to the traditional route of production. Mild reactional conditions, no side-reactions, and high-quality biodiesel manufacturing are some of the attractive qualities related with their use [242]. Many examples using different enzymes and oil sources have been recently reported. Bhangu *et al.* [243], used

lipase from *Candida rugosa* for the synthesis of biodiesel, from canola oil and methanol, using ultrasounds to increase the speed of the reactions [243]. Lipase from *Candida antarctica A* was used as a catalyst for the reaction between methanol and soybean oil [244]. Probiotic lipases (from *Lactobacillus plantarum* and *Lactobacillus brevis*) were used by Khan *et al.* [245]. The enzymes showed promising catalytic activity for the esterification reaction between olive oil and methanol [245].

Several other recent examples regarding the implementation of enzymes for biodiesel production can be found. The use of industrial wastes of fatty acids as renewable sources is also a common and suitable practice. Rubber seed oil [246], babassu oil [247], sardine oil [248], rapeseed oil [249], and palm oil [250] are only a few examples of hydrophobic compounds which were successfully converted into added value industrial products through enzymatic catalysis.

8.3. Improvement of enzymes' properties

Enzymatic catalysis is applied in many fields with diverse biotechnological applications. Nonetheless, the pursuit to enhance enzyme properties as well as to overcome some of their limitations is commonly undertaken. To achieve this purpose, two methodologies can be performed: protein engineering or chemical modification [251]. The first involves the direct evolution or site-directed mutagenesis. The second one, includes the chemical modification and/or immobilization of the enzyme on a solid support [251]. In this chapter, only the chemical approaches will be discussed, with a special focus on the chemical modification strategy.

The chemical modification of enzymes is a strategy often applied for the improvement of their catalytic performance. Increasing their activity, solvent tolerance, stability (temperature and pH), are some of the required properties (**Figure 8.2**). Different strategies can be undertaken for this purpose, which can be divided in two: the chemical conjugation with small molecules (< 1000 Da) or the conjugation with macromolecules (> 1000 Da).

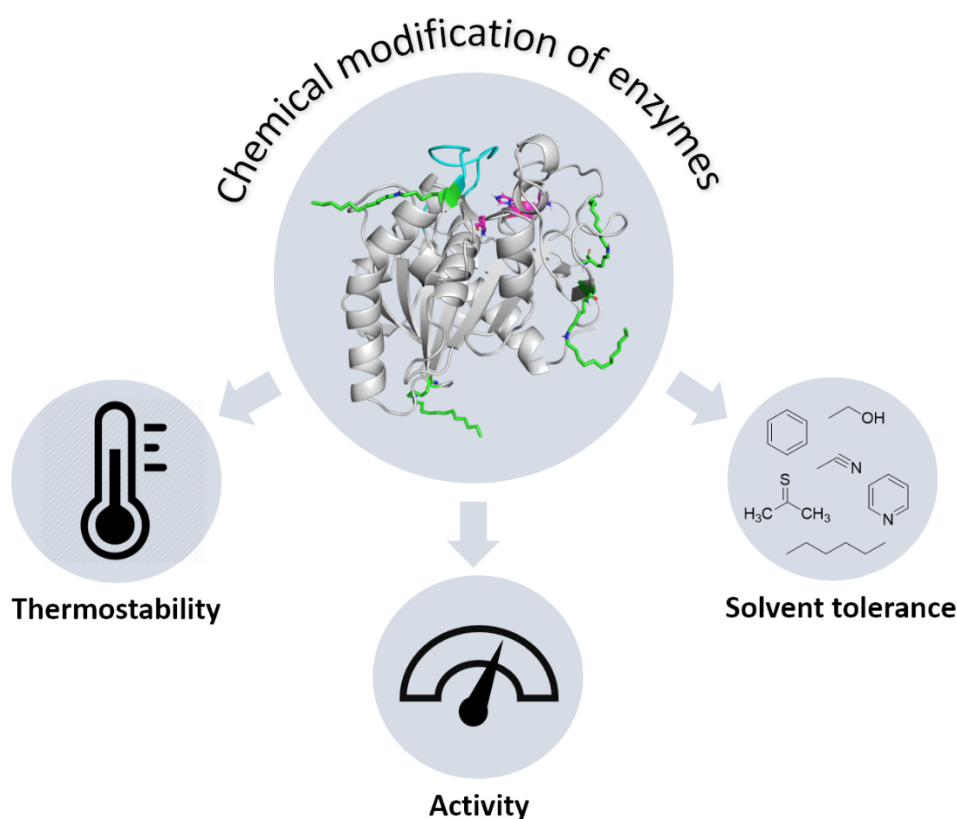


Figure 8.2. Some of the enzyme properties improved by chemical modification (enzyme represented: lipase from *Thermomyces lanuginosus*, PDB ID: 1TIB, modified aleatorily with four dodecyl chains through lysine residues using PyMOL).

Darby *et al.* [15], showed how diverse small “fragments” affected the activity of a bacterial glycoside hydrolase (BtGH84) after their covalent tethering. The strategy showed an high improvement of the catalytic activity (35-fold) and increase of the enzymes’ susceptibility to a certain classes of inhibitors [15].

Chen and co-workers [252], modified laccase from *Aspergillus oryzae* with thiourea dioxide and L-phenylalanine methyl ester hydrochloride. This approach increased the enzymes’ activity in 209 % and 50 %, respectively. However, the laccase stability was only improved when the L-phenylalanine was covalently attached. These enzymes showed potentiality for the treatment of pulp [252].

Another approach for the chemical modification of enzymes is the covalent bonding of macromolecules, like polymers. This strategy has been the most studied in the last years, since the application of the conjugates is not confined to enzymatic catalysis, but can be directly employed as therapeutics in biotechnology, and in medicine [253].

Kübelbeck *et al.* [254], have chemically modified protease from *Bacillus subtilis* and α -amylase from *Bacillus licheniformis* with different activated polymers (PEG, maltodextrin and carboxymethyl

cellulose). Besides observing that the enzymes suffered some activity loss, all the modified enzymes showed increased thermal stability and higher stability in a detergent formulation, comparing to their native counterparts [254].

Li and coworkers used a chitoooligosaccharide (5 kDa) to modify chemically pepsin. The strategy showed that the thermostability of the modified protein was significantly improved in all tested temperatures (from 4 to 65 °C) [72].

The attachment of poly(ethylene glycol) (PEG) to laccase from *Myceliophthora thermophila* was successfully achieved by Su and coworkers [114]. The modified enzyme showed to be more active than the native enzyme, in the biosynthesis of a polymer, poly(catechol) [114]. The PEGylated enzyme also showed high potentiality for the synthesis of other polymers with application for the bio-coloration of textiles [255, 256]. A diverse portfolio of enzymes can be chemically modified in order to enhance their catalytic properties. Among all the enzymes, lipases are the most explored catalysts for this purpose. The next section of this chapter is exclusively dedicated to this class of enzymes.

8.3.1. Chemical modification of lipases

8.3.1.1. Catalytic properties of lipases

Lipases (E.C. 3.1.1.3) are well-recognized enzymes classified as triacylglycerol acylhydrolases [257]. Their main function is the hydrolysis of triacylglycerols, producing glycerol and fatty acids [258]. Despite their natural purpose, lipases are extremely versatile, being able to hydrolyse non-natural substrates and catalyse esterification, transesterification, interesterification, aminolysis, thiolysis and acidolysis reactions (**Figure 8.3**) [259, 260]. Their enormous potential is well explored and has been highly reviewed in last year's [201, 202, 234, 240, 257-259, 261-265].

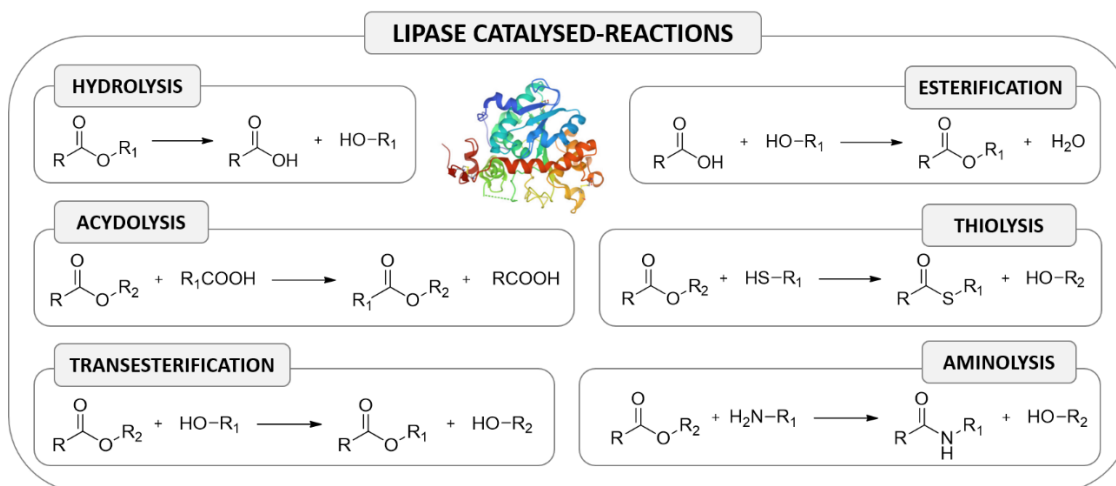


Figure 8.3. Examples of reactions performed by lipase-catalysis.

Their active site is composed of a catalytic triad, which comprises residues of serine, histidine, and aspartic acid (Ser-His-Asp), being the last amino acid replaced by a glutamic acid residue in few lipases (Ser-His-Glu) [257].

Another typical feature of lipases is the presence of a lid that surrounds the active site (**Figure 8.4**). This “flap” is commonly an α -helix which is responsible for the enzymes’ activity. In an aqueous medium, the active site is hindered by the lid, being the enzyme in a closed conformation. At an oil-water interface, the lid moves, and the accessibility of the substrate to the active site increases, being the enzyme able to efficiently catalyse the reaction. This phenomenon is called “interfacial activation” [262]. This feature makes lipases more prone to be used in the catalysis of hydrophobic compounds, given that no interfacial activation occurs in the absence of a lipophilic molecule or solvent. This event is necessary for almost all lipases, however, in some enzymes, the lid is very small and therefore the activation is not necessary [258].

Among the different possible sources, microbial lipases, more precisely, derivate from fungi are the ones with the highest interest for biotechnological industrial purposes [263]. Fungal lipases are expressed extracellularly, being easily extracted, and isolated in high yields and with low costs associated. These lipases have also remarkable properties, like stability at high temperatures, a broad range of pH, and high activity in organic solvents. Moreover, they can be easily manipulated genetically. These features make fungal lipases the ones more explored nowadays [259].

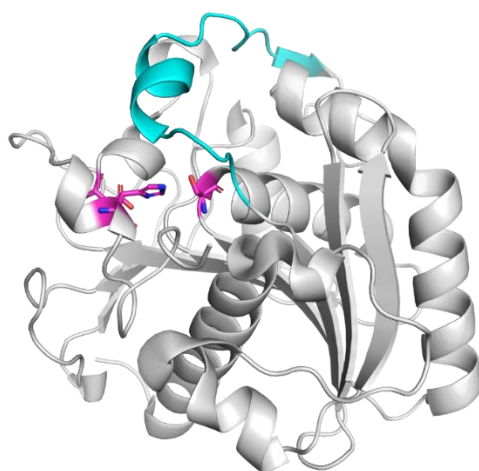


Figure 8.4. Structure of lipase from *Thermomyces lanuginosus* (PDB ID: 1TIB) elucidating the lid in cyan and the catalytic triad Ser-His-Asp in magenta.

These enzymes are ubiquitous in nature and can be produced by plants, animals, or microorganisms [259]. During catalysis, lipases can confer chemo-, enantio-, and regioselectivity to the produced compounds. These outstanding properties make their applications broader, including not only research, but also industry and other fields, such as food, detergent, pharmaceutical, oleochemical, pulp, paper, and textile industry, cosmetics, perfumery, organic synthesis, among others [264].

8.3.1.2. Modification of lipases with small molecules

The chemical modification of an enzymes' surface using small molecules, is mainly used to improve its catalytic properties. Besides enhancing the catalytic performance, other features may be improved like thermostability, organic solvent tolerance, enantioselectivity, etc [14, 15, 191, 192].

In the last decade, the most common strategy applied to achieve these goals is the grafting of ionic liquids to the enzymes' surface [266, 267]. However, in the past 5 years, the number of new reports regarding this strategy has been decreasing.

Chao and co-workers have grafted imidazolium and choline-based ionic liquid (IL) onto lipase from *Burkholderiacepacia* [268]. The authors observed a 1.2 fold increase in the lipases' relative activity and 1.4 fold in its thermostability, comparing to the native enzyme [268].

Jayawardena *et al.* [269] used benzoic anhydride for the modification of lipase from *Candida antarctica A* and greasex from *Humicola lanuginosa*. The modified enzymes showed higher

thermostability and productivity compared to their native forms, showing high potentiality for application in latex-based paint formulations.

A novel strategy was recently reported by Noro *et al.* [192] which modified lipase from *Thermomyces lanuginosus* with small hydrophobic compounds. Aromatic and aliphatic aldehydes and isothiocyanates were the selected compounds. The authors screened the modified lipases against many differentiated *p*-nitrophenyl substrates, comprising an aliphatic chain from 2 until 16 carbons. A non-natural substrate, *p*-nitrophenyl benzoate, was also tested. It was observed that all modified enzymes showed an improvement in their stability against high temperatures and a broad range of pH. The lipase modified with 4 dodecyl chains (from dodecyl aldehyde) revealed to be the most important finding, considering that its activity was exponentially improved. Besides being the only lipase with activity for the hydrolysis of the non-natural substrate, this modified enzyme also exhibited outstanding activity against the small substrates (until 10-fold increase for *p*-nitrophenyl acetate and butyrate). Later, the authors studied the transesterification (*p*-nitrophenyl palmitate) and esterification (oleic acid) activity of the modified lipases against different chain-length alcohols [270]. Similarly to the hydrolytic activity results, the modified lipase with 4 dodecyl chains grafted, showed outstanding catalytic activity for both reactions, comparing to the native enzyme. The increment of activity was more pronounced as the alcohol chain increased. For the first time, a practical application of the modified lipases with small molecules has been reported, underlining the potential of this lipase for the synthesis of valued-added industrial compounds.

8.3.1.3. Modification of lipases with macromolecules

The coupling of polymers is the most common strategy implemented to modify lipases. Between different polymeric structures, PEGylation is the most studied methodology. PEGylation is the attributed term for the covalent bonding of a polyethylene glycol (PEG) moiety to a molecule or macromolecule [271]. This strategy is being widely explored, considering many advantages associated to this polymer, such as low toxicity, higher stability [272], enhanced therapeutic activity [271], among others. The PEGylation of peptides/proteins is mostly explored for pharmaceutical purposes, due to several advantages including increased solubility, immunogenicity, and higher life-time circulation [273] being some PEGylated compounds/proteins already available in the market. It has also been reported that the PEGylation can potentiate the activity of enzymes [274]. However, the PEGylation of lipases for the improvement of their catalytic properties is still poorly explored.

Noro *et al.* [81] reported the PEGylation of three different enzymes, namely lipase from *Candida antarctica B* (CALB), lipase from *Thermomyces lanuginosus* (TL), and cutinase from *Fusarium solani pisi*, using a monofunctional PEG (5000 Da). The PEGylation resulted in the isolation of the enzymes with at least 50 % of their lysines modified. The hydrolytic activity of lipase TL was not affected after modification, while PEG-CALB and PEG-cutinase were 2-fold and 4-fold more active than the native lipase, respectively, after PEGylation. Moreover, the authors studied the effect of the PEGylation in the polymerase activity of the enzymes, for the production of a polyester, poly(ethylene glutarate). They observed that the polymerase activity, evaluated in terms of polymer conversion, of CALB and cutinase remained similar after PEGylation. PEG-lipase TL showed an outstanding activity for the production of the polyester (90 %), while the native enzyme was only able to convert 30 % of the monomers. This strategy showed the potential of the modified enzymes for the synthesis of polyesters which could be applied in differentiated fields like textiles or biomedical applications [81].

Kajiwara *et al.*, reported two similar strategies for the modification of lipase from *Candida cylindracea* with dextran (40 kDa). Differing in the coupling pH (5.5 and 8.9), and in the use or not of a reducing agent (borane-pyridine complex) [275] [276]. Both modifications led to similar organic solvent tolerance improvement.

As far as we know, no reports were found regarding the compilation of different methods for the chemical modification of lipases. In **Table 8.3** are described the different strategies for the chemical modification of lipases using small or macromolecules. A full compilation of molecules used, experimental conditions, and improved properties are described.

Table 8.3. Chemical modification of lipases: molecules grafted, experimental conditions and practical applications (2013-2020)

<i>Grafting small molecules (< 1000 Da)</i>				
Lipase	Molecules grafted	Experimental conditions	Improved properties/application	References
Lipase from <i>Candida antarctica B</i>	Ionic liquids: [HOOCMMIM][Cl]; [HOOCEMIM][Cl]; [HOOCBMIM][Cl]; [HOOCBMIM][H ₂ PO ₄]; [HOOCMMIM][PF ₆]	1) Ionic liquid (1 mmol) and carbonyldiimidazole (1 mmol) in 2 mL DMSO, 2 h at 25 °C in the dark. 2) 90 µL of the previous solution added to 5 mL CALB in deionized water (150 µM), 8 h at 4 °C.	Increased hydrolytic activity (<i>p</i> -nitrophenyl palmitate), thermostability and improved organic solvent tolerance.	[158]
Lipase from <i>porcine pancreas</i>	Ionic liquids: [HOOCMMIM][Cl]; [HOOCEMIM][Cl]; [HOOCBMIM][Cl]; [HOOCBMIM][H ₂ PO ₄]; [HOOCMMIM][PF ₆]; [choline][NO ₃]; [choline][H ₂ PO ₄]	1) Ionic liquid (500 mM) and carbonyldiimidazole (500 mM) in 2 mL DMSO, 2 h at 25 °C. 2) 200 µL of previous solution added to 10 mL lipase in deionized water (100 µM), 8 h at 4 °C.	Increased hydrolytic activity (<i>p</i> -nitrophenyl palmitate), enantioselectivity (racemic 1-phenethyl acetate hydrolysis), and thermostability.	[157]
Lipase from <i>Burkholderiacepacia</i>	Ionic liquids: [choline][NO ₃]; [choline][H ₂ PO ₄]; [HOOCBMIM][BF ₄]; [HOOCBMIM][PF ₆]; [HOOCEPEG ₃₅₀ Im][BF ₄]; [HOOCEPEG ₃₅₀ Im][Cl]	1) Ionic liquid (1 mmol) and carbonyldiimidazole (1 mmol) in 2 mL DMSO, 2 h at 25 °C in the dark. 2) 260 µL of the previous solution added to 15 mL of lipase (15 mg/mL), 24 h at 4 °C.	Increased relative activity (olive oil hydrolysis) and thermostability.	[268]

Lipase from <i>Candida rugosa</i>	Ionic liquids: [C ₂ OHmim][H ₂ PO ₄]; [C ₂ OHmim][Cl]; [C ₂ OHmim][BF ₄]; [HOOCMMIm][Cl]; [HOOCEPEG ₃₅₀ Im][H ₂ PO ₄]; [HOOCEPEG ₃₅₀ Im][Cl]; [HOOCEPEG ₃₅₀ Im][BF ₄]; [HOOCEPEG ₇₅₀ Im][Cl];	1) Ionic liquid (1 mmol) and carbonyldiimidazole (1 mmol) in 1 mL DMSO, 4 h at rt. 2) 260 μL of the previous solution added to 15 mL of lipase (5 mg/mL), 24 h at 4 °C.	Improved activity (hydrolysis of olive oil), organic solvent tolerance, thermostability, and adaptability to pH and temperature changes.	[277]
Lipase from <i>Candida antarctica A</i> and greases from <i>Humicola lanuginosa</i>	Benzoic anhydride	1) Benzoic anhydride (1 M) dissolved in 250 μL of DMSO. 2) 50 μL of the previous solution added to 9.9 mL of the lipases (10 mg in phosphate buffer, 0.1 M, pH 8.5), 30 min at 25 °C. 3) Addition of 50 μL of the benzoic acid solution, 1 h at 25 °C.	Increased thermostability, long-term stability and activity in paint-based formulations (<i>α</i> -naphthyl acetate)	[269]
Lipase from <i>Thermomyces lanuginosus</i>	1-naphtaldehyde, butyraldehyde, hexyl aldehyde, dodecyl aldehyde and 1-naphthyl isothiocyanate	<i>For the aldehydes:</i> Lipase (2 mL) in 5 mL of phosphate/NaBH ₃ CN (0.1 M/0.02 M, pH 5.1). Addition of the aldehyde (4:1 w/w aldehyde:lipase), overnight at 4 °C. <i>For the isothiocyanate:</i> Lipase (2 mL) in 5 mL of sodium carbonate buffer (0.1 M, pH 9). Addition of the isothiocyanate (5 mg in 50 μL DMSO), overnight at 4 °C.	Improved thermostability, and hydrolytic activity against differentiated size-chain substrates (<i>p</i> -nitrophenyl benzoate, <i>p</i> -nitrophenyl acetate, <i>p</i> -nitrophenyl butyrate, <i>p</i> -nitrophenyl hexanoate, <i>p</i> -nitrophenyl octanoate, <i>p</i> -nitrophenyl laurate and <i>p</i> -nitrophenyl palmitate). Higher transesterification (<i>p</i> -nitrophenyl palmitate) and esterification (oleic acid) activity (modified lipase with 4 dodecyl chains) against different chain-length alcohols.	[192, 270]

Grafting macromolecules (> 1000 Da)

Lipase	Molecules grafted	Experimental conditions	Improved properties/application	References
Lipase from <i>Candida antarctica B</i>	Pluronic F-127	1) Oxidation of Pluronic F-127 by Dess-Martin periodinane. 2) Oxidized Pluronic in phosphate buffer (10 mM, pH 7) added to CALB in phosphate buffer (5-10 mg/mL), 2 h. Addition of NaBH ₃ CN (10 % w/Pluronic), 15 h at rt.	Increased transesterification activity in the synthesis of lutein ester. Reusability of the catalyst through temperature-induced precipitation.	[278]
Lipase from <i>Candida rugosa</i> , lipase from <i>Candida antarctica B</i> and lipase from <i>Thermomyces lanuginosus</i>			Increased catalytic activity in the asymmetric ammonolysis of (<i>R</i>)- and (<i>S</i>)- phenylglycine methyl ester.	[279]
			Increased activity, stability, reusability, and selectivity. Higher conversions in the synthesis of an anti-cancer drug, valrubicin (2.1 times for modified lipase from <i>Thermomyces lanuginosus</i> and 6 times for modified lipase from <i>Candida antarctica B</i> . No activity for both forms of lipase from <i>Candida rugosa</i> were observed.	[280]
Lipase from <i>Thermomyces lanuginosus</i>	mPEG-propionaldehyde, mPEG-succinimidyl succinate ester, carboxymethyl cellulose or maltodextrin	<u>For the aldehydes:</u> 1) Lipase in phosphate buffer (0.1 mM, pH 9) with 50-fold molar excess of the aldehyde, 2 h at 22 °C; 2) Addition of NaBH ₃ CN (10-fold molar excess to the polymer), 24 h at rt. <u>For the mPEG-NHS:</u> Lipase in phosphate buffer (0.1 mM, pH 9) with 50-fold molar excess of the polymer, 24 h at 22 °C.	Increased thermal stability and stability in a detergent formulation.	[254]

Lipase from <i>Candida antarctica</i> B and lipase from <i>Thermomyces lanuginosus</i>	<i>O</i> [2-(6-oxocaproylamino)ethyl]- <i>O</i> -methylpolyethylene glycol (5 kDa)	Lipase (12 mg/mL) in phosphate/NaBH ₃ CN (0.1 M/0.02 M, pH 5.1). Addition of the PEG (4:1 w/w aldehyde:lipase), overnight at 4 °C.	Preserved or enhanced hydrolytic activity (<i>p</i> -nitrophenyl butyrate) and polymerase activity (synthesis of poly(ethylene glutarate, starting from ethylene glycol and diethyl glutarate).	[81]
Lipase from <i>Candida antarctica</i> B and lipase from <i>Thermomyces lanuginosus</i>	<i>In situ</i> polymerization using the monomers: <i>N</i> -(iso-butoxymethyl) acrylamide (NIBMA) or <i>N</i> {3-(dimethylamino)propyl} acrylamide (DMAPA)	1) Lipase (3 mg/mL) in phosphate-buffered saline (1x, pH 7.4) with 10 % glycerin. 2) Addition of CTA-NHS ^[a] (30 mg) in 2 mL DMSO, with a syringe pump, 2 h at rt. 3) Lipase-CTA conjugate (0.2 mM) added to DMAPA or NIBMA (0.2 mmol), Eosin Y (0.023 μmol), TEMED (0.0023 μmol) and 75 μL DMF. Bubbling N ₂ for 30 min. Blue light irradiation (λ _{max} = 460 nm) for 15 min.	Preserved or enhanced lipolytic activity (<i>p</i> -nitrophenyl palmitate hydrolysis).	[281]
Lipase from <i>Candida rugosa</i>	<i>In situ</i> polymerization using the monomers: carboxyl betaine methacrylate (CBMA), <i>tert</i> -butyl methacrylate (TBMA) or an equimolar mixture of the above.	1) NHS ester (200 mg/mL) in 450 μL DMSO added to 10 mL of lipase (20 mg/mL, in phosphate buffer, 20 mM, pH 7), 48 h at 4 °C. 2) Previous conjugate in 10 mL of phosphate buffer (20 mM, pH 7) with 5 mmol the respective monomer (TBMA or CBMA), 24 h at 4 °C. Then, Bpy, CuBr ₂ and CuBr where added. Molar ratios of TBMA, CBMA, Bpy, CuBr ₂ and CuBr tested: 100:0:20:1:10, 50:50:20:1:10 and 0:100:20:1:10.	Improved hydrolytic activity (<i>p</i> -nitrophenyl palmitate), pH tolerance, thermostability and higher efficiency and substrate affinity.	[282]

Lipase H from <i>Candida cylindracea</i>	Dextran (40 kDa)	1) Oxidation of dextran: 500 μmol NaIO_4 added to 10 mL of 1 % w/v dextran solution. Stirring, 2 h at rt followed by 24 h at 4 °C, in the dark. 2) Lipase (25 mg) in 8.215 mL of sodium borate buffer (50 mM, pH 7.4-8.9), added to 2.385 mL of oxidized dextran solution, 2 h at rt followed by 14 h at 4 °C, in the dark.	Improved stability in organic solvents.	[276]
		1) Oxidation of dextran as described above. 2) Lipase (25 mg) in 8.215 mL of sodium phosphate buffer (50 mM, pH 5.5-8.5), added to 2.385 mL of oxidized dextran solution, 2 h at rt followed by 13 h at 4 °C, in the dark. Addition of 54 μL of borane-pyridine complex, 1 h at 4 °C, in the dark.		[275]
Lipase A from <i>Bacillus subtilis</i>	Poly(4-acryloylmorpholine)	1) Poly(4-acryloylmorpholine)-NHS was added to a lipase solution (0.1 mg/mL) in sodium phosphate buffer (50 mM, pH 7.9, NaCl 200 mM, 3 vol % glycerol) at a molar ratio 20:1 (polymer:primary amine), 1 h at rt.	Enhanced transesterification (<i>p</i> -nitrophenyl butyrate with ethanol) activity in ionic liquids.	[14]

^[a]CTA-NHS: 2-(((ethylthio)-carbonothioyl)thio)propanoic acid (CTA) bearing a *N*-hydroxysuccinimidyl ester (NHS).

8.4. Immobilization of lipases onto solid supports

The modification of enzymes can also be undertaken by physical immobilization. This strategy is characterized by the attachment of the enzymes to an insoluble support [12]. These supports/carriers can be composites, hydrogels, polymeric membranes, nanofibers, nanoparticles, microspheres, and hybrid or bent support materials [283, 284]. Apart from different supports, several approaches can be implemented for the enzymes' immobilization. Physical adsorption, entrapment, covalent attachment, and cross-linked aggregates/crystals, are the most explored methodologies [12] (Figure 8.5).

This is the most explored approach conducted by the researchers, regarding the many advantages associated with their implementation. The increase of the enzymes' stability, reusability, easy recovery, and the possibility to shift the optimum pH of the enzyme, are the main motivations for its use [285]. Alike many techniques, the immobilization methodology has certain drawbacks. In most cases, there is a significant loss of the enzyme activity, correlated to the reduced mobility or stereochemical impediments promoted by the support [251].

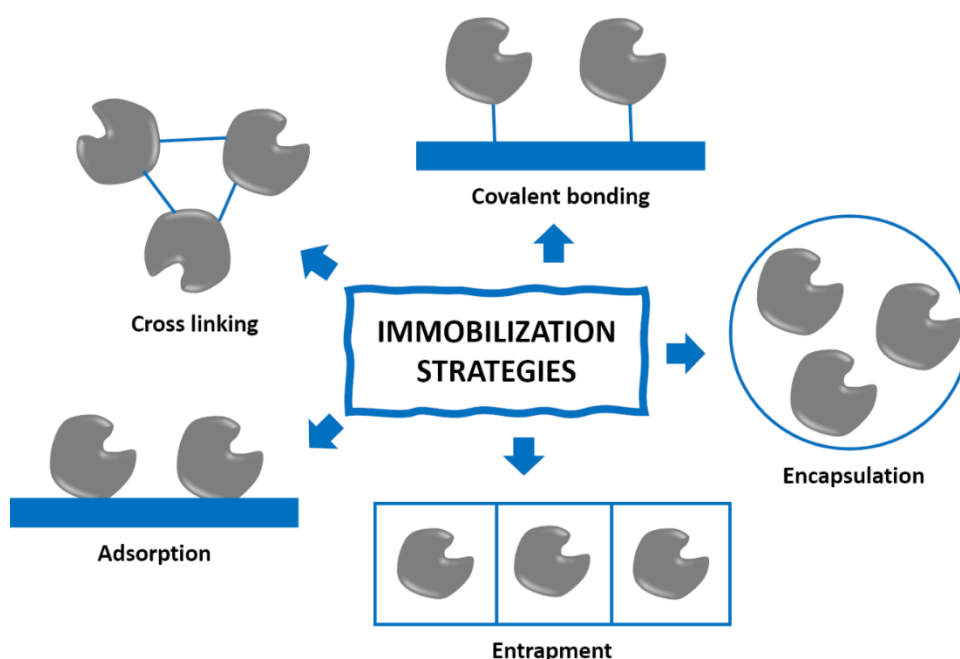


Figure 8.5. Examples of enzyme immobilization strategies.

8.4.1. Immobilization vs chemical modification: advantages and disadvantages

As earlier described, both chemical strategies have numerous advantages comparing to the use of the native enzymes. The immobilization onto solid supports is far the most common strategy, being

Novozymes 435 (lipase from *Candida Antarctica B* immobilized on acrylic resin) the most explored lipase [223, 286]. The possibility of reuse for multiple reactional cycles, with minimum activity loss, is the most appealing advantage of the immobilization strategy.

Most lipases need interfacial activation to initiate their catalytic activity. Both strategies are commonly applied to avoid or minimize this phenomenon, and therefore increase the broad range of possible substrates [192]. The compounds used for the lipases' grafting are usually hydrophobic, as well as the solid supports for their immobilization [287]. Consequently, the lid and/or the global structure of the enzyme is affected, increasing the accessibility through the active site. In this way, besides increasing the global stability of the enzyme at different temperatures or pH, unusual substrates become efficiently catalysed.

Comparing both strategies, the chemical modification is applied when the activity increase is required. This goal is more easily achieved when the modification is performed with small molecules rather than with polymers, since some mobility can be lost through the coupling of larger macromolecules. The same assumption can be postulated for the solid immobilization. This is the major drawback associated to this strategy. Moreover, this is usually a more expensive process (Figure 8.6). Nonetheless, both approaches can improve the enzymes' selectivity or specificity [191].

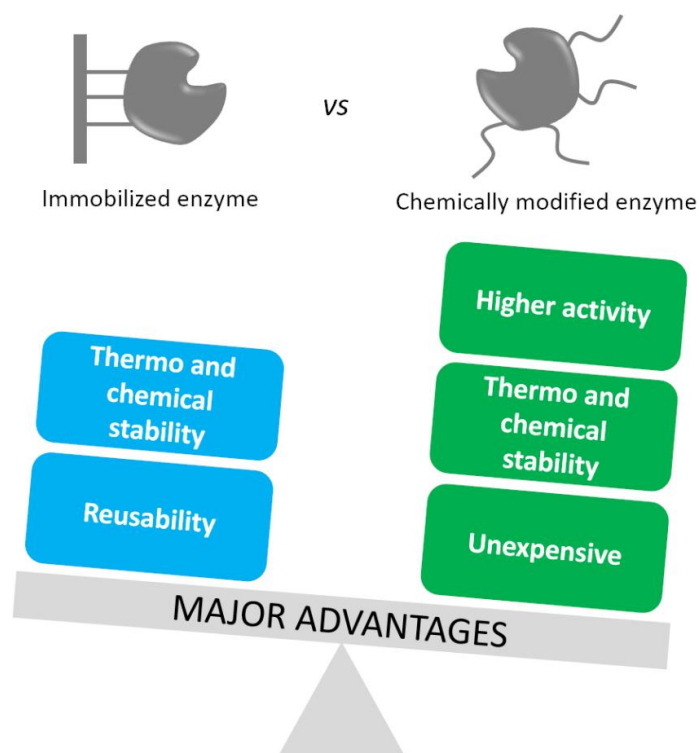


Figure 8.6. Major advantages of both strategies: immobilization vs chemical modification of enzymes.

8.5. Nanoemulsions for the encapsulation of hydrophobic compounds

8.5.1. General description

Nanoemulsions (NE) are generally formed by the mixture of two non-miscible phases. These systems can be classified as: i) water-in-oil (W/O), where water droplets are distributed in the oil phase; ii) oil-in-water (O/W), where oil droplets are distributed in the aqueous phase, and iii) bicontinuous nanoemulsions, where both small droplets of water and oil are interdispersed in the system [288]. The average size of the formed droplets is in the nanometres scale, comprised between 5 to 200 nm [289].

Regarding their formation, two different approaches can be undertaken: low- or high-energy methodologies. The first approach englobes methods like phase transitions, self-emulsification, and phase inversion temperature. The second one, includes ultrasonic emulsification and high-pressure homogenization [290].

8.5.2. Applications

Among the different types of nanodevices, NE stands out regarding their biotechnological applications. They are ideal for the solubilization and encapsulation of hydrophobic compounds given their lipophilic character [291, 292]. They are already available in many of our daily products, especially for cosmetics purposes [293].

Their several advantages make them desirable subjects for different fields of applications [294]. In the last years, this topic has been widely reviewed, in terms of applications in food, drug delivery and cosmetics [291-293, 295, 296].

Different types of compounds have been used to produce NE. Commonly, the oil phase is composed by fatty acids or tri-, di- or monoacylglycerols. Moreover, the presence of emulsifiers, like surfactants, proteins, phospholipids, or polysaccharides is frequently required [292].

Nonetheless, the search for novel emulsifier agents with different biotechnological applications continues to emerge. In **Table 8.4**, are described some examples of novel nanoemulsions produced using different emulsifier/surfactants compounds, and their applications. These NE are produced using nontoxic compounds, for the encapsulation of hydrophobic molecules.

Table 8.4. Recent examples of novel types of nanoemulsions encapsulating hydrophobic compounds, and their fields of applications

Nanoemulsion composition (oil phase)	Application	Hydrophobic compound(s) encapsulated	References
Lambda-cyhalothrin/alkyd resin	Agriculture	Lambda-cyhalothrin	[297]
Palmitoyl-cyclo-oligosaccharides	Pharmaceutical	Methotrexate	[131]
Lecithin/soybean oil	Pharmaceutical	Phenanthrene, diazepam, histamine and chloroquine	[298]
Perfluorohexane	Pharmaceutical	1,1'-dioctadecyl-3,3',3'-tetramethylindocarbocyanine	[299]
Poly(δ -decalactone)/ Pluronic F-68	Pharmaceutical	Prednisolone, carvedilol, griseofulvin, curcumin and cyclosporine A	[300]
Miglyol 812, Epikuron 145 V	Pharmaceutical	Curcumin	[301]
Polyoxyethylene castor oil, isopropyl myristate and glycerol	Cosmeceutical	Ellagic acid	[302]
Octenyl succinic anhydride-modified starches	Cosmeceutical	Vitamin E	[303]
Medium chain triglycerides and Tween	Food, cosmeceutical or pharmaceutical	Vitamin D	[304]

Noro *et al.* [131] synthesized highly hydrophobic compounds, through the coupling of palmitic chains to different oligosaccharides. The produced molecules, showed oily behaviour when heated, producing stable and narrow nanoemulsions after ultrasound treatment. MTX was encapsulated in this novel NE, showing a suitable release profile.

Another NE produced for pharmaceutical applications was developed by Haidar and co-workers [298]. Lecithin based soybean oil was produced for the encapsulation of differentiated hydrophobic drugs (phenanthrene, diazepam, histamine, and chloroquine) showing high versatility. Different starches modified with octenyl succinic anhydride were used by Hategekimana *et al.* for the encapsulation of vitamin E [303]. The many functions associated to this compound, potentializes the applications of these nanodevices, like drug or beverages development purposes [303].

The given examples show the importance of the developments regarding the new nanodevices, for the encapsulation of hydrophobic compounds as a stabilization approach, with different biotechnological applications.

8.6. Major remarks and future perspectives

The main goal of this thesis was to find different strategies for the stabilization, modification, and/or synthesis of hydrophobic compounds. Methotrexate was chosen as a model drug, because despite its current use for the treatment of many illnesses, several drawbacks are associated with its administration, and the development of strategies for its delivery/usage has become imperative. For this purpose, in **chapter 2** we demonstrated the synthesis of novel nanoemulsions for the encapsulation and delivery of MTX. This stabilization approach is one of the many strategies undertaken to overcome several side-effects associated with the administration of hydrophobic drugs. The novel nanoemulsions developed, based on the emulsifying properties of new hydrophobic cyclo-oligosaccharides, showed to be a promising route in the production of non-toxic nanodevices. However, it is important to state, that not all the cyclo-oligosaccharides fulfilled the desired parameters for pharmaceutical purposes. We found that the modification of β -cyclodextrin with palmitoyl chloride did not lead to stable nanoemulsions, contrarily to what occurred for γ -cyclodextrin and cyclosophoraose. We may assume that to afford suitable nanoemulsions, the size of the synthesized macromolecules is an important parameter to consider. Moreover, we could predict that the modification of α -cyclodextrin, the smallest cyclodextrin commercially available, would lead to a similar result, as obtained for the β -cyclodextrin. Another approach studied in this chapter was the introduction of BSA as a cover layer of the cyclo-oligosaccharides for the nanoemulsions formation. Besides decreasing the size, it incremented the polydispersity (0.2), and the toxicity of the nanodevices. Furthermore, these BSA-containing nanoemulsions were also highly susceptible to hydrolysis by a lipase. From this work we may conclude that the nanoemulsions composed exclusively by the modified cyclo-oligosaccharides (γ -cyclodextrin and cyclosophoraose) represent a novel and efficient route for the encapsulation and release of MTX.

In **chapter 3** and **4**, the biosynthesis of novel MTX-prodrugs was performed using two distinct enzymatic strategies. These works were performed to fulfil a literature gap on the use of enzymes for the synthesis of MTX-prodrugs. Firstly (**chapter 3**), the use of lipases (free *Thermomyces lanuginosus* and immobilized *Candida antarctica B*) was undertaken for the formation of MTX-ester prodrugs, by the reaction between MTX and triacylglycerols or cyclodextrins. The accurate enzyme selection was found to be a crucial parameter for the reactions, given the different selectivities observed by the lipases tested. Due to immobilization constraints, CALB was not able to catalyse the reaction between MTX and the long-chain triacylglycerols or cyclodextrins. On the contrary, lipase TL was able to perform both reactions, but not the synthesis of MTX with the small

triacylglycerols (glycerol tributyrate, glycerol trivalerate, and glycerol hexanoate). These findings underline the need of testing different lipases for a certain reaction. The use of an ultrasonic bath to perform the synthesis showed to increase the rate of the reactions, where a higher reactional yield was obtained comparing to the reactions carried out in a water bath. In this way, a green, fast, and environmentally friendly synthetic approach was developed for the synthesis of non-toxic MTX-prodrugs.

Secondly (**chapter 4**), the α -chymotrypsin from *bovine pancreas* was used for the self-polymerization of MTX. This procedure was performed taking advantage of the presence of amines and carboxylic acids in the MTX moiety, each one located in the extremity of its chemical structure. During synthesis, the size of the protease's active site revealed to be a limiting factor, hindering the achievement of products with high degree of polymerization ($DP_{max} = 6$). Apart from the control reaction, which did not lead to the oligomer synthesis, the performance of the enzyme was still limited, given that the oligomer was isolated with near 33 % of conversion rate. Nonetheless, a novel enzymatic approach for the synthesis of a MTX-prodrug was efficiently performed, underlining once again, the potential of enzymes in the synthesis/modification of MTX derivatives.

To enhance the catalytic properties of enzymes, their chemical modification was also explored. Two different approaches were undertaken for this purpose, one using a polymer (PEG) (**chapter 5**) and another using small hydrophobic molecules (**chapter 6**). In the first strategy, the PEGylation of three enzymes was performed: lipase TL, CALB and cutinase from *fusarium solani pisi*. All the enzymes were successfully modified, being their hydrolytic activity (*p*-nitrophenyl butyrate) preserved (TL) or enhanced (CALB and CUT). These findings were very interesting, given that most reports regarding the PEGylation of enzymes, showed a decrease of the enzyme activity after modification. Regarding the exploitation of their polymerase activity, we observed that the modification of CALB did not lead to a different reactional outcome for the synthesis of poly(ethylene glutarate). Both enzyme forms gave rise to oligomers with similar conversion rate and DP. In this way, the potential of this PEGylated enzyme should be explored for different applications, either for the synthesis of other ester compounds or for other synthetic purposes, taking advantage their hydrolytic activity enhancement.

PEGylated TL and PEGylated cutinase gave rise to higher conversion rates, and higher DP (PEG-TL), potentiating the use of these enzymes in different applications.

The other methodology undertaken was the grafting of small hydrophobic aldehydes or isothiocyanates to lipase TL (**chapter 6**). Concerning the modification strategy, we may conclude

that the most promising linkers are the aldehydes, more specifically, the aliphatic ones. Apart from the increase of the thermostability, higher hydrolytic activity was achieved. In the future, other aldehydes could be explored, varying even further the size of their aliphatic chain. Also, other enzymes, like proteases, or other lipases from different sources, could benefit from this modification and their catalytic properties improved.

Grafting of dodecyl aldehyde to the lipase did not only improve its hydrolytic activity, but also its transesterification and esterification abilities (**chapter 7**). The enlargement of the active site, promoted by the modification, showed an outstanding positive effect towards these reactions, opening new perspectives for the production of many added-value esters that can be synthesized in good yields. Furthermore, the practical purposes of this modified enzyme (TL5) are not restricted to one application, broadening its implementation for cosmetics, foods, pharmaceuticals, or the biofuel industry.

To achieve all the goals of this thesis, the modified lipases here developed should be applied on the modification of MTX. This study would demonstrate the potential of the chemically modified enzymes on the synthesis of pharmaceutical prodrugs. Furthermore, due to the high solubility challenges associated with MTX, the introduction of highly hydrophobic aliphatic chains, through esterification or transesterification reaction, would increase its encapsulation into the hydrophobic core of different nanoparticles. An higher stabilization effect promoted by the nanodevice, combined with the use of a prodrug, maybe a potential strategy to overcome several side-effects associated with its application.

References

- [1] Y. Bedoui, X. Guillot, J. Sélambarom, P. Guiraud, C. Giry, M.C. Jaffar-Bandjee, S. Ralandison, P. Gasque, Methotrexate an Old Drug with New Tricks, *International Journal of Molecular Sciences*, 20 (2019) 5023-5055.
- [2] A. Loureiro, A.S. Abreu, M.P. Sárria, M.C.O. Figueiredo, L.M. Saraiva, G.J.L. Bernardes, A.C. Gomes, A. Cavaco-Paulo, Functionalized protein nanoemulsions by incorporation of chemically modified BSA, *RSC Advances*, 5 (2015) 4976-4983.
- [3] R. Conway, J.J. Carey, Risk of liver disease in methotrexate treated patients, *World Journal of Hepatology*, 9 (2017) 1092-1100.
- [4] Z.A.A. Aziz, H. Mohd-Nasir, A. Ahmad, S.H. Mohd. Setapar, W.L. Peng, S.C. Chuo, A. Khatoon, K. Umar, A.A. Yaqoob, M.N. Mohamad Ibrahim, Role of Nanotechnology for Design and Development of Cosmeceutical: Application in Makeup and Skin Care, *Frontiers in Chemistry*, 7 (2019) 1-15.
- [5] J. Rautio, H. Kumpulainen, T. Heimbach, R. Oliyai, D. Oh, T. Järvinen, J. Savolainen, Prodrugs: design and clinical applications, *Nature Reviews Drug Discovery*, 7 (2008) 255-270.
- [6] K. Riebeseel, E. Biedermann, R. Löser, N. Breiter, R. Hanselmann, R. Mülhaupt, C. Unger, F. Kratz, Polyethylene Glycol Conjugates of Methotrexate Varying in Their Molecular Weight from MW 750 to MW 40000: Synthesis, Characterization, and Structure–Activity Relationships in Vitro and in Vivo, *Bioconjugate Chemistry*, 13 (2002) 773-785.
- [7] X. Duan, X. Yang, C. Li, L. Song, Highly Water-Soluble Methotrexate-Polyethyleneglycol-Rhodamine Prodrug Micelle for High Tumor Inhibition Activity, *AAPS PharmSciTech*, 20 (2019) 245-256.
- [8] G. Yousefi, S.M. Foroutan, A. Zarghi, A. Shafaati, Synthesis and characterization of methotrexate polyethylene glycol esters as a drug delivery system, *Chemical & Pharmaceutical Bulletin (Tokyo)*, 58 (2010) 147-153.
- [9] M. Yang, J. Ding, Y. Zhang, F. Chang, J. Wang, Z. Gao, X. Zhuang, X. Chen, Activated macrophage-targeted dextran–methotrexate/folate conjugate prevents deterioration of collagen-induced arthritis in mice, *Journal of Materials Chemistry B*, 4 (2016) 2102-2113.
- [10] A.M. Burger, G. Hartung, G. Stehle, H. Sinn, H.H. Fiebig, Pre-clinical evaluation of a methotrexate–albumin conjugate (MTX-HSA) in human tumor xenografts in vivo, *International Journal of Cancer*, 92 (2001) 718-724.
- [11] Z. Wu, A. Shah, N. Patel, X. Yuan, Development of methotrexate proline prodrug to overcome resistance by MDA-MB-231 cells, *Bioorganic & Medicinal Chemistry Letters*, 20 (2010) 5108-5112.

- [12] M. Bilal, Y. Zhao, S. Noreen, S.Z.H. Shah, R.N. Bharagava, H.M.N. Iqbal, Modifying biocatalytic properties of enzymes for efficient biocatalysis: a review from immobilization strategies viewpoint, *Biocatalysis and Biotransformation*, 37 (2019) 159-182.
- [13] N. Rueda, J.C.S. dos Santos, C. Ortiz, R. Torres, O. Barbosa, R.C. Rodrigues, Á. Berenguer-Murcia, R. Fernandez-Lafuente, Chemical Modification in the Design of Immobilized Enzyme Biocatalysts: Drawbacks and Opportunities, *The Chemical Record*, 16 (2016) 1436-1455.
- [14] G.R. Chado, E.N. Holland, A.K. Tice, M.P. Stoykovich, J.L. Kaar, Modification of Lipase with Poly(4-acryloylmorpholine) Enhances Solubility and Transesterification Activity in Anhydrous Ionic Liquids, *Biomacromolecules*, 19 (2018) 1324-1332.
- [15] J.F. Darby, M. Atobe, J.D. Firth, P. Bond, G.J. Davies, P. O'Brien, R.E. Hubbard, Increase of enzyme activity through specific covalent modification with fragments, *Chemical Science*, 8 (2017) 7772-7779.
- [16] Y. Ran, A. Jain, S.H. Yalkowsky, Solubilization and Preformulation Studies on PG-300995 (An Anti-HIV Drug), *Journal of Pharmaceutical Sciences*, 94 (2005) 297-303.
- [17] J.M.M. Terwogt, J.H.M. Schellens, W.W.t.B. Huinink, J.H. Beijnen, Clinical pharmacology of anticancer agents in relation to formulations and administration routes, *Cancer Treatment Reviews*, 25 (1999) 83-102.
- [18] F.A. Alvarez Núñez, S.H. Yalkowsky, Solubilization of Diazepam, *PDA Journal of Pharmaceutical Science and Technology*, 52 (1998) 33-36.
- [19] S.K. Han, G.Y. Kim, Y.H. Park, Solubilization of Biphenyl Dimethyl Dicarboxylate by Cosolvency, *Drug Development and Industrial Pharmacy*, 25 (1999) 1193-1197.
- [20] A.T.M. Serajuddin, Solid dispersion of poorly water-soluble drugs: Early promises, subsequent problems, and recent breakthroughs, *Journal of Pharmaceutical Sciences*, 88 (1999) 1058-1066.
- [21] L. Ana, G.A. Nuno, C.G. Andreia, C.-P. Artur, Albumin-Based Nanodevices as Drug Carriers, *Current Pharmaceutical Design*, 22 (2016) 1371-1390.
- [22] W.H. De Jong, P.J.A. Borm, Drug delivery and nanoparticles: applications and hazards, *International Journal of Nanomedicine*, 3 (2008) 133-149.
- [23] Z.A. Khan, R. Tripathi, B. Mishra, Methotrexate: a detailed review on drug delivery and clinical aspects, *Expert Opinion on Drug Delivery*, 9 (2012) 151-169.
- [24] S.S. Abolmaali, A. Tamaddon, G. Yousefi, K. Javidnia, R. Dinarvand, Sequential optimization of methotrexate encapsulation in micellar nano-networks of polyethyleneimine ionomer containing redox-sensitive cross-links, *International Journal of Nanomedicine*, 9 (2014) 2833-2848.

- [25] P. Chakkarapani, L. Subbiah, S. Palanisamy, A. Bibiana, F. Ahrentorp, C. Jonasson, C. Johansson, Encapsulation of methotrexate loaded magnetic microcapsules for magnetic drug targeting and controlled drug release, *Journal of Magnetism and Magnetic Materials*, 380 (2015) 285-294.
- [26] S. Massadeh, M. Alaamery, S. Al-Qatanani, S. Alarifi, S. Bawazeer, Y. Alyafee, Synthesis of protein-coated biocompatible methotrexate-loaded PLA-PEG-PLA nanoparticles for breast cancer treatment, *Nano Reviews & Experiments*, 7 (2016) 31996-32006.
- [27] D. Soto-Castro, J.A. Cruz-Morales, M.T.R. Apan, P. Guadarrama, Solubilization and anticancer-activity enhancement of Methotrexate by novel dendrimeric nanodevices synthesized in one-step reaction, *Bioorganic Chemistry*, 41-42 (2012) 13-21.
- [28] A. Loureiro, E. Nogueira, N.G. Azoia, M.P. Sárria, A.S. Abreu, U. Shimanovich, A. Rollett, J. Härmark, H. Hebert, G. Guebitz, G.J.L. Bernardes, A. Preto, A.C. Gomes, A. Cavaco-Paulo, Size controlled protein nanoemulsions for active targeting of folate receptor positive cells, *Colloids and Surfaces B: Biointerfaces*, 135 (2015) 90-98.
- [29] B. Gidwani, A. Vyas, A Comprehensive Review on Cyclodextrin-Based Carriers for Delivery of Chemotherapeutic Cytotoxic Anticancer Drugs, *Biomed Research International*, 2015 (2015) 198268-198268.
- [30] H. Kim, S.D. Dindulkar, D. Jeong, S. Park, B.-H. Jun, E. Cho, S. Jung, A synthetic encapsulating emulsifier using complex-forming pentacosadiynoyl cyclosophoraoses (cyclic β -(1, 2)-d-glucan), *Journal of Industrial and Engineering Chemistry*, 44 (2016) 195-203.
- [31] Y.-E. Kwon, E. Cho, I.-S. Lee, S. Jung, Synthesis and Characterization of Butyryl Cyclosophoraose, and its Inclusion Complexation Behavior for Some Flavonoids, *Bulletin of the Korean Chemical Society*, 32 (2011) 2779-2782.
- [32] K. Koizumi, Y. Okada, S. Horiyama, T. Utamura, T. Higashiura, M. Ikeda, Preparation of cyclosophoraose-A and its complex-forming ability, *Journal of Inclusion Phenomena*, 2 (1984) 891-899.
- [33] S.D. Dindulkar, D. Jeong, E. Cho, D. Kim, S. Jung, Microbial cyclosophoraose as a catalyst for the synthesis of diversified indolyl 4H-chromenes via one-pot three component reactions in water, *Green Chemistry*, 18 (2016) 3620-3627.
- [34] H. Kim, J.M. Choi, Y. Choi, M.N. Tahir, Y.-H. Yang, E. Cho, S. Jung, Enhanced solubility of galangin based on the complexation with methylated microbial cyclosophoraoses, *Journal of Inclusion Phenomena and Macrocyclic Chemistry*, 79 (2014) 291-300.

- [35] R. Silva, H. Ferreira, N.G. Azoia, U. Shimanovich, G. Freddi, A. Gedanken, A. Cavaco-Paulo, Insights on the Mechanism of Formation of Protein Microspheres in a Biphasic System, *Molecular Pharmaceutics*, 9 (2012) 3079-3088.
- [36] M.W. Breedveld, L.P. Zevenhuizen, A.J. Zehnder, Excessive excretion of cyclic beta-(1,2)-glucan by *Rhizobium trifolii* TA-1, *Applied and Environmental Microbiology*, 56 (1990) 2080-2086.
- [37] C. Kwon, Y. Choi, D. Jeong, J.G. Kim, J.M. Choi, S. Chun, S. Park, S. Jung, Inclusion complexation of naproxen with cyclophorases and succinylated cyclophorases in different pH environments, *Journal of Inclusion Phenomena and Macrocyclic Chemistry*, 74 (2012) 325-333.
- [38] S. Pronk, S. Páll, R. Schulz, P. Larsson, P. Bjelkmar, R. Apostolov, M.R. Shirts, J.C. Smith, P.M. Kasson, D. van der Spoel, B. Hess, E. Lindahl, GROMACS 4.5: a high-throughput and highly parallel open source molecular simulation toolkit, *Bioinformatics*, 29 (2013) 845-854.
- [39] B. Hess, H. Bekker, H.J.C. Berendsen, J.G.E.M. Fraaije, LINCS: A linear constraint solver for molecular simulations, *Journal of Computational Chemistry*, 18 (1997) 1463-1472.
- [40] H.J.C. Berendsen, J.P.M. Postma, W.F. van Gunsteren, A. DiNola, J.R. Haak, Molecular dynamics with coupling to an external bath, *The Journal of Chemical Physics*, 81 (1984) 3684-3690.
- [41] Z. Wu, B. Zhang, B. Yan, Regulation of enzyme activity through interactions with nanoparticles, *International Journal of Molecular Sciences*, 10 (2009) 4198-4209.
- [42] T. Matamá, F. Vaz, G.M. Gübitz, A. Cavaco-Paulo, The effect of additives and mechanical agitation in surface modification of acrylic fibres by cutinase and esterase, *Biotechnology Journal*, 1 (2006) 842-849.
- [43] S.K. Ramamoorthy, R. Hephziba, Acute renal failure post high dose methotrexate infusion successfully managed with high dose folinic Acid and high flux dialysis, *Indian Journal of Hematology & Blood Transfusion*, 29 (2013) 90-92.
- [44] O.M. Al-Quteimat, M.A. Al-Badaineh, Practical issues with high dose methotrexate therapy, *Saudi Pharmaceutical Journal*, 22 (2014) 385-387.
- [45] B.M. Liederer, R.T. Borchardt, Enzymes involved in the bioconversion of ester-based prodrugs, *Journal of Pharmaceutical Sciences*, 95 (2006) 1177-1195.
- [46] N. Kuznetsova, A. Kandyba, I. Vostrov, V. Kadykov, G. Gaenko, J. Molotkovsky, E. Vodovozova, Liposomes loaded with lipophilic prodrugs of methotrexate and melphalan as convenient drug delivery vehicles, *Journal of Drug Delivery Science and Technology*, 19 (2009) 51-59.

- [47] K.-E. Jaeger, T. Eggert, Lipases for biotechnology, *Current Opinion in Biotechnology*, 13 (2002) 390-397.
- [48] A.M. Klibanov, Improving enzymes by using them in organic solvents, *Nature*, 409 (2001) 241-246.
- [49] B.K. Liu, N. Wang, Z.C. Chen, Q. Wu, X.F. Lin, Markedly enhancing lipase-catalyzed synthesis of nucleoside drugs' ester by using a mixture system containing organic solvents and ionic liquid, *Bioorganic & Medicinal Chemistry Letters*, 16 (2006) 3769-3771.
- [50] J. Sun, S.-Q. Liu, Ester Synthesis in Aqueous Media by Lipase: Alcoholysis, Esterification and Substrate Hydrophobicity, *Journal of Food Biochemistry*, 39 (2015) 11-18.
- [51] J. Sun, B. Yu, P. Curran, S.-Q. Liu, Optimisation of flavour ester biosynthesis in an aqueous system of coconut cream and fusel oil catalysed by lipase, *Food Chemistry*, 135 (2012) 2714-2720.
- [52] C. Lecointe, E. Dubreucq, P. Galzy, Ester synthesis in aqueous media in the presence of various lipases, *Biotechnology Letters*, 18 (1996) 869-874.
- [53] D. Briand, E. Dubreucq, P. Galzy, Enzymatic fatty esters synthesis in aqueous medium with lipase from *Candida parapsilosis* (Ashford) Langeron and Talice, *Biotechnology Letters*, 16 (1994) 813-818.
- [54] X. Zhao, S.R. Bansode, A. Ribeiro, A.S. Abreu, C. Oliveira, P. Parpot, P.R. Gogate, V.K. Rathod, A. Cavaco-Paulo, Ultrasound enhances lipase-catalyzed synthesis of poly (ethylene glutarate), *Ultrasonics Sonochemistry*, 31 (2016) 506-511.
- [55] P. Tufvesson, J. Lima-Ramos, M. Nordblad, J.M. Woodley, Guidelines and Cost Analysis for Catalyst Production in Biocatalytic Processes, *Organic Process Research & Development*, 15 (2011) 266-274.
- [56] L.A. Lerin, R.A. Loss, D. Remonato, M.C. Zenevich, M. Balen, V.O. Netto, J.L. Ninow, C.M. Trentin, J.V. Oliveira, D. de Oliveira, A review on lipase-catalyzed reactions in ultrasound-assisted systems, *Bioprocess and Biosystems Engineering*, 37 (2014) 2381-2394.
- [57] F.I. Braginskaya, E.A. Zaitzeva, O.M. Zorina, O.M. Poltorak, E.S. Chukrai, F. Dunn, Low intensity ultrasonic effects on yeast hexokinase, *Radiation and Environmental Biophysics*, 29 (1990) 47-56.
- [58] K. Zhu, H. Liu, P. Han, P. Wei, Study of ultrasound-promoted, lipase-catalyzed synthesis of fructose ester, *Frontiers of Chemical Engineering in China*, 4 (2010) 367-371.

- [59] A.M. Gumel, M.S.M. Annuar, Y. Chisti, T. Heidelberg, Ultrasound assisted lipase catalyzed synthesis of poly-6-hydroxyhexanoate, *Ultrasonics Sonochemistry*, 19 (2012) 659-667.
- [60] S.-C. Lung, R.J. Weselake, Diacylglycerol acyltransferase: A key mediator of plant triacylglycerol synthesis, *Lipids*, 41 (2006) 1073-1088.
- [61] H.-D. Shin, J.-H. Kim, T.-K. Kim, S.-H. Kim, Y.-H. Lee, Esterification of hydrophobic substrates by lipase in the cyclodextrin induced emulsion reaction system, *Enzyme and Microbial Technology*, 30 (2002) 835-842.
- [62] P.P. Chiplunkar, X. Zhao, P.D. Tomke, J. Noro, B. Xu, Q. Wang, C. Silva, A.P. Pratap, A. Cavaco-Paulo, Ultrasound-assisted lipase catalyzed hydrolysis of aspirin methyl ester, *Ultrasonics Sonochemistry*, 40 (2018) 587-593.
- [63] E. Abreu Silveira, S. Moreno-Perez, A. Basso, S. Serban, R. Pestana Mamede, P.W. Tardioli, C. Sanchez Farinas, J. Rocha-Martin, G. Fernandez-Lorente, J.M. Guisan, Modulation of the regioselectivity of *Thermomyces lanuginosus* lipase via biocatalyst engineering for the Ethanolysis of oil in fully anhydrous medium, *BMC Biotechnology*, 17 (2017) 88-101.
- [64] L. Abdulrahman, O. Bakare, M. Abdulrahman, The Chemical Approach of Methotrexate Targeting, *Frontiers in Biomedical Sciences*, 1 (2017) 50-73.
- [65] C. Luna, C. Verdugo, E.D. Sancho, D. Luna, J. Calero, A. Posadillo, F.M. Bautista, A.A. Romero, Production of a biodiesel-like biofuel without glycerol generation, by using Novozym 435, an immobilized *Candida antarctica* lipase, *Bioresources and Bioprocessing*, 1 (2014) 11-24.
- [66] Z.-Z. Ou, J.-R. Chen, X.-S. Wang, B.-W. Zhang, Y. Cao, Synthesis of a water-soluble cyclodextrin modified hypocrellin and ESR study of its photodynamic therapy properties, *New Journal of Chemistry*, 26 (2002) 1130-1136.
- [67] J. Li, F. Yu, Y. Chen, D. Oupický, Polymeric drugs: Advances in the development of pharmacologically active polymers, *Journal of Controlled Release*, 219 (2015) 369-382.
- [68] R. Duncan, The dawning era of polymer therapeutics, *Nature Reviews Drug Discovery*, 2 (2003) 347-360.
- [69] P. Mishra, B. Nayak, R.K. Dey, PEGylation in anti-cancer therapy: An overview, *Asian Journal of Pharmaceutical Sciences*, 11 (2016) 337-348.
- [70] J. Suksiriworapong, V. Taresco, D.P. Ivanov, I.D. Styliari, K. Sakchaisri, V.B. Junyaprasert, M.C. Garnett, Synthesis and properties of a biodegradable polymer-drug conjugate: Methotrexate-poly(glycerol adipate), *Colloids and Surfaces B: Biointerfaces*, 167 (2018) 115-125.

- [71] D. Wang, L. Zou, Q. Jin, J. Hou, G. Ge, L. Yang, Human carboxylesterases: a comprehensive review, *Acta Pharmaceutica Sinica B*, 8 (2018) 699-712.
- [72] P. Philipps-Wiemann, Chapter 12 - Proteases—general aspects, in: C.S. Nunes, V. Kumar (Eds.) *Enzymes in Human and Animal Nutrition*, Academic Press 2018, pp. 257-266.
- [73] K. Yazawa, K. Numata, Recent advances in chemoenzymatic peptide syntheses, *Molecules* (Basel, Switzerland), 19 (2014) 13755-13774.
- [74] P.J. Baker, K. Numata, Chapter 9 - Polymerization of Peptide Polymers for Biomaterial Applications, 2013, pp. 229-246.
- [75] X. Qin, A.C. Khuong, Z. Yu, W. Du, J. Decatur, R.A. Gross, Simplifying alternating peptide synthesis by protease-catalyzed dipeptide oligomerization, *Chemical Communications*, 49 (2013) 385-387.
- [76] X. Qin, W. Xie, S. Tian, J. Cai, H. Yuan, Z. Yu, G.L. Butterfoss, A.C. Khuong, R.A. Gross, Enzyme-triggered hydrogelation via self-assembly of alternating peptides, *Chemical Communications*, 49 (2013) 4839-4841.
- [77] P. Cerqueira, J. Noro, S. Moura, D. Guimarães, C. Silva, A. Cavaco-Paulo, A. Loureiro, PTS micelles for the delivery of hydrophobic methotrexate, *International Journal of Pharmaceutics*, 566 (2019) 282-290.
- [78] J. Ren, Z. Fang, L. Yao, F.Z. Dahmani, L. Yin, J. Zhou, J. Yao, A micelle-like structure of poloxamer–methotrexate conjugates as nanocarrier for methotrexate delivery, *International Journal of Pharmaceutics*, 487 (2015) 177-186.
- [79] J. Noro, R.L. Reis, A. Cavaco-Paulo, C. Silva, Ultrasound-assisted biosynthesis of novel methotrexate-conjugates, *Ultrasonics Sonochemistry*, 48 (2018) 51-56.
- [80] C. Cupp-Enyard, Sigma's Non-specific Protease Activity Assay - Casein as a Substrate, *J Vis Exp*, (2008) 899-900.
- [81] J. Noro, T.G. Castro, F. Gonçalves, A. Ribeiro, A. Cavaco-Paulo, C. Silva, Catalytic Activation of Esterases by PEGylation for Polyester Synthesis, *ChemCatChem*, 11 (2019) 2490-2499.
- [82] N. Singh, T. Jabeen, S. Sharma, I. Roy, M.N. Gupta, S. Bilgrami, R.K. Somvanshi, S. Dey, M. Perbandt, C. Betzel, A. Srinivasan, T.P. Singh, Detection of native peptides as potent inhibitors of enzymes, *The FEBS Journal*, 272 (2005) 562-572.
- [83] T.J. Dolinsky, J.E. Nielsen, J.A. McCammon, N.A. Baker, PDB2PQR: an automated pipeline for the setup of Poisson-Boltzmann electrostatics calculations, *Nucleic Acids Research*, 32 (2004) 665-667.

- [84] G. Bussi, D. Donadio, M. Parrinello, Canonical sampling through velocity rescaling, *The Journal of Chemical Physics*, 126 (2007) 014101-014108.
- [85] R. Martoňák, A. Laio, M. Parrinello, Predicting Crystal Structures: The Parrinello-Rahman Method Revisited, *Physical Review Letters*, 90 (2003) 075503-075507.
- [86] M. Abraham;, B. Hess;, D.v.d. Spoel;, E. Lindahl;, a.t.G.d. team;, GROMACS User Manual version 5.1.5, DOI (2017).
- [87] W. Huang, Z. Lin, W.F. van Gunsteren, Validation of the GROMOS 54A7 Force Field with Respect to β -Peptide Folding, *Journal of Chemical Theory and Computation*, 7 (2011) 1237-1243.
- [88] N. Schmid, A.P. Eichenberger, A. Choutko, S. Riniker, M. Winger, A.E. Mark, W.F. van Gunsteren, Definition and testing of the GROMOS force-field versions 54A7 and 54B7, *European Biophysics Journal*, 40 (2011) 843-856.
- [89] T. Darden, D. York, L. Pedersen, Particle mesh Ewald: An $N \cdot \log(N)$ method for Ewald sums in large systems, *The Journal of Chemical Physics*, 98 (1993) 10089-10092.
- [90] B. Hess, P-LINCS: A Parallel Linear Constraint Solver for Molecular Simulation, *Journal of Chemical Theory and Computation*, 4 (2008) 116-122.
- [91] D. van der Spoel, P.J. van Maaren, H.J.C. Berendsen, A systematic study of water models for molecular simulation: Derivation of water models optimized for use with a reaction field, *The Journal of Chemical Physics*, 108 (1998) 10220-10230.
- [92] G.W.T.M.J. Frisch;, H.B. Schlegel;, G.E. Scuseria;, M.A. Robb;, J.R. Cheeseman;, G. Scalmani;, V. Barone;, G.A. Petersson;, H. Nakatsuji;, X. Li;, M. Caricato;, A. Marenich;, J. Bloino;, B.G. Janesko;, B.M. R. Gomperts, H.P. Hratchian, J.V. Ortiz, A.F. Izmaylov, J.L. Sonnenberg, D. Williams-Young, F. Ding, F. Lipparini, F. Egidi, J. Goings, B. Peng, A. Petrone, T. Henderson, D. Ranasinghe, V.G. Zakrzewski, J. Gao, N. Rega, G. Zheng, W. Liang, M. Hada, M. Ehara, K. Toyota, R. Fukuda, J. Hasegawa, M. Ishida, T. Nakajima, Y. Honda, O. Kitao, H. Nakai, T. Vreven, K. Throssell, J.A. Montgomery, Jr., J.E. Peralta, F. Ogliaro, M. Bearpark, J.J. Heyd, E. Brothers, K.N. Kudin, V.N. Staroverov, T. Keith, R. Kobayashi, J. Normand, K. Raghavachari, A. Rendell, J.C. Burant, S.S. Iyengar, J. Tomasi, M. Cossi, J.M. Millam, M. Klene, C. Adamo, R. Cammi, J.W. Ochterski, R.L. Martin, K. Morokuma, O. Farkas, J.B. Foresman, D. J. Fox. , Gaussian, Inc, Wallingford CT, Gaussian 09, nd gaussiancom/g09citation/, DOI.
- [93] J.J.P. Stewart, Optimization of parameters for semiempirical methods V: Modification of NDDO approximations and application to 70 elements, *Journal of Molecular Modeling*, 13 (2007) 1173-1213.

- [94] G.M. Morris, R. Huey, W. Lindstrom, M.F. Sanner, R.K. Belew, D.S. Goodsell, A.J. Olson, AutoDock4 and AutoDockTools4: Automated docking with selective receptor flexibility, *Journal of Computational Chemistry*, 30 (2009) 2785-2791.
- [95] G.M. Morris, D.S. Goodsell, R.S. Halliday, R. Huey, W.E. Hart, R.K. Belew, A.J. Olson, Automated docking using a Lamarckian genetic algorithm and an empirical binding free energy function, *Journal of Computational Chemistry*, 19 (1998) 1639-1662.
- [96] O. Pillai, R. Panchagnula, Polymers in drug delivery, *Current Opinion in Chemical Biology*, 5 (2001) 447-451.
- [97] V.R. Guarino, V.J. Stella, Prodrugs of Amides, Imides and Other NH-acidic Compounds, in: V.J. Stella, R.T. Borchardt, M.J. Hageman, R. Oliyai, H. Maag, J.W. Tilley (Eds.) *Prodrugs: Challenges and Rewards Part 1*, Springer New York, New York, NY, 2007, pp. 833-887.
- [98] R. Karaman, Prodrugs design based on inter- and intramolecular chemical processes, *Chemical Biology & Drug Design*, 82 (2013) 643-668.
- [99] J. Feher, 8.5 - Digestion and Absorption of the Macronutrients, in: J. Feher (Ed.) *Quantitative Human Physiology (Second Edition)*, Academic Press, Boston, 2017, pp. 821-833.
- [100] M. Custódio, A. Goulart, D. Marques, R.d. Giordano, R. Giordano, R. Monti, Hydrolysis of cheese whey proteins with trypsin, chymotrypsin and carboxypeptidase A, *Alimentos e Nutrição*, 16 (2005) 105-109.
- [101] S. Farhadian, B. Shareghi, L. Momeni, O.K. Abou-Zied, V.A. Sirotkin, M. Tachiya, A.A. Saboury, Insights into the molecular interaction between sucrose and α -chymotrypsin, *International Journal of Biological Macromolecules*, 114 (2018) 950-960.
- [102] S. Farhadian, B. Shareghi, A.A. Saboury, Exploring the thermal stability and activity of α -chymotrypsin in the presence of spermine, *Journal of Biomolecular Structure and Dynamics*, 35 (2017) 435-448.
- [103] H. Siddiqui, R. Farooq, B.P. Marasini, R. Malik, N. Syed, S.T. Moin, R. Atta ur, M.I. Choudhary, Synthesis and in vitro α -chymotrypsin inhibitory activity of 6-chlorobenzimidazole derivatives, *Bioorganic & Medicinal Chemistry*, 24 (2016) 3387-3395.
- [104] L. Yang, H. Li, P. Wu, A. Mahal, J. Xue, L. Xu, X. Wei, Dinghupeptins A–D, Chymotrypsin Inhibitory Cyclodepsipeptides Produced by a Soil-Derived Streptomyces, *Journal of Natural Products*, 81 (2018) 1928-1936.
- [105] J.K. Dozier, M.D. Distefano, Site-Specific PEGylation of Therapeutic Proteins, *International Journal Molecular Sciences*, 16 (2015) 25831-25864.

- [106] B. Yang, Y. Zhao, S. Wang, Y. Zhang, C. Fu, Y. Wei, L. Tao, Synthesis of Multifunctional Polymers through the Ugi Reaction for Protein Conjugation, *Macromolecules*, 47 (2014) 5607-5612.
- [107] C. Silva, M. Martins, S. Jing, J. Fu, A. Cavaco-Paulo, Practical insights on enzyme stabilization, *Critical Reviews in Biotechnology*, 38 (2018) 335-350.
- [108] V. Gaberc-Porekar, I. Zore, B. Podobnik, V. Menart, Obstacles and pitfalls in the PEGylation of therapeutic proteins, *Current Opinion in Drug Discovery & Development*, 11 (2008) 242-250.
- [109] F.M. Veronese, A. Mero, The impact of PEGylation on biological therapies, *BioDrugs : clinical immunotherapeutics, Biopharmaceuticals and Gene Therapy*, 22 (2008) 315-329.
- [110] C.J. Fee, J.M. Van Alstine, PEG-proteins: Reaction engineering and separation issues, *Chemical Engineering Science*, 61 (2006) 924-939.
- [111] F.M. Veronese, Peptide and protein PEGylation: a review of problems and solutions, *Biomaterials*, 22 (2001) 405-417.
- [112] H.A. Vandertol-Vanier, R. Vazquez-Duhalt, R. Tinoco, M.A. Pickard, Enhanced activity by poly(ethylene glycol) modification of *Coriopsis gallica* laccase, *Journal of Industrial Microbiology & Biotechnology*, 29 (2002) 214-220.
- [113] J.I. Lee, S.P. Eisenberg, M.S. Rosendahl, E.A. Chlipala, J.D. Brown, D.H. Doherty, G.N. Cox, Site-specific PEGylation enhances the pharmacokinetic properties and antitumor activity of interferon beta-1b, *Journal of Interferon Cytokine Research*, 33 (2013) 769-777.
- [114] J. Su, J. Noro, A. Loureiro, M. Martins, N.G. Azoia, J. Fu, Q. Wang, C. Silva, A. Cavaco-Paulo, PEGylation Greatly Enhances Laccase Polymerase Activity, *ChemCatChem*, 9 (2017) 3888-3894.
- [115] C. Vilela, A.F. Sousa, A.C. Fonseca, A.C. Serra, J.F.J. Coelho, C.S.R. Freire, A.J.D. Silvestre, The quest for sustainable polyesters – insights into the future, *Polymer Chemistry*, 5 (2014) 3119-3141.
- [116] Y. Yang, Y. Yu, Y. Zhang, C. Liu, W. Shi, Q. Li, Lipase/esterase-catalyzed ring-opening polymerization: A green polyester synthesis technique, *Process Biochemistry*, 46 (2011) 1900-1908.
- [117] C. Hedfors, E. Östmark, E. Malmström, K. Hult, M. Martinelle, Thiol End-Functionalization of Poly(ϵ -caprolactone), Catalyzed by *Candida antarctica* Lipase B, *Macromolecules*, 38 (2005) 647-649.

- [118] Y. Yang, W. Lu, J. Cai, Y. Hou, S. Ouyang, W. Xie, R.A. Gross, Poly(oleic diacid-co-glycerol): Comparison of Polymer Structure Resulting from Chemical and Lipase Catalysis, *Macromolecules*, 44 (2011) 1977-1985.
- [119] Z. Jiang, C. Liu, W. Xie, R.A. Gross, Controlled Lipase-Catalyzed Synthesis of Poly(hexamethylene carbonate), *Macromolecules*, 40 (2007) 7934-7943.
- [120] R. Araújo, C. Silva, A. O'Neill, N. Micaelo, G. Guebitz, C.M. Soares, M. Casal, A. Cavaco-Paulo, Tailoring cutinase activity towards polyethylene terephthalate and polyamide 6,6 fibers, *Journal of Biotechnology*, 128 (2007) 849-857.
- [121] K. Mayolo-Deloya, M. González-González, J. Simental-Martínez, M. Rito-Palomares, Aldehyde PEGylation of laccase from *Trametes versicolor* in route to increase its stability: effect on enzymatic activity, *Journal of Molecular Recognition*, 28 (2015) 173-179.
- [122] C. Silva, S. Da, N. Silva, T. Matamá, R. Araújo, M. Martins, S. Chen, J. Chen, J. Wu, M. Casal, A. Cavaco-Paulo, Engineered *Thermobifida fusca* cutinase with increased activity on polyester substrates, *Biotechnology Journal*, 6 (2011) 1230-1239.
- [123] B. Castillo, J. Méndez, W. Al-Azzam, G. Barletta, K. Griebenow, On the relationship between the activity and structure of PEG-alpha-chymotrypsin conjugates in organic solvents, *Biotechnology and Bioengineering*, 94 (2006) 565-574.
- [124] U. Derewenda, L. Swenson, Y. Wei, R. Green, P.M. Kobos, R. Joerger, M.J. Haas, Z.S. Derewenda, Conformational lability of lipases observed in the absence of an oil-water interface: crystallographic studies of enzymes from the fungi *Humicola lanuginosa* and *Rhizopus delemar*, *Journal of Lipid Research*, 35 (1994) 524-534.
- [125] J. Uppenberg, M.T. Hansen, S. Patkar, T.A. Jones, The sequence, crystal structure determination and refinement of two crystal forms of lipase B from *Candida antarctica*, *Structure*, 2 (1994) 293-308.
- [126] H.J.C. Berendsen, D. van der Spoel, R. van Drunen, GROMACS: A message-passing parallel molecular dynamics implementation, *Computer Physics Communications*, 91 (1995) 43-56.
- [127] S. Miyamoto, P.A. Kollman, Settle: An analytical version of the SHAKE and RATTLE algorithm for rigid water models, *Journal of Computational Chemistry*, 13 (1992) 952-962.
- [128] A.K. Malde, L. Zuo, M. Breeze, M. Stroet, D. Poger, P.C. Nair, C. Oostenbrink, A.E. Mark, An Automated Force Field Topology Builder (ATB) and Repository: Version 1.0, *Journal of Chemical Theory and Computation*, 7 (2011) 4026-4037.

- [129] M. Stroet, B. Caron, K.M. Visscher, D.P. Geerke, A.K. Malde, A.E. Mark, Automated Topology Builder Version 3.0: Prediction of Solvation Free Enthalpies in Water and Hexane, *Journal of Chemical Theory and Computation*, 14 (2018) 5834-5845.
- [130] PyMOL, The PyMOL Molecular Graphics System, Version 2.0 Schrödinger, LLC., n.d., DOI.
- [131] J. Noro, A. Loureiro, F. Gonçalves, N.G. Azoia, S. Jung, C. Silva, A. Cavaco-Paulo, Oil-based cyclo-oligosaccharide nanodevices for drug encapsulation, *Colloids and Surfaces B: Biointerfaces*, 159 (2017) 259-267.
- [132] I.W. Hamley, PEG–Peptide Conjugates, *Biomacromolecules*, 15 (2014) 1543-1559.
- [133] Y. Ikeda, J. Katamachi, H. Kawasaki, Y. Nagasaki, Novel Protein PEGylation Chemistry via Glutalaldehyde-Functionalized PEG, *Bioconjugate Chemistry*, 24 (2013) 1824-1827.
- [134] X. Zhao, J. Noro, J. Fu, H. Wang, C. Silva, A. Cavaco-Paulo, “In-situ” lipase-catalyzed cotton coating with polyesters from ethylene glycol and glycerol, *Process Biochemistry*, 66 (2018) 82-88.
- [135] S. Naik, A. Basu, R. Saikia, B. Madan, P. Paul, R. Chatterjee, J. Brask, A. Svendsen, Lipases for use in industrial biocatalysis: Specificity of selected structural groups of lipases, *Journal of Molecular Catalysis B: Enzymatic*, 65 (2010) 18-23.
- [136] C. Carvalho, M. Aires-Barros, J. Cabral, Cutinase structure, function and biocatalytic applications, *Electronic Journal of Biotechnology*, 1 (1998) 160-173.
- [137] C. Martinez, A. Nicolas, H. van Tilbeurgh, M.P. Egloff, C. Cudrey, R. Verger, C. Cambillau, Cutinase, a lipolytic enzyme with a preformed oxyanion hole, *Biochemistry*, 33 (1994) 83-89.
- [138] J. Skjold-Jørgensen, J. Vind, A. Svendsen, M.J. Bjerrum, Altering the Activation Mechanism in *Thermomyces lanuginosus* Lipase, *Biochemistry*, 53 (2014) 4152-4160.
- [139] M. Martinelle, M. Holmquist, K. Hult, On the interfacial activation of *Candida antarctica* lipase A and B as compared with *Humicola lanuginosa* lipase, *Biochimica et Biophysica Acta (BBA) - Lipids and Lipid Metabolism*, 1258 (1995) 272-276.
- [140] B. Stauch, S.J. Fisher, M. Cianci, Open and closed states of *Candida antarctica* lipase B: protonation and the mechanism of interfacial activation, *Journal of Lipid Research*, 56 (2015) 2348-2358.
- [141] T. Zisis, P.L. Freddolino, P. Turunen, M.C.F. van Teeseling, A.E. Rowan, K.G. Blank, Interfacial Activation of *Candida antarctica* Lipase B: Combined Evidence from Experiment and Simulation, *Biochemistry*, 54 (2015) 5969-5979.

- [142] N. Willems, M. Lelimosin, J. Skjold-Jørgensen, A. Svendsen, M.S.P. Sansom, The effect of mutations in the lid region of *Thermomyces lanuginosus* lipase on interactions with triglyceride surfaces: A multi-scale simulation study, *Chemistry and Physics of Lipids*, 211 (2018) 4-15.
- [143] S. Ali, F.I. Khan, W. Chen, A. Rahaman, Y. Wang, Open and closed states of Mrlip1 DAG lipase revealed by molecular dynamics simulation, *Molecular Simulation*, 44 (2018) 1520-1528.
- [144] T. Debuissy, E. Pollet, L. Avérus, Lipase-catalyzed synthesis of biobased and biodegradable aliphatic copolyesters from short building blocks. Effect of the monomer length, *European Polymer Journal*, 97 (2017) 328-337.
- [145] S. Brännström, M. Finnveden, M. Johansson, M. Martinelle, E. Malmström, Itaconate based polyesters: Selectivity and performance of esterification catalysts, *European Polymer Journal*, 103 (2018) 370-377.
- [146] Y. Jiang, A.J.J. Woortman, G.O.R. Alberda van Ekenstein, K. Loos, Environmentally benign synthesis of saturated and unsaturated aliphatic polyesters via enzymatic polymerization of biobased monomers derived from renewable resources, *Polymer Chemistry*, 6 (2015) 5451-5463.
- [147] R. Maheshwari, G. Bharadwaj, M.K. Bhat, Thermophilic fungi: their physiology and enzymes, *Microbiology and Molecular Biology Reviews*, 64 (2000) 461-488.
- [148] K. Arima, W.-H. Liu, T. Beppu, Isolation and Identification of the Lipolytic and Thermophilic Fungus, *Agricultural and Biological Chemistry*, 36 (1972) 1913-1917.
- [149] H. Lee, Y.M. Lee, Y. Jang, S. Lee, H. Lee, B.J. Ahn, G.-H. Kim, J.-J. Kim, Isolation and Analysis of the Enzymatic Properties of Thermophilic Fungi from Compost, *Mycobiology*, 42 (2014) 181-184.
- [150] W. Prathumpai, S.J. Flitter, M. McIntyre, J. Nielsen, Lipase production by recombinant strains of *Aspergillus niger* expressing a lipase-encoding gene from *Thermomyces lanuginosus*, *Applied Microbiology and Biotechnology*, 65 (2004) 714-719.
- [151] R. Fernandez-Lafuente, Lipase from *Thermomyces lanuginosus*: Uses and prospects as an industrial biocatalyst, *Journal of Molecular Catalysis B: Enzymatic*, 62 (2010) 197-212.
- [152] R. Xin, F.I. Khan, Z. Zhao, Z. Zhang, B. Yang, Y. Wang, A comparative study on kinetics and substrate specificities of Phospholipase A1 with *Thermomyces lanuginosus* lipase, *Journal of Colloid and Interface Science*, 488 (2017) 149-154.
- [153] A.A. Homaei, R. Sariri, F. Vianello, R. Stevanato, Enzyme immobilization: an update, *Journal of Chemical Biology*, 6 (2013) 185-205.

- [154] E.P. Cipolatti, A. Valério, J.L. Ninow, D. de Oliveira, B.C. Pessela, Stabilization of lipase from *Thermomyces lanuginosus* by crosslinking in PEGylated polyurethane particles by polymerization: Application on fish oil ethanolysis, *Biochemical Engineering Journal*, 112 (2016) 54-60.
- [155] A. de Vasconcellos, J. Bergamasco Laurenti, A.H. Miller, D.A. da Silva, F. Rogério de Moraes, D.A.G. Aranda, J.G. Nery, Potential new biocatalysts for biofuel production: The fungal lipases of *Thermomyces lanuginosus* and *Rhizomucor miehei* immobilized on zeolitic supports ion exchanged with transition metals, *Microporous and Mesoporous Materials*, 214 (2015) 166-180.
- [156] M. Marciello, M. Filice, J.M. Palomo, Different strategies to enhance the activity of lipase catalysts, *Catalysis Science & Technology*, 2 (2012) 1531-1543.
- [157] R. Jia, Y. Hu, L. Liu, L. Jiang, B. Zou, H. Huang, Enhancing Catalytic Performance of Porcine Pancreatic Lipase by Covalent Modification Using Functional Ionic Liquids, *ACS Catalysis*, 3 (2013) 1976-1983.
- [158] R. Jia, Y. Hu, L. Liu, L. Jiang, H. Huang, Chemical modification for improving activity and stability of lipase B from *Candida antarctica* with imidazolium-functional ionic liquids, *Organic & Biomolecular Chemistry*, 11 (2013) 7192-7198.
- [159] S.S.R. Bohr, P.M. Lund, A.S. Kallenbach, H. Pinholt, J. Thomsen, L. Iversen, A. Svendsen, S.M. Christensen, N.S. Hatzakis, Direct observation of *Thermomyces lanuginosus* lipase diffusional states by Single Particle Tracking and their remodeling by mutations and inhibition, *Scientific Reports*, 9 (2019) 16169-16180.
- [160] M.J. Abraham, T. Murtola, R. Schulz, S. Páll, J.C. Smith, B. Hess, E. Lindahl, GROMACS: High performance molecular simulations through multi-level parallelism from laptops to supercomputers, *SoftwareX*, 1-2 (2015) 19-25.
- [161] E. Jurrus, D. Engel, K. Star, K. Monson, J. Brandi, L.E. Felberg, D.H. Brookes, L. Wilson, J. Chen, K. Liles, M. Chun, P. Li, D.W. Gohara, T. Dolinsky, R. Konecny, D.R. Koes, J.E. Nielsen, T. Head-Gordon, W. Geng, R. Krasny, G.-W. Wei, M.J. Holst, J.A. McCammon, N.A. Baker, Improvements to the APBS biomolecular solvation software suite, *Protein Science*, 27 (2018) 112-128.
- [162] A.D. Becke, Density-functional thermochemistry. III. The role of exact exchange, *The Journal of Chemical Physics*, 98 (1993) 5648-5652.
- [163] G.M. Morris, R. Huey, A.J. Olson, Using AutoDock for Ligand-Receptor Docking, *Current Protocols in Bioinformatics*, 24 (2008) 1-40.

- [164] F.J. Solis, R.J.B. Wets, Minimization by Random Search Techniques, *Mathematics of Operations Research*, 6 (1981) 19-30.
- [165] J. Su, T.G. Castro, J. Noro, J. Fu, Q. Wang, C. Silva, A. Cavaco-Paulo, The effect of high-energy environments on the structure of laccase-polymerized poly(catechol), *Ultrasonics Sonochemistry*, 48 (2018) 275-280.
- [166] J.E. Reynolds Iii, M. Josowicz, P. Tyler, R.B. Vegh, K.M. Solntsev, Spectral and redox properties of the GFP synthetic chromophores as a function of pH in buffered media, *Chemical Communications*, 49 (2013) 7788-7790.
- [167] M.M. Hemdan, E.A. El-Bordany, Use of dodecanoyl isothiocyanate as building block in synthesis of target benzothiazine, quinazoline, benzothiazole and thiourea derivatives, *Chemical Papers*, 70 (2016) 1117-1125.
- [168] C.D. Spicer, B.G. Davis, Selective chemical protein modification, *Nature Communications*, 5 (2014) 4740-4754.
- [169] M.H. Sørensen, J.B.S. Ng, L. Bergström, P.C.A. Alberius, Improved enzymatic activity of *Thermomyces lanuginosus* lipase immobilized in a hydrophobic particulate mesoporous carrier, *Journal of Colloid and Interface Science*, 343 (2010) 359-365.
- [170] J. Yu, C. Wang, A. Wang, N. Li, X. Chen, X. Pei, P. Zhang, S.G. Wu, Dual-cycle immobilization to reuse both enzyme and support by reblossoming enzyme-inorganic hybrid nanoflowers, *RSC Advances*, 8 (2018) 16088-16094.
- [171] H. Chahinian, Y.B. Ali, A. Abousalham, S. Petry, L. Mandrich, G. Manco, S. Canaan, L. Sarda, Substrate specificity and kinetic properties of enzymes belonging to the hormone-sensitive lipase family: Comparison with non-lipolytic and lipolytic carboxylesterases, *Biochimica et Biophysica Acta (BBA) - Molecular and Cell Biology of Lipids*, 1738 (2005) 29-36.
- [172] G.R. Grimsley, J.M. Scholtz, C.N. Pace, A summary of the measured pK values of the ionizable groups in folded proteins, *Protein Science*, 18 (2009) 247-251.
- [173] D.G. Isom, C.A. Castañeda, B.R. Cannon, B. García-Moreno E, Large shifts in pKa values of lysine residues buried inside a protein, *Proceedings of the National Academy of Sciences*, 108 (2011) 5260-5265.
- [174] V. Oklejas, C. Zong, G.A. Papoian, P.G. Wolynes, Protein structure prediction: do hydrogen bonding and water-mediated interactions suffice?, *Methods*, 52 (2010) 84-90.

- [175] K.M. Gonçalves, L.R.S. Barbosa, L.M.T.R. Lima, J.R. Cortines, D.E. Kalume, I.C.R. Leal, L.S. Mariz e Miranda, R.O.M. de Souza, Y. Cordeiro, Conformational dissection of *Thermomyces lanuginosus* lipase in solution, *Biophysical Chemistry*, 185 (2014) 88-97.
- [176] P. Lozano, T. De Diego, J.L. Iborra, Dynamic Structure/Function Relationships in the α -Chymotrypsin Deactivation Process by Heat and pH, *European Journal of Biochemistry*, 248 (1997) 80-85.
- [177] S. Gautam, M.N. Gupta, Solid state fluorescence of proteins in high throughput mode and its applications, *F1000Research*, 2 (2013) 82-92.
- [178] S. Daneshjoo, N. Akbari, A.A. Sepahi, B. Ranjbar, R.-A. Khavarinejad, K. Khajeh, Imidazolium chloride-based ionic liquid-assisted improvement of lipase activity in organic solvents, *Engineering in Life Sciences*, 11 (2011) 259-263.
- [179] Y.I. Hassan, D. Trofimova, P. Samuleev, M.F. Miah, T. Zhou, Chapter 16 - Omics Approaches in Enzyme Discovery and Engineering, in: D. Barh, V. Azevedo (Eds.) *Omics Technologies and Bio-Engineering*, Academic Press 2018, pp. 297-322.
- [180] S. Ferreira-Dias, G. Sandoval, F. Plou, F. Valero, The potential use of lipases in the production of fatty acid derivatives for the food and nutraceutical industries, *Electronic Journal of Biotechnology*, 16 (2013) 1-28.
- [181] E.M.M. Abdelraheem, H. Busch, U. Hanefeld, F. Tonin, Biocatalysis explained: from pharmaceutical to bulk chemical production, *Reaction Chemistry & Engineering*, 4 (2019) 1878-1894.
- [182] M. Ashrafuzzaman, J. Pyo, C. Cheong, Sucrose Derivatives Preparation using *Thermomyces lanuginosus* Lipase and Their Application, *Bulletin of the Korean Chemical Society*, 35 (2014) 477-482.
- [183] L. Flores, H. Beltran, D. Arrieta-Baez, D. Reyes-Duarte, Regioselective Synthesis of Lactulose Esters by *Candida antarctica* and *Thermomyces lanuginosus* Lipases, *Catalysts*, 7 (2017) 263-278.
- [184] L. da Silva Corrêa, R.O. Henriques, J.V. Rios, L.A. Lerin, D. de Oliveira, A. Furigo, Lipase-Catalyzed Esterification of Geraniol and Citronellol for the Synthesis of Terpenic Esters, *Applied Biochemistry and Biotechnology*, 190 (2020) 574-583.
- [185] F.A.P. Lage, J.J. Bassi, M.C.C. Corradini, L.M. Todero, J.H.H. Luiz, A.A. Mendes, Preparation of a biocatalyst via physical adsorption of lipase from *Thermomyces lanuginosus* on hydrophobic

support to catalyze biolubricant synthesis by esterification reaction in a solvent-free system, *Enzyme and Microbial Technology*, 84 (2016) 56-67.

[186] Z. Amini, Z. Ilham, H.C. Ong, H. Mazaheri, W.-H. Chen, State of the art and prospective of lipase-catalyzed transesterification reaction for biodiesel production, *Energy Conversion and Management*, 141 (2017) 339-353.

[187] A. Kumari, P. Mahapatra, V.K. Garlapati, R. Banerjee, Enzymatic transesterification of Jatropha oil, *Biotechnology for Biofuels*, 2 (2009) 1-7.

[188] J. Mukherjee, M.N. Gupta, Dual bioimprinting of *Thermomyces lanuginosus* lipase for synthesis of biodiesel, *Biotechnology Reports*, 10 (2016) 38-43.

[189] P.B. Subhedar, C. Botelho, A. Ribeiro, R. Castro, M.A. Pereira, P.R. Gogate, A. Cavaco-Paulo, Ultrasound intensification suppresses the need of methanol excess during the biodiesel production with Lipozyme TL-IM, *Ultrasonics Sonochemistry*, 27 (2015) 530-535.

[190] D.N. Tran, K.J. Balkus, Perspective of Recent Progress in Immobilization of Enzymes, *ACS Catalysis*, 1 (2011) 956-968.

[191] N. Rueda, J.C. Dos Santos, C. Ortiz, R. Torres, O. Barbosa, R.C. Rodrigues, Á. Berenguer-Murcia, R. Fernandez-Lafuente, Chemical Modification in the Design of Immobilized Enzyme Biocatalysts: Drawbacks and Opportunities, *Chemical record (New York, N.Y.)*, 16 (2016) 1436-1455.

[192] J. Noro, T.G. Castro, A. Cavaco-Paulo, C. Silva, Substrate hydrophobicity and enzyme modifiers play a major role in the activity of lipase from *Thermomyces lanuginosus*, *Catalysis Science & Technology*, 10 (2020) 5913-5924.

[193] Y. Teng, Y. Xu, A modified para-nitrophenyl palmitate assay for lipase synthetic activity determination in organic solvent, *Analytical Biochemistry*, 363 (2007) 297-299.

[194] I. Bayout, N. Bouzemi, N. Guo, X. Mao, S. Serra, S. Riva, F. Secundo, Natural flavor ester synthesis catalyzed by lipases, *Flavour and Fragrance Journal*, 35 (2020) 209-218.

[195] Y.-T. Wang, Z. Fang, F. Zhang, Esterification of oleic acid to biodiesel catalyzed by a highly acidic carbonaceous catalyst, *Catalysis Today*, 319 (2019) 172-181.

[196] A. Alegría, J. Cuellar, Esterification of oleic acid for biodiesel production catalyzed by 4-dodecylbenzenesulfonic acid, *Applied Catalysis B: Environmental*, 179 (2015) 530-541.

[197] J.-P. Chen, J.-B. Wang, Wax ester synthesis by lipase-catalyzed esterification with fungal cells immobilized on cellulose biomass support particles, *Enzyme and Microbial Technology*, 20 (1997) 615-622.

- [198] D. Yu, E. Hornung, T. Iven, I. Feussner, High-level accumulation of oleyl oleate in plant seed oil by abundant supply of oleic acid substrates to efficient wax ester synthesis enzymes, *Biotechnology for Biofuels*, 11 (2018) 53-67.
- [199] G.A. Kovalenko, L.V. Perminova, A.B. Beklemishev, Catalytic properties of recombinant *Thermomyces lanuginosus* lipase immobilized by impregnation into mesoporous silica in the enzymatic esterification of saturated fatty acids with aliphatic alcohols, *Reaction Kinetics, Mechanisms and Catalysis*, 128 (2019) 479-491.
- [200] A. Mates, Inhibition of *Staphylococcus aureus* lipase activity by alcohol, *Lipids*, 8 (1973) 549-552.
- [201] J. Chapman, A. Ismail, C. Dinu, Industrial Applications of Enzymes: Recent Advances, Techniques, and Outlooks, *Catalysts*, 8 (2018) 238-264.
- [202] A.G.A. Sá, A.C.d. Meneses, P.H.H.d. Araújo, D.d. Oliveira, A review on enzymatic synthesis of aromatic esters used as flavor ingredients for food, cosmetics and pharmaceuticals industries, *Trends in Food Science & Technology*, 69 (2017) 95-105.
- [203] P. María, G. Gonzalo, A. Alcántara, Biocatalysis as Useful Tool in Asymmetric Synthesis: An Assessment of Recently Granted Patents (2014-2019), *Catalysts*, 9 (2019) 802-844.
- [204] D.L. Hughes, Highlights of the Recent U.S. Patent Literature: Focus on Biocatalysis, *Organic Process Research & Development*, 20 (2016) 700-706.
- [205] R.N. Patel, Biocatalysis for synthesis of pharmaceuticals, *Bioorganic & Medicinal Chemistry*, 26 (2018) 1252-1274.
- [206] Y.G. P. Fu, F. Gao, W. Kong, Y. Lu, Z. Min, S. Rong, C. Shu, R.W. C. Wang, J. Zhao, X. Zhao, Y. Zhao, J. Zhou, B., Martin., (Novartis), WO2020016749, (2020).
- [207] E. Ricklefs, M. Girhard, V.B. Urlacher, Three-steps in one-pot: whole-cell biocatalytic synthesis of enantiopure (+)- and (-)-pinoresinol via kinetic resolution, *Microbial Cell Factories*, 15 (2016) 78-89.
- [208] E.-M. Fischereeder, D. Pressnitz, W. Kroutil, Stereoselective Cascade to C3-Methylated Strictosidine Derivatives Employing Transaminases and Strictosidine Synthases, *ACS Catalysis*, 6 (2016) 23-30.
- [209] T.d.S. Fonseca, L.D. Lima, M.d.C.F. de Oliveira, T.L.G. de Lemos, D. Zampieri, F. Molinari, M.C. de Mattos, Chemoenzymatic Synthesis of Luliconazole Mediated by Lipases, *European Journal of Organic Chemistry*, 2018 (2018) 2110-2116.

- [210] A.d.S. de França, M.V.M. Silva, R.V. Neves, S.P. de Souza, R.A.C. Leão, C.M. Monteiro, Â. Rocha, C.A.M. Afonso, R.O.M.A. de Souza, Studies on the dynamic resolution of Crizotinib intermediate, *Bioorganic & Medicinal Chemistry*, 26 (2018) 1333-1337.
- [211] J.S. Carey, E. McCann, Lipase-Catalyzed Regioselective Ester Hydrolysis as a Key Step in an Alternative Synthesis of a Buprenorphine Pro-Drug, *Organic Process Research & Development*, 23 (2019) 771-774.
- [212] G.V. Lima, M.R. da Silva, T. de Sousa Fonseca, L.B. de Lima, M.d.C.F. de Oliveira, T.L.G. de Lemos, D. Zampieri, J.C.S. dos Santos, N.S. Rios, L.R.B. Gonçalves, F. Molinari, M.C. de Mattos, Chemoenzymatic synthesis of (S)-Pindolol using lipases, *Applied Catalysis A: General*, 546 (2017) 7-14.
- [213] A. Sikora, A. Tarczykowska, J. Chałupka, M. Marszał, Kinetic resolution of a β -adrenolytic drug with the use of lipases as enantioselective biocatalysts, *Medical Research Journal*, 3 (2018) 38-42.
- [214] J. Noro, T.G. Castro, A. Cavaco-Paulo, C. Silva, α -Chymotrypsin catalyses the synthesis of methotrexate oligomers, *Process Biochemistry*, 98 (2020) 193-201.
- [215] A.N. Bigley, T. Narindoshvili, F.M. Raushel, A Chemoenzymatic Synthesis of the (RP)-Isomer of the Antiviral Prodrug Remdesivir, *Biochemistry*, 59 (2020) 3038-3043.
- [216] X. Tang, M. Demiray, T. Wirth, R.K. Allemann, Concise synthesis of artemisinin from a farnesyl diphosphate analogue, *Bioorganic & Medicinal Chemistry*, 26 (2018) 1314-1319.
- [217] R.A. Sheldon, D. Brady, Broadening the Scope of Biocatalysis in Sustainable Organic Synthesis, *ChemSusChem*, 12 (2019) 2859-2881.
- [218] H. Luhavaya, R. Sigrist, J.R. Chekan, S.M.K. McKinnie, B.S. Moore, Biosynthesis of l-4-Chlorokynurenine, an Antidepressant Prodrug and a Non-Proteinogenic Amino Acid Found in Lipopeptide Antibiotics, *Angewandte Chemie International Edition*, 58 (2019) 8394-8399.
- [219] R.C. Peet, M.J. Kavarana, Biosynthesis of cannabinoid prodrugs and their use as therapeutic agents, US 2019/0382814 A1, (2019).
- [220] M.A. Huffman, A. Fryszkowska, O. Alvizo, M. Borra-Garske, K.R. Campos, K.A. Canada, P.N. Devine, D. Duan, J.H. Forstater, S.T. Grosser, H.M. Halsey, G.J. Hughes, J. Jo, L.A. Joyce, J.N. Kolev, J. Liang, K.M. Maloney, B.F. Mann, N.M. Marshall, M. McLaughlin, J.C. Moore, G.S. Murphy, C.C. Nawrat, J. Nazor, S. Novick, N.R. Patel, A. Rodriguez-Granillo, S.A. Robaire, E.C. Sherer, M.D. Truppo, A.M. Whittaker, D. Verma, L. Xiao, Y. Xu, H. Yang, Design of an in vitro biocatalytic cascade for the manufacture of islatravir, *Science*, 366 (2019) 1255-1259.

- [221] Y. Jiang, K. Loos, Enzymatic Synthesis of Biobased Polyesters and Polyamides, *Polymers*, 8 (2016) 243-296.
- [222] X. Zhao, A. Cavaco-Paulo, C. Silva, 4 - Biosynthesis of polyesters and their application on cellulosic fibers, in: A. Cavaco-Paulo, V.A. Nierstrasz, Q. Wang (Eds.) *Advances in Textile Biotechnology (Second Edition)*, Woodhead Publishing 2019, pp. 49-75.
- [223] S.K. Bhatia, R.K. Bhatia, Y.-H. Yang, Biosynthesis of polyesters and polyamide building blocks using microbial fermentation and biotransformation, *Reviews in Environmental Science and Bio/Technology*, 15 (2016) 639-663.
- [224] S. Kobayashi, Green polymer chemistry: new methods of polymer synthesis using renewable starting materials, *Structural Chemistry*, 28 (2017) 461-474.
- [225] J. Yang, Y. Liu, X. Liang, Y. Yang, Q. Li, Enantio-, Regio-, and Chemoselective Lipase-Catalyzed Polymer Synthesis, *Macromolecular Bioscience*, 18 (2018) 1800131-1800140.
- [226] Y. Liu, L. Song, N. Feng, W. Jiang, Y. Jin, X. Li, Recent advances in the synthesis of biodegradable polyesters by sustainable polymerization: lipase-catalyzed polymerization, *RSC Advances*, 10 (2020) 36230-36240.
- [227] P.D. Tomke, X. Zhao, P.P. Chiplunkar, B. Xu, H. Wang, C. Silva, V.K. Rathod, A. Cavaco-Paulo, Lipase-ultrasound assisted synthesis of polyesters, *Ultrasonics Sonochemistry*, 38 (2017) 496-502.
- [228] X. Zhao, J. Noro, J. Fu, C. Silva, A. Cavaco-Paulo, Strategies for the synthesis of fluorinated polyesters, *RSC Advances*, 9 (2019) 1799-1806.
- [229] M. Finnveden, P. Hendil-Forsell, M. Claudino, M. Johansson, M. Martinelle, Lipase-Catalyzed Synthesis of Renewable Plant Oil-Based Polyamides, *Polymers*, 11 (2019) 1730-1739.
- [230] H. Azim, A. Dekhterman, Z. Jiang, R.A. Gross, *Candida antarctica* Lipase B-Catalyzed Synthesis of Poly(butylene succinate): Shorter Chain Building Blocks Also Work, *Biomacromolecules*, 7 (2006) 3093-3097.
- [231] R. García-Arrazola, D.A. López-Guerrero, M. Gimeno, E. Bárzana, Lipase-catalyzed synthesis of poly-L-lactide using supercritical carbon dioxide, *The Journal of Supercritical Fluids*, 51 (2009) 197-201.
- [232] Y. Zhang, P. Lu, Q. Sun, T. Li, L. Zhao, X. Gao, F. Wang, J. Liu, Lipase-mediated direct in situ ring-opening polymerization of ϵ -caprolactone formed by a chemo-enzymatic method, *Journal of Biotechnology*, 281 (2018) 74-80.

- [233] E. Stavila, R.Z. Arsyi, D.M. Petrovic, K. Loos, *Fusarium solani* pisi cutinase-catalyzed synthesis of polyamides, *European Polymer Journal*, 49 (2013) 834-842.
- [234] S. Wu, R. Snajdrova, J.C. Moore, K. Baldenius, U.T. Bornscheuer, *Biocatalysis: Enzymatic Synthesis for Industrial Applications*, *Angewandte Chemie International Edition*, 60 (2020) 88-119.
- [235] K.S. Jaiswal, V.K. Rathod, Enzymatic synthesis of cosmetic grade wax ester in solvent free system: optimization, kinetic and thermodynamic studies, *SN Applied Sciences*, 1 (2019) 949-960.
- [236] N.R. Khan, S.V. Jadhav, V.K. Rathod, Lipase catalysed synthesis of cetyl oleate using ultrasound: Optimisation and kinetic studies, *Ultrasonics Sonochemistry*, 27 (2015) 522-529.
- [237] P. Ungcharoenwivat, A. H-Kittikun, Enzymatic synthesis of coconut oil based wax esters by immobilized lipase EQ3 and commercial lipozyme RMIM, *Electronic Journal of Biotechnology*, 47 (2020) 10-16.
- [238] H.R. da Silva Corrêa L, Rios JV, Lerin LA, de Oliveira D, Furigo A Jr., Lipase-Catalyzed Esterification of Geraniol and Citronellol for the Synthesis of Terpenic Esters, *Applied Biochemistry and Biotechnology*, 190 (2020) 574-583.
- [239] S. Cong, K. Tian, X. Zhang, F. Lu, S. Singh, B. Prior, Z.X. Wang, Synthesis of flavor esters by a novel lipase from *Aspergillus niger* in a soybean-solvent system, *3 Biotech*, 9 (2019) 244-251.
- [240] I. Antonopoulou, S. Varriale, E. Topakas, U. Rova, P. Christakopoulos, V. Faraco, Enzymatic synthesis of bioactive compounds with high potential for cosmeceutical application, *Applied Microbiology and Biotechnology*, 100 (2016) 6519-6543.
- [241] B. Thangaraj, P.R. Solomon, B. Muniyandi, S. Ranganathan, L. Lin, Catalysis in biodiesel production—a review, *Clean Energy*, 3 (2019) 2-23.
- [242] J.H. C. Wancura, M.V. Tres, S.L. Jahn, J.V. de Oliveira, Lipases in liquid formulation for biodiesel production: Current status and challenges, *Biotechnology and Applied Biochemistry*, 67 (2020) 648-667.
- [243] S.K. Bhangu, S. Gupta, M. Ashokkumar, Ultrasonic enhancement of lipase-catalysed transesterification for biodiesel synthesis, *Ultrasonics Sonochemistry*, 34 (2017) 305-309.
- [244] Y. Lv, S. Sun, J. Liu, Biodiesel Production Catalyzed by a Methanol-Tolerant Lipase A from *Candida antarctica* in the Presence of Excess Water, *ACS Omega*, 4 (2019) 20064-20071.
- [245] I. Khan, R. Ganesan, J.R. Dutta, Probiotic lipase derived from *Lactobacillus plantarum* and *Lactobacillus brevis* for biodiesel production from waste cooking olive oil: an alternative feedstock, *International Journal of Green Energy*, 17 (2020) 62-70.

- [246] J. Sebastian, C. Muraleedharan, A. Santhiagu, Enzyme catalyzed biodiesel production from rubber seed oil containing high free fatty acid, *International Journal of Green Energy*, 14 (2017) 687-693.
- [247] K. Moreira, L. Júnior, R. Monteiro, A. Oliveira, C. Valle, T. Freire, P. Fechine, M. Souza, G. Fernández-Lorente, J. Guisan, J. Santos, Optimization of the Production of Enzymatic Biodiesel from Residual Babassu Oil (*Orbignya sp.*) via RSM, *Catalysts*, 10 (2020) 414-434.
- [248] A. Arumugam, V. Ponnusami, Production of biodiesel by enzymatic transesterification of waste sardine oil and evaluation of its engine performance, *Heliyon*, 3 (2017) 486-504.
- [249] M. Santaraite, E. Sendzikiene, V. Makareviciene, K. Kazancev, Biodiesel Production by Lipase-Catalyzed in Situ Transesterification of Rapeseed Oil Containing a High Free Fatty Acid Content with Ethanol in Diesel Fuel Media, *Energies*, 13 (2020) 2588-2600.
- [250] N. Rachmadona, J. Amoah, E. Quayson, S. Hama, A. Yoshida, A. Kondo, C. Ogino, Lipase-catalyzed ethanolysis for biodiesel production of untreated palm oil mill effluent, *Sustainable Energy & Fuels*, 4 (2020) 1105-1111.
- [251] Y. Zhang, J. Ge, Z. Liu, Enhanced Activity of Immobilized or Chemically Modified Enzymes, *ACS Catalysis*, 5 (2015) 4503-4513.
- [252] Y. Chen, J. Wan, Q. Wu, Y. Ma, Chemical Modification of Laccase from *Aspergillus oryzae* and its Application in OCC Pulp, *BioResources*, 12 (2017) 673-683.
- [253] Y. Wang, C. Wu, Site-Specific Conjugation of Polymers to Proteins, *Biomacromolecules*, 19 (2018) 1804-1825.
- [254] S. Kübelbeck, J. Mikhael, H. Keller, R. Konradi, A. Andrieu-Brunsen, G. Baier, Enzyme-Polymer Conjugates to Enhance Enzyme Shelf Life in a Liquid Detergent Formulation, *Macromolecular Bioscience*, 18 (2018) 1800095-1800103.
- [255] J. Su, J. Noro, J. Fu, Q. Wang, C. Silva, A. Cavaco-Paulo, Enzymatic polymerization of catechol under high-pressure homogenization for the green coloration of textiles, *Journal of Cleaner Production*, 202 (2018) 792-798.
- [256] J. Su, J. Noro, J. Fu, Q. Wang, C. Silva, A. Cavaco-Paulo, Coloured and low conductive fabrics by in situ laccase-catalysed polymerization, *Process Biochemistry*, 77 (2019) 77-84.
- [257] S.R. Bansode, V.K. Rathod, An investigation of lipase catalysed sonochemical synthesis: A review, *Ultrasonics Sonochemistry*, 38 (2017) 503-529.
- [258] N.B. Melani, E.B. Tambourgi, E. Silveira, Lipases: From Production to Applications, *Separation & Purification Reviews*, 49 (2020) 143-158.

- [259] A. Mehta, U. Bodh, R. Gupta, Fungal lipases: A review, *Journal of Biotech Research*, 8 (2017) 58-77.
- [260] L. Ramos-Sánchez, M. Cujilema, M. Julián Ricardo, J. Cordova, P. Fickers, Fungal Lipase Production by Solid-State Fermentation, *Bioprocessing & Biotechniques*, 5 (2015) 1-9.
- [261] D. Guerrand, Lipases industrial applications: focus on food and agroindustries, *OCL*, 24 (2017) 1-7.
- [262] N. Sarmah, D. Revathi, G. Sheelu, K. Yamuna Rani, S. Sridhar, V. Mehtab, C. Sumana, Recent advances on sources and industrial applications of lipases, *Biotechnology Progress*, 34 (2018) 5-28.
- [263] P. Priyanka, Y. Tan, G.K. Kinsella, G.T. Henehan, B.J. Ryan, Solvent stable microbial lipases: current understanding and biotechnological applications, *Biotechnology Letters*, 41 (2019) 203-220.
- [264] A.K. Sharma;, V. Sharma;, J. Saxena, A Review on Applications of Microbial Lipases, *International Journal of Biotech Trends and Technology*, 6 (2016) 1-5.
- [265] N.C. Goodwin, J.P. Morrison, D.E. Fuerst, T. Hadi, Biocatalysis in Medicinal Chemistry: Challenges to Access and Drivers for Adoption, *ACS Medicinal Chemistry Letters*, 10 (2019) 1363-1366.
- [266] T. Itoh, Ionic Liquids as Tool to Improve Enzymatic Organic Synthesis, *Chemical Reviews*, 117 (2017) 10567-10607.
- [267] M. Moniruzzaman, N. Kamiya, M. Goto, Activation and stabilization of enzymes in ionic liquids, *Organic & Biomolecular Chemistry*, 8 (2010) 2887-2899.
- [268] C. Xu, X. Yin, C. Zhang, H. Chen, H. Huang, Y. Hu, Improving Catalytic Performance of Burkholderiacepacia Lipase by Chemical Modification with Functional Ionic Liquids, *Chemical Research in Chinese Universities*, 34 (2018) 279-284.
- [269] M.B. Jayawardena, L.H. Yee, A. Poljak, R. Cavicchioli, S.J. Kjelleberg, K.S. Siddiqui, Enhancement of lipase stability and productivity through chemical modification and its application to latex-based polymer emulsions, *Process Biochemistry*, 57 (2017) 131-140.
- [270] J. Noro, A. Cavaco-Paulo, C. Silva, Chemical modification of lipase from *Thermomyces lanuginosus* enhances transesterification and esterification activity, Submitted to: *ACS Catalysis*, (2021).

- [271] M. Joseph, H.M. Trinh, A.K. Mitra, Chapter 7 - Peptide and Protein-Based Therapeutic Agents*, in: A.K. Mitra, K. Cholkar, A. Mandal (Eds.) *Emerging Nanotechnologies for Diagnostics, Drug Delivery and Medical Devices*, Elsevier, Boston, 2017, pp. 145-167.
- [272] J.K. Dozier, M.D. Distefano, Site-Specific PEGylation of Therapeutic Proteins, *International Journal of Molecular Sciences*, 16 (2015) 25831-25864.
- [273] P.L. Turecek, M.J. Bossard, F. Schoetens, I.A. Ivens, PEGylation of Biopharmaceuticals: A Review of Chemistry and Nonclinical Safety Information of Approved Drugs, *Journal of Pharmaceutical Sciences*, 105 (2016) 460-475.
- [274] d.-S.-F. Débora, B.-F. Johara, A. Eliane Candiani, PEGylation: a successful approach to improve the biopharmaceutical potential of snake venom thrombin-like serine protease, *Protein & Peptide Letters*, 22 (2015) 1133-1139.
- [275] S. Kajiwara, K. Komatsu, R. Yamada, T. Matsumoto, M. Yasuda, H. Ogino, Modification of lipase from *Candida cylindracea* with dextran using the borane-pyridine complex to improve organic solvent stability, *Journal of Biotechnology*, 296 (2019) 1-6.
- [276] S. Kajiwara, K. Komatsu, R. Yamada, T. Matsumoto, M. Yasuda, H. Ogino, Improvement of the organic solvent stability of a commercial lipase by chemical modification with dextran, *Biochemical Engineering Journal*, 142 (2019) 1-6.
- [277] X. Li, C. Zhang, S. Li, H. Huang, Y. Hu, Improving Catalytic Performance of *Candida rugosa* Lipase by Chemical Modification with Polyethylene Glycol Functional Ionic Liquids, *Industrial & Engineering Chemistry Research*, 54 (2015) 8072-8079.
- [278] M. Hou, R. Wang, X. Wu, Y. Zhang, J. Ge, Z. Liu, Synthesis of Lutein Esters by Using a Reusable Lipase-Pluronic Conjugate as the Catalyst, *Catalysis Letters*, 145 (2015) 1825-1829.
- [279] X. Wu, R. Wang, Y. Zhang, J. Ge, Z. Liu, Enantioselective Ammonolysis of Phenylglycine Methyl Ester with Lipase-Pluronic Nanoconjugate in Tertiary Butanol, *Catalysis Letters*, 144 (2014) 1407-1410.
- [280] Y. Zhang, Y. Dai, M. Hou, T. Li, J. Ge, Z. Liu, Chemo-enzymatic synthesis of valrubicin using Pluronic conjugated lipase with temperature responsiveness in organic media, *RSC Advances*, 3 (2013) 22963-22966.
- [281] M. Kovaliov, M.L. Allegranza, B. Richter, D. Konkolewicz, S. Averick, Synthesis of lipase polymer hybrids with retained or enhanced activity using the grafting-from strategy, *Polymer*, 137 (2018) 338-345.

- [282] N. Chen, C. Zhang, X. Dong, Y. Liu, Y. Sun, Activation and stabilization of lipase by grafting copolymer of hydrophobic and zwitterionic monomers onto the enzyme, *Biochemical Engineering Journal*, 158 (2020) 107557-107565.
- [283] M. Bilal, T. Rasheed, Y. Zhao, H.M.N. Iqbal, J. Cui, "Smart" chemistry and its application in peroxidase immobilization using different support materials, *International Journal of Biological Macromolecules*, 119 (2018) 278-290.
- [284] M. Bilal, H.M.N. Iqbal, Naturally-derived biopolymers: Potential platforms for enzyme immobilization, *International Journal of Biological Macromolecules*, 130 (2019) 462-482.
- [285] S.Y. Zaitsev, A.A. Savina, I.S. Zaitsev, Biochemical aspects of lipase immobilization at polysaccharides for biotechnology, *Advances in Colloid and Interface Science*, 272 (2019) 102016-102030.
- [286] C. Ortiz, M.L. Ferreira, O. Barbosa, J.C.S. dos Santos, R.C. Rodrigues, Á. Berenguer-Murcia, L.E. Briand, R. Fernandez-Lafuente, Novozym 435: the "perfect" lipase immobilized biocatalyst?, *Catalysis Science & Technology*, 9 (2019) 2380-2420.
- [287] E.A. Manoel, J.C.S. dos Santos, D.M.G. Freire, N. Rueda, R. Fernandez-Lafuente, Immobilization of lipases on hydrophobic supports involves the open form of the enzyme, *Enzyme and Microbial Technology*, 71 (2015) 53-57.
- [288] T.G. Singh, S. Dhiman, M. Jindal, I.S. Sandhu, M. Chitkara, Chapter 13 - Nanobiomaterials: Applications in biomedicine and biotechnology, in: A.M. Grumezescu (Ed.) *Fabrication and Self-Assembly of Nanobiomaterials*, William Andrew Publishing 2016, pp. 401-429.
- [289] M. Gnanadesigan, V. Nandagopalan, G. Kapildev, M. Gundappa, Chapter 16 - Nano Drugs for Curing Malaria: The Plausibility, in: S.S. Mohapatra, S. Ranjan, N. Dasgupta, R.K. Mishra, S. Thomas (Eds.) *Applications of Targeted Nano Drugs and Delivery Systems*, Elsevier 2019, pp. 451-467.
- [290] A. Ostróžka-Cieślík, B. Sarecka-Hujar, Chapter 7 - The Use of Nanotechnology in Modern Pharmacotherapy, in: A.M. Grumezescu (Ed.) *Multifunctional Systems for Combined Delivery, Biosensing and Diagnostics*, Elsevier 2017, pp. 139-158.
- [291] E. Sánchez-López, M. Guerra, J. Dias-Ferreira, A. Lopez-Machado, M. Ettcheto, A. Cano, M. Espina, A. Camins, M.L. Garcia, E.B. Souto, Current Applications of Nanoemulsions in Cancer Therapeutics, *Nanomaterials (Basel)*, 9 (2019) 821-850.
- [292] J.B. Aswathanarayan, R.R. Vittal, Nanoemulsions and Their Potential Applications in Food Industry, *Frontiers in Sustainable Food Systems*, 3 (2019) 1-21.

- [293] Z.A.A. Aziz, H. Mohd-Nasir, A. Ahmad, S.H. Mohd Setapar, W.L. Peng, S.C. Chuo, A. Khatoon, K. Umar, A.A. Yaqoob, M.N. Mohamad Ibrahim, Role of Nanotechnology for Design and Development of Cosmeceutical: Application in Makeup and Skin Care, *Frontiers in Chemistry*, 7 (2019) 739-739.
- [294] N. Azrini, A. Elgharbawy, S. Rezaei Motlagh, N. Samsudin, H. Mohd, Nanoemulsions: Factory for Food, Pharmaceutical and Cosmetics, *Processes*, 7 (2019) 617-651.
- [295] P.J.P. Espitia, C.A. Fuenmayor, C.G. Otoni, Nanoemulsions: Synthesis, Characterization, and Application in Bio-Based Active Food Packaging, *Comprehensive Reviews in Food Science and Food Safety*, 18 (2019) 264-285.
- [296] A. Bahuguna, S. Ramalingam, M. Kim, Formulation, Characterization, and Potential Application of Nanoemulsions in Food and Medicine, in: D. Thangadurai, J. Sangeetha, R. Prasad (Eds.) *Nanotechnology for Food, Agriculture, and Environment*, Springer International Publishing, Cham, 2020, pp. 39-61.
- [297] H. Qin, X. Zhou, D. Gu, L. Li, C. Kan, Preparation and Characterization of a Novel Waterborne Lambda-Cyhalothrin/Alkyd Nanoemulsion, *Journal of Agricultural and Food Chemistry*, 67 (2019) 10587-10594.
- [298] I. Haidar, I.H. Harding, I.C. Bowater, A.W. McDowall, Physical characterisation of drug encapsulated soybean oil nano-emulsions, *Journal of Drug Delivery Science and Technology*, 55 (2020) 101382-101393.
- [299] D.A. Fernandes, D.D. Fernandes, Y. Li, Y. Wang, Z. Zhang, D. Rousseau, C.C. Gradinaru, M.C. Kolios, Synthesis of Stable Multifunctional Perfluorocarbon Nanoemulsions for Cancer Therapy and Imaging, *Langmuir*, 32 (2016) 10870-10880.
- [300] J. Wik, K.K. Bansal, T. Assmuth, A. Rosling, J.M. Rosenholm, Facile methodology of nanoemulsion preparation using oily polymer for the delivery of poorly soluble drugs, *Drug Delivery and Translational Research*, 10 (2020) 1228-1240.
- [301] S. Guerrero, M. Inostroza-Riquelme, P. Contreras-Orellana, V. Diaz-Garcia, P. Lara, A. Vivanco-Palma, A. Cárdenas, V. Miranda, P. Robert, L. Leyton, M.J. Kogan, A.F.G. Quest, F. Oyarzun-Ampuero, Curcumin-loaded nanoemulsion: a new safe and effective formulation to prevent tumor recurrence and metastasis, *Nanoscale*, 10 (2018) 22612-22622.
- [302] H. Zhang, Y. Zhao, X. Ying, Z. Peng, Y. Guo, X. Yao, W. Chen, Ellagic Acid Nanoemulsion in Cosmetics: The Preparation and Evaluation of a New Nanoemulsion Method as a Whitening and Antiaging Agent, *IEEE Nanotechnology Magazine*, 12 (2018) 14-20.

[303] J. Hategekimana, K.G. Masamba, J. Ma, F. Zhong, Encapsulation of vitamin E: Effect of physicochemical properties of wall material on retention and stability, *Carbohydrate Polymers*, 124 (2015) 172-179.

[304] M. Guttoff, A.H. Saberi, D.J. McClements, Formation of vitamin D nanoemulsion-based delivery systems by spontaneous emulsification: Factors affecting particle size and stability, *Food Chemistry*, 171 (2015) 117-122.